SELF-INHIBITION OF RUBISCO BY INHIBITORY BY-PRODUCTS

A thesis submitted by Frederick Grant Pearce for the degree of Doctor of Philosophy at the Australian National University

Molecular Plant Physiology Group
Research School of Biological Sciences
The Australian National University

November 2003

Candidate's Statement

Except where otherwise acknowledged, the work presented in this thesis is my own

Grant Pearce

Publications Arising From This Thesis

The effect of the L335V mutation on the reaction kinetics and ligand binding properties of tobacco Rubisco were published in 2003 as:

> Pearce F.G. & Andrews T.J., (2003) 'The Relationship between Side Reactions and Slow Inhibition of Ribulose-bisphosphate Carboxylase Revealed by a Loop 6 Mutant of the Tobacco Enzyme' *The Journal of Biological Chemistry*, **278**(35): 32526-32536

An anonymous reviewer commented that:

> "This is a very detailed and elegant accounting of the many ways that the reaction catalysed by Rubisco can come off the tracks. The landscape is rough and even if the overall trajectory for the carboxylation reaction is downhill there are alternate basins of attraction into which the unsuspecting intermediate can fall. The contours of the landscape aren't fixed, however. Mutations raise the barriers to some basins, lower them to others."
>
> "This is a textbook example of how a complex enzymatic reaction involving several intermediates can partition to a variety of other products that can only be detected after a lot of very careful analytical chemistry; of how mutations within the active site induce changes in these partitionings. This is quite beautiful."

Results of this thesis were also presented at the following conferences:

> Pearce F.G. & Andrews T.J. (2003): Not All Rubiscos Are Created Equal, ComBio 2003, Melbourne, Australia (poster presentation).
>
> Pearce F.G., Whitney S.M. & Andrews T.J. (2002): Why Doesn't a Mutant Higher Plant Rubisco Show Fallover ?, Gordon Research Conference on CO_2 Fixation & Metabolism in Green Plants, Mt Holyoke College, MA, USA (poster presentation).
>
> Pearce F.G., Andrews T.J., Kane H.J. & Whitney S.M. (2001): A Mutation in Rubisco Reduces Fallover, ComBio 2001, Canberra, Australia (oral presentation).
>
> Pearce F.G., Andrews T.J., Kane H.J. & Whitney S.M. (2001): A Mutation in the Rubisco Large Subunit Reduces the Decline in Activity during Catalysis, 12th International Congress on Photosynthesis, Brisbane, Australia (poster presentation).

It is anticipated that the results from this thesis will form the basis of two further publications: one comparing the differences in ligand binding properties of different Rubisco enzymes, and the other comparing the differences in catalytic side-reactions of different Rubisco enzymes.

Acknowledgements

"Whoever could make two ears of corn or two blades of grass to grow upon a spot of ground where only one grew before, would deserve better of mankind, and do more essential service to his country than the whole race of politicians put together."

The King of Brobdingnag

Gulliver's Travels, By Jonathon Swift (1726)

The production of this thesis is the culmination of several years work, which would not have been possible without the support of many people. The support of my partner, Magda, has been unwavering, and the sacrifices we have made, while difficult at the time, seem less significant now.

I would like to also acknowledge the participation of the people around me in MPP. My supervisor, John, for the support he provided, both in the lab, and especially out of it. My other supervisors, Heather and Spencer, for showing me how to carry out experiments, and the many discussions, some of which were even relevant to this work. Other people in the lab also participated in the project, both directly and indirectly, and big thanks also go out to Rob, Dan, Dave, Ivana, Ollie, and Jason, and the numerous other people in MPP.

My network of friends, both within RSBS, and especially outside of it, provided a chance to forget about the lab for a while, usually over a few drinks. The opportunity to do this is often vastly under-rated and should be encouraged.

The support of my family was also greatly appreciated during this time, as they patiently listened to my stories of active sites and inhibitors. Financial support from the ANU is also acknowledged.

This thesis is dedicated to the memory of Andy Rae, 1976–2001

Abstract

A long term goal of photosynthesis research is to improve the efficiency of the CO_2 fixing enzyme Rubisco in higher plants by the replacement or modification of the endogenous enzyme. Despite its crucial role in photosynthesis, Rubisco appears to have inefficient properties, and is often limited by its inability to distinguish between CO_2, and the competitive substrate O_2. Unfortunately, structural studies have failed to explain the basis for the natural variation in the efficiency of different Rubisco enzymes, and despite extensive mutational studies, there has been little success in improving the efficiency of the enzyme.

Many kinetic studies have been carried out on Rubisco enzymes, but have only measured a few of the kinetic parameters, usually focussing on the catalytic rate and the specificity for the carboxylation reaction. This thesis involves out a comprehensive study of the catalytic chemistry and binding of ligands for a range of naturally occurring classes of Rubisco, and how mutation can influence the higher plant enzyme. The comparison is based on elucidating the differences that have previously been observed in the pattern of self-inhibition between different forms of Rubisco enzymes.

During *in vitro* assays, some forms of purified Rubisco enzymes have shown a decrease in activity over time, due to the formation of inhibitory compounds through side-reactions that bind to the active site of the enzyme. Other forms of the enzyme have not shown a decline in activity, which may be due to either a reduction in the production of inhibitors during catalysis or a decrease in the binding of inhibitors, although the basis for this difference has not previously been fully investigated.

Formation of inhibitors has been observed in the past, but these studies have often not been extended to other Rubisco enzymes. This thesis extends the observations for all forms of Rubisco, and formation was greatest when the reaction conditions promoted the formation of the potentially reactive 2-peroxy-3-keto-D-arabinitol-1,5-bisphosphate intermediate compound, or the reaction was limited by the addition of the substrate, CO_2, increasing the opportunity for the enediol intermediate to undergo alternate processing. The formation of side-reactions is determined by the stability of the intermediate compound in the active site, and measuring the rate of side-reactions allows inferences to be made about the catalytic chemistry of the active site.

Many Rubisco enzymes do not show a decrease in activity over time because the side-products do not bind to the active site. Since the rate of binding and release of

ligands correlates to the extent to which the ligand mimics a reaction intermediate or substrate, measuring the interaction of different ligands with Rubisco also provides information about the active site geometry. While some forms of the enzyme bind inhibitors very tightly, other forms are very loosely inhibited. Similarly, while some inhibitors bind very tightly to the enzyme, others only form loose associations.

The catalytic chemistry and ligand interactions reveal the important relationship between enzyme structure and function. Reducing the structural rigidity of the active site increases the tendency for side-reactions, because the reaction intermediates are not well stabilised in the active site. Increased flexibility of the active site also reduces the tightness of ligand binding, due to a higher tendency for conformational change. Higher plants have a Rubisco enzyme with a tight active site; however this can be loosened by mutations. Rubisco from other groups may have a tighter or looser active site, and thus altered kinetic parameters that must be taken into account when modelling how different enzymes function.

Table of Contents

List of Figures

5 CONTINUOUS MEASUREMENT OF SIDE- AND PARTIAL- REACTIONS

6 INTERACTION OF RUBISCO WITH LIGANDS

List of Tables

Abbreviations and Notations

ATP	adenosine triphosphate
ATPase	enzyme that carries out ATP hydrolysis
Carboxyarabinitol-1-P	2'-carboxy-D-arabinitol-1-phosphate
Carboxyarabinitol-P_2	2'-carboxy-D-arabinitol-1,5-bisphosphate
Carboxyketone	2-carboxy-3-keto-D-arabinitol-1,5-bisphosphate
Carboxytetritol-P_2	2'-carboxytetritol-1,5-bisphosphate
CBB cycle	Calvin-Benson-Bassham cycle
Deoxy-pentodiulose-P	1-deoxy-D-glycero-2,3-pentodiulose-5-phosphate
Dihydroxyacetone-P	dihydroxyacetone-3-phophate
DNA	deoxyribonucleic acid
DTT	dithiothreitol
E	uncarbamylated enzyme
E. coli	*Escherichia coli*
E:ribulose-P_2	complex between E and ribulose-P_2
E:xylulose-P_2	complex between E and xylulose-P_2
ECM	carbamylated enzyme with coordinated Mg^{2+}
ECM:carboxyarabinitol-1-P	complex between ECM and carboxyarabinitol-1-P
ECM:carboxyarabinitol-P_2	complex between ECM and carboxyarabinitol-P_2
EDTA	ethylenediamine tetra-acetic acid
EI	loose complex between enzyme and inhibitor
EI*	tight complex between enzyme and inhibitor
EPPS	4-(2-hydroxyethyl)-1-piperazinepropanesulphonic acid
FPLC	fast performance liquid chromatography
G. sulphuraria	*Galdieria sulphuraria*
Glycolaldehyde-P	glycolaldehyde-2-phosphate
His-*Rubrum*	*R. rubrum* Rubisco with an N-terminal His tag

HPLC	high performance liquid chromatography
IPTG	isopropyl-β-D-thiogalactopyranoside
k_1, k_2	rate constants for rapid inhibitor binding
k_3	rate constant for slow tight inhibitor binding
k_4	rate constant for slow tight inhibitor release
K_{app}	observed Michaelis constant
keto-arabinitol-P_2	3-keto-D-arabinitol-1,5-bisphosphate
keto-ribitol-P_2	3-keto-D-ribitol-1,5-bisphosphate
K_i	inhibition constant
K_m	Michaelis constant
k_{obs}	observed first order rate constant
LSU	large subunit of Rubisco
M_r	molecular weight
NAD^+	nicotinamide adenine dinucleotide (oxidised form)
NADH	nicotinamide adenine dinucleotide (reduced form)
NaP_i	mixture of NaH_2PO_4 and Na_2HPO_4
Ni-NTA	nickel-nitrilotriacetic acid
NMWL	nominal molecular weight limit
PCO cycle	photorespiratory carbon oxidation
PEG_{3350}	polyethylene glycol, molecular weight 3,350 $g.mol^{-1}$
peroxyketone	2-peroxy-3-keto-D-arabinitol-1,5-bisphosphate
P-glycerate	3-phospho-D-glycerate
P-glycolate	2-phosphoglycolate
PMSF	phenyl-methylsulphonyl-fluoride
R. rubrum	*Rhodospirillum rubrum*
*rbc*L	gene encoding the Form I Rubisco large subunit
*rbc*M	gene encoding the Form II Rubisco large subunit

*rbc*S	gene encoding the Rubisco small subunit
Ribulose-P_2	D-ribulose-1,5-bisphosphate
Rubisco	ribulose-P_2 carboxylase/oxygenase
SDS	Na dodecyl sulphate
SSU	small subunit of Rubisco
v_f	final steady-state rate
v_i	initial rate
Xylulose-P_2	D-xylulose-1,5-bisphosphate
τ	specificity factor

Sequence numbering is shown according to the spinach Rubisco sequence, with the corresponding *R. rubrum* sequence number shown in parenthesis where appropriate. An alignment of some sequences is shown in Hudson et al. (1990).

Mutated residues are indicated by the single letter code of the wild-type residue followed by the sequence number and the single letter code of the mutant residue (e.g. L335V has valine instead of leucine at position 335).

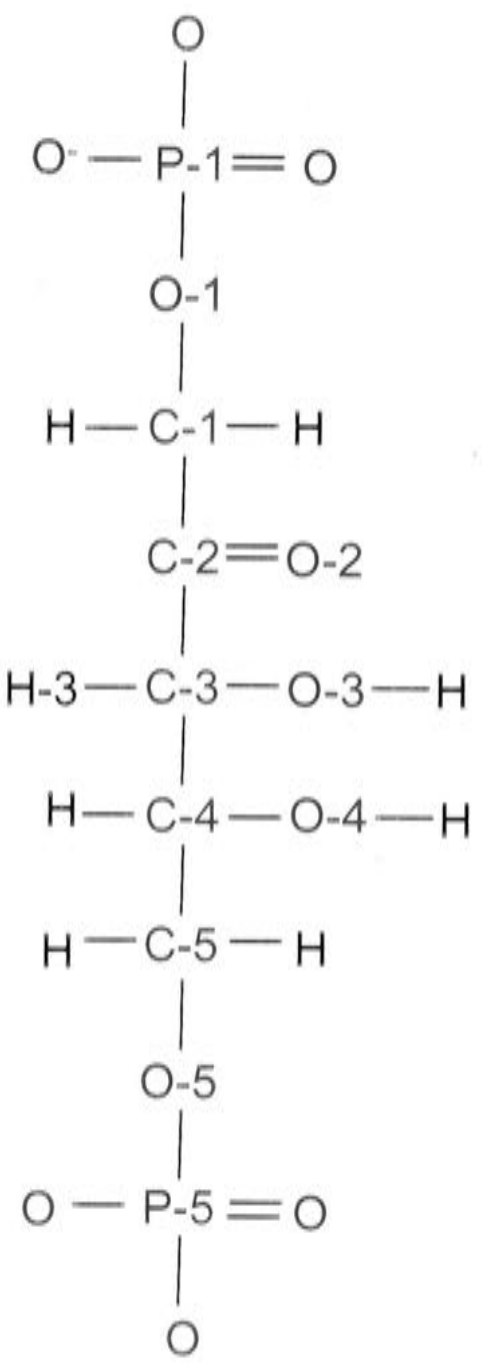

Figure 0.1. The Structure and Labelling of Ribulose-P_2

Ribulose-P_2 is a five-carbon sugar phosphate that is the substrate of Rubisco. Atoms that will be specifically referred to are labelled above, with carbon atoms shown in blue, oxygen atoms shown in red, and phosphate atoms shown in green.

1 Introduction

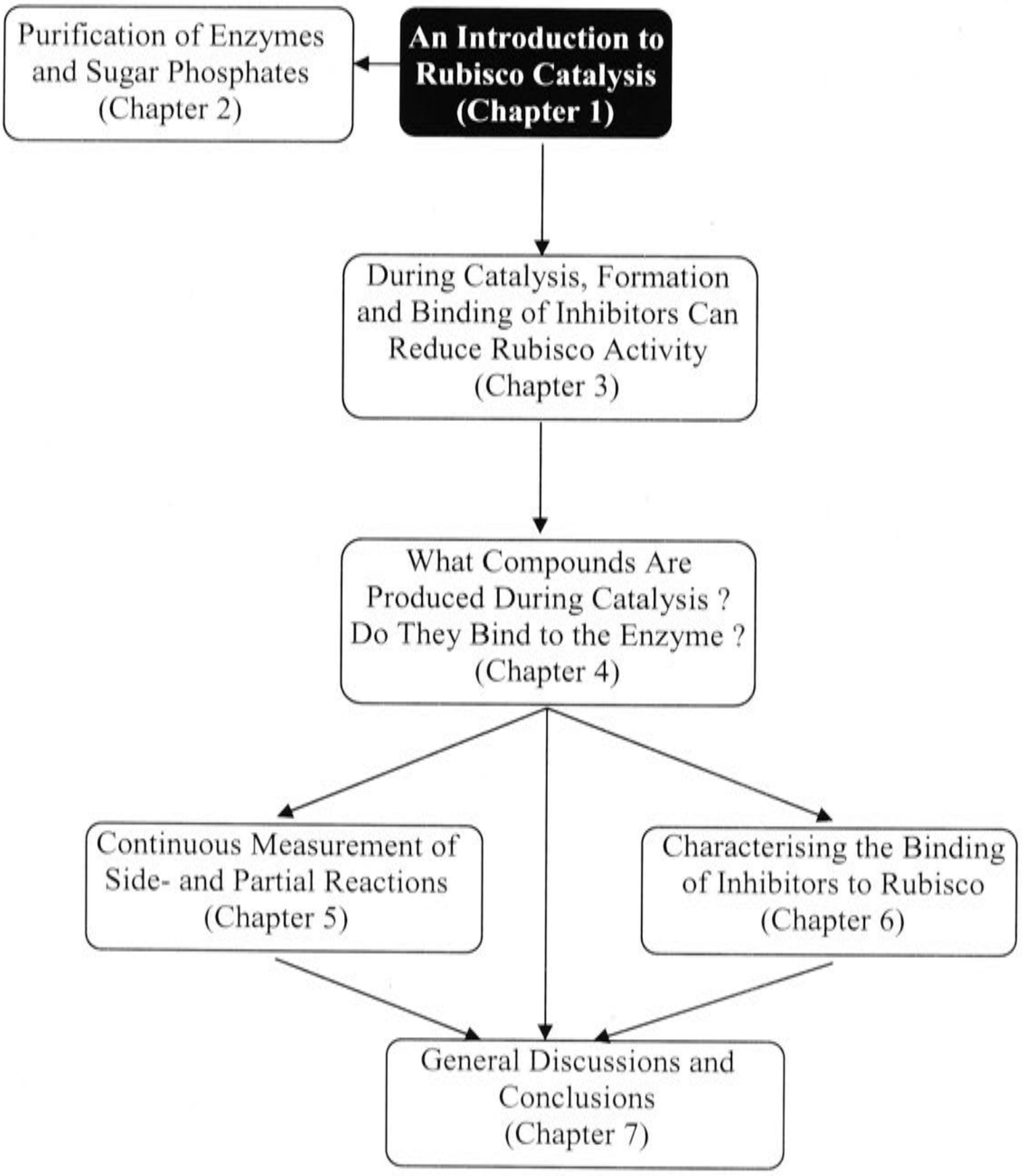

1.1 Historical Perspective

Nearly all of the carbon atoms that are present in living organisms have passed through the active site of the enzyme ribulose-P_2 carboxylase/oxygenase (Rubisco EC 4.1.39). It is responsible for nearly all of the conversion of inorganic CO_2 into organic carbon, and is probably the most abundant protein in the world (Ellis 1979).

Elucidation of the Calvin-Benson-Bassham cycle described each of the steps involved in the fixation of CO_2 during photosynthesis (Calvin and Benson 1948), and further studies identified an enzyme that catalysed the carboxylation of ribulose-P_2, a five-carbon sugar, to produce two molecules of P-glycerate, a three-carbon sugar acid (Weissbach et al. 1954). This work coincided with the observation of the 'Fraction 1' protein, which could be extracted from spinach as 50 % of the soluble leaf protein. The identity of the 'Fraction 1' protein as the ribulose-P_2 carboxylating enzyme was confirmed (Dorner et al. 1957), and it was named 'carboxydismutase'.

Throughout the 50's and 60's, research focussed on the purification and catalytic characterisation of the enzyme, which involved the observation that O_2 was a competitive inhibitor with respect to CO_2. In the early 1970's, it was discovered that the carboxydismutase enzyme could actually catalyse the oxygenation of ribulose-P_2 to form P-glycolate, a two-carbon sugar acid, in the first step of the photorespiratory pathway (Ogren and Bowes 1971). Hence the acronym 'Rubisco' was first used at a symposium in 1979, to encapsulate *r*ib*u*lose-*bis*phosphate *c*arboxylase/*o*xygenase.

Following the discovery of the competing oxygenase reaction, many studies focussed on finding or engineering Rubisco enzymes that could discriminate accurately between CO_2 and O_2. It was discovered that there was natural variation in the carboxylase/oxygenase ratios of Rubisco enzymes from different classes of organisms, with all higher plants having a similar ratio. The possibility of improving the efficiency of Rubisco gained momentum in the 1980's, using the developing fields of X-ray crystallographic studies and site-directed mutagenesis of bacterial Rubisco enzymes. It was hoped that the crystal structures of different Rubisco enzymes would provide an insight into the reasons for the kinetic differences, thereby giving greater direction to mutagenic strategies of modifying the active site configuration. Unfortunately, despite difference in the primary amino acid structure, nearly every Rubisco structure solved so far has an active site that can be superimposed over the other enzymes, indicating that the structural differences that impose the variation in catalytic chemistry between

Rubisco enzymes are not the consequence of gross structural differences in the active site (Andersson and Taylor 2003).

Mutation of the Rubisco enzyme has aimed to establish the functional importance of many different residues in the enzyme, and to improve the ability of the enzyme to distinguish between CO_2 and O_2. Traditionally, comprehensive biochemical characterisations of the mutated Rubisco enzymes were undertaken, enabling a more comprehensive understanding of the catalytic chemistry in the active site and confirming the role of different residues in catalysis. Unfortunately, few of the current mutational studies involve full characterisations, and tend to concentrate only on measuring the catalytic rate and substrate specificity.

Although the goal of mutational studies has been to improve the efficiency of Rubisco, nearly all results so far have produced an enzyme that is less efficient. It is most likely that any improvement of kinetic parameters will be due to a synergistic approach, in which several different changes are required simultaneously, rather than any one substitution being responsible. What seems to be overlooked in recent years is that modified and different Rubisco enzymes provide material to improve our understanding of the enzyme, and unravel the consequences that subtle changes to the active site geometry can have on the catalytic chemistry of the enzyme.

Over the last decade, the tools for modifying Rubisco in higher plants have become more sophisticated, such that it is now feasible to mutate the higher plant enzyme, modifying the amount of enzyme expressed and transplanting foreign Rubisco enzymes to supplement and even replace the endogenous form. The substitution of Rubisco in higher plants has shown that the photosynthetic characteristics of the whole plant reflects the kinetic parameters of the enzyme (Whitney et al. 1999), therefore it is vital to have a detailed understanding of how the enzyme works. Recent work has also uncovered the realisation that higher plant Rubisco enzymes are by no means the pinnacle of evolution. The Rubisco enzyme from a variety of red algae have kinetic properties that outperform the higher plant enzyme, and provide an irresistible opportunity for transplantation into higher plant chloroplasts.

There is a lot of information to be learnt from the comparison of modified and different Rubisco enzymes, and the goal of this thesis is to take a comprehensive look at the catalytic chemistry and ligand interactions of some naturally occurring classes of Rubisco, as well as how the parameters for the higher plant enzyme can be influenced by mutation. This increased understanding of how subtle changes in the active site

influence the catalytic chemistry of the enzyme will have ramifications for the future work involved in the rational design or selection of Rubisco enzymes, with the long term goal of improving the efficiency of photosynthesis in crop plants, and thus increasing the level of sustainability.

1.2 Rubisco Function

As previously mentioned, Rubisco is a key component of the CBB cycle, and catalyses the carboxylation of ribulose-P_2. In the CBB cycle, ribulose-P_2, a five-carbon sugar, is carboxylated with CO_2 from the atmosphere to produce two three-carbon carboxylic acids. These carboxylic acids are then reduced to form a carbohydrate, with some being used to regenerate ribulose-P_2 to accept more CO_2 (Figure 1.1).

In addition to carboxylation, Rubisco is also able to catalyse the oxygenation of ribulose-P_2 to form a 3-carbon sugar acid and a 2-carbon sugar acid. This process is the primary reaction in the photorespiratory carbon oxidation (PCO) cycle (Figure 1.1). Photorespiration involves the recovery of a 3-carbon sugar from the 2-carbon sugar, but is expensive in terms of energy and reducing power, and involves the loss of CO_2.

In higher plants, CO_2 and O_2 enter the leaf through pores on the leaf called stomata, through which water vapour is also lost. When the stomatal aperture is reduced during times of water stress, the CO_2 concentration in the leaf becomes limiting resulting in increased photorespiration. A more efficient and selective Rubisco enzyme could sustain CO_2 fixation at a lower internal CO_2 concentration, permitting smaller stomatal apertures in increasing the water use efficiency.

It is possible that the oxygenase activity of the enzyme is important when the plant is under stress. If there is high intensity but low CO_2 levels, the light reactions will still produce ATP and reducing power. The oxygenase reaction uses oxygen that is liberated from the light reactions, and may be a way of dissipating the excess energy to prevent damage to the components of the light reactions.

The level of photorespiration depends on the ratio of carboxylation to oxygenation rates and the relative concentrations of O_2 and CO_2 in the Rubisco environment. Organisms such as higher plants have developed strategies that compensate for photorespiration by having a higher tendency to carry out carboxylation rather than oxygenation. Other organisms, including cyanobacteria and algae, use a CO_2 concentrating mechanism to increase the concentration of CO_2 relative to O_2 in close proximity to Rubisco. This strategy is also used by some higher plants, including many

tropical grasses, in which the Rubisco enzyme is located in the interior of the leaf, away from the higher concentration of oxygen. CO_2 is transported to the inner part of the leaf by a C4 carbon assimilation cycle, in which phosphoenolpyruvate, a three-carbon compound, is carboxylated to form the four-carbon compound oxaloacetic acid, which may be reduced to form malate or aspartate. The four-carbon compound is transported to the inner cells, where Rubisco is localised, and decarboxylated to form CO_2 and pyruvate, a three-carbon compound, which is returned to the outer cells. This process is energy-expensive, in that transport of each CO_2 requires 2 ATP molecules, but is compensated for by the reduced proportion of oxygenase activity carried out by the Rubisco enzyme.

The proficiency of Rubisco is also limited by its low catalytic efficiency. The substrate-saturated rate is very slow compared to other enzymes, and the ratio of catalytic rate to substrate affinity is also low. As a result, organisms have to invest vast amounts of protein (up to 50 % of soluble leaf protein) in order to compensate for this inefficiency.

If the process of photosynthesis could be made more efficient, the requirements of higher plants for water, nutrients and sunlight could be reduced. Plants currently need to invest much protein into Rubisco due to its slow catalytic rate. Increasing the catalytic rate would reduce the amount of Rubisco enzyme that needs to be produced, and would improve the nitrogen efficiency of the plant. Reducing the tendency of Rubisco to carry out the oxygenation reaction would decrease the amount of energy that is lost through photorespiration, and so lessen the requirement of the plant for energy from sunlight. By increasing the efficiency with which Rubisco uses CO_2, the loss of water fom the plant would be reduced by reducing the stomatal aperture, reducing the requirements of the plant for water.

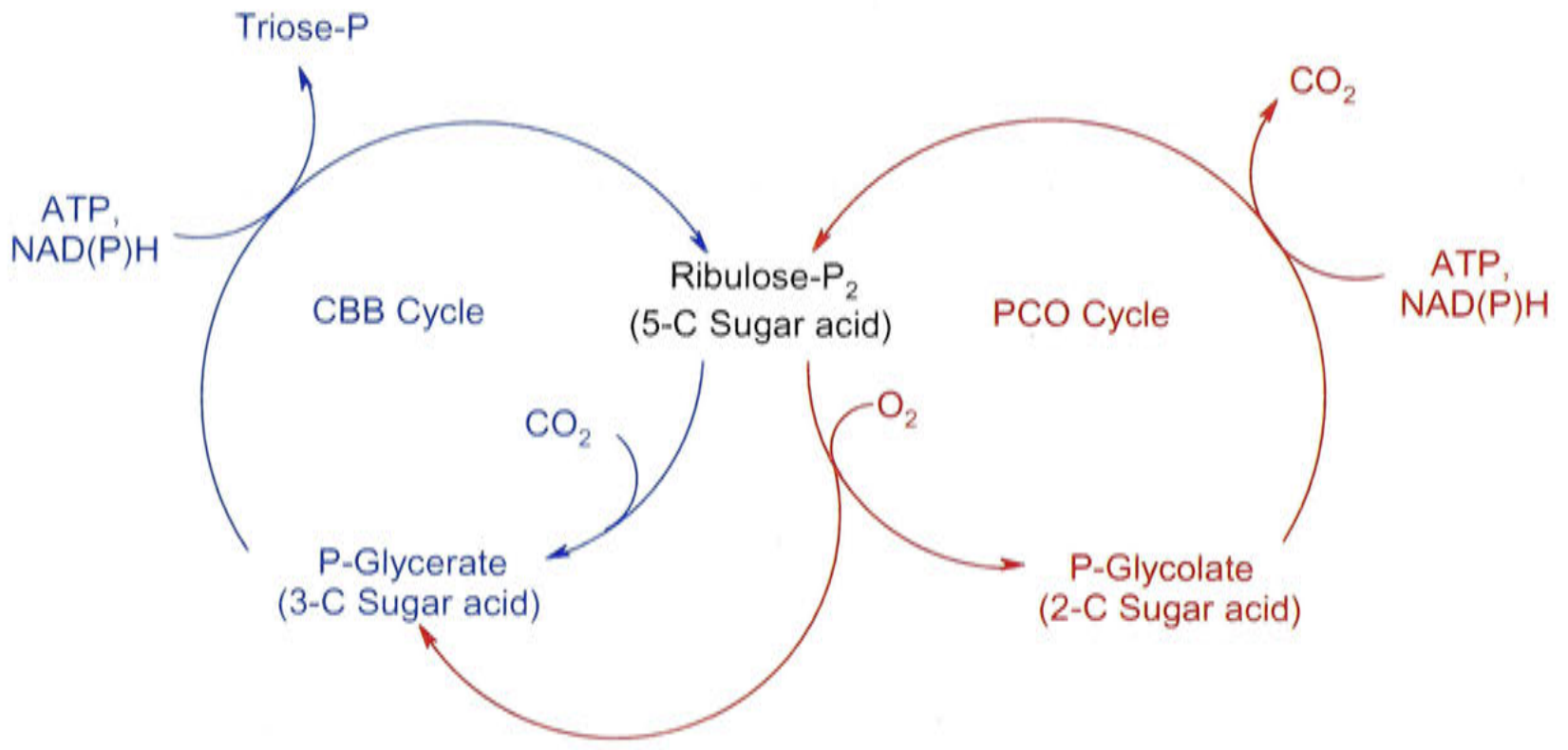

Figure 1.1 Carboxylation and Oxygenation of Ribulose-P_2.

Rubisco can catalyse the carboxylation and oxygenation of ribulose-P_2. Carboxylation produces P-glycerate, which enters the CBB Cycle (shown in blue), and produces triose-phosphates that can be used to produce sucrose and starch. Oxygenation produces P-glycerate and P-glycolate. The P-glycolate enters the PCO cycle (shown in red), which requires energy and releases CO_2 in the process of regenerating ribulose-P_2.

1.3 Rubisco Structure

1.3.1 Introduction

The initial characterisation of Rubisco showed that there were differences in the kinetic parameters of the enzyme from different classes of organisms, and further studies attempted to identify the differences in enzyme structure that are responsible for the variation in enzyme activity. Much of the early research compared the amino acid sequences of different enzymes, which was soon followed by the elucidation of X-ray crystallographic data. Through the recent developments in genome mapping, there is a wealth of information available, with more than 15,000 different Rubisco nucleotide sequences included in the GenBank database alone. Increased computational power has also aided in solving crystallographic data, and there are currently more than 25 different X-ray crystal structures for Rubisco from a range of organisms available from the Protein Data Bank, up to a resolution of 1.6 Å. However, while the primary amino acid sequences can differ greatly between different classes of organisms, the structure of the enzyme is highly conserved.

1.3.2 Rubisco Phylogeny

Rubisco from higher plants, cyanobacteria and algae is a large enzyme, composed of a combination of large (55 kDa) and small (15 kDa) subunits. The resulting Rubisco holoenzyme is a hexadecamer composed of eight large and eight small subunits, which is referred to as Form I Rubisco. Some prokaryotes and dinoflagellates have a Form II Rubisco consisting of large subunits only (Whitney et al. 1995), which may be arranged as a dimer with different degrees of oligimerisation.

Phylogenetic trees constructed using Rubisco large subunit amino acid sequences show distinct divisions between Rubisco enzymes from different species, as shown in Figure 1.2 (Delwiche and Palmer 1996; Watson and Tabita 1997; Tabita 1999). One of the main differences is between Form I Rubisco, which has both small and large subunits, and Form II Rubisco, which has only large subunits. Form I Rubisco enzymes can be further divided into two major types, 'green-like' and 'red-like'. 'Green-like' Rubisco subdivides into a group from cyanobacteria and plants, and a group from purple bacteria. 'Red-like' Rubisco also subdivides into a group from purple bacteria and a group from non-green algae. However the α, β and γ-proteobacteria are divided between the red and green classes, and the phylogenies differ from those constructed

using other genes. This is consistent with multiple occurrences of horizontal gene transfer and gene duplication (Delwiche and Palmer 1996).

Some archaebacteria also contain Rubisco sequences, termed Form III Rubisco, due to their differences in sequence from Form I and Form II enzyme sequences. Only the enzyme from *Thermococcus* (previously *Pyrococcus*) *kodakaraenis* has been purified and characterised (Ezaki et al. 1999). Like Form II Rubisco, these enzymes lack small subunits, but the large subunit dimers are arranged in a $(LSU_2)_5$ decameric structure (Kitano et al. 2001). This arrangement appears to allow for high thermostability (Maeda et al. 2002), but the physiological role of the enzyme is unknown, because as yet, no putative ribulose-5-phosphate kinase, which is required for the production of ribulose-P_2, the substrate of Rubisco, has been identified (Ezaki et al. 1999).

Sequences encoding genes with homology to Rubisco have also been identified from the Gram-positive bacterium *Bacillus subtilis* (Kunst et al. 1997), the green-sulphur bacterium *Chlorobium tepidium* (Hanson and Tabita 2001) and the sulphur metabolising archeobacterium *Archeoglobus fulgidus* (Klenk et al. 1997). Because of their differences in sequence from other Rubisco genes, they are termed Form IV Rubisco. These Rubisco enzymes lacked several active site residues, and did not show any ribulose-P_2 dependant CO_2 or O_2 fixation (Hanson and Tabita 2001; Ashida et al. 2003), and are referred to as 'Rubisco-like' proteins. These proteins appear to be involved with sulphur metabolism, as mutants of *C. tepidium* lacking the protein accumulated elemental sulphur globules, due to an inability to oxidise the sulphur (Hanson and Tabita 2001). Further studies showed that the enzyme from *B. subtilis* catalysed a reaction in the methionine salvage pathway (Ashida et al. 2003), and that mutants lacking the enzyme were unable to grow on media which contained methylthioadenosine as the sole sulphur source. Interestingly, replacing the Form IV Rubisco with the Form II Rubisco from *R. rubrum* restored the phenotype, and *in vitro* studies showed that the enzyme was also able to catalyse the methionine salvage reaction.

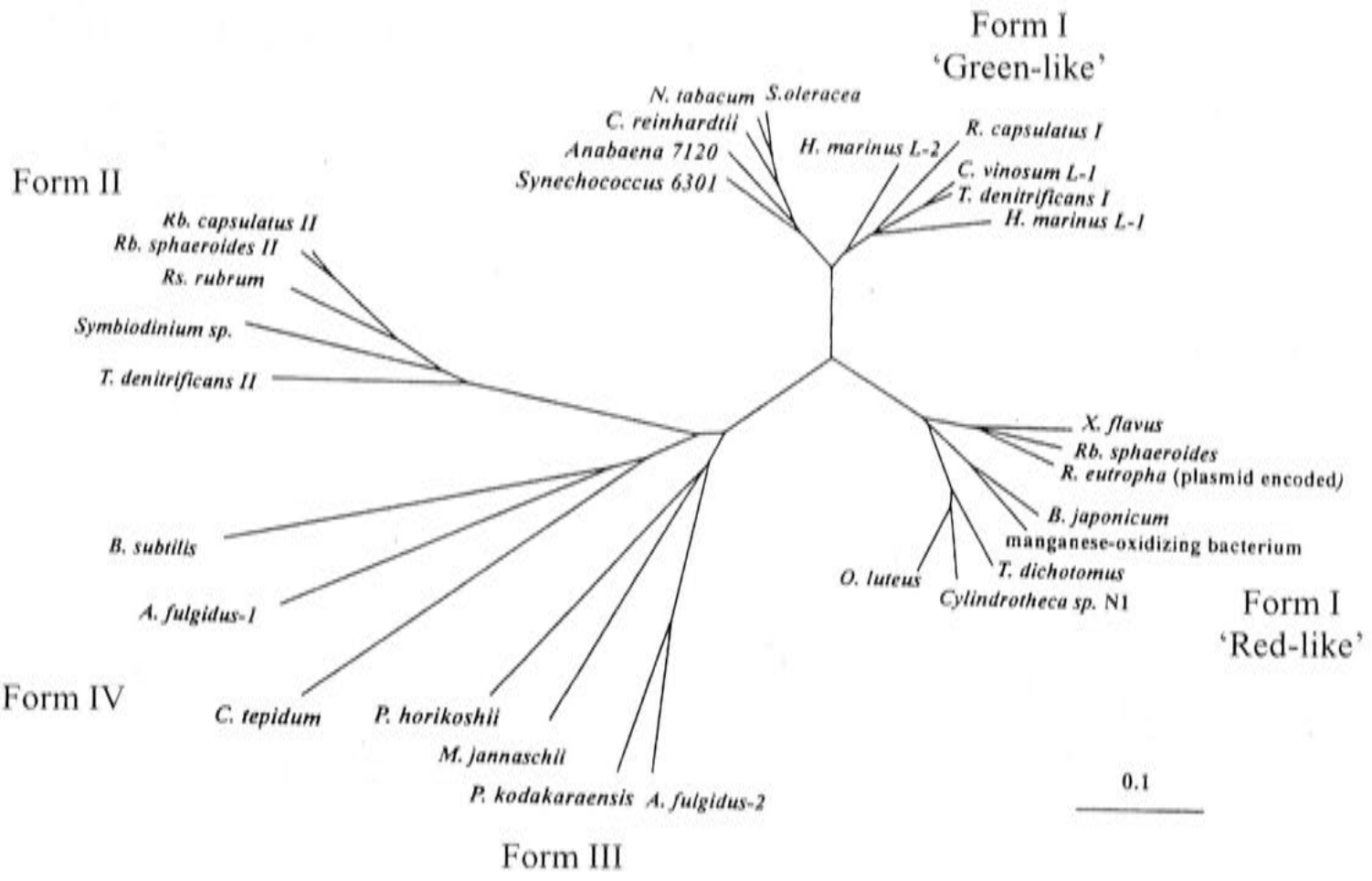

Figure 1.2 Molecular Phylogenetic Tree of Selected Rubisco Large Subunit Amino Acid Sequences (Tabita 1999)

The marker in the lower right corner refers to 0.1 substitutions per site. Form I Rubisco enzymes are divided into a 'green-like' group and a 'red-like' group. The 'green-like' group is further divided into one set containing mostly green plastids and cyanobacteria, and another containing proteobacteria. Similarly the 'red group' is divided into a group of non-green algae, and one of proteobacteria.

Abbreviations: *A. fulgidus, Archaeglobus fulgidus; B. subtilis, Bacillus subtilis; B. japonicum, Bradyrhizobium japonicum; C. tepidium, Chlorobium tepidium; C. reinhardtii, Chlamydomonas reinhardtii; C. vinosum, Chromatium vinosum; H. marinus, Hydrogenovibrio marinus; M. jannaschii, Methanococcus jannaschii; N. tabacum, Nicotiana tabacum; O. luteus, Orconectes luteus; P. horikoshii, Pyrococcus horikoshii; P. kokokaraensis, Pyrococcus kodokaraensis; R. capsulatus, Rhodobactor capsulatus; R. eutropha, Ralstonia eutropha; R. sphaeroides, Rhodobactor sphaeroides; Rs. rubrum, Rhodospirillum rubrum; S. oleracea, Spinacia oleracea; T. denitrificans, Thiobacillus denitrificans; T. dichotomus, Trematocarpus dichotomus; X. flavus, Xanthobactor flavus,*

The observation that these Rubisco-like proteins are involved in sulphur metabolism suggests that the gene for Rubisco enzyme may have a common ancestral gene with an enzyme involved in sulphur metabolism (Ashida et al. 2003). The ancestral enzyme may have been involved in sulphur metabolism, and later evolved an ability to carry out the carboxylation and oxygenation of ribulose-P_2.

1.3.3 Organisation of Rubisco Genes

For Form I Rubisco, the large subunit is encoded by the *rbc*L gene, while the *rbc*S gene encodes the small subunit. In higher plants and green algae, a single copy of the *rbc*L gene is encoded in the chloroplast genome, while the *rbc*S gene is encoded in a nuclear multigene family (Berrylow et al. 1982; Dean et al. 1985). Alternatively, in cyanobacteria, proteobacteria and non-green algae, the *rbc*L and *rbc*S genes are located together as part of the same operon under the control of a single promoter (Shinozaki and Sugiura 1983; Nierzwicki-Bauer et al. 1984). Proteobacteria have a large operon that encodes for many enzymes involved in the CBB cycle. As such the *rbc*L and *rbc*S genes are denoted as *cbb*L and *cbb*S respectively (Tabita 1995). Form II Rubisco only has the large subunit of Rubisco, encoded by the *rbc*M gene (Somerville and Somerville 1984).

1.3.4 Assembly of Large and Small Subunits in Higher Plants

In higher plants, the holoenzyme of Rubisco is located in the chloroplast. As the small subunits are expressed from the nucleus, a transit peptide sequence must be included that targets the polypeptides to the chloroplast. These precursor proteins are imported into the chloroplast through the chloroplast inner and outer translocon complex in an ATP-dependant process. The transit peptide is cleaved by the stromal processing peptidase, and the N^{α}-methylase enzyme methylates the N-terminus α-amino group (Grimm et al. 1997).

After being imported into the chloroplasts and subjected to N-terminal methylation, the small subunits are able to assemble with chloroplast encoded large subunits. The correct folding and assembly of small and large subunits requires interactions with molecular chaperones. The chloroplast chaperones Cpn60 and Cpn21 are similar to the chaperones GroEL and GroES from *E. coli*. Rubisco large subunits associate with Cpn60 prior to assembly into the holoenzyme (Barraclough and Ellis 1980). Studies have shown that relocation of the *rbc*S gene to the chloroplast genome in tobacco is limited by inefficient translation or assembly (Whitney and Andrews 2001a).

Few chloroplast encoded small subunits were assembled into the L_8S_8 complex, possibly because the nuclear encoded small subunits form a complex with the chaperones during translocation into the chloroplast. This gives the translocated small subunits better access to the large subunits that are bound to the chaperones (Whitney and Andrews 2001a).

In higher plants, the Rubisco large subunit undergoes post-translational modification (Houtz and Portis 2003). Trimethylation of the Lys-14 residue is observed in some species, such as tobacco, but not in others, such as spinach (Houtz et al. 1989). Truncation and acetylation of the N-terminal of the large subunit at Pro-3 was observed in all higher plant Rubisco enzymes (Houtz et al. 1992). The reason for these post-translational modifications is currently unknown, but they may be involved in regulating the interactions of the enzyme with other proteins or maintaining the stability of the enzyme.

1.3.5 Expression and Assembly in a Foreign Host

Experimental manipulation of the Rubisco enzyme is often carried out in a foreign host. The *rbc*M gene from *R. rubrum* was the first Rubisco to be expressed and assembled in *E. coli*, resulting in high levels of fully functional enzyme (Somerville and Somerville 1984). This was followed by the expression of active hexadecameric Rubisco genes from prokaryotic organisms such as *Synechococcus* PCC6301 (Gatenby et al. 1985), although as yet, assembly of higher plant Rubisco in *E. coli* has not been attained.

In order to construct a functional enzyme, the subunits must be expressed and assembled into a holoenzyme complex. Expression of foreign Rubisco genes is often impaired in foreign hosts (Whitney and Andrews 2001b), but translation is not usually the limiting step in producing a functional enzyme. Rubisco subunits may have strict requirements for specific chaperones, which must be present in order for assembly to occur.

Form II Rubisco appears to only require a few chaperones to allow assembly of functional Rubisco, and the enzyme from *R. rubrum* can be expressed and assembled in *E. coli* (Somerville and Somerville 1984) or higher plant chloroplasts (Whitney and Andrews 2001b). When the tobacco Rubisco was replaced with that from *R. rubrum*, the growth characteristics of the plant reflected those of the substituted enzyme, which is described further in Section 1.7.3. Cyanobacterial Rubisco enzymes also can be expressed and assembled in *E. coli* to produce a functional enzyme, because the

chaperones that are naturally occurring in the host are sufficient to meet the requirements for folding and assembly (Gibson and Tabita 1986).

The higher plant Rubisco enzymes require chaperones that are not present in *E. coli* or cyanobacteria, therefore while the gene is expressed, no assembly occurs (Gatenby and Castleto 1982). Substitution of the *rbc*L gene in tobacco with the *rbc*L gene from sunflower resulted in the synthesis and assembly of sunflower large subunits in tobacco chloroplasts, because the chaperones are similar in higher plants (Kanevski et al. 1999). Rubisco from non-green algae are also expressed, but do not assemble in *E. coli*, cyanobacteria or higher plant chloroplasts (Whitney et al. 2001), presumably because they require additional chaperones that are not present.

1.3.6 X-Ray Crystallography Studies

Nearly all of the characteristics of enzymes are dependent on their structure, and X-ray crystallography provides a tool to elucidate the structure of Rubisco. One of the earliest X-ray structures of Rubisco was the enzyme from *R. rubrum* (Schneider et al. 1986a), which showed a dimer of large subunits. Structures of higher plant Rubisco were resolved soon after (Andersson et al. 1989; Knight et al. 1989; Knight et al. 1990), allowing an insight into the organisation of the enzyme. As a hexadecamer, the molecule consists of four L_2 dimers ($(LSU_2)_4$) arranged together with four-fold symmetry (Figure 1.3). The small subunits are arranged into two groups of four subunits ($(SSU_4)_2$) located at the ends of the LSU_2 dimers, with a small subunit located in the gap between adjacent dimers. Each small subunit makes contacts with three large subunits and two other small subunits. In the centre of the molecule there is a solvent channel between the LSU_2 dimers.

In the large subunit there is an N-terminal domain, consisting of residues 1-150, and a larger C-terminal domain, consisting of residues 151-475. The N-terminal domain is made up of a 5-stranded β-sheet with two α-helices on one side, while the C-terminal domain is made up of eight consecutive α/β units that form an α/β barrel structure, with eight β-sheets surrounded by the eight α-helices (Knight et al. 1990). The active site is located at the intra-dimer interface between the C-terminal domain of one subunit, and the N-terminal domain of the second subunit (Figure 1.4).

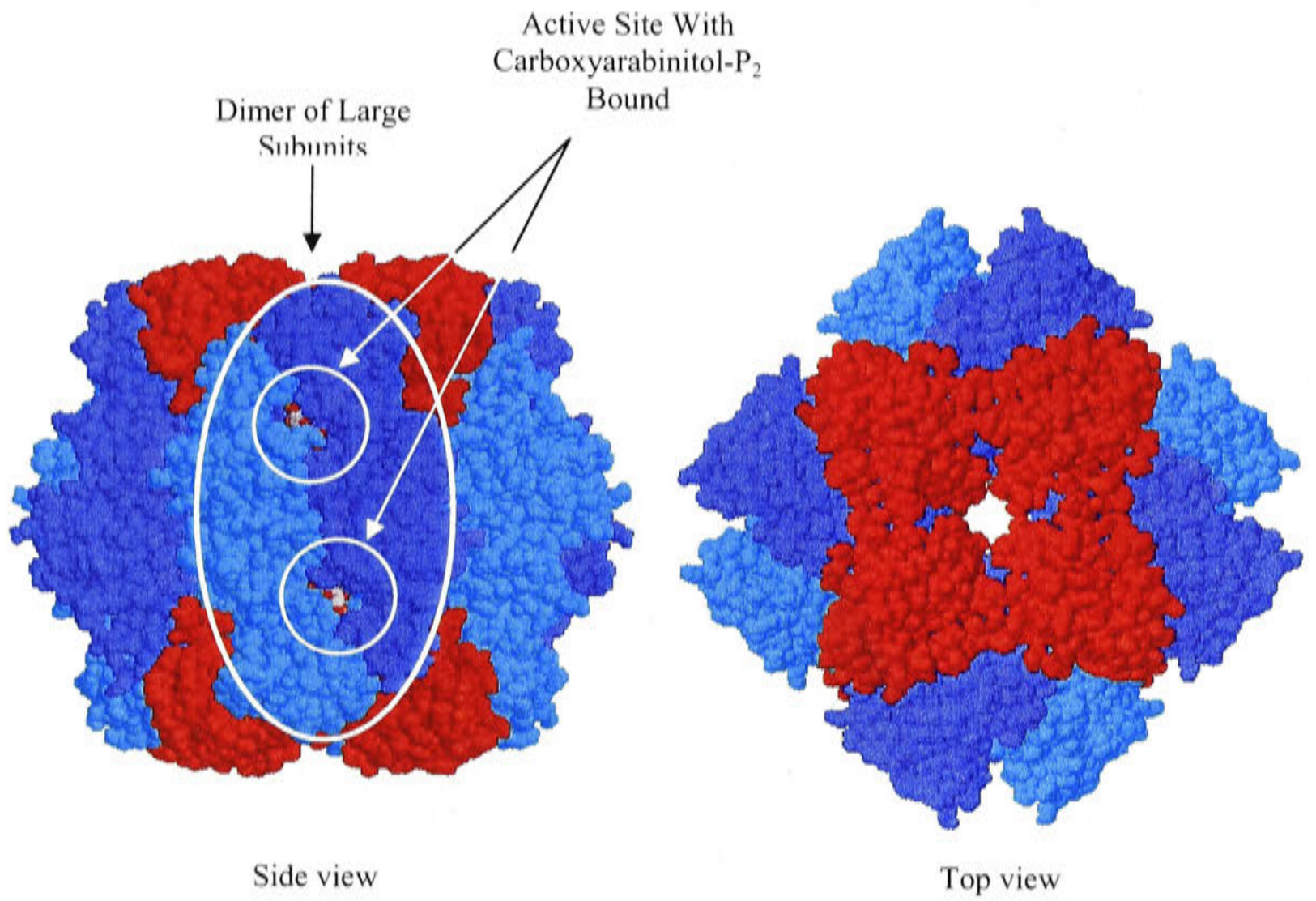

Figure 1.3 Structure of the Rubisco Hexadecamer with Carboxyarabinitol-P_2 Bound

Form I Rubisco consists of small (shown in red) and large (shown in blue and cyan) subunits. The large subunits are arranged as 4 dimers, and 4 small subunits are located at each end of the dimers. The active sites are located at the interface of the dimers. The structure is that of spinach Rubisco complexed with carboxyarabinitol-P_2 (Andersson 1996).

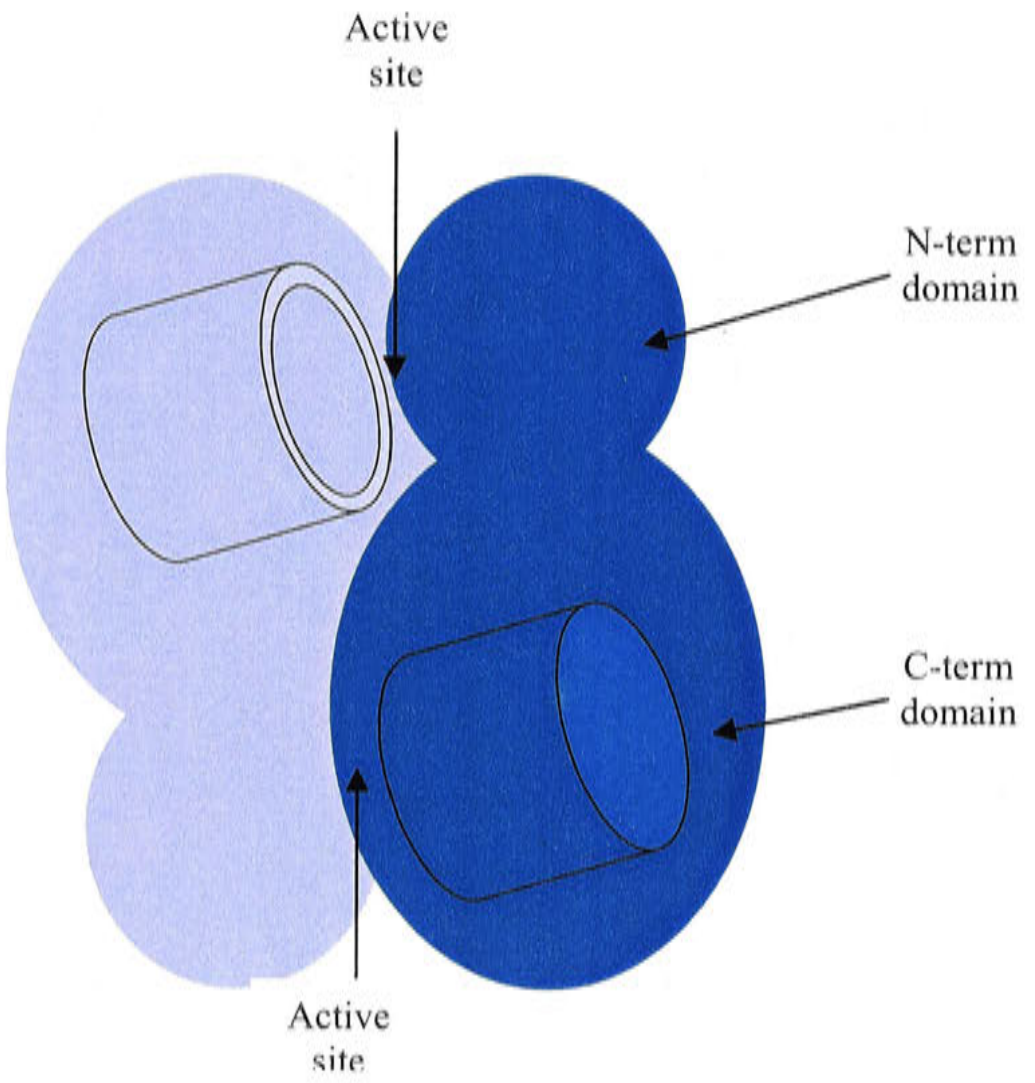

Figure 1.4 Schematic Diagram of the L_2 Dimer

The basic form of Rubisco is a dimer of large subunits. Each subunit is made up of a small N-terminal domain and a larger C-terminal domain. The active site is located at the entrance to an α/β barrel located in the C-terminal domain, and has active site residues contributed by the N-terminal domain of the other subunit.

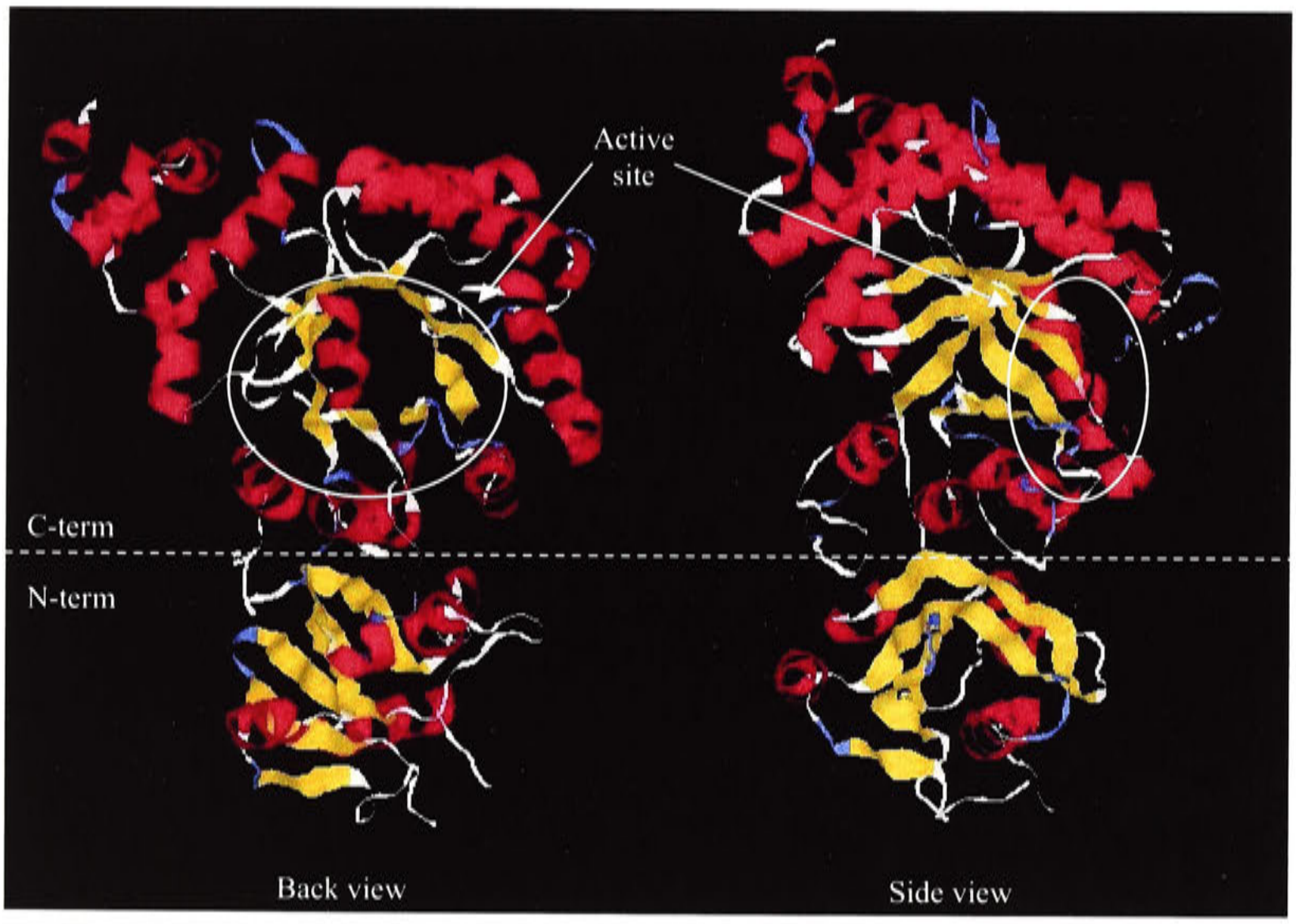

Figure 1.5 Structure of the Rubisco Large Subunit

The Rubisco large subunit consists of the N-terminal domain, which has a β-sheet flanked by α-helices, and the larger C-terminal domain, which contains the active site. The active site is located at the entrance of an 8-stranded α/β barrel. The structure is that of Rubisco from *R. rubrum* (Lundqvist and Schneider 1989b).

Despite only 25% sequence identity between the amino acid sequences of the large subunits of the Form I and Form II enzymes, the folding of the subunit is very similar in all resolved structures, with highly conserved regions in the active site (Knight et al. 1990; Taylor et al. 2001). The N-terminal end of the α/β-barrel is closed by an α-helix, while the active site is located at the C-terminal end as shown in Figure 1.5 (Andersson et al. 1989). Most of the active site residues are located on the loops between the C-terminal of a β-strand and the N-terminal of an α-helix, but there are also residues from two loop regions of the N-terminal domain of the second large subunit in the dimer.

Within the active site there are two phosphate binding sites, which act to bind the sugar phosphate groups during catalysis. The P-1 binding site involves residues from loops 7 and 8 in the C-term, as well as some from the N-terminal of the adjoining subunit. The second phosphate-binding site is made up of residues from loops 5 and 6 of the C-terminal domain (Knight et al. 1990).

A critical residue in the active site is Lys-201, which is located in the middle of the active site, and reacts with CO_2 to form a carbamate, as shown in Figure 1.7 (Lorimer and Miziorko 1980). Mg^{2+} is also be present in the active site, and is essential for catalysis. It is co-ordinated by the carbamylated Lys-201 carboxyl group and the hydroxyl groups of Asp-203 and Glu-204, with the remaining co-ordination sites being occupied by water molecules, or the C-2 and C-3 hydroxyl groups of bound sugar-phosphates (Knight et al. 1990). This is discussed in Section 1.4.2.

In Form I Rubisco, small subunits are arranged at each end of holoenzyme, making interactions with the large subunits. The Rubisco small subunit from higher plants has 123 residues, which are arranged as a four-stranded antiparallel β-sheet with two α-helices on one side (Knight et al. 1989). In higher plants, the two strands β-A and β-B are joined by a long loop (22 residues) which extends into the central solvent channel and forms interactions with two large subunits. Green algae have a longer loop between the β-A and β-B strands (28 residues), which results in a narrowing of the central solvent channel, and increases the interactions (Taylor et al. 2001). Prokaryotes and non-green algae have a much shorter loop with only 10 residues (Newman and Gutteridge 1993), however non-green algae have small subunits with a long C-terminal that has two extra β-strands which also extend into the central solvent channel and form interactions with the large subunits (Sugawara et al. 1999). It is possible that the differences that occur in activity between enzymes from different classes of organism

are due to altered interactions between the loops or termini of the small subunits with the large subunits, which in turn alters the conformation of the active site.

1.3.7 The Structure of Rubisco Bound to Ligands

Further information about the functioning of Rubisco has been provided by X-ray crystallographic structures of Rubisco enzymes complexed with a range of ligands. These include the transition state analogue carboxyarabinitol-P_2 (Newman and Gutteridge 1993; Zhang et al. 1994; Shibata et al. 1996; Taylor et al. 1996; Taylor et al. 2001), the substrate ribulose-P_2 (Lundqvist and Schneider 1991; Taylor and Andersson 1997b), the product P-glycerate (Lundqvist and Schneider 1989a; Taylor and Andersson 1997a), and the inhibitor xylulose-P_2 (Newman and Gutteridge 1994; Taylor et al. 1996).

Carbamylation of Lys-201 and co-ordination of Mg^{2+} to the carbamate causes few conformation changes in the active site (Taylor and Andersson 1996). However, there is a difference between the structures of liganded and non-liganded Rubisco enzymes (Schreuder et al. 1993a). After a ligand has bound to the active site, loop 6 at the C-terminal of the α/β-barrel closes over the active site, making it inaccessible to solvent. This loop, corresponding to residues 333-337 of the large subunit, is normally disordered in the unliganded enzyme, as are residues 464-475 of the C-terminal and residues 1-19 of the N-terminal (Schreuder et al. 1993a; Taylor and Andersson 1996). Closure of loop 6 over the active site is accompanied by the ordering of the C-terminal residues and the N-terminal residues, which hold loop 6 in the closed position. The N-terminal domain of the adjacent large subunit and a small subunit move towards the α/β-barrel, excluding the active site from the bulk solvent, and bringing several residues from loop 6 within binding distance of the ligand where they can participate in catalysis. Closure of loop 6 over the active site is also important in excluding the solvent from the active site of the enzyme. The structure of non-green Rubisco from *Galdieria partita* shows a unique hydrogen bond between the Val-332 residue on loop 6 and Gln-386 of the same large subunit, which may assist in stabilising loop 6 in the closed state (Okano et al. 2002).

Binding of ligands such as ribulose-P_2, xylulose-P_2 and 4-carboxyarabinitol-P_2 to non-carbamylated Rubisco induces closure of loop 6 over the active site. Activated Rubisco that lacks substrate or is bound to P-glycerate has a disordered loop 6, allowing access of the solvent to the active site (Taylor and Andersson 1997a). When Rubisco was carbamylated and coordinated with Ca^{2+}, rather than Mg^{2+}, it was able to bind

ribulose-P_2 but was not able to carry out catalysis. This complex also had loop 6 in the disordered, open state (Taylor and Andersson 1997b). Non-activated Rubisco that is bound to 2-carboxyarabinitol-P_2 has loop 6 in the disordered, open state (Zhang et al. 1994), while the complex between 2-carboxyarabinitol-P_2 and activated Rubisco has loop 6 in the ordered state, closed over the active site (Schreuder et al. 1993b). The only observation of loop closure when there is no bisphosphate compound present is for the structure of *Galdieria partita* enzyme, in which loop 6 of non-activated Rubisco was closed over that active site that had a sulphate ion bound at the P-2 site (Okano et al. 2002).

While the exact trigger for loop closure and opening is unclear, it is possible that the distance between the P-1 and P-2 phosphate initiates loop closure. A comparison of structures showed that if the inter-phosphate distance was less than 9.1 Å then the active site closes, and if the distance is more than 9.4 Å the loop remains open (Duff et al. 2000). Closure of loop 6 over the active is likely to be triggered by the binding of substrate to the active site. The binding causes loop 6, as well as the N-terminal and C-terminal to become ordered, which restricts access of the bulk solvent to the active site and brings several residues closer to the active site, enabling them to participate in catalysis. Closing the active site off from the bulk solvent would assist in stabilising the intermediates of catalysis, and maintaining the correct conformation of the active site. When the reaction is complete, loop 6 is no longer constrained in an ordered state, and becomes disordered, allowing the products of catalysis to be released from the active site. Some inhibitors can trigger the ordering of loop 6 and the N-terminal and C-terminal by mimicking the binding of ribulose-P_2, by binding to either the carbamylated form in the case of carboxyarabinitol-P_2, or to the uncarbamylated form in the case of xylulose-P_2.

1.3.8 Role of the Small Subunits

The sequences and structures of Rubisco small subunits show greater diversity than those of large subunits, suggesting that they may be partly responsible for the differences in kinetic parameters that occur between different Rubisco enzymes from different species. As Form II Rubisco does not have any small subunits, these are apparently not essential for catalysis, and indeed removing the small subunits from the Form I Rubisco of cyanobacterial enzymes reduced, but did not abolish catalysis, showing that they are not crucial for enzyme activity (Andrews 1988; Morell et al. 1997). Each small subunit in the SSU_4 clusters at the ends of the $(LSU_2)_4$ core makes

contacts with two other small subunits and three different large subunits (Knight et al. 1990), indicating that small subunits may also have a role in stabilising the four LSU_2 dimers together.

Small subunits must be able to influence the reaction mechanism by altering the conformation of the active site to alter the reaction mechanism. Removal of small subunits from *Synechococcus* PCC6301 Form I Rubisco greatly reduced the rate of catalysis, but not the ability of the enzyme to distinguish between CO_2 and O_2 as substrates. The activity could be restored by the application of isolated small subunits from separate species, which still did not alter the specificity for CO_2 over O_2 (Andrews 1988). Hybrid enzymes consisting of sunflower Rubisco large subunits and tobacco Rubisco small subunits had a similar specificity to the native tobacco enzyme, but a reduced catalytic rate (Kanevski et al. 1999), confirming that while the small subunits are important for catalysis, they do not appear to have a significant role in influencing Rubisco specificity.

However, there have been some examples in which small subunits have been observed to influence specificity. The hybrid enzyme of large subunits from *Synechococcus* PCC6301 and small subunits from *Cylindrotheca* (a diatom) had an increased specificity relative to the native enzyme from *Synechococcus* PCC6301 (Lee et al. 1991). Rubisco from *Synechococcus* PCC6301 lacking small subunits showed an increased tendency to carry out β-elimination of the enediol intermediate (Morell et al. 1997), demonstrating their importance in stabilising reaction intermediates during catalysis.

The small subunit is likely to influence catalysis through interactions between the small subunit and helix α8 of the large subunit. The position of the α8-helix is different between Form I and Form II Rubisco enzymes, as is the position of loop 8, which has a role in the P-1 binding site (Schneider et al. 1989). In this way, changes in the small subunit shape can influence the conformation of the active site in the large subunit, and subsequently affect the catalytic mechanism.

1.4 The Rubisco Reaction mechanism

1.4.1 Introduction

Models for the reaction mechanism of Rubisco catalysis have been proposed based on the isolation of intermediate compounds formed during catalysis, measuring the consumption of proposed intermediate compounds, using mutational studies to

demonstrate the role of key amino acid residues, and using computational methods to model the reaction. Recent advances in technology have greatly increased the ability to model the reaction mechanism using computational methods (King et al. 1998; Mauser et al. 2001), and these predictions are often confirmed by biochemical methods.

The reaction of Rubisco is ordered, with the substrate ribulose-P_2 binding before the addition of substrate CO_2 or O_2 (Pierce et al. 1986b). Carboxylation and oxygenation of ribulose-P_2 involves a similar sequence of intermediate compounds, as shown in Figure 1.6. Initially ribulose-P_2 is enolised to form an enediol compound, which is then attacked by O_2 or CO_2 to form a peroxyketone or carboxyketone intermediate compound. The ketones are hydrated, before cleavage between C-2 and C-3. In the carboxylation reaction, another step is required to protonate the *aci*-acid. A detailed knowledge of the Rubisco reaction mechanism is vital in establishing how the enzyme structure influences the functioning of the enzyme.

1.4.2 Carbamylation of the Active Site

Initial observations showed that incubating Rubisco with Mg^{2+} and HCO_3^- before assay increased the enzyme activity (Pon et al. 1963; Badger and Andrews 1974; Andrews et al. 1975; Laing and Christeller 1976), due to the binding of CO_2 and Mg^{2+} to the active site. The activating CO_2 that binds within the active site is distinct from the substrate CO_2 (Lorimer 1979), and this binding is the reversible, rate-limiting step before rapid coordination of Mg^{2+} (Lorimer et al. 1976). The activating CO_2 forms a carbamate on the ε amino group of Lys-201 within the active site, as shown in Figure 1.7 (Lorimer 1981), resulting in the conversion of the positively charged lysine side chain into a negatively charged carboxyl group. Mutational substitution of the Lys-201 residue results in an enzyme with no enolisation activity (Gutteridge et al. 1988). One of the carbonyl O atoms coordinates with Mg^{2+}, which is also coordinated by the hydroxyl groups from the neighbouring residues Asp-203 and Glu-204. While some divalent metal ions, such as Mn^{2+} and Fe^{2+} can also bind to Rubisco and support catalysis at a reduced rate, others, including Ca^{2+} and Cu^{2+} showed no activity (Barcena 1983).

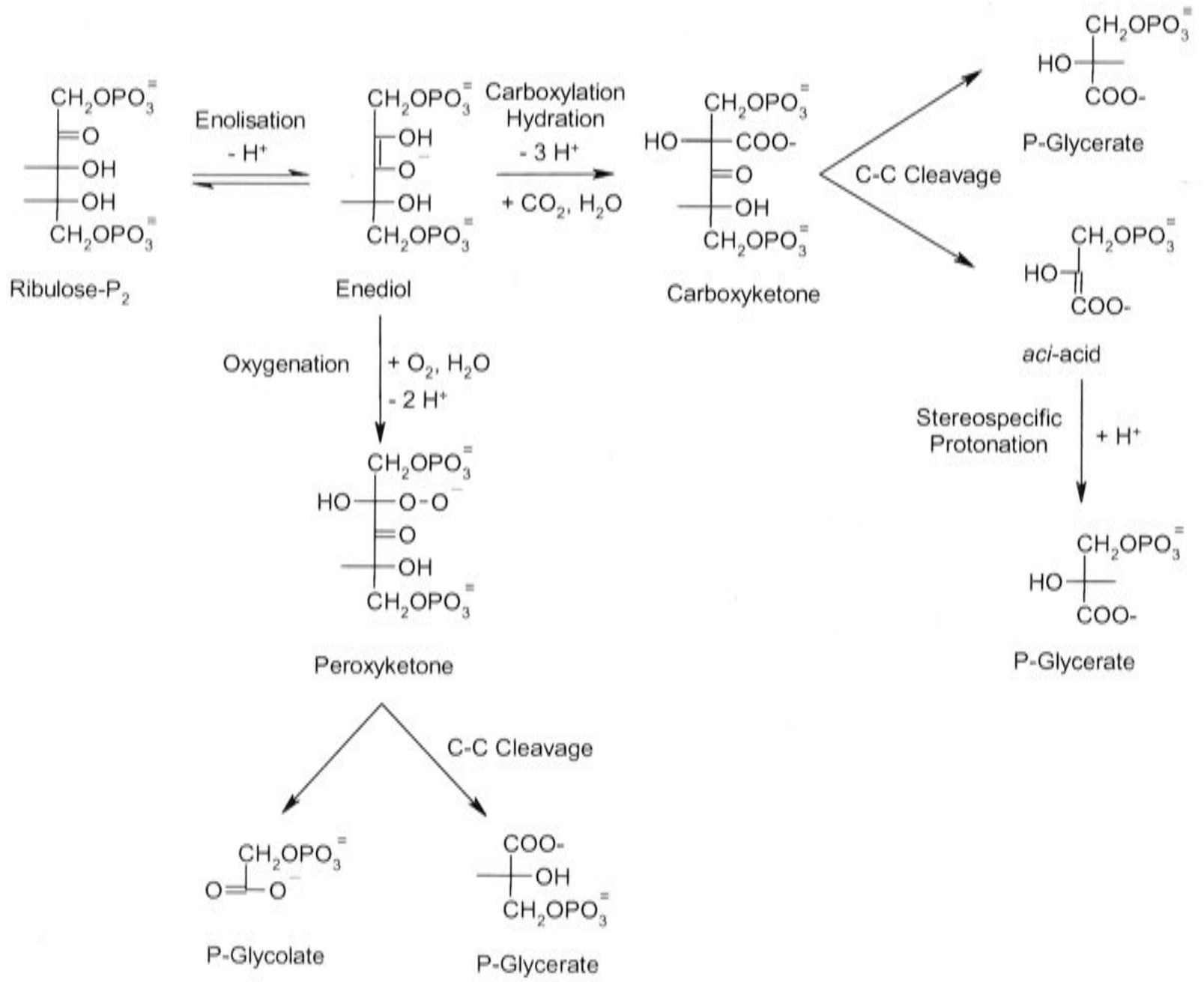

Figure 1.6 Carboxylation and Oxygenation of Ribulose-P_2 by Rubisco

Rubisco catalyses the carboxylation or oxygenation of ribulose-P_2, producing two molecules of P-glycerate or a molecule of P-glycerate and a molecule of P-glycolate respectively. The initial enolisation step is common for both pathways, and is followed by the addition of CO_2 or O_2 to form the carboxyketone or peroxyketone intermediates respectively. C-C cleavage of the carboxyketone yields one molecule of P-glycerate and one molecule of the *aci*-acid, which is protonated to form P-glycerate, while cleavage of the peroxyketone intermediate yields one molecule of P-glycerate and one molecule of P-glycolate.

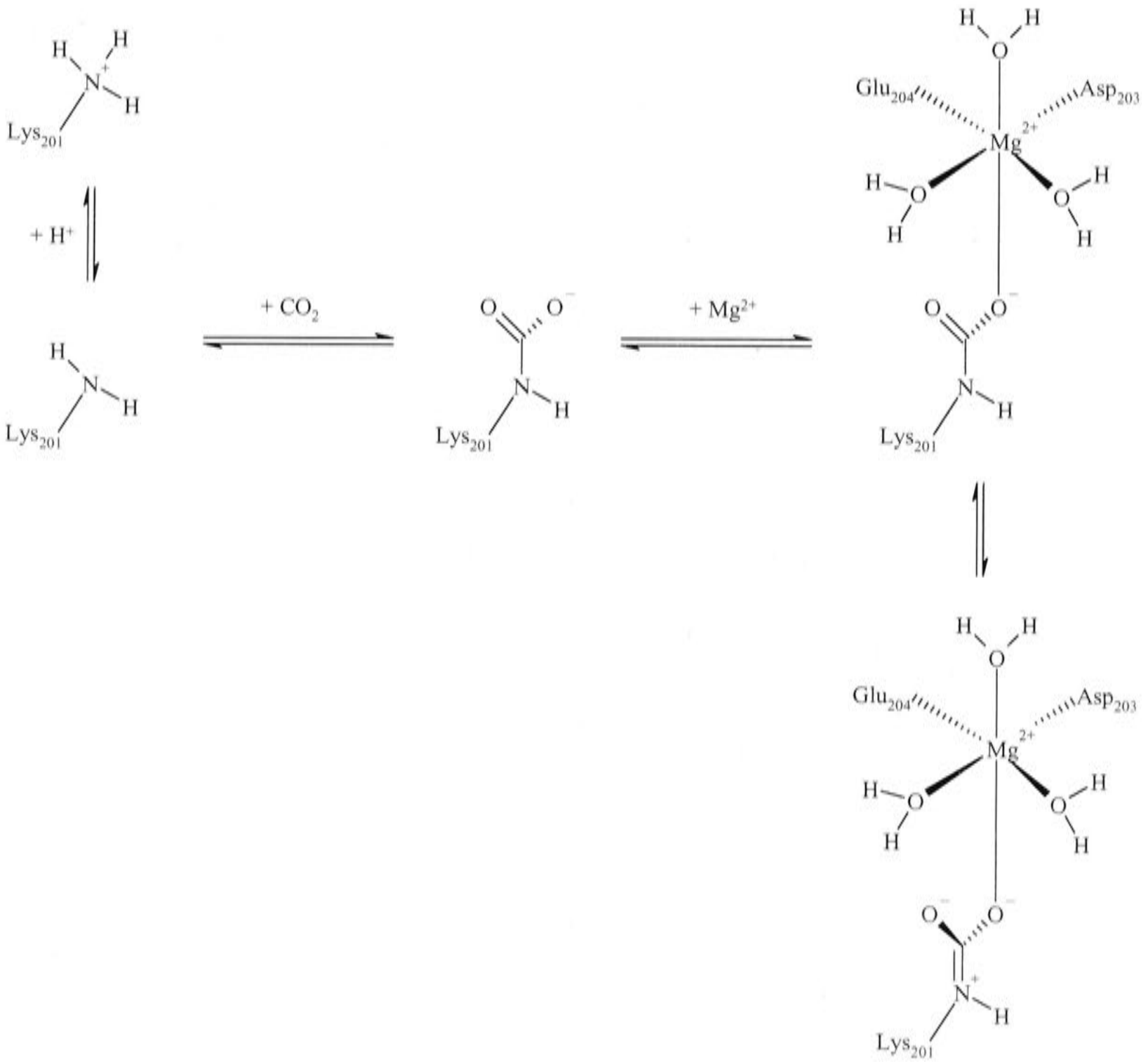

Figure 1.7 Activation of the Active Site

CO_2 forms a carbamate on the ε-N of Lys-201. Along with Glu-204 and Asp-203, the carbamate is involved in the coordination of Mg^{2+}. The other Mg^{2+} coordination sites are occupied by water molecules.

1.4.3 Enolisation of Ribulose-P_2

The first step of catalysis involves the deprotonation of C-3, and protonation of O-2 of ribulose-P_2 (Figure 1.8). Deprotonation of O-3 also assists in the binding of gaseous substrate in the next step. Several possible candidates could act as the base to accept the proton from C-3. Directed mutational studies showed that the Lys-175 residue is essential for enolisation (Hartman et al. 1987; Hartman and Lee 1989) and replacement with other residues caused a significant reduction in enolisation and a subsequent reduction in the general reaction rate. However the position and orientation of Lys-175 does not appear to meet the requirements for it to act to deprotonate C-3 (Roy and Andrews 2000).

The carbamylated Lys-201 residue is appropriately positioned to accept a proton from C-3, with 3.1 Å between C-3 and the uncoordinated carbamate O atom in the Ca^{2+} activated enzyme/ribulose-P_2 and Mg^{2+} activated enzyme/carboxyarabinitol-P_2 structures, which would allow proton abstraction to occur (Andersson 1996; Taylor and Andersson 1997b). There are several residues surrounding the carbamate that could assist in maintaining a double negative charge, including a cluster of histidine residues (His-292, His-294, His-325 and His-327) that could act as a proton sink (Taylor and Andersson 1997b). Therefore it is likely that the deprotonation of C-3 is performed by the carbamylated Lys-201 O atom.

Protonation of the O-2 atom of ribulose-P_2 requires an acidic residue, which is likely to be the ε-amino group of Lys-175. This step could be carried out by the carbamate residue that has been previously protonated (Cleland et al. 1998), however structural studies have shown that Lys-175 is in a suitable orientation to protonate O-2 (Taylor and Andersson 1997b). Mutational studies have confirmed the importance of Lys-175 in catalysis, with substitution of the residue greatly reducing the rate of enolisation (Lorimer and Hartman 1988; Harpel et al. 2002), and computational studies have shown that Lys-175 is likely to be charged before enolisation commences (King et al. 1998).

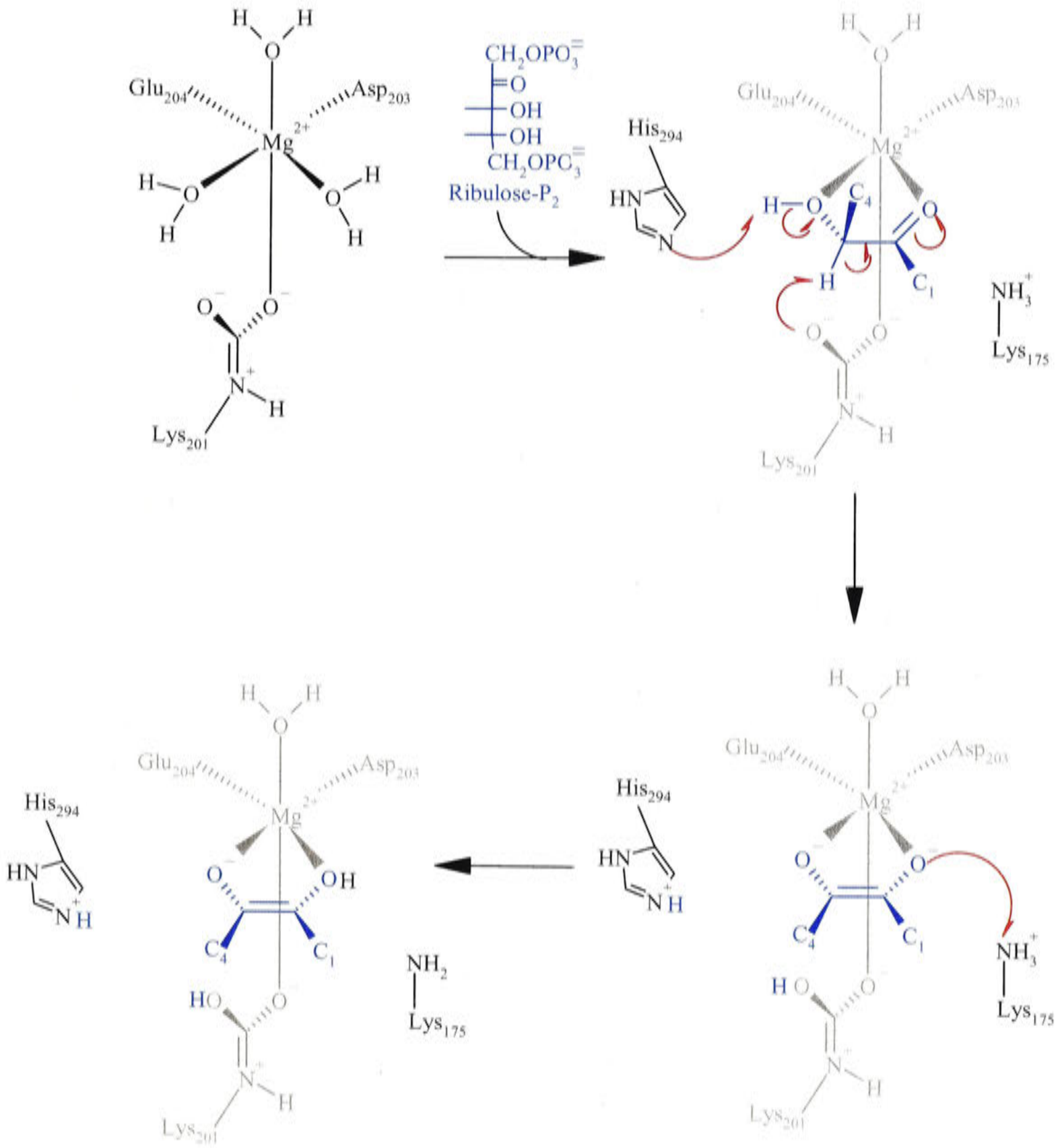

Figure 1.8 Enolisation of Ribulose-P_2

The active site consists of a Mg^{2+} ion coordinated by three water molecule and three amino acid residues, one of which is a carbamylated lysine. Ribulose-P_2 (shown in blue) displaces two water molecules, and is coordinated around the metal ion. A histidine residue is involved in the deprotonation of O-3, while the carbamylated lysine residue accepts a proton from C-3. This proton is then transferred to protonate O-2, resulting in the formation of the enediolate.

To direct the attack of CO_2 to C-2, rather than the otherwise identical C-3, deprotonation of O-3 is required. There is some currently some uncertainty as to the identity of the residue responsible for this abstraction. Structural studies show that the nitrogen of His-294 is 3.1 Å away from O-3 in the activated complex, which is a suitable distance to allow the residue to abstract a proton (Taylor and Andersson 1997b). Mutagenesis of His-294 also prevented catalysis (Harpel et al. 1998), with the mutants being restricted in both enolisation and in processing the intermediate compound carboxy-keto-arabinitol-P_2. Alternatively, the carbamate could be reused for a second proton abstraction, providing it the surrounding environment has been able to act as a proton sink (Mauser et al. 2001).

1.4.4 Addition of Gaseous Substrate

Carboxylation occurs as a result of electrophilic attack of CO_2 at C-2 of the enediolate (Figure 1.9). The electrons from O-3 form a double bond with C-3, followed by the attack on C-2 by CO_2. The positively charged Mg^{2+} and H^+-His-294 are located close to O-3, and can assist it in maintaining a negative charge. The new carboxyl group attached to C-2 also needs to be stabilised. After displacing water, one oxygen of the carboxyl group becomes coordinated to Mg^{2+} and the other oxygen atom forms an interaction with Lys-334 from loop six (Taylor and Andersson 1997b). Computational studies have shown no evidence for the binding of substrate CO_2 or O_2 in the absence of ribulose-P_2 (Mauser et al. 2001).

The product of CO_2 addition to the enediol is the free carbonyl of carboxy-keto-arabinitol-P_2, which is then hydrated. The structure of Rubisco complexed with Ca^{2+} and ribulose-P_2 showed a water molecule located 3.8 Å from C-3 of ribulose-P_2, which can form H-bonds with Gln-401, Ser-379, Thr-173 and the carbamate (Taylor and Andersson 1997b). His-327 is located 3.5 Å from the water molecule and was initially proposed to deprotonate the water molecule. However, substitution of this residue reduced, but did not completely eliminate catalysis or enolisation (Harpel et al. 1991), and it is more likely that the proton is abstracted by the carbamylated residue, which is supported by computational studies (Mauser et al. 2001).

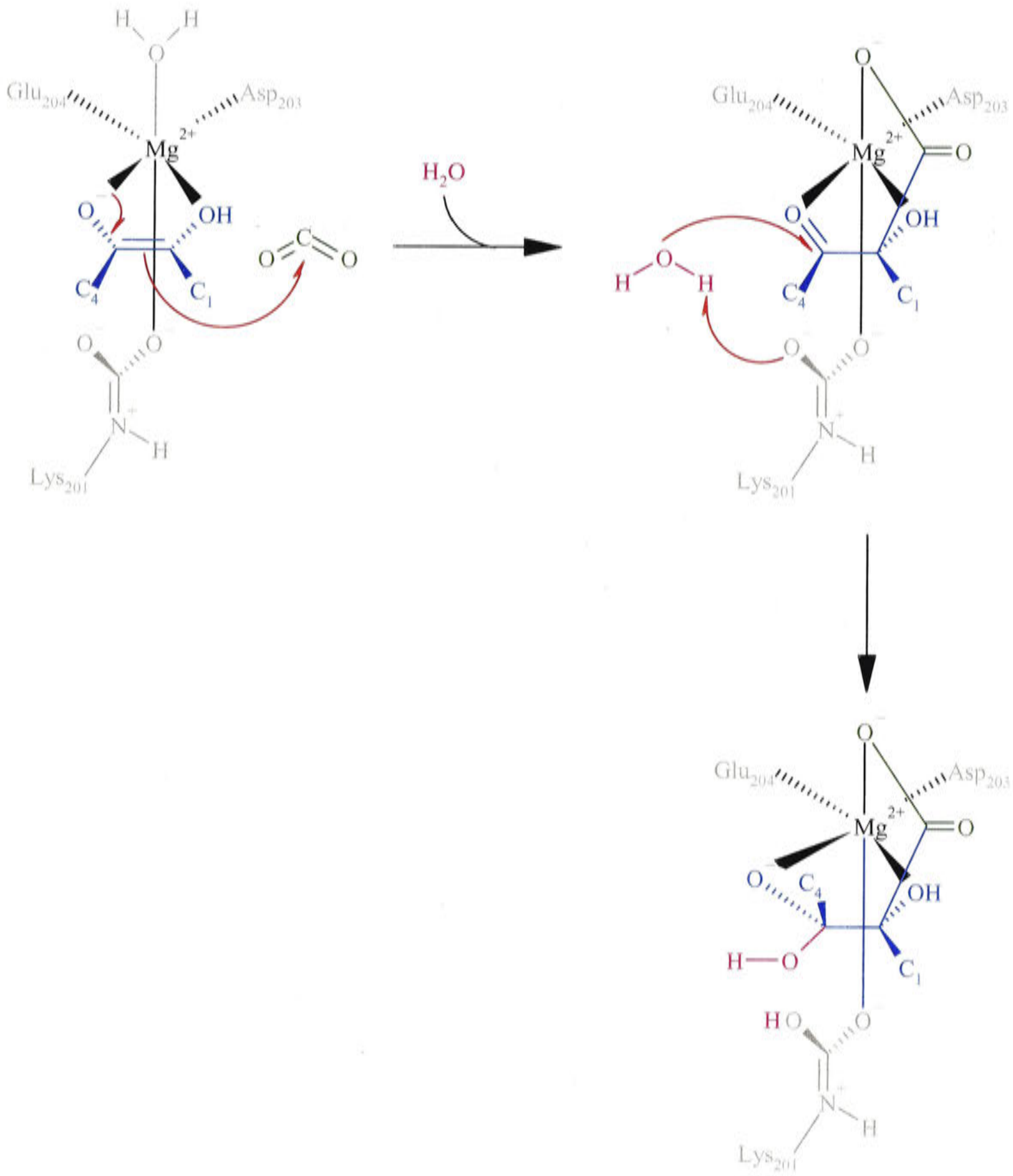

Figure 1.9 Addition of CO_2

Carboxylation of the enediolate involves an electrophilic attack on C-2 by CO_2 (shown in green). This is preceded by the electrons from O-3 forming a double bond with C-3. One oxygen atom of the carboxyl group displaces water and becomes coordinated to the metal ion. A histidine residue deprotonates a water molecule (shown in purple), which then hydrates C-3.

It is not known for certain whether the hydration step occurs simultaneously with gas addition, or if it occurs sequentially, but computational studies have shown that the intermediate transition state would be stable, and supported the addition of CO_2 and H_2O in two discrete steps (Mauser et al. 2001). While applying the free carbonyl form of carboxy-keto-arabinitol-P_2 to Rubisco resulted a very slow production of P-glycerate (Pierce et al. 1986a), suggesting that while Rubisco can catalyse hydration, the free carbonyl may not be a true intermediate, the apparent reduction in catalysis could be due to limitations in the binding of carboxy-keto-arabinitol-P_2 to the active site (Pierce et al. 1980; Pierce et al. 1986a).

1.4.5 C-C Cleavage

Cleavage between C-2 and C-3 of carboxy-keto-arabinitol-P_2 is initiated by the deprotonation of the uncoordinated hydroxyl group attached to C-3, causing the conversion from a *gem*-diol to a carboxylate, and resulting in the deprotonation of both *gem*-diol O atoms (Figure 1.10). One O atom is already deprotonated, and is stabilised in this state by H^+-His-294 and Mg^{2+}. The second O atom points towards the carbamate, which would be able to accept the proton if the previously accepted protons had been transferred away. It is likely that these protons are lost into the network of histidine residues surrounding the carbamate.

1.4.6 Stereospecific Protonation

Cleavage of the C-C bond results in the formation of one molecule of P-glycerate (the 'lower' molecule), and the *aci*-acid form of P-glycerate. While P-glycerate can be released, the *aci*-acid requires protonation on the *Si* face to produce the second, 'upper', P-glycerate molecule (Figure 1.10). The proton donor must be on the opposite side to the carbamate, and structural studies suggest that Lys-175 would be ideally located (Taylor and Andersson 1997b). Mutagenesis studies also show that while Lys-175 mutants are able to process carboxy-keto-arabinitol-P_2 (Lorimer and Hartman 1988), they produce pyruvate instead of P-glycerate (Harpel and Hartman 1996). As this residue has already donated a proton to O-2 during enolisation, the proton may come back from O-2 to C-2 via Lys-175, rather than Lys-175 acting as the ultimate source (Roy and Andrews 2000).

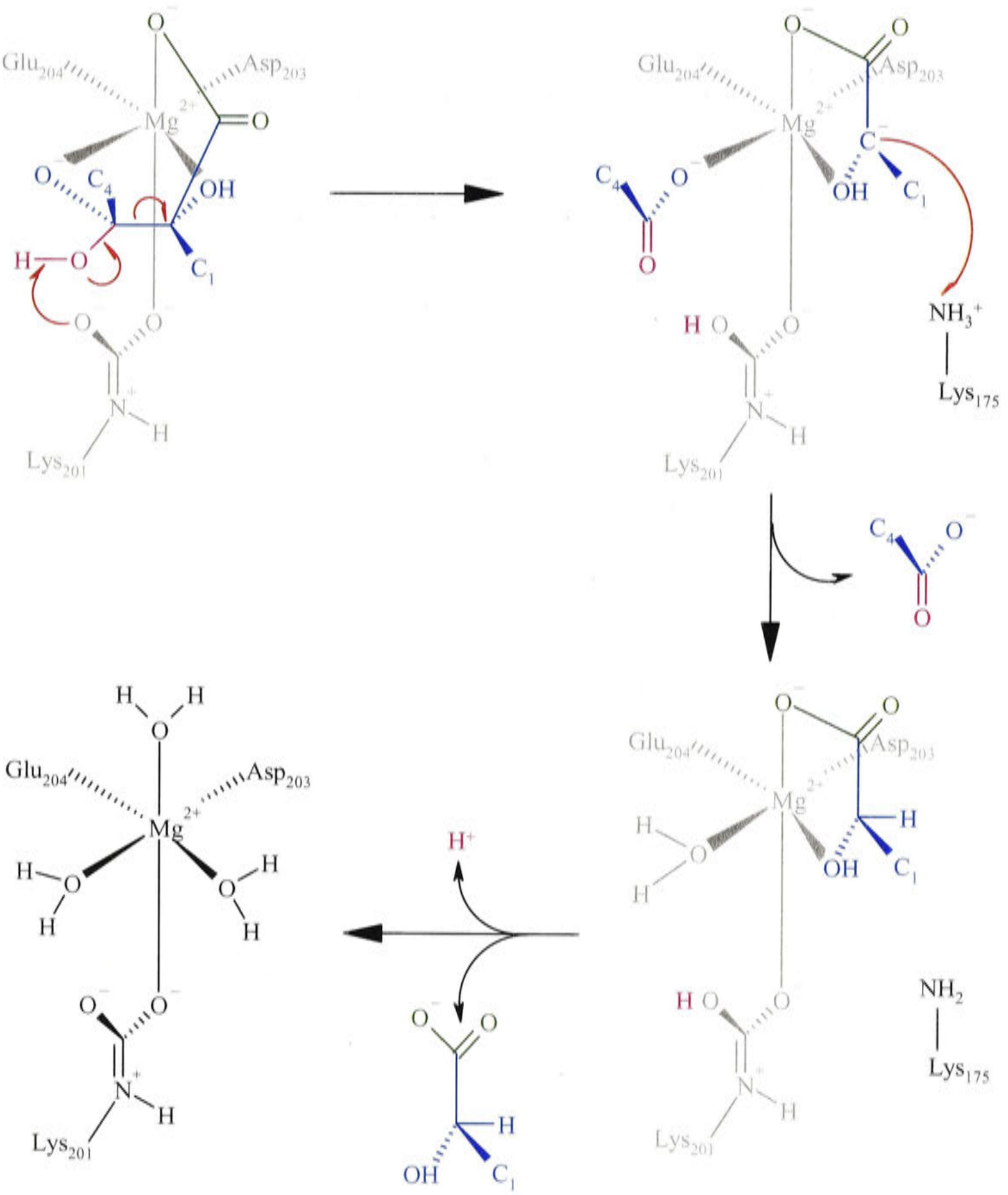

Figure 1.10 Cleavage of the C-C Bond

Initially, the carbamylated lysine residue carries out the deprotonation of O-3. This allows cleavage between C-2 and C-3 to occur, forming one P-glycerate molecule and the *aci*-acid form of P-glycerate. While the P-glycerate molecule can be released immediately, the *aci*-acid requires protonation by a lysine residue.

1.4.7 The Oxygenation Reaction

Attack of the enediol by O_2 is thought to follow a similar pathway to the carboxylation pathway. Normally, addition of O_2 in the triplet ground state to the enediol in the singlet state is chemically unfavourable. There have been two mechanisms proposed for the addition of O_2, but there is little direct evidence for either. A radical mechanism would involve a caged radical pair, consisting of a superoxide radical anion and a enediol radical cation (Andrews and Lorimer 1987). Alternatively, there may be activation of the enediol to the triplet state by geometric deformation (Tapia and Andrés 1992; Andrés et al. 1993).

Other than the novel side products pentodiulose-P_2 and carboxytetritol-P_2 produced by the E48Q and K334A mutants of *R. rubrum*, no intermediates unique to the oxygenase pathway have been isolated (Chen & Hartman 1995, Harpel et al 1995). These compounds support the involvement of a peroxyketone intermediate, which could undergo H_2O_2 elimination to produce pentodiulose-P_2, followed by a benzylic-acid type rearrangement to form carboxytetritol-P_2.

Cleavage of the C-2 to C-3 bond in the peroxyketone intermediate would be accompanied by heterolytic cleavage of the peroxyl O to O bond, producing one molecule of P-glycerate, and one of P-glycolate. Unlike the upper molecule of P-glycerate produced by carboxylation, P-glycolate does not require a final protonation step.

1.4.8 Selecting Between CO_2 and O_2

The relative specificity of the Rubisco enzyme for CO_2 (v_c) compared with O_2 (v_o) is a function of the V_{max}/K_m values for the two substrates multiplied by the ratios of the concentrations of the gaseous substrates, as indicated below:

$$v_c/v_o = V_c/K_c \,/\, V_o/K_o \cdot [CO_2]/[O_2] = \tau \cdot [CO_2]/[O_2] \qquad \textbf{Equation 1.1}$$

Where τ is the specificity factor, and V_c, V_o, and K_c, K_o are the v_{max} and K_m values for CO_2 and O_2 respectively (Laing et al. 1974). τ varies for different Rubisco enzymes from 10 for Form II Rubisco enzymes, up to 200 for some thermophilic non-green algae, and 80 for higher plants.

If it is assumed that CO_2 and O_2 react with the same form of the enediol, the specificity factor can be simplified to the ratio of the second order rate constants for the addition of CO_2 and O_2 (Pierce et al. 1986a; Lorimer et al. 1993). This also takes into

account the observation that decarboxylation of the carboxyketone intermediate is not catalysed by activated Rubisco (Pierce et al. 1986a), and that reverse partitioning of the peroxyketone intermediate is also likely to be minimal.

As a result, the specificity factor is related to the difference in free energy between the carboxyketone and peroxyketone intermediate states (Lorimer et al. 1993). Differences in specificity factors between different Rubisco enzymes are the result of very small differences in the relative free energies of transition states in the active sites (Roy and Andrews 2000). In comparing the specificity of Rubisco from *R. rubrum* and spinach, which is 8-fold greater in the latter, there is only a 1.2 kcal.mol^{-1} difference in the activation energies (Lorimer et al. 1993). This is similar to the energy contributed by a single hydrogen bond.

1.4.9 The Importance of Structure

The functioning of an enzyme is greatly influenced by the structure of the active site. Active site residues need to be positioned so that they are able to act as a proton acceptor or donor during catalysis. The ability of Rubisco to distinguish between CO_2 and O_2 as substrates depends on the relative free energies of the peroxyketone and carboxyketone transition states, which in turn is dependent on the interaction with the active site.

In the case of Rubisco, there are also several steps of catalysis that require precise positioning of the substrate in order to prevent formation of other compounds. To prevent β-elimination, the planarity of the enediol bond needs to be maintained to avoid formation of deoxy-pentodiulose-P (Paech et al. 1978; Morell et al. 1994), and the planarity of the *aci*-acid also needs to be maintained to prevent formation of pyruvate (Andrews and Kane 1991). The enediol can undergo misprotonation, forming xylulose-P_2 (Edmondson et al. 1990d), while the peroxyketone intermediate can eliminate H_2O_2 to form pentodiulose-P_2 (Chen and Hartman 1995).

1.5 Regulation of Rubisco Activity

1.5.1 Introduction

The CBB cycle is an important metabolic pathway, and Rubisco is often the rate limiting step in the cycle (Hudson et al. 1992; von Caemmerer et al. 1997). Other enzymes in the pathway are also regulated, often by illumination via a reduction path from the light reactions. By regulating the activity of the enzymes, the flux of

metabolites through the metabolic pathway can be controlled, which is important in maintaining a steady level of metabolites.

In the chloroplast, Rubisco is exposed to the substrate, ribulose-P_2, as well as a range of other sugar-phosphate compounds. The binding of these compounds to the enzyme can play a role in the regulation of Rubisco activity, as has been reviewed extensively (Gutteridge and Gatenby 1995; Andersson and Taylor 2003; Parry et al. 2003; Portis 2003). If conditions are unfavourable for photosynthesis, such as low light conditions, high temperatures, low CO_2 levels or water stress, Rubisco must be down-regulated so that the rate of ribulose-P_2 consumption is balanced to the rate of ribulose-P_2 regeneration.

Sugar phosphate compounds are able to bind either to Rubisco that lacks the carbamylated lysine residue and Mg^{2+} (termed E), or to Rubisco that has been activated by carbamylation and binding of Mg^{2+} (termed ECM), as shown in Figure 1.11. Inhibitors can be formed by Rubisco itself, or through other pathways in the chloroplast. Release of the inhibitors from the Rubisco active site is facilitated by the action of other enzymes. The interaction of regulatory ligands with Rubisco enzymes from different classes of organisms provides an insight into how the binding of compounds may be related to the reaction mechanism, and how there may be a correlation between ligand binding and catalysis.

1.5.2 Slow, Tight Binding Inhibitors

Some inhibitors can bind to the enzyme at very low concentrations, sometimes at levels similar to that of the enzyme itself(Morrison 1982). These inhibitors are often analogues of substrates or intermediate compounds formed during catalysis (Figure 1.12). One of the benefits of this type of inhibition is that very low levels of inhibitor can inhibit the enzyme (Schloss 1988b).

This inhibition is referred to as slow, tight-binding inhibition (Morrison 1982), because the rate of binding and release of inhibitors is slow, but eventually very tight because of an even slower rate of release. Slow, tight-binding inhibition frequently involves two distinct steps. The first step is a rapid equilibrium step to form EI, similar to that observed for competitive inhibition. This is followed by a slow conformational change to form EI*, the tightly bound enzyme-inhibitor complex from which release of the inhibitor is slow, or sometimes undetectable.

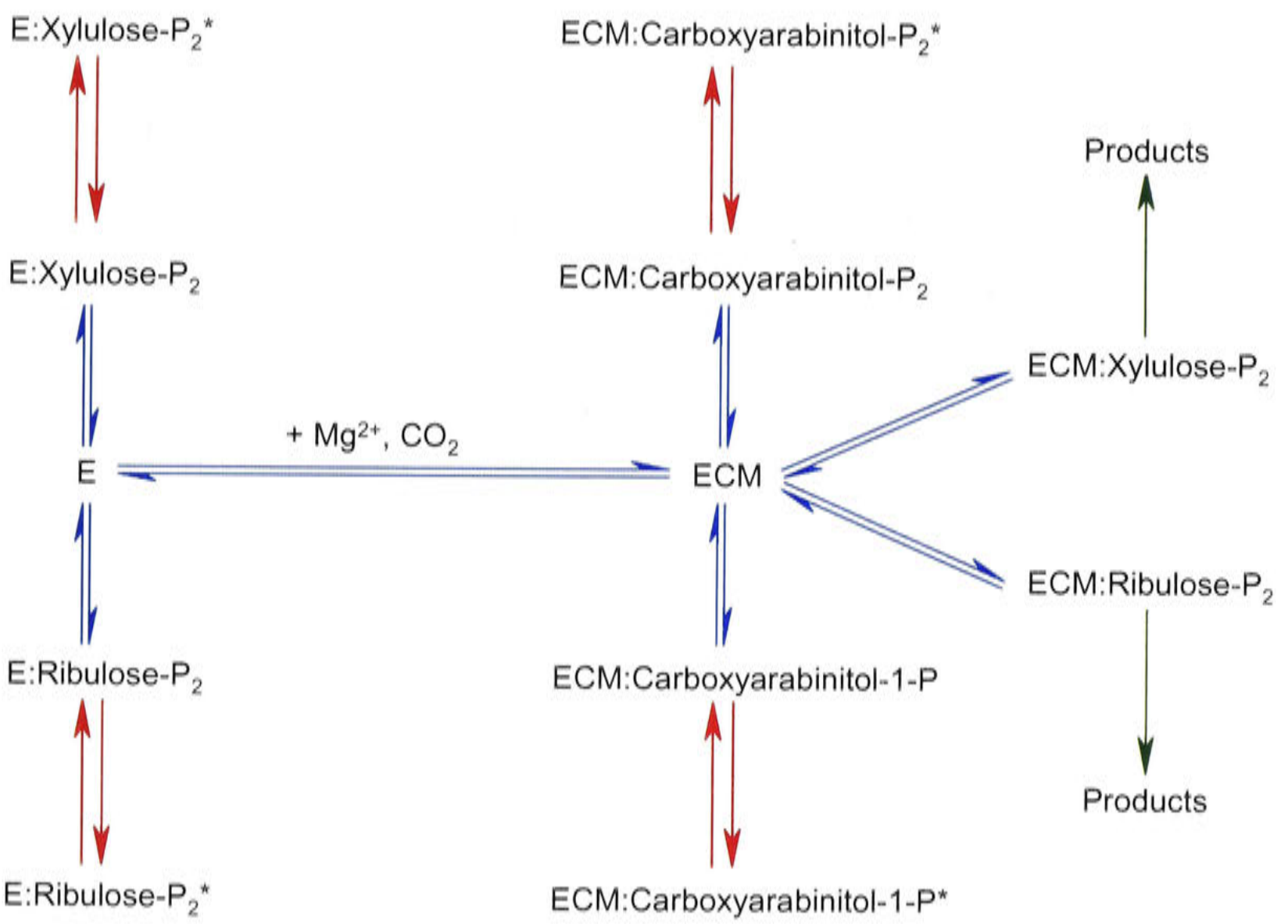

Figure 1.11 Interactions of Rubisco with Different Ligands.

Rubisco requires carbamylation and coordination of a Mg^{2+} ion to carry out catalysis. In the absence of these (termed 'E') Rubisco can interact with the substrate, ribulose-P_2, and xylulose-P_2. The activated form (termed 'ECM') can interact with carboxyarabinitol-P_2, carboxyarabinitol-1-P, ribulose-P_2, and xylulose-P_2. Some interactions involve only a rapid equilibria (shown with blue arrows), while others may include a slower binding step to form a tight complex (shown with red arrows and indicated by an asterisk). The complex may also give rise to products that are released, as indicated by the green arrows.

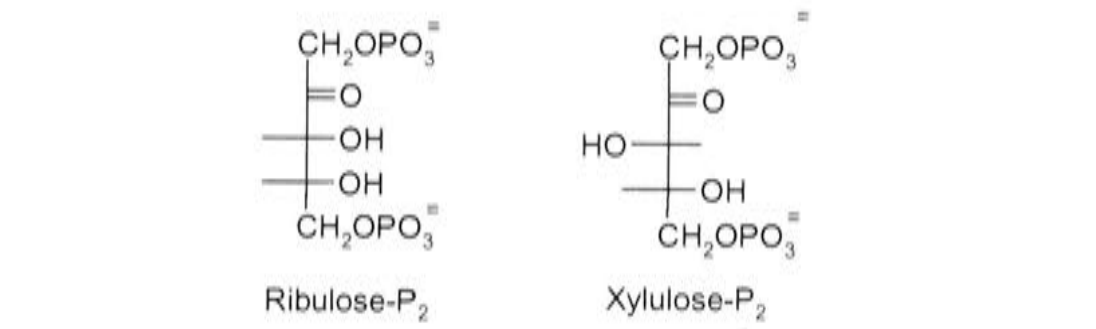

Figure 1.12 Comparison of Substrate, Intermediate and Inhibitor Structures.

Most inhibitors have a similar structure to reaction intermediates or substrates. Xylulose-P_2 has a similar structure to ribulose-P_2, the normal substrate. Carboxyarabinitol-P_2 and carboxyarabinitol-1-P have structures that are similar to the carboxyketone compound that is an intermediate compound in the carboxylation pathway.

1.5.3 Ribulose-P_2, the Natural Substrate

Early studies showed that exposing the Rubisco enzyme to the substrate, ribulose-P_2, prior to activation with HCO_3^- and Mg^{2+} resulted in inhibition of the enzyme activity, which was slowly reversed after exposure to HCO_3^- and Mg^{2+} (Pon et al. 1963; Laing and Christeller 1976). This inhibition was due to the binding of ribulose-P_2 to active sites that have not been carbamylated to form what is referred to as the E:ribulose-P_2 complex.

Binding of ribulose-P_2 to uncarbamylated Rubisco is rarely complete, with some activity remaining at high concentrations of ribulose-P_2. Rubisco from *R. rubrum* showed a maximum inhibition of 75 %, even at ribulose-P_2 levels nearly 1000-fold greater than the K_d (Jordan and Chollet 1983). Release of ribulose-P_2 from E:ribulose-P_2 is slow for Rubisco from higher plants and Form I non-sulphur purple bacteria, taking up to 15 min for full activation (Gibson and Tabita 1979; Jordan and Chollet 1983). However there is faster release from Form II Rubisco enzymes, and Rubisco from cyanobacteria (Andrews and Abel 1981), rhodophytes (Newman et al. 1989) and *Thiobacillus denitrificans* (Hernandez et al. 1996), which show full activation within a matter of minutes.

X-ray crystallographic studies showed that when non-carbamylated spinach Rubisco is complexed with ribulose-P_2, loop 6 is closed over the active site (Taylor and Andersson 1997b). This prevents carbamylation occurring until the loop is opened again, and ribulose-P_2 is released. The degree of carbamylation depends on the levels of CO_2 and Mg^{2+} and the activity of Rubisco activase (described in Section 1.5.6).

Formation of the E:ribulose-P_2 complex may be a way of regulating Rubisco activity during photosynthesis. The concentration of CO_2 in the chloroplast is often lower than the concentration of CO_2 that is required for activation (Portis et al. 1986), and decarbamylation of Rubisco can occur, promoting the formation of the E:ribulose-P_2 complex (Portis et al. 1995). If the level of CO_2 drops, the inactive E:ribulose-P_2 complex will form, reducing Rubisco activity. As the CO_2 concentration increases again, E:ribulose-P_2 will slowly release ribulose-P_2 and be activated again (Woodrow and Berry 1988).

1.5.4 Carboxyarabinitol-1-P, the Night-Time Inhibitor

The leaves of soybean and French bean plants have reduced Rubisco activity when sampled before dawn (Vu et al. 1984; Servaites 1985a). This is due to the

presence of an inhibitor, which was identified as carboxyarabinitol-1-P (Gutteridge et al. 1986; Berry et al. 1987). Carboxyarabinitol-1-P is a bisphosphate sugar that mimics the structure of the carboxyketone intermediate (as shown in Figure 1.12). Unlike the regulation by ribulose-P_2, carboxyarabinitol-1-P was found to bind to carbamylated sites to form an ECM:carboxyarabinitol-1-P complex (Seemann et al. 1985). Incubation of Rubisco inhibited by carboxyarabinitol-1-P in the presence of alkaline phosphatase or ribulose-P_2 restored Rubisco activity, showing that the inhibition is reversible (Seemann et al. 1985; Robinson and Portis 1988).

Inhibition by carboxyarabinitol-1-P is found in some plant species, but not in others. The French bean shows high levels of dark inhibition, and has similarly high levels of carboxyarabinitol-1-P, while other plants, such as spinach, do not accumulate carboxyarabinitol-1-P, and do not show a great reduction in activity at night (Seemann et al. 1990). There appears to be no real pattern to the level of inhibition between different species.

In related experiments, an enzyme was isolated that dephosphorylated carboxyarabinitol-1-P into carboxyarabinitol that was stimulated by ribulose-P_2 and NADH and inhibited by ATP and P_i (Salvucci et al. 1988; Holbrook et al. 1989). It is possible that carboxyarabinitol acts as a precursor to carboxyarabinitol-1-P, but this pathway has not yet been established. Carboxyarabinitol-1-P may be produced when photosynthesis is limited by low light conditions, and act to maintain the enzyme in a carbamylated state.

1.5.5 Daytime Inhibitors

In a similar pattern of regulation, wheat leaves accumulate an inhibitor during the day. Analysis of the inhibitor showed that it was not carboxyarabinitol-1-P or xylulose-P_2, but that it had a similar structure to ribulose-P_2 (Keys et al. 1995). The inhibitor was prone to degradation, and did not show inhibition in Tris buffers, which indicates the presence of a carbonyl group. This pattern of inhibition was also seen in tobacco Rubisco (Paul et al. 1996).

From the properties described for this inhibitor, it is likely to be pentodiulose-P_2 that is produced by peroxide elimination of the peroxyketone intermediate compound. This intermediate is produced when the enediol is using O_2 as a substrate rather than CO_2, thus when conditions favour oxygenation rather than carboxylation, more inhibitor will be produced, and Rubisco will be down-regulated. Xylulose-P_2 may have a similar regulatory role during catalysis.

1.5.6 Rubisco Activase

A consequence of slow, tight-binding is the associated reduced rate of inhibitor release. To accelerate this process, plants contain Rubisco activase, an enzyme that interacts with Rubisco and facilitates the release of inhibitors from the active site in a process that requires energy from ATP hydrolysis (Robinson and Portis 1989a).

Identification of Rubisco activase came from the initial observations of the Arabidopsis *rca* mutant, which had low Rubisco activity and accumulated ribulose-P_2 (Somerville et al. 1982). The mutant lacked a 47 kDa protein that was required for full activation of the E:ribulose-P_2 complex at low CO_2 levels (Salvucci et al. 1985). The protein did not affect the rate of Rubisco deactivation, but increased the rate at ribulose-P_2 was released from the E:ribulose-P_2 complex (Portis et al. 1986). It was also shown that Rubisco activase could increase the rate of carboxyarabinitol-1-P release (Robinson and Portis 1988) and alleviate the inhibition of Rubisco activity that is observed during *in vitro* assays (Robinson and Portis 1989b), as described in Chapter 3.

As yet, no crystal structure of Rubisco activase is available; however it is a member of the AAA+ family of ATPases, which typically form a ring-structure (Neuwald et al 1999). The interaction of Rubisco activase with Rubisco is unclear, although one electron microscopy study suggested that Rubisco activase encircled the Rubisco holoenzyme (Buchen-Osmond et al 1992). Rubisco activase has been observed to show species specificity (Wang et al. 1992), and regions have been identified on the Rubisco large subunit that affect the interactions with Rubisco activase (Portis 1995; Larson et al. 1997; Ott et al. 2000).

Several similar models have been proposed for the mechanism by which Rubisco activase releases inhibitors from Rubisco (Andrews et al. 1995; Salvucci and Ogren 1996). It is thought that the binding of inhibitors to Rubisco causes loop 6 to close over the active site, forming a tight complex. An oligomer of Rubisco activase subunits then associates with Rubisco and forces the loops open, allowing the inhibitor to disassociate. In the process, Rubisco activase uses energy from ATP to convert from an inactive to an active form, or to promote interactions with Rubisco.

A gene encoding the Rubisco activase protein has also been identified in cyanobacteria (Li et al. 1993). While the Rubisco activase product had no effect on the *in vitro* activation of carboxyarabinitol-1-P inhibited enzyme, mutant strains of *Anabaena* sp. that lacked the gene had slower *in vivo* growth rates, suggesting that the

product of the gene has an important physiological role (Li and Tabita 1997; Li et al. 1999).

In non-green algae, the *rbc*L and *rbc*S genes are often in the same operon as the *cbb*X gene, whose function is unknown. However mutant strains of *Rhodobacter sphaeroides* lacking the gene have impaired photoautotrophic growth (Gibson and Tabita 1997) and it is possible that the product of the *cbb*X gene has a similar function to that of Rubisco activase.

1.6 Previous Structure-Function Studies

1.6.1 Introduction

The discovery that there was natural variation in the catalytic efficiency of different Rubisco enzymes lead to a concerted effort to establish the basis for this disparity, by correlating changes in structure with changes in catalytic chemistry. Nearly all studies of how the enzyme structure influences the function have been based on site-directed mutagenesis, naturally occurring mutations, and comparing sequence variation between different species. Structural studies have shown that there are no gross inconsistencies between different Rubisco enzymes, and that the shape and residues of the active site are highly conserved (Knight et al. 1990). Thus the differences in catalytic properties must be due to subtle changes in the configuration of the active site that are too discreet to be observed using current structural information.

Mutational studies allow some elucidation of the importance of different structural features (Table 1.1). Most studies have involved work on *R. rubrum* and *Synechococcus* PCC6301 Rubisco, due to the ease of enzyme expression and assembly in *E. coli*. Directed mutagenesis of Rubisco in the green alga *Chlamydomonas* is also becoming routine (Bateman and Purton 2000; Esquivel et al. 2002). While most mutations that influence catalysis are located in the active site, some are not directly associated and others are located in the small subunit.

1.6.2 Mutation of Active Site Residues

Mutations in the active site may be located at the metal binding site, the P-1 or P-2 binding sites, or at loop 6. Many mutations of active site residues completely abolish activity, confirming the importance of the residue in catalysis, however they do not always provide information about their function. An example of this is the Lys-201 residue that is carbamylated before catalysis, in which mutant enzymes in *R. rubrum* did not carry out any enolisation or processing of the six-carbon intermediate (Gutteridge et

al. 1988). Mutagenesis studies in which the kinetic parameters are altered, but still measurable, allow better inferences to be made.

Lys-175 (166) has an important role as an acid-base catalyst during enolisation and carboxylation reactions (Roy and Andrews 2000). While Lys-175 mutants of *R. rubrum* have some limited enolisation activity, most of the enediol undergoes β-elimination to form deoxy-pentodiulose-P, suggesting that the mutant enzyme is limited in carboxylation and oxygenation of the enediol (Harpel et al. 2002). The K175G mutant enzyme can catalyse hydrolysis of the carboxyketone intermediate (Lorimer and Hartman 1988), and the substitution of Lys-175 also increased the production of pyruvate by the enzyme (Harpel and Hartman 1996). Chemical rescue of the mutants by aminoethylation or aminopropylation restored the enolisation rate, but resulted in increased formation of pentodiulose-P_2 and carboxytetritol-P_2 by some mutants (Harpel et al. 2002). This suggests that the residue is important in stabilising the peroxyketone intermediate.

Another residue, His-294 (287) also has an important role during catalysis. The residue is located within 5 Å of C-3 of ribulose-P_2 bound to the enzyme, and forms interactions with Glu-204 and the carbamylated Lys-201 residue (Taylor and Andersson 1997b). Mutating the His-294 residue of *R. rubrum* Rubisco enzyme greatly reduced carboxylation and enolisation of ribulose-P_2, increased the binding of carboxyarabinitol-P_2 to the active site, and increased the formation of carboxytetritol-P_2, xylulose-P_2 and deoxy-pentodiulose-P (Harpel et al. 1998).

The E60Q (48) mutant of *R. rubrum* also had a significant reduction in carboxylation rate and specificity. Glu-60 (48) is located in the N-terminal domain above the active site, and forms a salt bridge with Lys-168 of an adjacent subunit in the inactivated form, and with Lys-334 (329) in the carbamylated form. It accumulated xylulose-P_2 and keto-arabinitol-P_2 under assay conditions, which were eventually processed to form P-glycerate and P-glycolate (Lee et al. 1993). Later studies revealed that the keto-arabinitol-P_2 had been misidentified, and was actually pentodiulose-P_2 (Chen and Hartman 1995). The accumulation of xylulose-P_2 and pentodiulose-P_2 suggests that the mutant enzyme has difficulty in preventing misprotonation of the enediol and stabilising the peroxyketone intermediate.

Residue	Organism	Carboxylation Rate	Enolisation Rate	Specificity	Ligand Binding	Reference
Lys-201	*R.rubrum*	ND[a]	Abolished	ND	ND	(Gutteridge et al. 1988)
Lys-175	*R.rubrum*	ND	Limited	ND	ND	(Lorimer and Hartman 1988)
His-294	*R.rubrum*	Reduced	Reduced	ND	Increased	(Harpel et al. 1998)
Glu-60	*R.rubrum*	Reduced	ND	Reduced	ND	(Lee et al. 1993)
Thr-65	*Synechococcus PCC6301*	Reduced	ND	Reduced	ND	(Morell et al. 1994)
His-327	*R.rubrum*	Reduced	Reduced	ND	Reduced	(Harpel et al. 1991)
Ser-379	*R.rubrum*	Reduced	ND	ND	Increased	(Harpel et al. 1991)
Lys-334	*R.rubrum*	Abolished	Limited	ND	ND	(Hartman and Lee 1989), (Lorimer et al. 1993)
Met-335	*R.rubrum*	Reduced	ND	Unchanged	Reduced	(Terzaghi et al. 1986)
Leu-335	Tobacco	Reduced	Similar[b]	Reduced	Reduced[b]	(Whitney et al. 1999)
C-terminal domain of SSU	*Synechococcus* PCC6301	Slight decrease	ND	Slight decrease	ND	(Flachmann et al. 1997)

[a] Not Determined

[b] Results from this thesis

Table 1.1 The Effect of Some Rubisco Mutations on Kinetic Parameters

Mutations in the Rubisco enzyme can alter the kinetic parameters, including the rate of carboxylation and enolisation, the ability to distinguish between CO_2 and O_2 as substrates, and the binding of ligands to the active site.

The P-1 phosphate of ribulose-P_2 is held in position by 5 amino acid residues, Thr-65 (53) and Asn-66 (54) from the N-terminal of one large subunit, and Gly-381 (370), Gly-403 (393), and Gly-404 (394) from the C-terminal of the other large subunit. Mutation of these residues in *R. rubrum* greatly reduced the rate of catalysis, specificity and affinity for ribulose-P_2 (Larimer et al. 1994). Reducing the interaction with P-1 also increased the release of carboxyarabinitol-P_2 by the enzyme, and the tendency of the enzyme to produce pyruvate and deoxy-pentodiulose-P during catalysis. Substitution of this Thr-65 in *Synechococcus* PCC6301 reduced carboxylation, specificity, and pyruvate production (Morell et al. 1994). The T65V mutant enzymes also had an increased tendency to produce side products, including deoxy-pentodiulose-P and xylulose-P_2.

His-327 (321) interacts with P-2 group of the substrate. Mutations of the His-327 residue in *R. rubrum* reduced the carboxylation rate with a proportional drop in enolisation rate, suggesting that His-327 is involved in the initial deprotonation step (Harpel et al. 1991). These mutants showed an increase in the rate of carboxyarabinitol-P_2 release.

Ser-379 (368) forms a H-bond with O-3 during catalysis. Mutants of the Ser-379 residue in *R. rubrum* had reduced carboxylation rates, and also had a slower rate of carboxyarabinitol-P_2 release (Harpel et al. 1991).

1.6.3 Mutation of Loop 6 Residues

Lys-334 is a catalytically essential residue located in loop 6, which closes over the active site after ribulose-P_2 binds (Knight et al. 1990). Mutants in *R. rubrum* effectively abolished carboxylation and oxygenation activity, because of the importance of the residue in the addition of CO_2 or O_2, but the mutants retained some ability to carry out the enolisation of ribulose-P_2 (Hartman and Lee 1989; Lorimer et al. 1993). Replacement of a charged group by chemical rescue using aminoethylation or aminopropylation recovered some carboxylation activity, but the specificity was reduced (Harpel et al. 2002).

Residue-335 is conserved as a leucine residue in all L_8S_8 enzymes, but is conserved as methionine in all L_2 Rubisco enzymes. Leu-335 is located near the apex of loop 6 and makes van der Waals contacts with the P-2 phosphate of ribulose-P_2 (Knight et al. 1990). Conversion of Met-335 (330) to leucine in *R. rubrum* reduced the catalytic rate and increased the kinetic constants for CO_2 and ribulose-P_2, but did not affect the specificity (Terzaghi et al. 1986). The binding of carboxyarabinitol-P_2 to the mutant

enzyme was also reduced, suggesting that the mutation resulted in reduced stability of the enediol intermediate.

The L335V mutant of tobacco Rubisco was the first site-directed mutant of higher plant Rubisco. The substitution successfully reduced the CO_2/O_2 specificity and the Michaelis constants for CO_2, O_2, and ribulose-P_2, while retaining sufficient substrate-saturated activity to allow growth under CO_2 enrichment. The changes were readily apparent in the photosynthetic characteristics of the leaves of the mutant plant (Whitney et al. 1999).

1.6.4 Mutation of Other Residues

The C-terminal domain of the SSU is highly conserved among species. Mutations in this region of the *Synechococcus* SSU (F92S, Q99G and P108L) resulted in a small decrease in carboxylation rate and specificity, and a change in affinity for CO_2 (Flachmann et al. 1997). The Q99G and P108L mutations also increased the rate of xylulose-P_2 production.

Rubisco enzymes from C4 plants have higher turnover rates and lower affinities for CO_2 than enzyme from C3 plants. Comparisons of the Rubisco amino acid sequences from C3 and C4 plants revealed only three to six substitutions, all of which were remote from the active site (Hudson et al. 1990). Residue 309 is usually methionine in C3 plants, and isoleucine in C4 plants and *Synechococcus* PCC6301. The I309M mutant of *Synechococcus* PCC6301 had negligible difference in the kinetic parameters, while substitution with other amino acid residues prevented folding of the enzyme (Morell et al. 1992).

1.6.5 Mutations Alter the Kinetic Parameters

Nearly all of the mutant Rubisco enzymes produced to date have an impaired catalytic ability. Mutations in the enzyme can reduce individual or several of the enolisation, carboxylation, oxygenation or hydration steps during catalysis. Other changes in the active site can also affect the partitioning of products by the enzyme. Reducing the stability of the enediol increased the probability of misprotonation to form xylulose-P_2 or β-elimination to form deoxy-pentodiulose-P. If the peroxyketone is not stabilised, it can form pentodiulose-P_2, which may then be rearranged to form carboxytetritol-P_2. The carbanion requires protonation to form P-glycerate, but is prone to β-elimination to form pyruvate. Changes to the structure of the active site can alter this partitioning.

Interactions of Rubisco with ligands can also be affected by mutations to the enzyme. Many mutations reduced the affinity of the enzyme for ribulose-P_2 or CO_2, while other mutations had an effect on the release of carboxyarabinitol-P_2 from the enzyme.

1.7 Site-Directed Mutagenesis of Higher Plants

Much of the current Rubisco research is focussed on the genetic modification of Rubisco in higher plants, with the intention of replacing the endogenous enzyme with a different, more efficient form. It is now possible to carry out many different manipulations of the higher plant chloroplast (Andrews and Whitney 2003), however, to date, only one such mutation has been generated in higher plants (Whitney et al. 1999).

One of the limitations of working with higher plant Rubisco is that it can only be produced in its native species. Unlike the Rubisco from *R. rubrum* or *Synechococcus* PCC6301, higher plant Rubisco is unable to be assembled when expressed in *E. coli*, which means that any transformations must be carried out in the higher plant.

1.7.1 Transformation of the Chloroplast

In higher plants, the *rbc*L gene is located in the chloroplast genome, which creates added challenges for transforming the gene. The plastid contains up to several hundred copies of the genome, and combined with the large number of plastids per cell, resulting in many copies of the gene per cell. The initial transformation event is only likely to transform one copy of the gene, and this copy must then reach homoplasmy, in which all copies of the plastid genome are identical. Transplastomic lines will be genetically stable only if each of their plastid-genomes is uniformly altered, which does not necessarily require all copies to be transformed in the initial event.

Plastid transformation requires a method for DNA delivery through the double membrane of the plastid, integration of the heterologous DNA and efficient selection for the transformed plastome (Maliga 1993). To select for the single transformed gene, a selection marker must be coupled to the transforming construct. These selection genes confer an advantage to the transformed cells, allowing them to proliferate over non-transformed cells. The gene may encode for resistance to antibiotics, the ability to detoxify harmful compounds, or resistance to herbicides.

Transformation is achieved by the recombination of a gene construct with the gene in the plastid. Recombination occurs when homologous regions pair up, and

exchange a portion of the sequence. This can result in the insertion of a new gene, or the substitution of the native gene for one containing a site-specific mutation.

The gene construct is composed of a selection marker, regions of homology, and the gene of interest. This can be introduced into the cell by several methods, including microparticle bombardment. In this method, the construct is coated onto gold particles, which are then propelled into the plant cell by a blast of high pressure helium. Recombination can then occur between the introduced gene construct and the plastid DNA.

Limitations to this method of site-specific mutation are due to the unlinking of the selection gene from the gene of interest (Whitney et al. 1999), and the selection of transformed plastids. In order to develop an efficient transformation system, these limitations need to be overcome.

When a single change is made to a gene, to generate a site-specific mutation, the construct has several regions of homology to the native plastid. The initial transformation event is likely to incorporate the entire construct, recombining at either end of the construct. However there is often another homologous region between the mutation and the selection gene. Recombination between the transformed plasmid and an untransformed plasmid can occur between this region and the homologous region following the selection gene to unlink the selection gene from the mutation. This hinders the ability to use the selection gene to select for the mutation.

To alleviate this problem, the homologous region between the mutation and the selection gene must be reduced. This can be achieved by transforming the mutated gene into a plant cell that either lacks an *rbc*L gene, or has an *rbc*L gene with less homology than the native gene. Because this method requires two transformation steps, two independent selection genes would be required.

Another option to using two separate selection genes is to remove the selection pressure after the initial exposure, and then allow the removal of the gene. This can be achieved by including some tandem repeats on either side of the gene (Iamtham and Day 2000). In the absence of the selection agent, recombination between the tandem repeats results in excision of the gene.

1.7.2 Genes for the Selection of Transformants

The most commonly used selection gene for plastid transformation, aminoglycoside 3"-adenyltransferase, *aad*A, confers resistance to spectinomycin.

Spectinomycin inhibits plastid protein synthesis (Svab and Maliga 1993). Initially, all cells will grow because sucrose media alleviates the need for photosynthesis. Resistant, transformed cells are green, while sensitive cells are white, due to inhibition of plastid-protein synthesis. Since plastid-protein synthesis is required for organelle maintenance, spectinomycin sensitive chloroplasts will degrade, while transformed spectinomycin resistant chloroplasts will be preferentially maintained.

Kanamycin is an antibiotic than inhibits cell division, and prevents growth of plant tissue. The gene encoding neomycin phosphotransferase, *npt*II, has been used to confer resistance to kanamycin, unfortunately it is 20-30 times less efficient than selection using spectinomycin, with a transformation event occurring for every 25 bombardments (Carrer et al. 1993). Another gene encoding for the aminoglycoside phosphotransferase enzyme APH(3')-VI has also been used as a selection gene for kanamycin resistance (Bateman and Purton 2000).

Selection genes can also confer resistance to toxic substances. Betaine aldehyde dehydrogenase allows plant cells to grow on media containing betaine aldehyde, which is normally toxic to tobacco plants (Daniell et al. 2001). However current work in this laboratory has shown that the method is not as efficient as initially proposed, with a high rate of background resistance.

1.7.3 Previous Manipulation of Rubisco in Higher Plants

Many studies have been carried out that involve the transformation of Rubisco genes in higher plants (Andrews and Whitney 2003). It has shown that the *rbc*L gene can be deleted from the chloroplast and relocated to the nucleus. The chloroplast *rbc*L gene was replaced with the *aad*A gene, which confers resistance to spectinomycin. The resulting plants were photosynthetically incompetent, but could be maintained on sucrose media (Kanevski and Maliga 1994). The *rbc*L gene was then introduced into the nuclear genome (linked with the *npt*II gene and a transit peptide) with a partial restoration of Rubisco levels and activity.

Other studies tested whether the native *rbcL* of tobacco could be replaced with the large subunit of another species (sunflower and *Synechococcus* PCC6301) and still fold into an active holoenzyme by assembling with tobacco Rubisco small subunits (Kanevski et al. 1999). The gene construct contained the *rbc*L gene from *Synechococcus* PCC6301 or sunflower linked to the *aadA* gene and flanked by homologous regions. The Rubisco hybrid consisting of tobacco LSUs and sunflower SSUs showed some Rubisco activity, while the Rubisco hybrid consisting of tobacco LSUs and

Synechococcus PCC6301 SSUs did not have any activity. In 50-70 % of lines *aadA* integration was not linked to the heterologous *rbcL* sequences, due to recombination in the *rbcL* 3' UTR.

Conversely, the *rbc*S gene was returned to its pre-endosymbiotic location in the chloroplast (Whitney and Andrews 2001a). These plants retained the native nuclear *rbc*S genes and it was found that the nuclear encoded small subunits bound preferentially to the hexadecameric enzyme. While small subunits were expressed from the chloroplast genome, they were inefficiently incorporated into the holoenzyme.

Recent studies have also replaced the tobacco *rbc*L gene with the *rbc*M from *R. rubrum* (Whitney and Andrews 2001b). The resulting plants were able to grow autotrophically when supplemented with CO_2, and the photosynthetic characteristics of the transformants matched those predicted using the parameters for the Form II enzyme.

In order to efficiently generate site-specific mutations in tobacco Rubisco, the mutant gene must be transformed into either null-*rbc*L tobacco plants or tobacco plants containing an *rbc*L gene with sufficiently less homology. This requires the use of two separate selection genes, or the ability to excise the selection gene to allow its reuse.

1.8 Aims of this Thesis

A long-term goal of Rubisco research is to improve the efficiency of Rubisco in crop plants, which would result in a more efficient use of the available resources to provide agricultural products. Achieving this goal requires a detailed knowledge of how catalysis is influenced by the structure of the enzyme. This thesis aims to extend this knowledge by investigating how the subtle differences in active site geometry of naturally occurring Rubisco enzymes and mutational modifications of the higher plant enzyme influence catalysis and interactions with ligands.

Initially, observations are made about the formation and binding of alternate compounds during catalysis for a range of Rubisco enzymes from different phylogenetic groups. These studies are then expanded to directly measure the rate of side- and partial-reactions, and the rate of binding and release of inhibitory ligands. The pattern of catalytic chemistry can then be used to make inferences about differences in the geometry of the active site.

2 General Methods

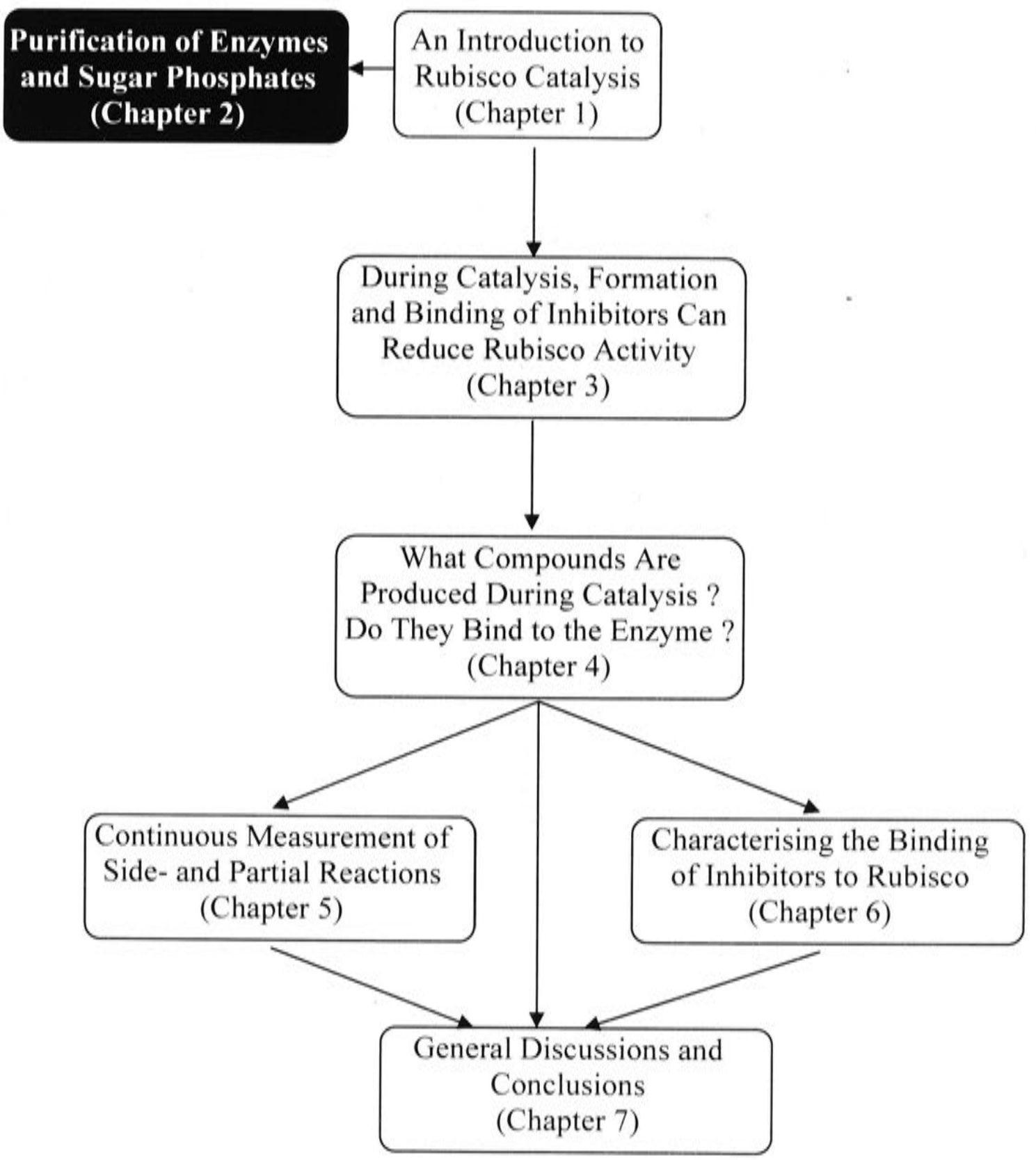

2.1 Introduction

Different groups of Rubisco enzymes have differences in structure and catalytic properties. In order to elucidate how subtle differences in the structure of the Rubisco enzyme influence the catalytic chemistry, Rubisco enzymes from different phylogenetic groups were selected as representatives for comparison.

2.1.1 Higher Plant Rubisco

Higher plants contain a 'green-type' Form I Rubisco, which consists of a hexadecamer of eight small subunits and eight large subunits. Higher plant Rubisco enzymes tend to have a moderate catalytic rate (3 sec^{-1}) and CO_2/O_2 substrate specificity (~ 80). Tobacco was chosen because of the availability of crystal structures (Curmi et al. 1992), ease of cultivation, and the availability of an active site mutant (Whitney et al. 1999).

2.1.2 Cyanobacterial Rubisco

Cyanobacteria are photoautotrophic prokaryotes that also have a 'green-type' Form I Rubisco enzyme. They occur naturally in both seawater and freshwater, and were among the earliest photosynthetic organisms. Cyanobacterial Rubisco enzymes are characterised by a high catalytic rate (10 sec^{-1}), low to moderate CO_2/O_2 substrate specificity (~ 40), and a low affinity for CO_2. This low affinity is associated with the presence of a carbon concentrating mechanism, which allows an increase in the CO_2 concentration around the Rubisco enzyme. *Synechococcus* PCC6301 (also known as *Anacystis nidulans*) was chosen because the Rubisco enzyme can be expressed and assembled in prokaryotic foreign hosts, and also because of the availability of its crystal structures (Newman and Gutteridge 1993; Newman and Gutteridge 1994).

2.1.3 'Red-type' Rubisco

Rhodophytes (red algae) are photoautotrophic eukaryotes that have a 'red-like' Form I Rubisco enzyme. They live mostly in salt water, but some are also found in freshwater. Red algal Rubisco have a high specificity for CO_2 over O_2, and a moderate catalytic rate (1.5–2.6 sec^{-1}). The thermophilic red algae *Galdieria partita* and *Cyanidium caldarium* have specificities of 238 and 222 respectively at 25°C (Uemura et al. 1997). *Galdieria sulphuraria* is a unicellular red alga that occurs mainly in hot volcanic springs, at a pH between 0.05 and 3. It was chosen due to its ease of culture in

the laboratory, and the availability of crystal structures (Sugawara et al. 1999; Okano et al. 2002).

2.1.4 Form II Rubisco

The simplest form of the enzyme, Form II Rubisco, occurs in some prokaryotes and dinoflagellates, and is composed of a dimer of large subunits. *Rhodospirillum rubrum* is a purple, non-sulphur bacterium that occurs naturally in pond water and mud. It is a phototrophic bacterium, and can grow autotrophically or heterotrophically. It was chosen because the Rubisco can be expressed in prokaryotic foreign hosts, and the crystal structures are available (Schneider et al. 1986b; Lundqvist and Schneider 1989a; Lundqvist and Schneider 1989b; Lundqvist and Schneider 1991).

2.1.5 Rubisco Activase

Rubisco activase is a protein that interacts with higher plant Rubisco, inducing the release of inhibitors from the active site. It is thought to use the energy from ATP hydrolysis to trigger the opening of loop 6 over the Rubisco active site, as described in Section 1.5.6 (Portis 2003).

2.1.6 Sugar Phosphate Compounds

With the exception of the gaseous substrates CO_2 and O_2, the majority of molecules that interact with Rubisco are sugars with one or two phosphate groups. These include the substrate, ribulose-P_2, as well as the inhibitors xylulose-P_2, carboxyarabinitol-1-P, and carboxyarabinitol-P_2.

2.1.7 Specific Aims and Objectives

This chapter describes the purification of Rubisco enzymes from a range of different sources, the synthesis and purification of several different sugar phosphate compounds, and the spectrophotometric assay for measuring Rubisco activity. These enzymes and sugar phosphates are used in experiments in later chapters, which also use variations of the spectrophotometric assay.

Protein extraction from natural or foreign hosts and purification was performed using anion exchange or affinity chromatography, while sugar phosphates compounds were synthesised by multi-step enzymatic reactions and purified by anion exchange chromatography.

2.2 Materials, Methods & Results

2.2.1 Materials

Chemicals were generally purchased from Sigma Chemical Company or Merck Pty Ltd. Enzymes were obtained as lyophilised powders or saturated $(NH_4)_2SO_4$ suspensions from Roche Biochemicals or Sigma Chemical Company. Enzymes used in spectrophotometric assays were desalted by dialysis prior to use, to remove residual sulphate. Radiochemicals were obtained from Amersham Biosciences. Ion exchange resins were obtained from Bio-Rad or Amersham Biosciences. Ribulose-P_2 was synthesised and purified as described (Kane et al 1998) by H.J Kane. *Synechococcus* PCC6301 Rubisco was purified as described (Andrews 1988) by Y.B.C Arvidsson & H. J. Kane. Unless otherwise stated, purification of proteins, and synthesis and purification of sugar phosphates was carried out at 0–4°C.

2.2.2 The Spectrophotometric Rubisco Assay

Rubisco activity was determined at 25°C using a spectrophotometric assay in which the consumption of P-glycerate is coupled to the oxidation of NADH, as shown in Figure 2.1 (Lilley and Walker 1974). The oxidation of NADH can be monitored spectrophotometrically, as NADH absorbs light at 340 nm ($\varepsilon_{NADH} = 6.22 \times 10^3$ $M^{-1}.cm^{-1}$), while NAD^+, the reduced form, does not. Under carboxylating conditions, four NADH molecules are oxidised per ribulose-P_2 consumed in the reaction. Prior to assay, Rubisco was activated in buffer containing 100 mM EPPS-NaOH pH 8.0, 20 mM $MgCl_2$, 1 mM EDTA and 20 mM $NaHCO_3$ and tobacco Rubisco was incubated at 50°C for 10 min (Kawashima et al. 1971). Each assay (2 ml) contained 100 mM EPPS-NaOH, pH 8.0, 20 mM $MgCl_2$, 1 mM EDTA, 0.5 mM DTT, 0.2 mM NADH, 2 mM ATP, 10 mM phosphocreatine, 5–50 mM $NaHCO_3$, 25 $units.ml^{-1}$ creatine phosphokinase, 0.1 $mg.ml^{-1}$ carbonic anhydrase, 20 $units.ml^{-1}$ 3-phosphoglycerate kinase, 20 $units.ml^{-1}$ glyceraldehyde-3-phosphate dehydrogenase, 50 $units.ml^{-1}$ triosephosphate isomerase, and 20 $units.ml^{-1}$ glycerol-3-phosphate dehydrogenase. The reaction was initiated by the addition of Rubisco or 5-1200 μM ribulose-P_2, and the absorbance at 340 nm was measured over time.

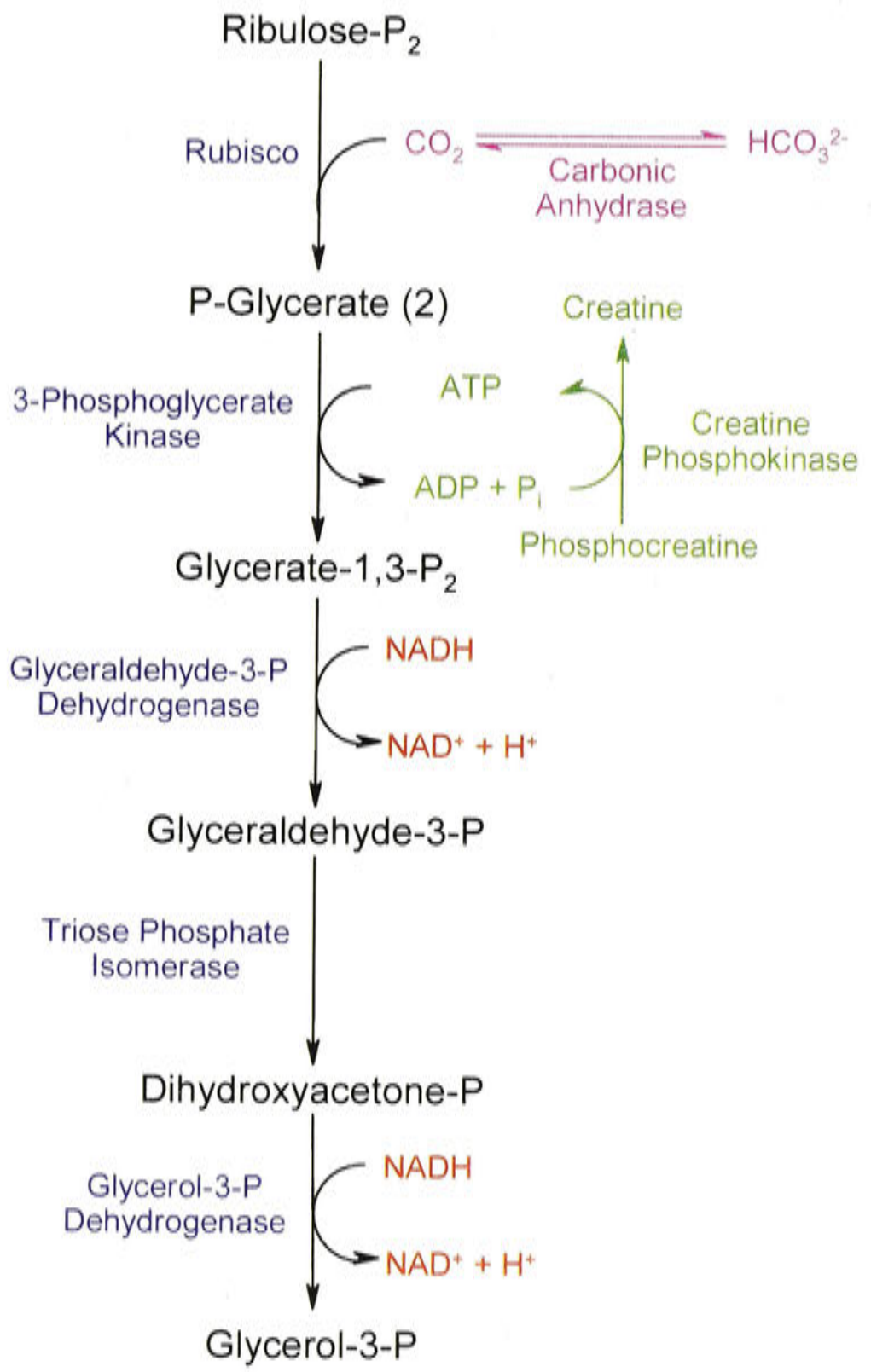

Figure 2.1 The Coupled Spectrophotometric Assay for Rubisco Activity

To measure the rate at which P-glycerate is produced by Rubisco, other enzymes (shown in blue) are included in the assay that couple the consumption of P-glycerate to the oxidation of NADH (shown in red). This oxidation can be measured by monitoring the absorbance at 340 nm, and required the inclusion of an ATP regenerating system (shown in green). Carbonic anhydrase is also included to maintain the equilibrium between CO_2 and HCO_3^- (shown in purple).

The coupling enzymes must be present in excess to ensure that the rate of NADH oxidation is directly proportional to the Rubisco reaction rate. On occasions, a lag period was observed due to the coupling enzymes not being sufficiently in excess. In these cases, the concentration of coupling enzymes was increased, or the concentration of Rubisco decreased to reduce the reaction rate.

The Rubisco concentration was also manipulated so that a change in absorbance of approximately 0.2 AU was observed over the course of the assay. This ensured that the reaction was unlikely to be limited by the consumption of components of the coupled assay. Typically this resulted in a higher concentration of L335V tobacco and *G. sulphuraria* Rubisco, due to the reduced reaction rates, and lower concentration of His-*Rubrum* and *Synechococcus* PCC6301 Rubisco, because of their higher catalytic rates.

The $NaHCO_3$ concentration used for each enzyme was adjusted to correspond to the affinity of each enzyme for CO_2 ($K_m(CO_2)$). The concentration was designed to be at saturating levels of CO_2, but not sufficiently high to cause inhibition, which can be seen at high $NaHCO_3$ concentrations due to HCO_3^- binding to the active site (Andrews and Hatch 1971). *G. sulphuraria* Rubisco was assayed at 5 mM $NaHCO_3$ due to a low $K_m(CO_2)$, while tobacco Rubisco was assayed at 20 mM $NaHCO_3$ because of a high $K_m(CO_2)$. *R. rubrum* and *Synechococcus* PCC6301 Rubisco enzymes have a higher $K_m(CO_2)$ than tobacco and *G. sulphuraria* Rubisco, and were assayed at 50 mM $NaHCO_3$.

2.2.3 Rubisco Purification

2.2.3.1 Tobacco Rubisco

Rubisco was purified from wild-type and L335V tobacco plants by crystallisation as previously described (Servaites 1985b), or by anion exchange chromatography. Wild-type tobacco (*Nicotiana tobacum* L. cv Petit Havana [N,N]) was grown in soil under naturally illuminated glasshouse conditions in ambient CO_2. Plastome mutants that produce Rubisco with a Leu to Val mutation at residue 335 (Whitney et al. 1999) were grown in an artificially illuminated growth cabinet in an atmosphere containing 0.3 % (v/v) CO_2. Leaves (20–40 g) were collected, deveined, snap frozen in liquid N_2, and ground to a fine powder with a mortar and pestle, before being added to 50 ml of buffer containing 50 mM Tris-HCl, pH 7.4, 20 mM $MgCl_2$, 20 mM $NaHCO_3$, 0.5 mM EDTA, 50 mM β-mercaptoethanol, 10 $mg.ml^{-1}$ casein, 20 $mg.ml^{-1}$ poly-vinyl-polypyrrolidone, 1 mM PMSF and 10 % (v/v) glycerol. The solution was filtered

through two layers of cheesecloth and Miracloth, clarified by centrifugation (27,000 x g, 10 min, 4°C), and applied batch-wise to 20 ml of AG1-X8 (Cl^-) (Bio-Rad) resin, which was removed by filtration. 60 % (w/v) PEG_{3350} was added dropwise to the solution to a final concentration of 10 %, and the solution stirred on ice for 30 min before being centrifuged again (27,000 x g, 10 min, 4°C). The green pellet was discarded, and 60 % (w/v) PEG_{3350} added to the green/yellow supernatant to a final concentration of 20 %. The sample was centrifuged (27,000 x g, 10 min, 4°C), and the white pellet resuspended in buffer containing 50 mM Tris-HCl, pH 7.4, 20 mM $MgCl_2$, 20 mM $NaHCO_3$, and 0.5 mM EDTA.

Insoluble material was removed by centrifugation (27,000 x g, 10 min, 4°C), and the supernatant was dialysed at 4°C for up to four days against buffer containing 25 mM Tris-HCl, pH 7.6 and 0.2 mM EDTA, that was frequently changed. Crystals were collected by centrifugation (12,000 x g, 10 min, 4°C) and resuspended in buffer containing 10 mM NaP_i, pH 7.6, 50 mM NaCl, 1 mM EDTA and 10 % (v/v) glycerol. The solution was assayed for Rubisco activity and concentration, snap frozen, and stored at –80 °C.

Some preparations of L335V tobacco Rubisco included an ion-exchange chromatography step on an AKTA Explorer FPLC system using a Waters HR Q column (125 ml, 250 mm x 25 mm) and a 0–0.35 M NaCl gradient over 28 column volumes (5 $ml.min^{-1}$), similar to the procedure used for spinach Rubisco (Morell et al. 1997). Fractions containing Rubisco activity eluted at 220 mM NaCl (Figure 2.2A), were pooled, dialysed overnight against storage buffer (10 mM NaP_i, pH 7.6, 50 mM NaCl, 1 mM EDTA, 10 % (v/v) glycerol), snap frozen, and stored at –80 °C.

Rubisco concentration was estimated from the absorbance at 280 nm, under the assumption that the protein concentration in $mg.ml^{-1}$ is given by A_{280} x 0.7 (Kung et al. 1980), which agreed with that calculated from the binding of [^{14}C]carboxyarabinitol-P_2 (Hall et al. 1981). The yield was typically 40 mg of Rubisco from 80 g (wet weight) of tobacco leaves, and SDS-PAGE analysis showed only two proteins with molecular weights of 52 and 14 kDa as the major components, which correspond to the large and small Rubisco subunits respectively.

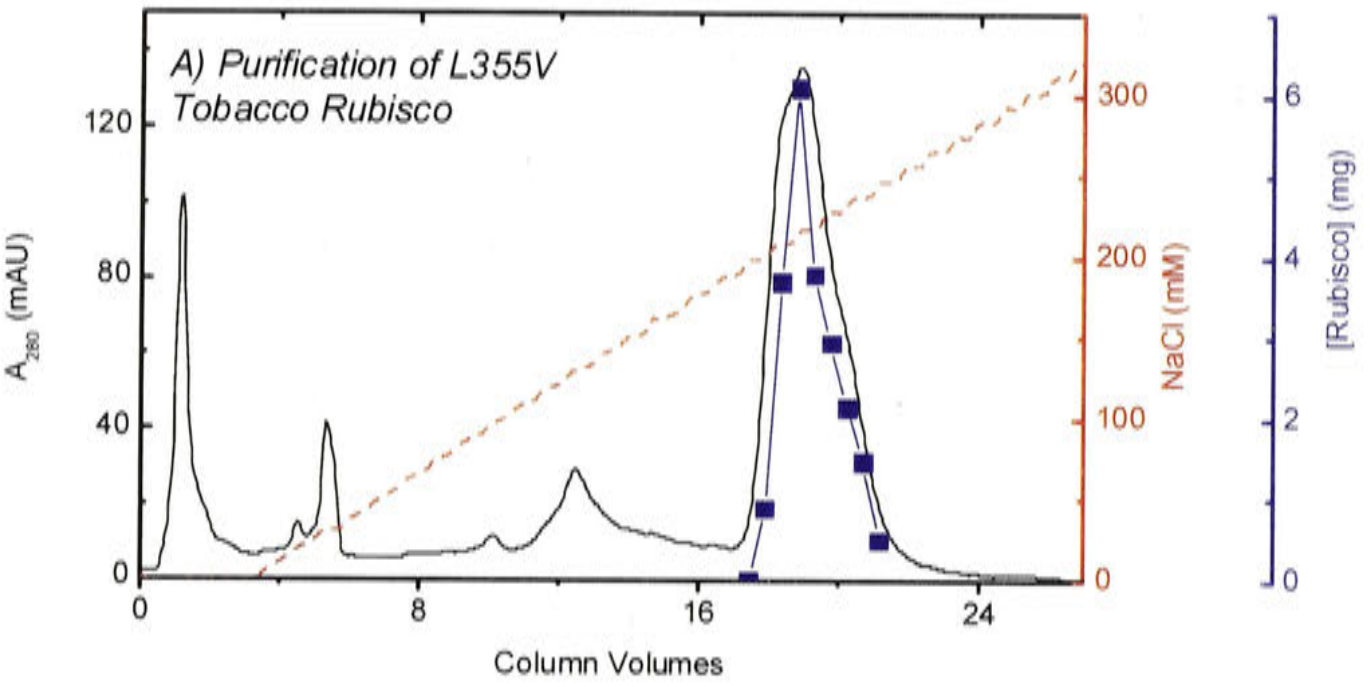

Figure 2.2 Purification of Rubisco by Anion Exchange Chromatography.

L335V tobacco (*A*) and *G. sulphuraria* (*B*) extracts were initially fractionated using polyethylene glycol precipitation. The precipitated protein was resuspended, and Rubisco was purified using anion exchange chromatography on a Waters HR Q column (125 ml, 250 mm x 25 mm) (L335V tobacco Rubisco) or an Amersham Biosciences Mono-Q HR 5/5 column (*G. sulphuraria*) using a 0-0.35 M NaCl gradient (50 mM Tris-HCl, pH 8.0, 1 mM EDTA), shown as -- on the right ordinate. The A_{280} was monitored to detect protein elution. Fractions were collected, and the relative Rubisco activity measured using a spectrophotometric assay (shown by ■, far right ordinate).

2.2.3.2 G. sulphuraria *Rubisco*

Cultures of *G. sulphuraria* were grown in liquid cultures, and the Rubisco was purified by anion exchange chromatography. Cells were grown in Cyanidium medium (Allen 1959) in 10-20 l glass containers at 30°C under constant illumination (480-660 µmol quanta.m^{-2}.s^{-1} at the surface) and vigorous sparging with air. Cells were harvested by using a continuos flow centrifuge, and were resuspended in three volumes of extraction buffer (100 mM EPPS-NaOH, pH 8.0, 20 mM $MgCl_2$, 1 mM EDTA, 1 mM PMSF, 1 mM DTT). The cells were lysed in a French Press (16,000 psi) and clarified by centrifugation (10 min, 13,000 x g, 4°C). 60 % (w/v) PEG_{3350} was added dropwise to the solution to a final concentration of 10 %, and the solution was stirred on ice for 30 min before being centrifuged again (10 min, 13,000 x g, 4°C). The green pellet was discarded, and 60 % (w/v) PEG_{3350} added to the blue supernatant to a final concentration of 20 %. The sample was centrifuged (10 min, 13,000 x g, 4°C), and the blue pellet was resuspended in buffer containing 100 mM EPPS-NaOH, pH 8.0, 20 mM $MgCl_2$ and 1 mM EDTA.

The Rubisco was separated on an AKTA Explorer FPLC system using a MonoQ HR 5/5 column (Amersham Biosciences) eluted with 50 mM Tris-HCl, pH 8.0, 1 mM EDTA and a 0-0.35 M NaCl gradient over 30 column volumes (1 ml.min^{-1}). Fractions containing Rubisco activity eluted at 150 mM NaCl (Figure 2.2B), were pooled, dialysed overnight at 4°C against storage buffer (20 mM K_2HPO_4, pH 8.0, 1 mM EDTA), before glycerol was added to 10 % (v/v) and the samples were snap-frozen, and stored at –80°C.

Rubisco concentration was estimated using Coomassie Plus Protein Reagent (Pierce) with bovine serum albumin as a standard, which showed agreement to that calculated from the binding of [^{14}C]carboxyarabinitol-P_2 (Hall et al. 1981). The yield was typically 6 mg Rubisco from 12 g (wet weight) cells, and SDS-PAGE analysis showed two proteins with molecular weights of 54 and 17 kDa as the major components (> 90%), which correspond to the large and small Rubisco subunits respectively.

2.2.3.3 R. rubrum *Rubisco*

Rather than direct purification of Rubisco from *R. rubrum*, a plasmid containing the gene encoding the protein was used to transform *E.coli* cells, and the enzyme was then purified using affinity chromatography. The p*Rr*His plasmid contains the gene for Rubisco from *R. rubrum* fused to a 5' hexahystidyl coding sequence (Whitney and

Andrews 2001b), the product of which will be referred to as His-*Rubrum* in this thesis. *E. coli* BL 21, pLysS, p*Rr*His cells were grown at 25°C in 2YT media containing kanamycin (30 $\mu g.ml^{-1}$), and when the A_{600} was 0.4, the culture was induced with 0.2 mM IPTG. After six h, the cells were harvested by centrifugation (10 min, 13,000 x g, 4°C) and resuspended in three volumes of extraction buffer (50 mM NaH_2PO_4, pH 8.0, 20 mM imidazole, 300 mM NaCl). The cells were lysed in a French Press (16,000 psi) and clarified by centrifugation (10 min, 13,000 x g, 4°C) and the supernatant was applied to a Ni-NTA (Qiagen) column (20 ml) on an AKTA Explorer FPLC system. The column was washed with extraction buffer (1 $ml.min^{-1}$) for 3.5 column volumes, and the A_{280} monitored. Elution buffer (50 mM NaH_2PO_4, pH 8.0, 250 mM imidazole, 300 mM NaCl) was then used to elute the sample (1 $ml.min^{-1}$) (Figure 2.3). Fractions containing Rubisco activity were pooled, and dialysed overnight at 4°C against storage buffer (10 mM NaP_i, pH 7.6, 1 mM EDTA, 50 mM NaCl), before glycerol was added to 10 % (v/v) and the samples were snap-frozen, and stored at –80°C.

Rubisco concentration was estimated using Coomassie Plus Protein Reagent with bovine serum albumin as a standard, which showed agreement to that calculated from the binding of [^{14}C]carboxyarabinitol-P_2 (Hall et al. 1981). The yield was typically 30 mg Rubisco from 3 g (wet weight) of cells, and SDS-PAGE analysis showed a single protein with a molecular weights 55 kDa, corresponding to the Rubisco large subunit.

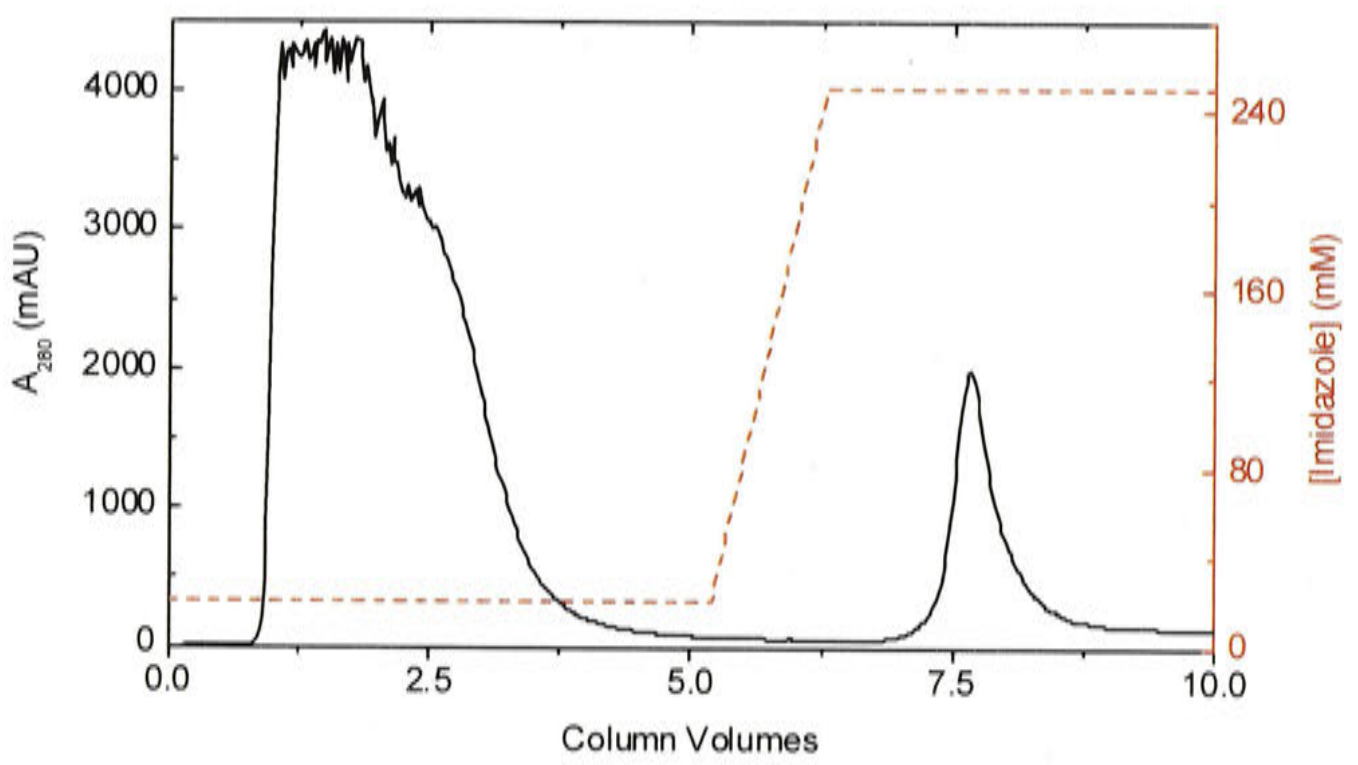

Figure 2.3. Purification of His-*Rubrum* Rubisco by Affinity Chromatography.

His-*Rubrum* Rubisco was initially extracted by lysis of *E. coli* cells. The supernatant was purified by affinity chromatography using Ni-NTA resin (20 ml, 120 mm x 20 mm). The column was washed with buffer (50 mM NaH_2PO_4, 20 mM imidazole, 300 mM NaCl, pH 8.0) before bound proteins were eluted using 250 mM imidazole (--, shown on right ordinate). The A_{280} was monitored to detect protein elution.

2.2.4 Rubisco Activase Purification

Rather than direct purification of Rubisco activase from tobacco plants, a plasmid encoding the Rubisco activase gene was used to transform E.coli cells, and the expressed enzyme was purified using affinity chromatography. The pET-ActH plasmid contains the gene for Rubisco activase from tobacco fused to a 5' hexahystidyl coding sequence. *E. coli* BL 21, pLysS, pET-ActH cells were grown at 37°C in LB media containing kanamycin (30 $\mu g.ml^{-1}$), and when the A_{600} was 0.4, the culture was induced with 0.4 mM IPTG. After three h, the cells were harvested by centrifugation (10 min, 13,000 x g, 4°C) and resuspended in three volumes of extraction buffer (50 mM Tris-HCl, pH 8.0, 10 mM imidazole, 300 mM NaCl, 10 mM $MgCl_2$). The cells were lysed in a French Press (10,000 psi), and clarified by centrifugation (10 min, 13,000 x g, 4°C). The supernatant was applied to 5 ml of Ni-NTA resin, and the column was washed with four column volumes of extraction buffer. Elution buffer (50 mM Tris-HCl, pH 8.0, 200 mM imidazole, 300 mM NaCl, 10 mM $MgCl_2$) was used to elute the protein.Fractions were assayed for protein using Coomassie Plus Protein Reagent, using bovine serum albumin as a standard, and those containing protein were pooled, and dialysed overnight at 4°C against storage buffer (10 mM NaP_i, pH 7.2, 1 mM EDTA, 50 mM NaCl), before glycerol was added to 10 % (v/v) and samples were snap-frozen, and stored at –80°C. The yield was typically 30 mg protein from 4 g (wet weight) of cells, and SDS-PAGE analysis showed only a protein with a molecular weight of approximately 43 kDa, which corresponds to the Rubisco activase monomer.

2.2.5 ^{3}H-Ribulose-P_2 Synthesis

[1-^{3}H]Ribulose-P_2, the substrate of Rubisco, was synthesised from [2-^{3}H]glucose using an enzymatic process and purified by anion exchange chromatography (Kane et al. 1994; Kane et al. 1998). Initially, [2-^{3}H]glucose (0.06 µmol, 14.0 $Ci.mmol^{-1}$) was combined with non-labelled glucose (1.75 µmol) to reduce the specific radioactivity (final activity, 465 $mCi.mmol^{-1}$). Hexokinase (4 $units.ml^{-1}$) and glucose-6-P dehydrogenase (4 $units.ml^{-1}$) were used to convert [1-^{3}H]glucose (1.8 µmol) into [1-^{3}H]gluconate-6-P (1.8 µmol) in buffer containing 50 mM Tris-HCl, pH 8.0, 10 mM $MgCl_2$, 0.3 mM ATP, 0.6 mM NADH and an ATP regenerating system consisting of 1 mM creatine phosphate and 10 $units.ml^{-1}$ creatine phosphokinase. The absorbance at 340 nm was monitored, and showed a rapid increase of 1.1 absorbance units, implying full conversion of glucose into gluconate-6-P. The pH was adjusted to 10.0 using 5N NaOH, and reduced to 7.5 with 1N HCl after 5 min incubation at 25°C.

6-Phosphogluconate dehydrogenase (1.2 units.ml^{-1}) was then added to convert the [1-^{3}H]gluconate-6-P into [1-^{3}H]ribulose-5-P (1.5 µmol). The absorbance at 340 nm was again monitored, and showed an increase of 0.9 absorbance units over eight min. Phosphoribulokinase (0.5 units.ml^{-1}) and 10 mM DTT were then added to the solution, which was incubated at 25°C to allow conversion of [1-^{3}H]ribulose-5-P into [1-^{3}H]ribulose-P_2 (1.5 µmol). After 60 min, the pH was adjusted to 2.8 using AG50W-X8 beads and the solution was applied to a charcoal column (0.1 g charcoal and 0.5 g cellulose powder) and was eluted with two volumes of water, to remove any residual ATP.

The eluted solution was applied to a AG1-X8 (Cl^-) column (5 ml, 15 mm x 50 mm, Bio-Rad) and purified on an AKTA Explorer FPLC system by anion exchange chromatography using with a 40-250 mM NaCl gradient over 10 column volumes in 3 mM HCl (2 ml.min^{-1}). [1-^{3}H]Ribulose-P_2 eluted at 200 mM NaCl (Figure 2.4A), and fractions were pooled, and stored in buffer containing 3 mM HCl and 200 mM NaCl under liquid N_2.

2.2.6 Xylulose-P_2 Synthesis

Xylulose-P_2, an epimer of ribulose-P_2 which acts as an inhibitor of Rubisco, was synthesised from glycolaldehyde phosphate and dihydroxyacetone phosphate using aldolase, as previously described (Byrne and Lardy 1954), and purified by anion exchange chromatography. Glycolaldehyde phosphate is not available commercially, but could be synthesised by the periodate oxidation of ribose-5-P, as previously described (Loring et al. 1956). Oxidation of ribose-5-P (1030 µmol) was carried out on ice with 60 mM NaIO4, and the pH was maintained at 6.20 by the addition of 0.05 M NaOH. The pH stabilised after 60 min, after yielding five protons per ribose-5-P oxidised. Barium acetate (0.4 M) was added to the solution, which was incubated at 4°C overnight before the removal of insoluble barium salts by filtration, adjusting the pH to 5.0 using 10 % H_2SO_4 and applying the solution to 5 ml of AG50W-X8 (Na^+) resin. The pH of the resulting solution containing glycolaldehyde phosphate (~500 µmol) was increased to 6.5 using 1N NaOH, before the addition of dihydroxyacetone-P (132 µmol) and aldolase (0.04 mg.ml^{-1}). This solution was incubated at 37°C, during which aldolase catalysed the production of xylulose-P_2 (10 µmol), before being applied to a AG1-X8 (Cl^-) column (400 ml, 35 mm x 300 mm).

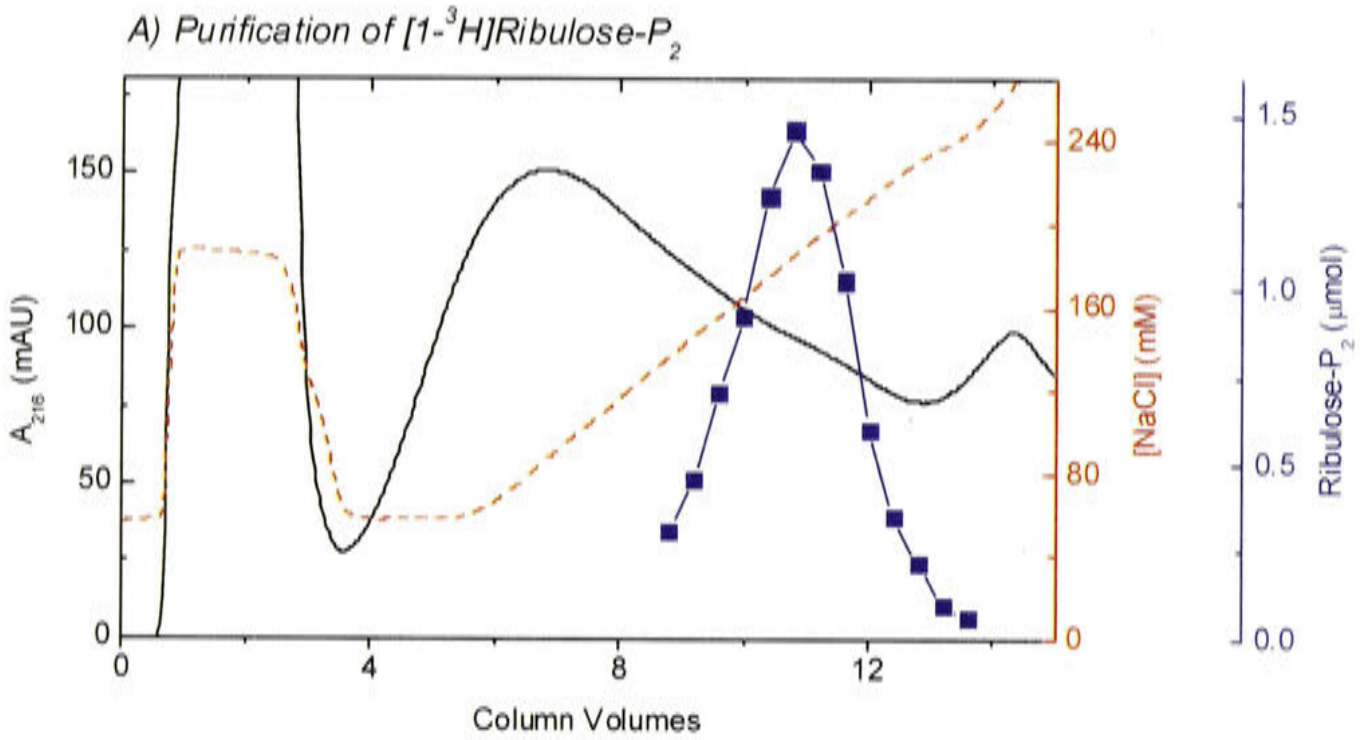

Figure 2.4. Purification of [1-^{3}H]Ribulose-P_2 and Xylulose-P_2 by Anion Exchange Chromatography.

[1-^{3}H]Ribulose-P_2 (*A*) and xylulose-P_2 (*B*) were purified by anion exchange chromatography using AG1-X8 (Cl^-) resin ([1-^{3}H]ribulose-P_2, 10 mm x 50 mm, xylulose-P_2 35 mm x 300 mm). Samples were eluted in 3 mM HCl using a NaCl gradient (-- shown on right ordinate). Elution of compounds was monitored by measuring A_{216} or A_{254}, and fractions were collected. The relative [1-^{3}H]ribulose-P_2 concentration (■, far right ordinate) was determined by measuring the radioactivity in the fractions. Relative xylulose-P_2 concentration (■, far right ordinate) was measured using spectrophotometric assays.

Xylulose-P_2 was purified on an AKTA Explorer FPLC system by anion exchange chromatography using an 80-250 mM NaCl gradient over five column volumes in 3 mM HCl (8 $ml.min^{-1}$). The xylulose-P_2 concentration was determined using a coupled spectrophotometric assay containing 100 mM EPPS-NaOH, pH 8.0, 0.2 mM NADH, 1 mM EDTA, glycerol-3-phosphate dehydrogenase (2.5 $\mu g.ml^{-1}$) and aldolase (200 $\mu g.ml^{-1}$) by monitoring the decrease in absorbance at 340 nm. Xylulose-P_2 eluted at 230 mM NaCl (Figure 2.4B), after the elution of dihydroxyacetone-P, and fractions were pooled and dried down using a rotary evaporator. The sample was then desalted on an AKTA Explorer FPLC system using size exclusion chromatography on a Sephadex G-10 column (66 ml, 15 mm x 300 mm Amersham Biosciences) eluted with 3 mM HCl (0.5 $ml.min^{-1}$), and the desalted fractions containing xylulose-P_2 were dried down again using a rotary evaporator and stored in 3 mM HCl under liquid N_2.

2.2.7 Carboxyarabinitol-P_2 Synthesis

Carboxypentitol-P_2, an inhibitor of Rubisco, was synthesised by treating ribulose-P_2 with an excess of cyanide to produce a mixture of carboxyarabinitol-P_2 and carboxyribitol-P_2, as previously described (Pierce et al. 1980), and purified by anion exchange chromatography. Ribulose-P_2 was produced enzymatically from ribulose-5-P (690 µmol) in a solution adjusted to pH 7.0 with 1 N NaOH, that contained 40 mM MgCl2, 0.23 mM ATP, 5 mM DTT, 8 $units.ml^{-1}$ phosphoribose-isomerase, 1.5 $units.ml^{-1}$ phosphoribose-kinase, and a coupling system to regenerate ATP consisting of 15 mM creatine phosphate and 1.5 $units.ml^{-1}$ creatine phosphokinase (Kane et al. 1994; Kane et al. 1998). This solution was incubated at 25°C for 60 min, before the pH was adjusted to 3.4 by the addition of AG50W-X8 (H^+) resin, which was subsequently removed by filtration. Spectrophotometric assays, as described in Section 2.2.2, were used to measure the concentration of ribulose-P_2 (630 µmol), before the pH was adjusted to 8.3 by the addition of 1 M Tris-HCl. An excess (1200 µmol) of KCN was added to the solution, which was incubated at 25°C for 48 h before removing the unreacted KCN by adding AG50W-X8 (H^+) resin (Bio-Rad) and drying down the solution using a rotary evaporator. The solution was stored over P_2O_5 to ensure complete removal of H_2O and lactonisation of carboxypenitol-P_2. Excess ATP was removed by applying the solution to a charcoal column (1 g charcoal and 5 g cellulose powder) and eluting with two volumes of H_2O.

The eluted solution was applied to a AG1-X8 (Cl^-) column (260 ml, 30 mm x 350 mm), and the carboxyarabinitol-P_2 lactone was separated from carboxyribitol-P_2 lactone

and the free acid forms by anion exchange chromatography using and a 100-300 mM NaCl gradient over 15 column volumes in 3 mM HCl (5 $ml.min^{-1}$) on an AKTA Explorer FPLC system. The lactone form of carboxyarabinitol-P_2 eluted at 240 mM NaCl (Figure 2.5A), after the free acids and lactone of carboxyribitol-P_2. Carboxyarabinitol-P_2 concentration was determined by treating with calf intestinal alkaline phosphatase and measuring inorganic phosphate using the Chifflet assay (Chifflet et al. 1988). Fractions containing carboxyarabinitol-P_2 were pooled and dried down using a rotary evaporator, before being desalted using size exclusion chromatography on a Sephadex G-10 column (66 ml, 15 mm x 300 mm) eluted with H_2O (0.5 $ml.min^{-1}$) on an AKTA Explorer FPLC system, before being dried down again using a rotary evaporator, and stored in 50 mM Bicine (pH 9.3) at –80°C. Carboxy-^{14}C-labelled carboxypentitol-P_2 was produced using ^{14}C labelled cyanide.

2.2.8 Carboxyarabinitol-1-P Synthesis

Carboxyarabinitol-1-P, an inhibitor of Rubisco, was synthesised by removing the 5-P group from carboxyarabinitol-P_2 , as previously described (Moore et al. 1991), and purified by anion exchange chromatography. Carboxyarabinitol-P_2 (20 μM) was incubated with acid phosphatase (3 $units.ml^{-1}$, from potato) in 50 mM Na Formate, pH 5.7, for three h at room temperature, before AG50W-X8 (H^+) resin was added to stop the reaction.

The solution was then applied to a AG1-X8 (Cl^-) column (5 ml, 15 mm x 50 mm), and carboxyarabinitol-1-P was separated from carboxyarabinitol-P_2 , carboxyarabinitol, and inorganic phosphate by anion exchange chromatography on an AKTA Explorer FPLC system using with a 0-200 mM NaCl gradient over 10 column volumes in 3 mM HCl (5 $ml.min^{-1}$). Carboxyarabinitol-1-P (6.6 μmol) eluted at 90 mM NaCl (Figure 2.5B), which was coincident with inorganic phosphate (PO_4^{3-}) (16.2 μmol). Fractions were pooled and desalted using size exclusion chromatography on a Sephadex G-10 column (66 ml, 15 mm x 300 mm) eluted with H_2O (0.5 $ml.min^{-1}$), before being dried down again using a rotary evaporator, and stored in 50 mM Bicine (pH 9.3) at –80°C. The size exclusion chromatography also separated the carboxyarabinitol-1-P from inorganic phosphate.

The carboxyarabinitol-1-P concentration was determined comparing the amount of free phosphate in the sample with the amount of phosphate after treating the with calf intestinal alkaline phosphatase. Inorganic phosphate concentrations were determined using the Chifflet assay (Chifflet et al. 1988).

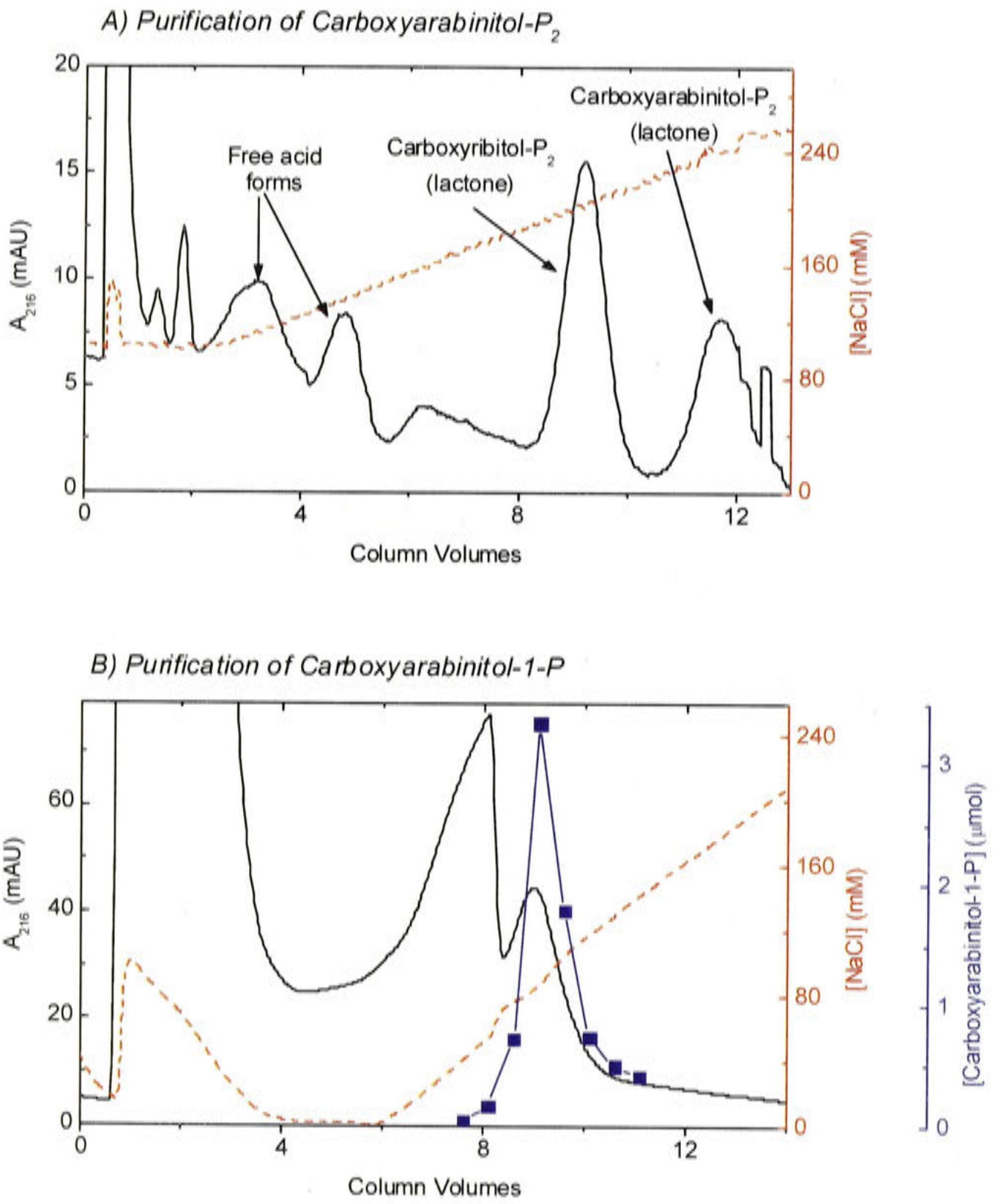

Figure 2.5. Purification of Carboxyarabinitol-P_2 and Carboxyarabinitol-1-P by Anion Exchange Chromatography.

Carboxyarabinitol-P_2 (*A*) and carboxyarabinitol-1-P (*B*) were purified by anion exchange chromatography using AG1-X8 (Cl^-) resin (carboxyarabinitol-P_2, 30 mm x 350 mm, carboxyarabinitol-1-P 10 mm x 50 mm). Samples were eluted in 3 mM HCl using a NaCl gradient (-- shown on right ordinate). Elution of compounds was monitored by measuring A_{216}, and fractions were collected. The relative carboxyarabinitol-1-P concentration (■, far right ordinate) was determined by measuring the concentration of inorganic phosphate after treatment with alkaline phosphatase.

3 Self-Inhibition of Rubisco

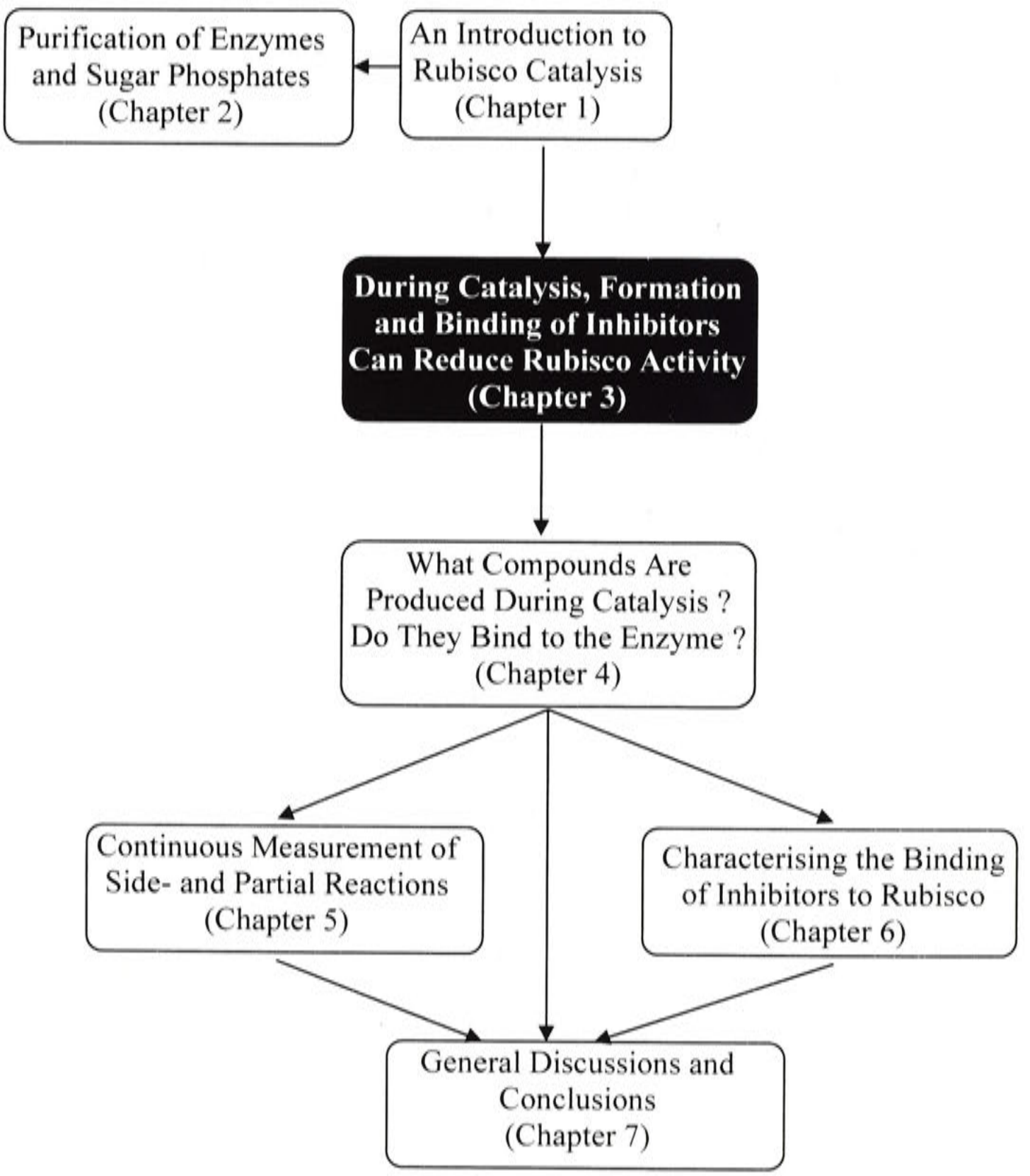

3.1 Introduction

Many *in vitro* studies of purified Rubisco have observed variations in the activity of the enzyme, but these changes in activity are not always fully characterised. The first purification of Rubisco from spinach yielded an enzyme that formed P-glycerate from ribulose-P_2 and CO_2, but was inhibited by high concentrations (above 0.5 mM) of ribulose-P_2 (Weissbach et al. 1956; Paulsen and Lane 1966). Conversely, later studies suggested that high ribulose-P_2 concentrations actually stimulated the activity of the enzyme (Yokota 1991b). The change in activity over time was attributed to the binding of ribulose-P_2 to an allosteric regulatory site (Chu and Bassham 1975) or by the formation of inhibitory compounds from ribulose-P_2, which would be present in higher concentrations at higher ribulose-P_2 concentrations (Paech et al. 1978).

Further studies directly showed that purified enzyme from higher plants exhibited an *in vitro* decline in activity over time (Chu and Bassham 1975). The activity decreased exponentially to a final steady state (v_f) that was less than the initial rate (v_i), in a process that was referred to as 'fallover' (Edmondson et al. 1990a). The v_f/v_i ratio was typically around 0.3, and the time for half of the decrease to happen ($t_{(1/2)}$) was around seven min at pH 8.3. Fallover could not be attributed to substrate exhaustion, product accumulation or protein degradation, and could not be reversed by diluting the enzyme or by the complete consumption of ribulose-P_2. The degree of fallover was dependant on the CO_2 concentration and the pH, with a lower v_f/v_i ratio at lower CO_2 concentrations and lower pH (Edmondson et al. 1990a). Varying the ribulose-P_2 concentration had negligible effect on the rate or degree of fallover. Both the rate and extent of fallover were lessened by the addition of H_2O_2 or 6-phosphogluconate.

3.1.1 Distribution of Fallover

The fallover phenomenon does not appear to be ubiquitous *in vitro*. All measured higher plants have a 'green-type' Form I Rubisco that shows a decrease in activity over time (Edmondson et al. 1990a). The 'green-type' Form I enzyme from the purple bacterium *Rhodobacter capsulatus* also exhibited fallover (Horken and Tabita 1999b), although the 'red-type' Form I Rubisco from *Rhodobacter sphaeroides* did not (Gibson and Tabita 1979).

Conversely, several 'green-type' Form I Rubisco enzymes show no inhibition; cyanobacterial Rubisco, such as that from *Anabaena*, does not show any self-inhibition

(Li and Tabita 1997). The 'green-type' Form I Rubisco from *Thiobacillus denitrificans*, a chemoautotrophic bacterium, also did not show fallover (Hernandez et al. 1996).

Fallover was reported for 'red-type' Form I Rubisco from unicellular red algae and red macroalgae (Uemura et al. 1998). However these experiments used commercially prepared ribulose-P_2, which was later shown to contain inhibitory compounds that accentuate the drop in activity (Mizohata et al. 2003).

Fallover is much less apparent in Form II Rubisco enzymes, which show little or no decrease in activity over time. The only exception is some mutant enzymes, which exhibit a decrease in activity over time (Lee et al. 1993).

3.1.2 Proposed Explanations for Fallover

Several different explanations have been proposed for the observed decline in activity during catalysis. Rubisco could lose the catalytically important carbamylated lysine residue and Mg^{2+} ion, resulting in the formation of an inactive complex between uncarbamylated Rubisco and ribulose-P_2 (Paech et al. 1977). Alternatively, ribulose-P_2 could bind reversibly to a regulatory site separate to the active site, which regulates activity (Chu and Bassham 1975; Yokota 1991b). Other models suggest slow, tight-binding inhibition by isomerization or degradation products derived from ribulose-P_2 during storage or under assay conditions (Paech et al. 1978).

If the Rubisco enzyme became decarbamylated during the assay, the inactive E:ribulose-P_2 complex could form. A dual-isotope method used to monitor carbamylation status during catalysis showed that no decarbamylation occurred during the assay, in the presence of ribulose-P_2 and $NaHCO_3$. When activated Rubisco was incubated in the absence of $NaHCO_3$, decarbamylation happened much more quickly in the absence of ribulose-P_2 than if ribulose-P_2 was included in the assay (Edmondson et al. 1990c). Zhu and Jensen (1991a) observed no change in carbamylation during the assay at pH 8.5 and only moderate loss at pH 7.5, showing that the loss of activity was not due to the decarbamylation of the active site. This showed that the decrease in activity was not due to the decarbamylation of the active site.

The 'hysteresis' theory proposed that fallover is due the binding of ribulose-P_2 to an allosteric site which is separate from the catalytic site. It was suggested that after ribulose-P_2 binds to the catalytic site, the Rubisco enzyme slowly undergoes a conformational change into a form that has less activity. Binding of ribulose-P_2 to the regulatory site causes further conformational changes that alters the activity of the

enzyme (Yokota and Kitaoka 1989; Yokota 1991b). This model was based on the observation that the decrease in activity occurred to a lesser extent at higher ribulose-P_2 concentrations. However, these observations were complicated by the use of commercially prepared ribulose-P_2, which has been shown to increase the rate of fallover due to the presence of ribulose-P_2 oxidation and degradation products (Kane et al. 1998; Mizohata et al. 2003). The observation that highly pure ribulose-P_2 causes less inhibition of the enzyme shows that contaminating compounds may be inhibitory, and it is unlikely that there is an allosteric binding site for ribulose-P_2 on the Rubisco enzyme.

The most likely explanation for inhibition during *in vitro* assay is the binding of inhibitory compounds during catalysis. Edmondson et al. (1990b) carried out a full characterisation of the fallover phenomenon, with the aim of finding the reason for fallover inhibition. Some of the enzyme activity that had been lost over the course of the assay could be recovered by gel filtration, with almost complete recovery when 200 mM $(NH_4)_2SO_4$ was included, suggesting that inhibition was due to the binding of inhibitors. This was also supported by the partial recovery of activity after incubation for 24 h at room temperature or incubation with alkaline phosphatase. An extract (0.07 % of the initial concentration of ribulose-P_2) was isolated by gel filtration of inhibited enzyme followed by acid precipitation of enzyme, which was inhibitory when applied to Rubisco, with increasing rate of decline as the inhibitor concentration was increased. Complete inhibition was not observed, with the same steady state value being reached at saturating inhibitor concentrations.

With the isolation of the inhibitory mixture, further characterisation of the inhibition could be carried out. The inhibitor was stable at pH 2.0, but not at pH 8.3, and was not affected by incubation with H_2O_2 or *o*-phenylene-diamine, suggesting it was not an α-dicarbonyl compound. The inhibition was destroyed by acid phosphatase, showing that it is phosphorylated. The inhibitor concentration was dependent on the number of turnovers rather than the time taken to use up the ribulose-P_2, and substrate CO_2 was not incorporated into the compound. These observations suggested that the inhibitor is likely to be produced as a side-product of the Rubisco reaction mechanism, possibly misprotonation of the enediol. At lower CO_2 concentrations, the level of enzyme with enediol in the active site would be higher, resulting in increased chance of misprotonation or other reactions, and a higher rate of self-inhibition. At higher pH there are fewer protons available in solution. Since misprotonation of the enediol

involves the attack of a proton, this reaction will be reduced as the protons become less available at increased pH, and hence the reduction of self-inhibition.

3.1.3 Identification of Inhibitors

Once it was established that inhibition was due to slow, tight binding inhibitors, experiments were carried out to establish the identity of the inhibitors. Borohydride reduction of a ketone compound can produce several different isomers, depending on the structure of the initial compound. Ribulose-P_2 produces ribitol and arabinitol, while xylulose-P_2 produces arabinitol and xylitol, and keto-arabinitol-P_2 would produce only arabinitol. Isolated inhibitory compounds were dephosphorylated and reduced with [^{3}H]borohydride, which yielded arabinitol and xylitol, suggesting that the inhibitor contained at least xylulose-P_2 as well as the possibility of some keto-arabinitol-P_2 (Edmondson et al. 1990b).

The presence of xylulose-P_2 was further confirmed by using aldolase, which catalyses the cleavage of xylulose-P_2 into glycolaldehyde phosphate and dihydroxyacetone-P. Assays of the catalysis products showed xylulose-P_2 to be present as 0.26 % of the initial ribulose-P_2 concentration (Edmondson et al. 1990d). Treatment of the inhibitory mixture with aldolase partially reduced the inhibitory concentration, showing that while xylulose-P_2 was indeed present as an inhibitor, there was also another inhibitory compound present.

Incubation of the inhibitory mixture at pH 12.4 also reduced the concentration of inhibitor, but would have no effect on xylulose-P_2, suggesting that inhibition was due to two different compounds. The second compound, which was unstable at high pH, was most likely thought to be keto-arabinitol-P_2 (Edmondson et al. 1990d).

Production of xylulose-P_2 and keto-arabinitol-P_2 by Rubisco was also observed by Zhu and Jensen (1991a), with little change in carbamylation over the course of the assay. Xylulose-P_2 and keto-arabinitol-P_2 were identified as the inhibitors bound to the enzyme, with proportionally more xylulose-P_2 at pH 7.5 than at pH 8.5. Similar experiments showed that a lower pH favoured xylulose-P_2 formation, consistent with a higher proton availability increasing the rate of proton attack on the enediol, and that xylulose-P_2 bound preferentially to decarbamylated sites (Zhu and Jensen 1991b).

However, the identification of the inhibitors as keto-arabinitol-P_2 and xylulose-P_2 did not explain why the inhibition was sensitive to H_2O_2 (Edmondson et al. 1990a), as both of these compounds should be stable in the presence of peroxide. Later studies

isolated another inhibitory compound that bound tightly to Rubisco (Kane et al. 1998). Incubation of the inhibitor with *o*-phenylene-diamine yielded a quinoxaline compound, showing that the inhibitor was a dicarbonyl compound. Treatment with H_2O_2 and catalase produced P-glycolate and P-glycerate, which was consistent with the inhibitor being pentodiulose-P_2, which can be derived from the peroxyketone intermediate during catalysis, or by the non-enzymatic oxidation of ribulose-P_2 in the presence of metal ions.

While Rubisco formed some inhibitors during catalysis, the extent and rate of decline were observed to vary between different preparations of ribulose-P_2, suggesting that inhibitory compounds were present in preparations of ribulose-P_2. It was found that different preparations of substrate contained varying concentrations of pentodiulose-P_2 (Kane et al. 1998), xylulose-P_2 (McCurry and Tolbert 1977) and deoxy-pentodiulose-P, (Paech et al. 1978), which could be present in different batches of ribulose-P_2 preparations in amounts as high as 1 % of the ribulose-P_2 concentration.

Storage of ribulose-P_2 was shown to have an effect on the inhibitor concentration, due to the formation or removal of pentodiulose-P_2. Little inhibition was observed when ribulose-P_2 was stored in the absence of O_2, which prevents the oxidation to form pentodiulose-P_2, or after pre-treatment with H_2O_2, which reacts with pentodiulose-P_2 to yield P-glycerate and P-glycolate (Kane et al. 1998). Negligible inhibition was also observed when ribulose-P_2 was stored in Tris buffer, which can react with the dicarbonyl group. The presence of inhibitory compounds in some preparations of ribulose-P_2 increases the rate of inhibition, and often necessitates further purification for complete separation of ribulose-P_2 from inhibitors (Mizohata et al. 2003).

Previous studies are likely to have misidentified one of the inhibitors as keto-arabinitol-P_2 instead of pentodiulose-P_2. Initial identification of the inhibitor as keto-arabinitol-P_2 was based on the observation of arabinitol as the only product of borohydride reduction, however Chen and Hartman (1995) showed that under some conditions pentodiulose-P_2 reduction gives rise to arabinitol-P_2 almost exclusively, rather than a combination of arabinitol, ribitol and xylitol. They also showed the formation of the quinoxaline complex between pentodiulose-P_2 and *o*-phenylene-diamine, reaction of pentodiulose-P_2 with H_2O_2 to form P-glycolate and P-glycerate, and that pentodiulose-P_2 is stabilised by the presence of borate.

Later experiments showed that fallover inhibition was greater when oxygen was present (Kane et al. 1998), due to an increase in the formation of inhibitors. While

xylulose-P_2 production increased as the levels of CO_2 or O_2 decreased, due to an increased chance of misprotonation of an enediol intermediate bound to enzyme active sites, the formation of keto-arabinitol-P_2 was dependent on the presence of O_2 suggesting that it was derived from an intermediate of the oxygenase reaction (Zhu et al. 1998). Identification of one inhibitor as keto-arabinitol-P_2 was based on the products of borohydride reduction, and it is likely that the compound was pentodiulose-P_2. This supports the idea that the increased fallover at higher oxygen levels was due to increased production of pentodiulose-P_2 from the peroxyketone intermediate.

3.1.4 Rubisco Activase

To prevent the total inhibition of Rubisco *in vivo*, higher plants contain the enzyme Rubisco activase, which uses the energy from the hydrolysis of ATP to loosen the active site, allowing the release of inhibitors, as described in Section 1.5.6. Addition of Rubisco activase to *in vitro* assays reduces the level of Rubisco inhibition (Robinson and Portis 1989b), due to the release of inhibitory compounds from the active site.

3.1.5 Specific Aims and Objectives

This chapter compares the level and pattern of inhibition of different Rubisco enzymes during *in vitro* assays using spectrophotometric assays. Previous observations for the activity of Rubisco from higher plants, cyanobacteria, and *R. rubrum* are confirmed, and studies are extended to include the L335V tobacco Rubisco mutant and the 'red-like' Form I enzyme from *G. sulphuraria*. This work clarifies some of the previous studies of self-inhibition that may have been influenced by the use of ribulose-P_2 preparations that contained inhibitory compounds The effect of oxygen on the level and pattern of inhibition is confirmed for higher plant Rubisco, as is the effect of the activating protein Rubisco activase, and studies are extended to test the effect of oxygen levels and Rubisco activase on the L335V tobacco Rubisco mutant.

3.2 Materials and Methods

3.2.1 Assaying Self-Inhibition of Rubisco

Rubisco activity was measured using the spectrophotometric assay described in Section 2.2.2. The reaction was initiated by the addition of activated Rubisco (0.2–0.8 $\mu g.ml^{-1}$) and the absorbance at 340 nm was measured at five second intervals for up to 2000 s. Assays were carried out in duplicate, and at least two separate runs were performed. Data for product accumulation versus time was pooled, and fitted to the following equation (Edmondson et al. 1990a), which is also referred to in Section 6.2.9,

$$[product] = v_f .t + \frac{(v_i - v_f)(1 - e^{-k_{obs} .t})}{k_{obs}} \qquad \textbf{(Equation 3.1)}$$

to calculate the initial rate (v_i), final steady-state rate (v_f), and the observed first-order rate constant (k_{obs}) using non-linear regression software (OriginLab, Northampton, MA). Residual activity versus time was plotted using the parameter estimates obtained and the differentiated form of Equation 3.1, in Equation 3.2.

$$\frac{v}{v_i} = \left(1 - \frac{v_f}{v_i}\right) e^{-k_{obs} .t} + \frac{v_f}{v_i} \qquad \textbf{(Equation 3.2)}$$

Anaerobic assays were carried out in septum-capped cuvettes in which the headspace was flushed with N_2, and using buffer that had been sparged with N_2.

3.2.2 The Effect of Activating Proteins

Rubisco activase can alleviate the self-inhibition of Rubisco activity (Robinson and Portis 1989b). Rubisco activity was measured using a spectrophotometric assay as described in Section 2.2.2, but in a buffer containing 100 mM Tricine-KOH, pH 8.0, 10 mM $MgCl_2$, 20 mM KCl, 6 % (w/v) PEG_{3350}, 0.5 mM ribulose-P_2, 0.5 mM DTT, 0.2 mM NADH, 2 mM ATP, 10 mM phosphocreatine, 20 mM $NaHCO_3$, 25 $units.ml^{-1}$ creatine phosphokinase, 500 $units.ml^{-1}$ carbonic anhydrase, 22.5 $units.ml^{-1}$ 3-phosphoglycerate kinase, 20 $units.ml^{-1}$ glyceraldehyde-3-phosphate dehydrogenase, 56 $units.ml^{-1}$ triose-phosphate-isomerase, and 20 $units.ml^{-1}$ glycerol-3-phosphate dehydrogenase, as described previously (Lan and Mott 1991; Salvucci 1992). Rubisco activase (0–100 $\mu g.ml^{-1}$) was added to the assays after 900 s.

3.3 Results

3.3.1 Self-Inhibition of Rubisco

Under aerobic conditions, at saturating $NaHCO_3$ concentrations, the activity of wild-type and L335V tobacco Rubisco decreased slowly over time after addition of ribulose-P_2 during *in vivo* assays (Figure 3.1), as is always seen for higher plant Rubisco enzymes. Equation 3.1 was used to give an estimate of the kinetic parameters (Table 3.1). Wild-type tobacco Rubisco fitted the data well, decreasing to a final rate that was 32 % of the initial rate with a half-time of 6 min. L335V tobacco Rubisco did not fit the data as well, with the rate appearing to decrease to zero, but exhibiting a very slow rate of decline. A better fit was obtained when v_f was set to zero, which gave similar values for v_i and k_{obs}.

Assays performed under anaerobic conditions showed less decline in activity than those performed under aerobic conditions (Table 3.1, Figure 3.1). Wild-type tobacco Rubisco activity dropped to 74 % of the initial rate, with a slightly faster rate of decline than under aerobic conditions, while L335V tobacco Rubisco showed no decline in activity over time under anaerobic conditions.

Rubisco from *G. sulphuraria*, *Synechococcus* PCC6301 and His-*Rubrum* showed no decrease in activity under aerobic conditions (Figure 3.2). A linear equation was used to calculate the reaction rate (Table 3.1)

3.3.2 The Effect of Rubisco Activase on Fallover

When Rubisco activase was added to fallover assays after 900 s (Figure 3.3), the pattern of inhibition was altered. There was an initial lag period after addition of the protein, followed by an increase in activity. In the presence of Rubisco activase, the activity was linear, and did not decrease further over time. The new steady state of activity was proportional to the concentration of Rubisco activase. L335V tobacco Rubisco did not respond to Rubisco activase to the same extent as wild-type tobacco Rubisco.

	v_i (s^{-1})	v_f/v_i	k_{obs} (s^{-1})	r^2
Wild-Type Tobacco				
Aerobic	2.82 ± 0.01	0.32	1.93 ± 0.05 x 10^{-3}	0.9991
Anaerobic	2.84 ± 0.01	0.74	2.25 ± 0.09 x 10^{-3}	0.9997
L335V Tobacco				
Aerobic	0.477 ± 0.004	-0.08	0.28 ± 0.18 x 10^{-3}	0.9999
Anaerobic	0.463 ± 0.001	1	NA[a]	0.9997
G. sulphuraria	1	1	NA	0.9989
Synechococcus PCC6301	11	1	NA	o.9992
His-*Rubrum*	7	1	NA	0.9994

NA[a], not applicable (no decrease in activity)

Table 3.1. Kinetic Parameters for the Decline in Rubisco Activity Over Time.

Activated Rubisco was added to spectrophotometric assays containing 0.5 mM ribulose-P_2 under CO_2 saturating conditions. Parameters (± S.E.) were calculated by fitting the data of Figure 3.1 and Figure 3.2 to Equation 3.1, or using linear regression where appropriate.

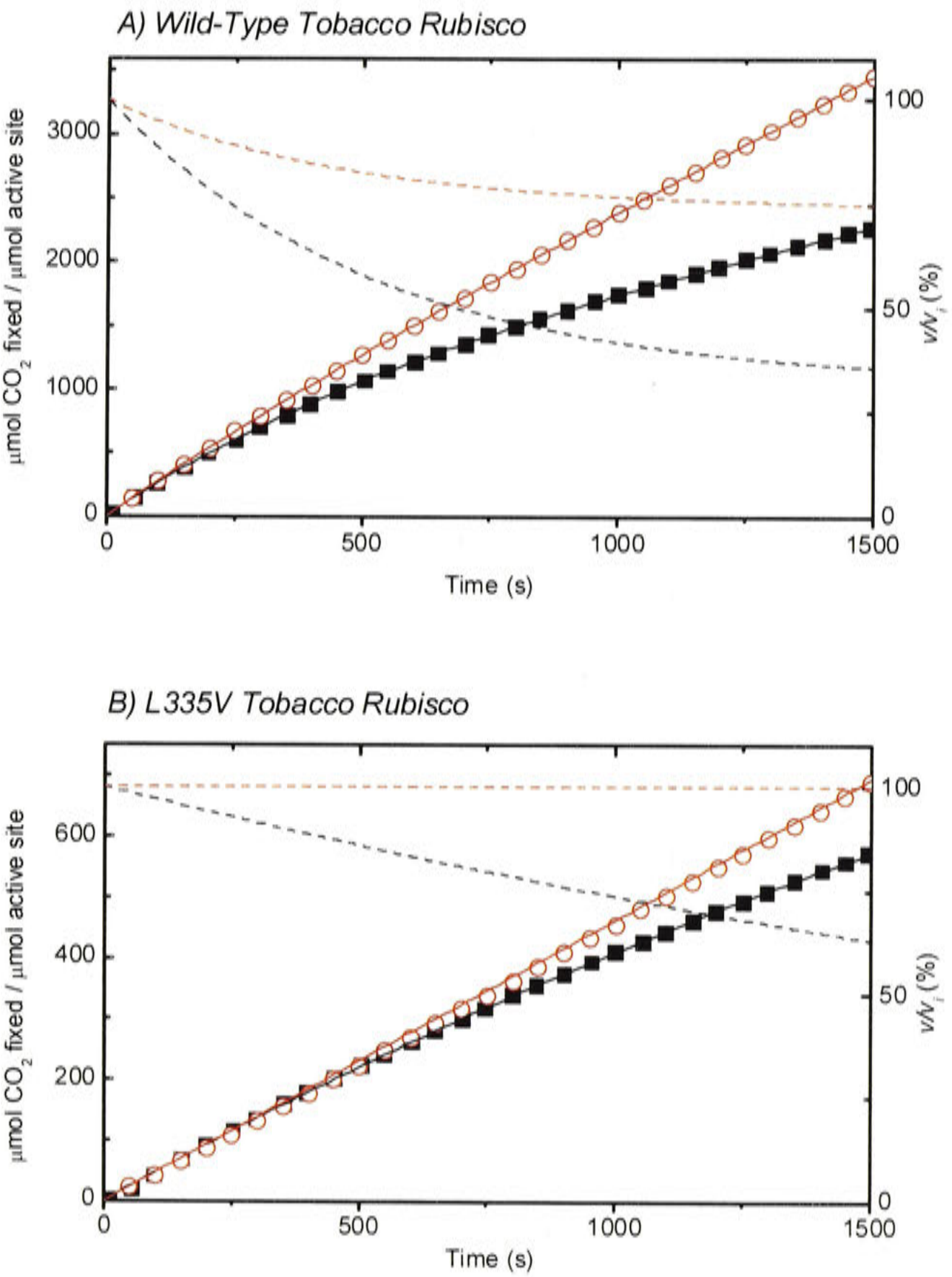

Figure 3.1. Decline in the Activity of Wild-Type and L335V Tobacco Rubisco.

Pre-activated wild-type (*A*) and L335V (*B*) tobacco Rubisco was added to an otherwise complete reaction mixture to initiate the reaction. Carboxylase activity was measured spectrophotometrically at saturating CO_2 under aerobic (■) or anaerobic conditions (○). The data for product accumulation (left ordinate, every tenth 5-s data point shown) versus time were fitted to equation 3.1, and the values for v_i, v_f and k_{obs} were estimated (Table 3.1). Using these estimates, curves for the percentage of the initial activity remaining (right ordinate, dashed lines) as a function of time were plotted using Equation 3.2.

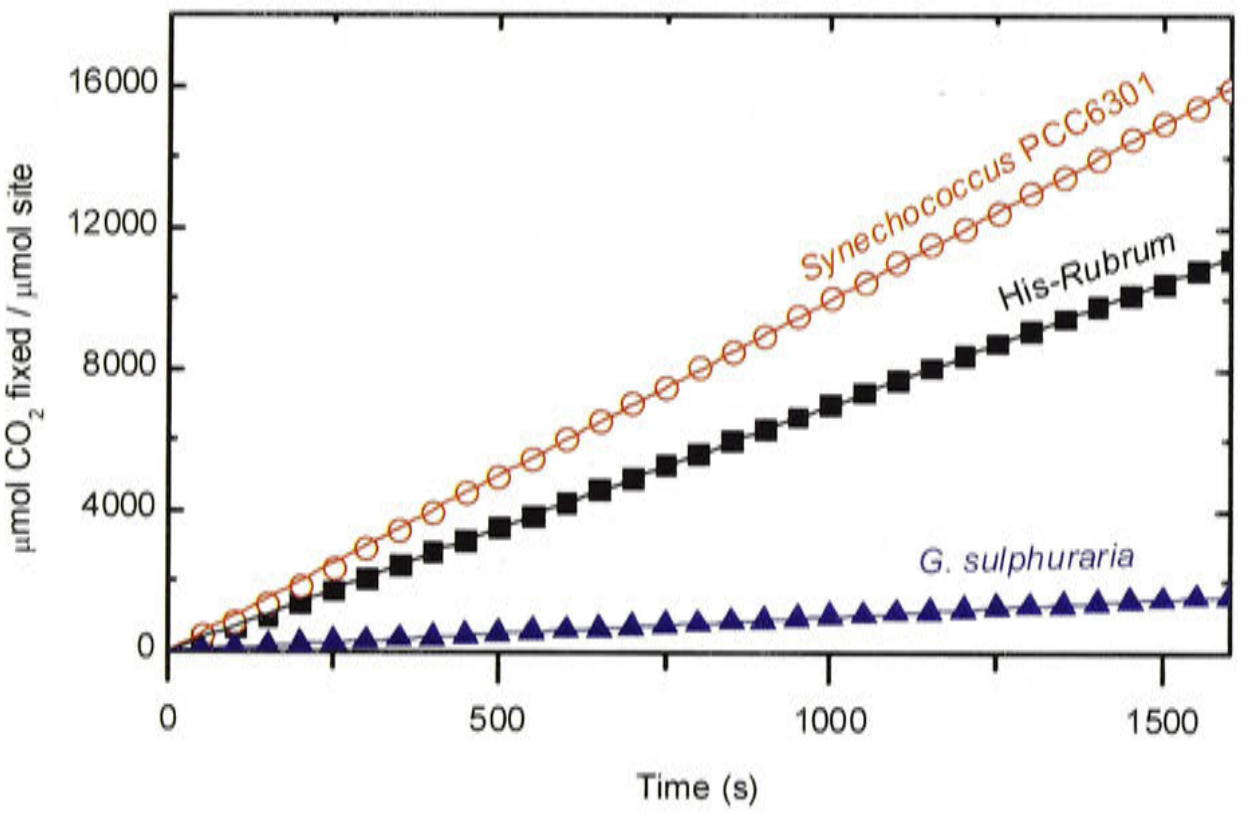

Figure 3.2. Constant Rubisco Activity During Catalysis.

Pre-activated *G. sulphuraria* (▲), *Synechococcus* PCC6301 (○) and His-*Rubrum* (■) Rubisco was added to an otherwise complete aerobic reaction mixture to initiate the reaction. Carboxylase activity was measured spectrophotometrically at saturating CO_2 under aerobic conditions. The data for product accumulation (every tenth 5-s data point shown) versus time were fitted to a linear equation to calculate the rate (Table 3.1).

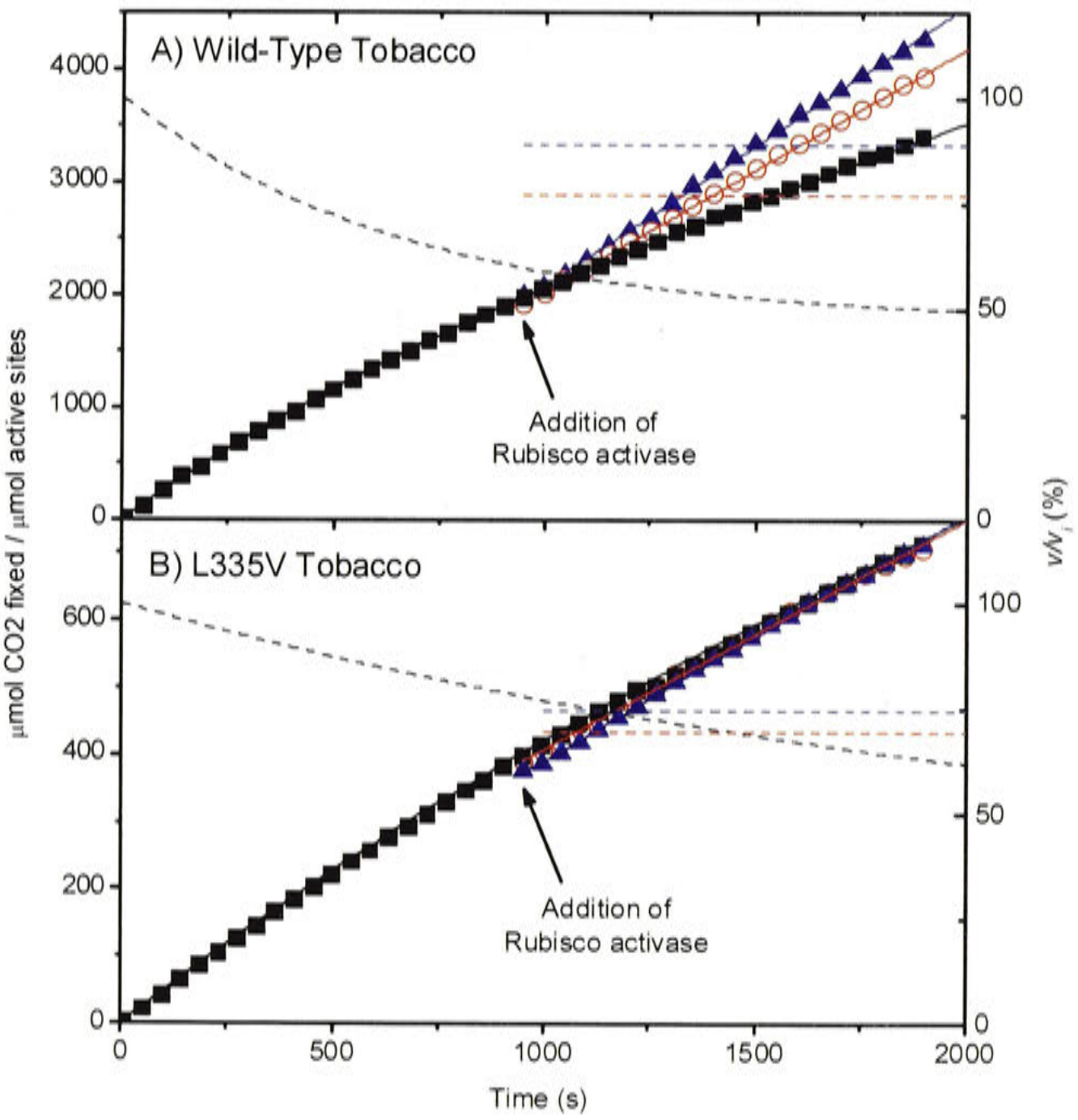

Figure 3.3 Alleviation of Fallover by Rubisco Activase

Pre-activated wild-type (*A*) and L335V (*B*) tobacco Rubisco was added to an otherwise complete aerobic reaction mixture to initiate the reaction. Carboxylase activity was measured spectrophotometrically at saturating CO_2 conditions. After 900 s, Rubisco activase was added to the assay (■, 0 $\mu g.ml^{-1}$, ○ 50 $\mu g.ml^{-1}$, ▲ 100 $\mu g.ml^{-1}$). The data for product accumulation (left ordinate, every tenth 5-s data point shown) versus time were fitted to Equation 3.1 or a linear equation, and the values for v_i, v_f and k_{obs} were estimated. Using these estimates, curves for the percentage of the initial activity remaining (right ordinate, dashed lines) as a function of time were plotted using Equation 3.2.

3.4 Discussion

Some previous studies undertaken to evaluate the self-regulation of Rubisco over time have been limited by the use of commercially produced ribulose-P_2, which has been shown to contain inhibitory compounds that accentuate the decline in enzyme activity. The experiments described in this chapter use highly pure ribulose-P_2 preparations that are unlikely to contain inhibitory compounds that may influence the *in vitro* Rubisco activity. By keeping the time between the addition of ribulose-P_2 and enzyme to a minimum, the chance of inhibitors being formed in the reaction mix prior to the addition of enzyme was kept to a minimum.

3.4.1 Slow Inhibition of Tobacco Rubisco

Self-inhibition of wild-type and L335V tobacco Rubisco was evident, as shown by a decrease in activity over time. This decline is consistent with the view that fallover inhibition is due to the slow, tight binding of inhibitors at the active site (Edmondson et al. 1990c; Edmondson et al. 1990b). Data for activity versus time showed a good fit to Equation 3.1 (Figure 3.1), which can be derived from the models for the two-step, slow isomerisation model for inhibitor binding (Morrison 1982).

The model of binding is complicated, as there are at least two different inhibitors involved in binding. The inhibitors are also present at very low concentrations during the assay, and are generated during the assay itself by non-enzymatic oxidation of ribulose-P_2 (Kane et al. 1998) or misprotonation of the enediol by Rubisco itself (Edmondson et al. 1990d).

Under aerobic conditions, in the presence of atmospheric concentrations of O_2, there was a high level of inhibition. Wild-type tobacco Rubisco activity decreased over time before reaching a finite steady-state, with a $t_{(1/2)}$ of 6 min. The L335V mutation greatly reduced the speed of fallover inhibition and altered the pattern of inhibition (Figure 3.1). While less inhibition was observed for the L335V tobacco Rubisco during the 30 min assay period, the best fit of the data to the fallover model suggested that inhibition would proceed to completion (i.e. $v_f \sim 0$), but that this would take much longer than the 30 min assay period. This suggests that the inhibition seen with the L335V mutant is caused by an inhibitor whose rate of release from the tight complex (EI*) is close to zero, unlike wild-type fallover where the finite steady-state v_f indicates that release of inhibitors must be balanced with the binding of inhibitors.

When O_2 was excluded from the assay, the extent of fallover inhibition was decreased for wild-type tobacco enzyme, and completely eliminated for the L335V tobacco mutant Rubisco. This is consistent with previous observations that non-enzymatic oxidation of ribulose-P_2 to pentodiulose-P_2 occurring during the assay was one of the main causes of the fallover phenomenon (Kane et al. 1998). Total abolition of fallover inhibition of the L335V tobacco enzyme under the same conditions (Figure 3.1) is consistent with pentodiulose-P_2, or a product derived from it, being the sole cause of the residual inhibition seen with the mutant under aerobic conditions.

3.4.2 Constant Activity of Other Rubisco

Rubisco from *G. sulphuraria*, *Synechococcus* PCC6301 and His-*Rubrum* did not show a decline in activity over the 20 minute assay (Figure 3.2). A lack of self-inhibition suggests that inhibitors are not binding to the active sites, either due to reduced binding affinity or that less inhibitory compounds were being formed during the assay. These assays were performed under aerobic conditions, therefore the enzymes would have been exposed to the inhibitors formed by non-enzymatic oxidation of ribulose-P_2. It is likely that the inhibitors are present, but that they do not bind to the enzyme, or that the enzyme is able to convert the inhibitors into non-inhibitory compounds.

3.4.3 Reversal of Inhibition by Rubisco Activase

Rubisco activase acts to remove inhibitors from the active site of Rubisco, and could restore some of the decline in activity when it was added to the *in vitro* assays. Wild-type tobacco Rubisco was more responsive to Rubisco activase than L335V tobacco Rubisco, suggesting that either Rubisco activase does not recognise L335V tobacco Rubisco, or that the inhibitors are too tightly bound to be released by the protein. The degree of restoration of activity correlated to the concentration of Rubisco activase protein, demonstrating that the rate of inhibitor release is increased when there is more Rubisco activase protein available to associate with the Rubisco enzyme and trigger loop opening.

3.4.4 Conclusions

Rubisco from wild-type tobacco and the mutant L335V tobacco Rubisco showed a decrease in activity over time, which was not observed for Rubisco from *G. sulphuraria*, *Synechococcus* PCC6301 or His-*Rubrum*. The inhibition of wild-type and L335V tobacco Rubisco was higher under aerobic conditions than anaerobic conditions,

with slower inhibition observed for L335V tobacco Rubisco, but with inhibition appearing to proceed to completion. Rubisco activase could restore the inhibition of wild-type tobacco Rubisco, but not the inhibition of L335V tobacco Rubisco. This suggests that the nature of inhibition during *in vitro* assays is different for different forms of the enzyme.

4 Products of Rubisco Catalysis

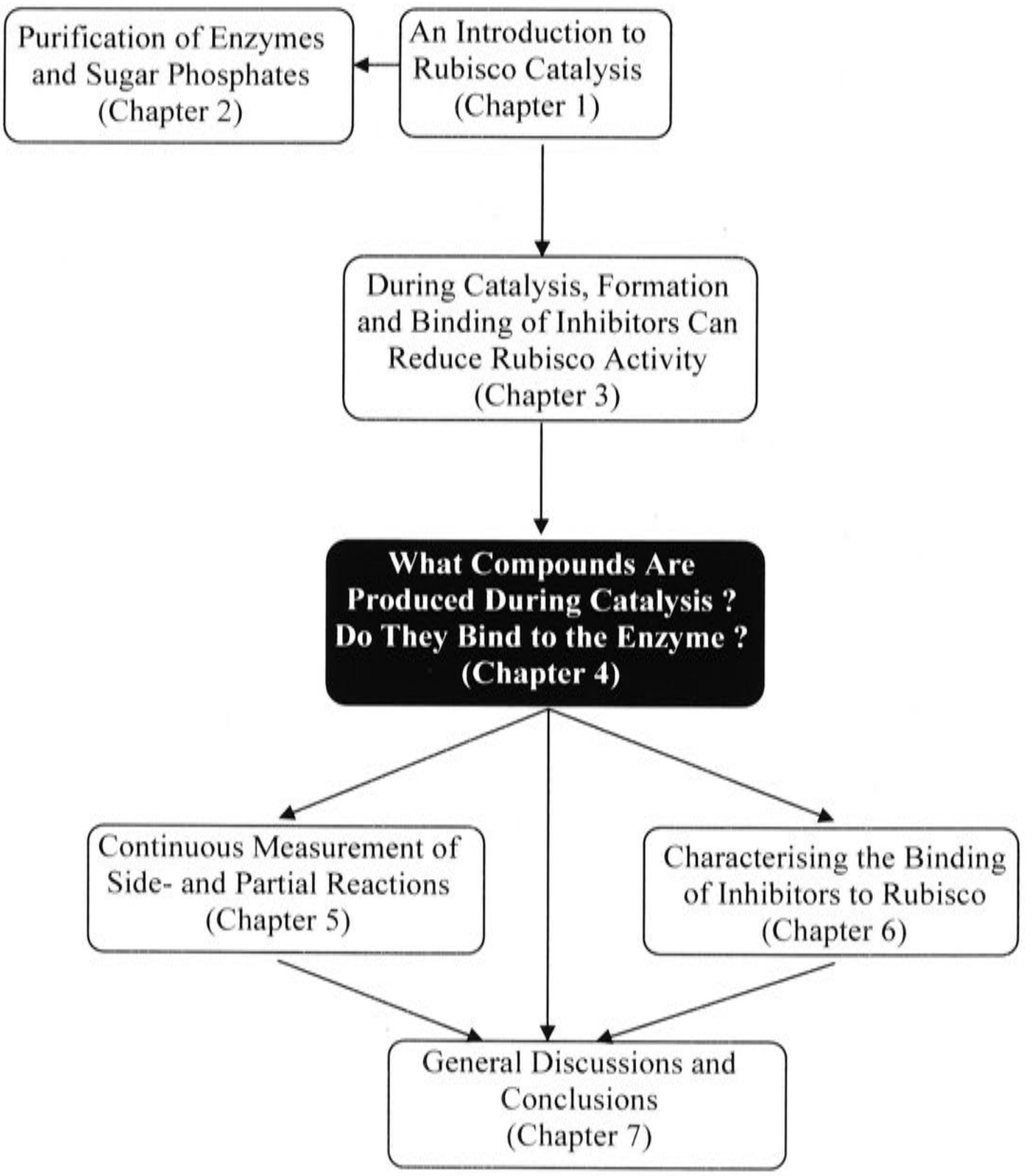

4.1 Introduction

Self-inhibition of Rubisco activity appears to be due to the formation of side-products by the enzyme that bind tightly to the active site. Alternate processing of intermediate compounds during catalysis can result in Rubisco producing compounds other than P-glycolate and P-glycerate (Figure 4.1), and these side-products are likely to be able to bind to the active site. Some of these products are derived from the highly reactive enediol, which must be stabilised to avoid these side reactions. Misprotonation of the enediol yields xylulose-P_2, while β-elimination produces deoxy-pentodiulose-P. The peroxyketone intermediate formed during oxygenation can eliminate H_2O_2 to produce pentodiulose-P_2, which may then be rearranged to form carboxytetritol-P_2. The *aci*-acid formed during carboxylation may also undergo β-elimination, yielding pyruvate. Some products remain tightly bound to the enzyme, while others are released from the active site.

4.1.1 Misprotonation of the Enediol

Xylulose-P_2 can be produced as a catalytic by-product by misprotonation of the enediol intermediate (Edmondson et al. 1990d). Rubisco was allowed to completely consume ribulose-P_2, and the enzyme was removed by treatment with acid, leaving only the products of catalysis. Quantification of xylulose-P_2 can be achieved by cleavage with aldolase to produce dihydroxyacetone-P and glycolaldehyde-P. The dihydroxyacetone-P can then be measured by using glycerol-3-phosphate dehydrogenase and monitoring the consumption of NADH. This assay showed that the initial ribulose-P_2 contained less than 0.05 % xylulose-P_2. However, in the reaction solution containing the products of catalysis, xylulose-P_2 was detected at a level equivalent to 0.26 % of the ribulose-P_2 concentration.

When spinach Rubisco was incubated with ribulose-P_2 at pH 8.5 under carboxylating conditions, 0.07 % of the initial ribulose-P_2 was converted into inhibitory compounds and 0.02 % was converted to xylulose-P_2 (Zhu and Jensen 1991a). The remainder was thought to be 3-keto-arabinitol-P_2, but is more likely to be pentodiulose-P_2, due to its misidentification as discussed in Section 3.1.3. At pH 7.5 a similar total level of inhibitors was observed, but a greater proportion was xylulose-P_2. There was also a greater drop in carbamylated sites observed at the lower pH (Zhu and Jensen 1991a), which is consistent with xylulose-P_2 binding tightly to decarbamylated ribulose-P_2 binding sites (Zhu and Jensen 1991b).

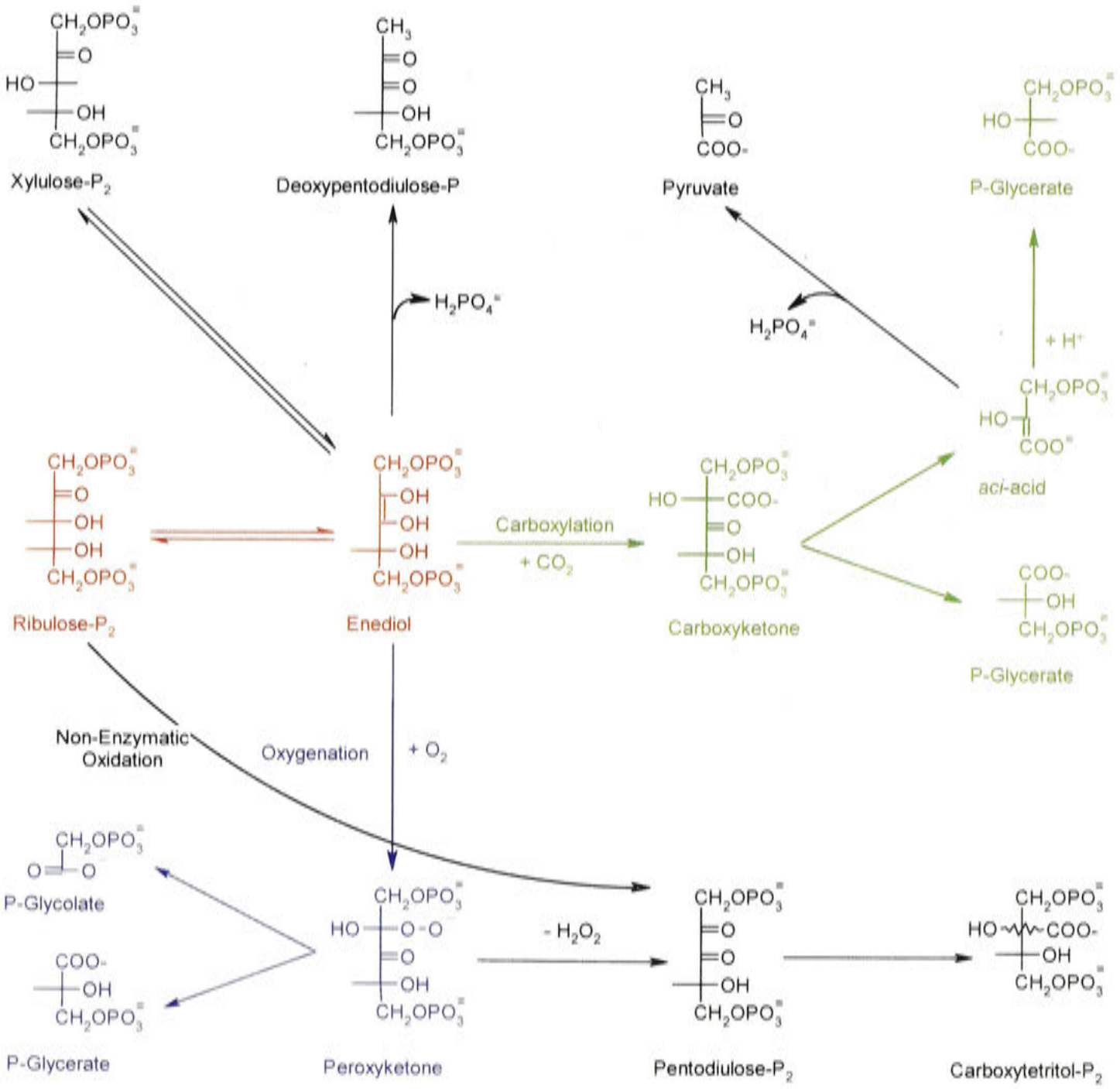

Figure 4.1 Side Reactions Catalysed by Rubisco

The predominant reactions carried out by Rubisco are the carboxylation or oxygenation of ribulose-P_2. The initial reaction, which is common to both pathways, is the formation of an enediol (shown in red). The enediol can then react with CO_2 (pathway shown in green) or O_2 (pathway shown in blue) to produce P-glycerate and P-glycolate. Intermediate compounds may also be partitioned to produce other products, some of which are shown here, and ribulose-P_2 may undergo non-enzymatic oxidation to form pentodiulose-P_2, as indicated by the dashed arrow.

The amount of xylulose-P_2 produced by Rubisco showed correlation to the concentrations of CO_2 and O_2 (Zhu et al. 1998). At the concentrations of 32 μM CO_2 and 7 μM O_2, 0.31 % of the initial ribulose-P_2 was converted into xylulose-P_2 and increasing the concentration of either gas decreased the rate of formation.

Reprotonation of the enediol C-2 to produce 3-keto-arabinitol-P_2 or 3-keto-ribitol-P_2 is also theoretically possible, but has not been conclusively shown to occur. Previous reports of the production of these compounds by Rubisco (Zhu and Jensen 1991b; Morell et al. 1994; Morell et al. 1997; Zhu et al. 1998) based the identification on the detection of arabinitol-P_2 after borohydride reduction. However, under some conditions, arabinitol-P_2 is also produced by the borohydride reduction of pentodiulose-P_2, which can occur as a byproduct of the oxygenase reaction (Chen and Hartman 1995; Harpel et al. 1995), or as a contaminant in ribulose-P_2 preparations (Kane et al. 1998). Therefore there is no direct evidence for reprotonation at C-2 of the enediol, and previous studies may have misidentified the pentodiulose-P_2 as 3-keto-arabinitol-P_2.

4.1.2 Reactions of the Peroxyketone Intermediate

Like the enediol intermediate, the peroxyketone intermediate of the oxygenation pathway is also unstable and prone to side reactions, as shown in Figure 4.2. Elimination of H_2O_2 from the peroxyketone results in the formation of pentodiulose-P_2, which is a dicarbonyl compound. Pentodiulose-P_2 was first identified as a transient product formed by the E60Q (48) mutant of *R. rubrum* Rubisco (Chen and Hartman 1995). The formation of pentodiulose-P_2 was oxygen-dependent and resulted in the production of H_2O_2, which is consistent with H_2O_2 elimination from the peroxyketone intermediate. Identification of the molecule as pentodiulose-P_2 was confirmed by the reaction with *o*-phenylene-diamine to form a coloured quinoxaline compound, cleavage by H_2O_2 to form P-glycerate and P-glycolate, and the products of borohydride reduction. Pentodiulose-P_2 was also a substrate for the E60Q (48) mutant, producing P-glycerate and P-glycolate.

Pentodiulose-P_2 has also been detected in some preparations of ribulose-P_2 (Kane et al. 1998). The formation of pentodiulose-P_2 was dependant on the types of buffer used, the pH of the storage solution, and exposure to O_2 and transition metals. It formed a tight complex with spinach Rubisco that could be isolated by gel filtration.

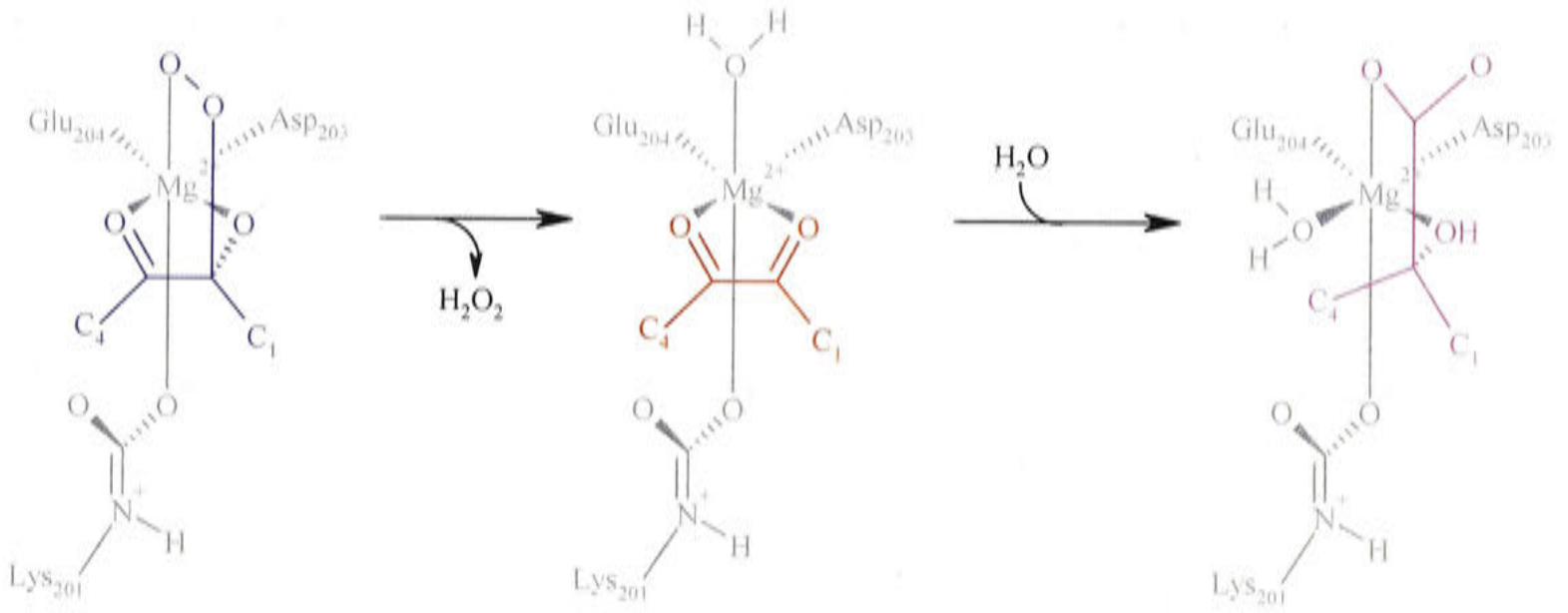

Peroxyketone Intermediate

Pentodiulose-P_2

Carboxytetritol-P_2

Figure 4.2 Reactions of the Peroxyketone Intermediate

After the enediol reacts with O_2, a peroxyketone intermediate is formed (shown in blue). This compound is normally cleaved between C-2 and C-3, but may also undergo other reactions. Pentodiulose-P_2 (shown in red) is formed by the elimination of peroxide. This may then be rearranged to form carboxytetritol-P_2 (shown in pink).

Another side product, carboxytetritol-P_2, was observed from a mutant of *R. rubrum* Rubisco. In the K334A (329) mutant of *R. rubrum* Rubisco, the lysine residue in loop 6 that normally stabilises the reaction intermediates, is mutated to a non-charged residue (Harpel and Hartman 1994). One of the products of catalysis was identified as carboxytetritol-P_2 by mass spectrometry, ^{1}H-, ^{13}C- and ^{31}P-NMR spectroscopy, and periodate oxidation (Harpel et al. 1995). Incubation of the K334A (329) mutant enzyme with pentodiulose-P_2 resulted in the production of carboxytetritol-P_2, due to a benzylic acid-type rearrangement. This reaction was not O_2-dependant, and did not occur in the absence of Rubisco.

Production of pentodiulose-P_2 and carboxytetritol-P_2 was also observed by the aminopropylated K175C (166)-C73S (58) mutant of *R. rubrum* Rubisco, in which the charged lysine group that is essential for protonation of the *aci*-acid during catalysis is replaced by a lysine analogue with one of the methylene carbon atoms of the side chain substituted by a sulphur atom (Harpel et al. 2002).

4.1.3 Specific Aims and Objectives

This chapter aims to confirm the observations of self-inhibition by identifying and comparing products formed by different Rubisco enzymes under varying assay conditions, and to investigate the binding of products to the enzyme. Previous studies have identified the formation of sugar phosphate compounds, including xylulose-P_2, pentodiulose-P_2, and carboxytetritol-P_2 during catalysis, and this work confirms and extends these observations.

Experiments are carried out using radiolabelled ribulose-P_2 under conditions that promote carboxylation or oxygenation and by applying oxidised ribulose-P_2 mixtures to Rubisco. Reaction products are then separated using anion-exchange chromatography and separate bound and non-bound radioactivity by size-exclusion chromatography.

4.2 Materials & Methods

4.2.1 Products of the Carboxylase Reaction

Rubisco was incubated with radiolabelled ribulose-P_2 to observe the products formed under conditions that promote carboxylation. Rubisco (final concentration 250 $\mu g.ml^{-1}$) was activated as described in Section 2.2.2. 200-1000 µl assays were carried out in buffer containing 100 mM EPPS-NaOH, pH 8.0, 20 mM $MgCl_2$, 1 mM EDTA, and 1 µM [1-^{3}H]ribulose-P_2 (3.2 $MBq.nmol^{-1}$). The buffer was sparged with N_2 before the addition of 20 mM $NaHCO_3$. After 20 min incubation at room temperature, SDS was added to a final concentration of 2 % (w/v) and borate was added to a final concentration of 10 mM. The denatured proteins were removed using an Ultrafree-MC filter unit (M_r cut-off 10,000 NMWL, Millipore). The filtrate was loaded onto a Mono-Q HR 5/5 column equilibrated with 10 mM EPPS-NaOH, pH 8.0, and 10 mM borate. The ribulose-P_2 derivatives were separated on an HPLC system (Waters) using a 50–225 mM NaCl gradient over 85 column volumes (1 $ml.min^{-1}$) and the radioactively labelled compounds were detected by online scintillation counting (Packard, Canberra). At least two separate assays were performed for each enzyme, and peak areas were calculated for each run, and then averaged.

4.2.2 Products of the Oxygenase Reaction

To promote the oxygenase activity, 200-1000 µl assays were carried out in buffer containing 100 mM EPPS-NaOH, pH 8.0, 20 mM $MgCl_2$, 1 mM EDTA, and 1 µM [1-^{3}H]ribulose-P_2 that had been sparged with oxygen. Rubisco was activated separately in a small volume of buffer, as described in Section 2.2.2, and was added to initiate the assays (final Rubisco concentration of 250 $\mu g.ml^{-1}$; final HCO_3^- concentration of 100 µM). The reaction was incubated at room temperature for 30 min, before SDS was added to a final concentration of 2 % (w/v) and borate was added to a final concentration of 10 mM. The denatured proteins were removed using an Ultrafree-MC filter unit (M_r cut-off 10,000 NMWL, Millipore), and the ribulose-P_2 derivatives were separated on an HPLC system, as described in Section 4.2.1. At least two separate assays were performed for each enzyme, and peak areas were calculated for each run, and then averaged.

4.2.3 Determination of the 40 Min Peak

Because both ribulose-P_2 and xylulose-P_2 elute at 40 min, further separation is required. Separation methods have been established that involve chromatography of the

phosphate free sugars (Morell et al. 1994). The sample was separated using a Mono-Q HR 5/5 column as described in Section 4.2.1, and the fractions containing radioactivity were pooled. Alkaline phosphatase (5 $\mu g.ml^{-1}$) was added, and the pH was adjusted to final value of 9.3 using NH_4OH (1 M) before the solution was incubated overnight at room temperature and then applied to an AG1-X8 (formate) column (5 ml, 10 mm x 50 mm, Bio-Rad). The column was washed with 3 column volumes of H_2O and the eluent was collected and dried down under nitrogen before being resuspended in H_2O. The sample was applied to an HPX-87C column (Bio-Rad) and eluted with H_2O (85 °C, 0.5 $ml.min^{-1}$) using ion moderated partition chromatography, and compared to known standards.

4.2.4 Reaction Products that Remain Bound

To investigate compounds that remained bound, Rubisco was incubated with [1-^{3}H]ribulose-P_2 as described in Section 4.2.1, but the unbound compounds were removed by exchanging the reaction buffer using an Ultrafree-MC filter unit (M_r cut-off 10,000 NMWL), which was repeated four times. SDS was then added to a final concentration of 2 % (w/v) and the denatured enzyme was removed using the same device. The filtrate was analysed using anion exchange chromatography on a Mono-Q HR 5/5 column described in Section 4.2.1. At least two separate assays were performed for each enzyme, and peak areas were calculated for each run, and then averaged.

Separation of the bound and unbound components could be achieved much more rapidly by gel filtration on a Sephadex G-50 fine column (150 ml, 10 mm x 200 mm, Amersham Biosciences) equilibrated with the same buffer solution (0.5 $ml.min^{-1}$) using the Akta Explorer FPLC system (Amersham Biosciences) or the HPLC system. The protein peak was collected and the radioactivity it contained was measured and released by adding SDS to 2 % (w/v). Denatured protein was removed by ultrafiltration using an Ultrafree-MC filter unit (M_r cut-off 10,000 NMWL), and an aliquot of the filtrate was analysed using anion exchange chromatography on a Mono-Q HR 5/5 column, as described in Section 4.2.1.

4.2.5 Conversion of Pentodiulose-P_2 to Carboxytetritol-P_2

4.2.5.1 Oxidation of Ribulose-P_2

In order to produce a mixture containing a variety of the products of ribulose-P_2 oxidation and further degradation, [1-^{3}H]ribulose-P_2 (50 μM) was oxidised for three h in

buffer containing 100 mM EPPS-NaOH, pH 8.0, with 1 mM $CuSO_4$ as described (Kane et al. 1998).

4.2.5.2 Products of Rubisco from Oxidised Ribulose-P_2

The mixture of ribulose-P_2 oxidation and degradation products was then incubated with Rubisco to determine the effects on catalysis. Reactions were carried out in 100 mM EPPS-NaOH pH 8.0, 20 mM $MgCl_2$, 1 mM EDTA, 10 mM $NaHCO_3$, 650 $\mu g.ml^{-1}$ activated Rubisco, and 8 μM oxidised [1-^{3}H]ribulose-P_2. The reaction was incubated at room temperature for 10 min, before concentrating the sample with an Ultrafree-MC filter unit (M_r cut-off 10,000 NMWL). The reaction buffer was then exchanged four times, and the retentate was resuspended in 10 mM EPPS-NaOH, pH 8.0, 10 mM borate, 2 % (w/v) SDS. After centrifuging again, the filtrate was analysed using anion exchange chromatography as described in Section 4.2.1. The radioactivity of wash fractions was measured by scintillation counting (Ultima Gold, Packard). At least two separate assays were performed for each enzyme, and peak areas were calculated for each run, and then averaged.

Separation of the bound and unbound components could also be achieved by gel filtration using Sephadex G-50 fine, as described in Section 4.2.4.

4.2.5.3 The Effect of H_2O_2 on Conversion of Pentodiulose-P_2

In some experiments, 5 mM H_2O_2 was included in the solution during consumption of the oxidised ribulose-P_2 by Rubisco. In others, addition of the H_2O_2 was delayed until 5 min after mixing the oxidised ribulose-P_2 with Rubisco. Rubisco-bound radioactivity was measured by separation using gel filtration using Sephadex G-50 fine (150 ml, 10 mm x 200 mm) equilibrated with buffer solution containing 100 mM EPPS-NaOH pH 8.0, 20 mM $MgCl_2$, 1 mM EDTA, and 10 mM $NaHCO_3$.

4.3 Results

4.3.1 Products of Catalysis

The side-reaction products of tobacco Rubisco could be observed by chromatographic analysis of the products of conversion of [1-^{3}H]ribulose-P_2 by Rubisco under conditions that promoted oxygenation or carboxylation. Radioactivity was detected using an online scintillation counter, which allowed detected of products up to 0.1% of the initial radioactivity. Chromatography of the initial [1-^{3}H]ribulose-P_2 sample showed that no inhibitory products were present (Figure 4.3).

In most cases, conversion was complete, however under some circumstances traces of ribulose-P_2 remained. *G. sulphuraria* consistently had ribulose-P_2 remaining after 30 min of incubation due its high Michaelis constant for ribulose-P_2 (K_m*(ribulose-P_2)*) of > 100 μM. With a low binding affinity for the substrate, the rate of catalysis was slow at the 1 μM ribulose-P_2 concentration in the assay. *Synechococcus* PCC6301 also had ribulose-P_2 remaining after 30 min of incubation under low CO_2 concentrations, due to a very high $K_m(O_2)$ that limits the reaction rate at the low O_2 concentrations that are present under assay conditions.

The NaCl gradient was optimised to allow good separation of bisphosphate compounds by chromatography. Ribulose-P_2 was identified by comparison with known standards and previous studies, as were the elution of P-glycerate, P-glycolate, carboxytetritol-P_2 and pentodiulose-P_2 (Table 4.1). Ribulose-P_2 and xylulose-P_2 eluted at the same time, thus fractions were collected and dephosphorylated to form ribulose and xylulose respectively. Ribulose and xylulose were then identified by separation using ion moderated partition chromatography on an HPX-87C column, and compared with known standards. Xylulose typically eluted after 11.2 min, while ribulose eluted after 17.1 min.

Unfortunately, any deoxy-pentodiulose-P produced during the reaction would be expected to co-elute with the other mono-phosphate compounds P-glycerate and P-glycolate or in the initial wash prior to the start of the gradient. This meant that it was not possible to accurately identify the deoxy-pentodiulose-P, as it was masked by the other mono-phosphate or non-phosphorylated compounds that were present in much higher concentrations.

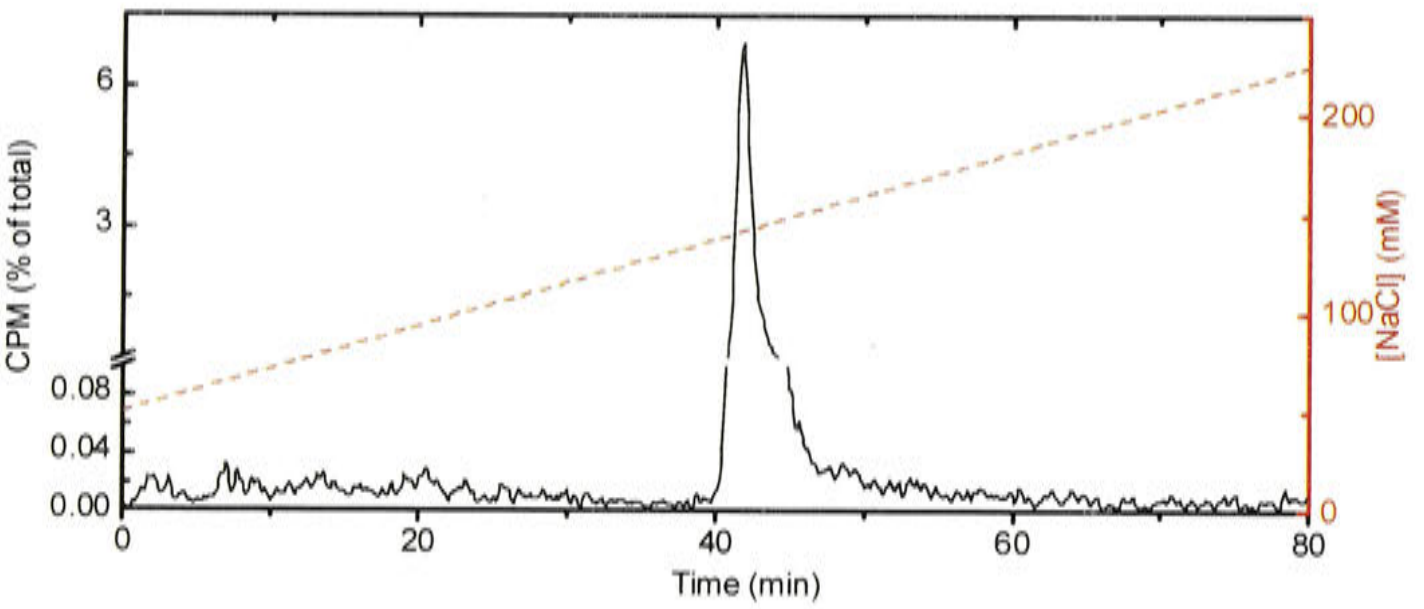

Figure 4.3 Chromatography of Purified Ribulose-P_2

[1-3H]ribulose-P_2 was chromatographed on a Mono-Q HR 5/5 column with a 50-225 mM NaCl gradient over 80 column volumes (indicated as -- on the right ordinate) in buffer containing 10 mM EPPS-NaOH (pH 8.0) and 10 mM Borate at a flow rate of 1 $ml.min^{-1}$.

Some early-eluting labelled compounds were observed for many of the chromatographic analyses. These non-phosphorylated compounds were likely to include any pyruvate that was produced, and also the products formed by any contaminating phosphatase enzymes that were present under assay conditions. Due to the long incubation times that were used, only traces of phosphatase enzymes would need to be present in the assay to dephosphorylate some of the labelled compounds.

4.3.2 Side Reactions Under Carboxylating Conditions

Under conditions that promoted carboxylase activity, all Rubisco enzymes produced P-glycerate nearly exclusively (Figure 4.4, Figure 4.5, Figure 4.6, Figure 4.7, Figure 4.8, Table 4.2). In addition, 1-2 % of the total counts were present as early-eluting, non-phosphorylated compounds that may include pyruvate.

4.3.3 Side Reactions Under Predominantly Oxygenating Conditions

When the assay conditions promoted oxygenase activity, the predominant products were P-glycerate and P-glycolate for all Rubisco enzymes (Table 4.2). Absolute oxygenating conditions were not possible due to a carryover of 100 μM $NaHCO_3$ from the activation buffer, which is necessary to carbamylate the active site and allow coordination of the Mg^{2+} ion, allowing catalysis to occur. The assay uses tritium labelled ribulose-P_2, in which radiolabelled ^3H is attached to C-1 of the ribulose-P_2. During catalysis, oxygenation of [1-^{3}H]ribulose-P_2 produces one molecule of [1-^{3}H]P-glycolate and one molecule unlabelled P-glycerate, while carboxylation produces one molecule of [1-^{3}H]P-glycerate and one molecule of unlabelled P-glycerate. As a result, the proportion of [1-^{3}H]P-glycerate to [1-^{3}H]P-glycolate gives an indication of the proportion of carboxylation and oxygenation reactions, and hence the specificity of each Rubisco for CO_2 rather than O_2. His-*Rubrum* Rubisco, which has a specificity of 10, carried out 17 oxygenase reactions for every carboxylase reaction (Figure 4.8B), while wild-type tobacco Rubisco, which has a specificity of 80, carried out 2.2 oxygenations for every carboxylation (Figure 4.4B). Rubisco with a high specificity, such as that from *G. sulphuraria*, carried out only 1.4 oxygenations for every carboxylation (Figure 4.6B).

In addition to P-glycerate and P-glycolate, other products, including xylulose-P_2, pentodiulose-P_2 and carboxytetritol-P_2, were also observed in the separation of reaction products, as shown in Table 4.2. All types of Rubisco enzyme studied produced some xylulose-P_2, varying from low production by His-*Rubrum* Rubisco (Figure 4.8B) up to

high production by L335V tobacco Rubisco (Figure 4.5B). Tobacco Rubisco produced some pentodiulose-P_2, while only His-*Rubrum* and L335V tobacco Rubisco produced carboxytetritol-P_2 (Figure 4.5B and Figure 4.8B).

4.3.4 Binding of Reaction Products to Rubisco

Identification of products that bound tightly to Rubisco could be carried out in two possible ways. Compounds that bind very tightly to Rubisco were separated from unbound compounds using ultrafiltration. The enzyme was washed by exchanging the reaction buffer four times, reducing the concentration of unbound [1-^{3}H] products to less than 0.5 % of the total radioactivity. SDS was then added to denature the enzyme and release the compounds, which were then separated and identified by chromatography. This method had the advantage that multiple samples could be run in parallel under the same conditions.

Alternatively, the products that remained bound to the enzyme were separated from unbound compounds by gel filtration. This method gave similar results for the proportion of radioactivity binding to Rubisco, but had the benefit that the separation was quicker, allowing separation in 20 min, as opposed to 3 h required for ultrafiltration. This increased speed of separation reduced the opportunity for inhibitor release or degradation of the reaction products.

Under assay conditions, the concentration of Rubisco active sites was greater than the concentration of ribulose-P_2. This promoted the binding of inhibitors to the enzyme, as there was an excess of active sites to which the inhibitors could bind.

Under carboxylating conditions, very few products remained bound to Rubisco (Figure 4.9). For wild-type tobacco, His-*Rubrum*, *Synechococcus* PCC6301, and *G. sulphuraria* Rubisco, less than 0.1 % of products remained bound to the enzyme. Some carboxytetritol-P_2 (0.3 % of the initial ribulose-P_2 concentration) remained bound to L335V tobacco Rubisco.

When conditions favoured the oxygenase reaction, more products remained bound to Rubisco (Figure 4.10). Pentodiulose-P_2 (0.4 % of the initial ribulose-P_2 concentration) bound tightly to *G. sulphuraria* Rubisco, while carboxytetritol-P_2 (0.8 %) bound tightly to L335V tobacco Rubisco and xylulose-P_2 (0.3 %) was the only compound that bound to wild-type tobacco Rubisco. No compounds were observed to bind to His-*Rubrum* or *Synechococcus* PCC6301 Rubisco.

Compound	Retention Time (± S.D, min)	[NaCl] (mM)
Non-phosphorylated compounds	1.4 ± 0.2	50
P-Glycerate	21.2 ± 2.5	90
P-Glycolate	23.4 ± 1.9	96
Ribulose-P_2	36.5 ± 2.2	125
Xylulose-P_2	36.5 ± 2.2	125
Pentodiulose-P_2	46.7 ± 2.1	145
Carboxytetritol-P_2	56.9 ± 2.2	169

Table 4.1 Elution of Compounds Using Anion Exchange Chromatography

Reaction products and known standards were chromatographed on a MonoQ HR 5/5 column using a 50–225 mM NaCl gradient over 80 column volumes in buffer containing 10 mM EPPS-NaOH (pH 8.0) and 10 mM Borate (1 $ml.min^{-1}$).

	P-Glycerate	P-Glycolate	Xylulose-P_2	Pentodiulose-P_2	Carboxytetritol-P_2
Wild-Type Tobacco Rubisco					
Carboxylase	98.6 ± 0.4 %	< 0.1 %	< 0.1 %	< 0.1 %	< 0.1 %
Oxygenase	29.8 ± 0.4 %	67.6 ± 2.0 %	1.1 ± 0.4 %	0.3 ± 0.1 %	< 0.1 %
L335V Tobacco Rubisco					
Carboxylase	98.7 ± 1.0 %	< 0.1 %	< 0.1 %	< 0.1 %	< 0.1 %
Oxygenase	6.3 ± 1.4 %	88.2 ± 6.4 %	2.4 ± 1.0 %	0.5 ± 0.2 %	1.2 ± 0.2 %
G. sulphuraria Rubisco					
Carboxylase	96.6 ± 0.1 %	< 0.1 %	< 0.1 %	< 0.1 %	< 0.1 %
Oxygenase	39.3 ± 3.8 %	56.1 ± 4.5 %	2.1 ± 0.4 %	< 0.1 %	< 0.1 %
Synechococcus PCC6301 Rubisco					
Carboxylase	98.8 ± 0.1 %	< 0.1 %	< 0.1 %	< 0.1 %	< 0.1 %
Oxygenase	17.4 ± 2.5 %	77.4 ± 4.2 %	2.8 ± 0.5 %	< 0.1 %	< 0.1 %
His-*Rubrum* Rubisco					
Carboxylase	98.0 ± 0.2 %	< 0.1 %	< 0.1 %	< 0.1 %	< 0.1 %
Oxygenase	5.6 ± 2.5 %	92.0 ± 2.2 %	0.9 ± 0.4 %	< 0.1 %	0.6 ± 0.1 %

Table 4.2 Products of Rubisco Catalysis After Complete Consumption of [1-^{3}H]Ribulose-P_2.

Activated Rubisco was added to assays containing [1-^{3}H]ribulose-P_2 under conditions that promoted carboxylase or oxygenase activity (as described in Section 4.2.1and 4.2.2). Although oxygenase activity was promoted, residual amounts of CO_2 were also present, allowing some carboxylation to occur. Values shown are the amount of each radiolabelled product as a percentage of ribulose-P_2 consumed during the reaction (± S.D.). The proportion of initial ribulose-P_2 that was present as early eluting non-phosphorylated compounds is not shown.

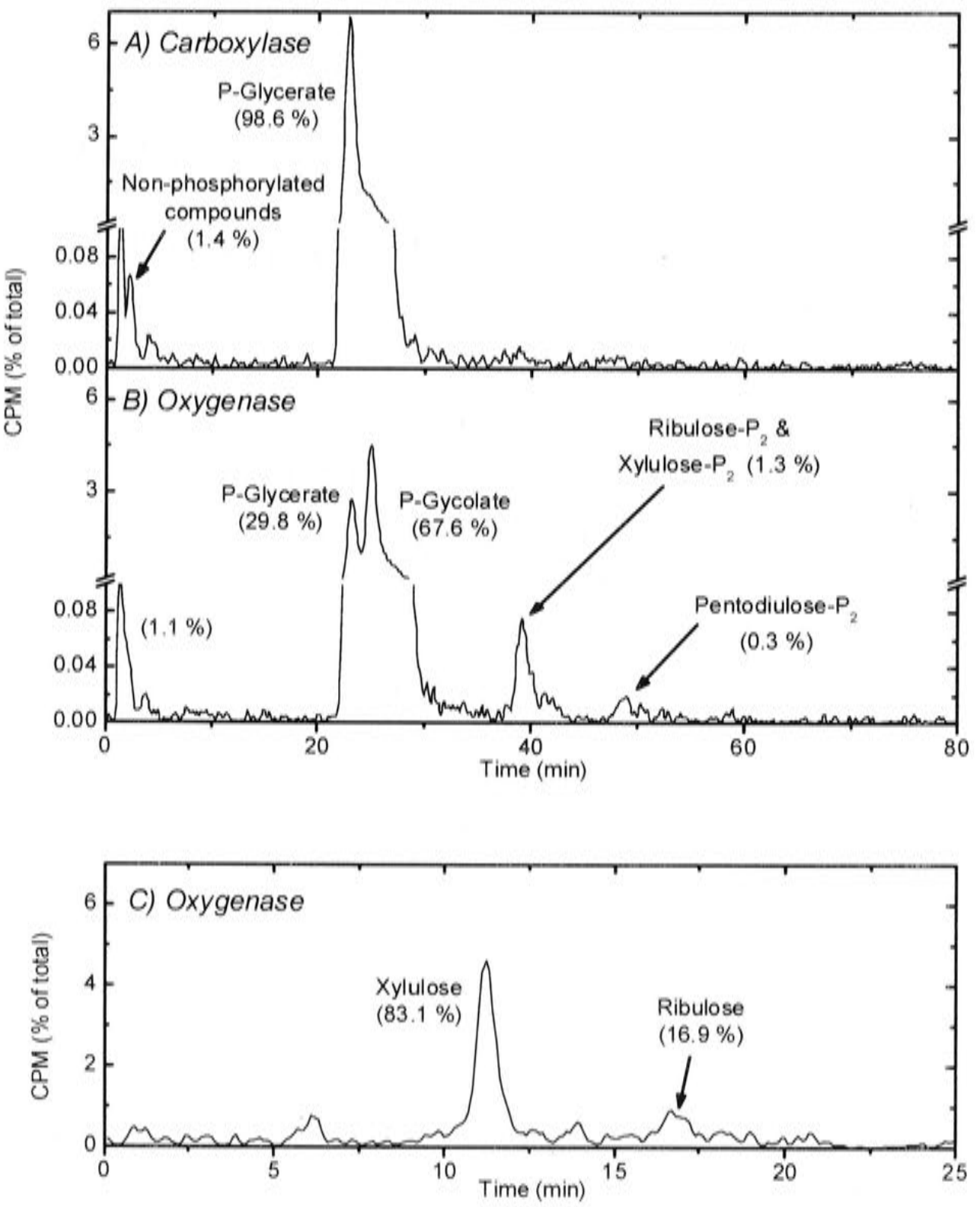

Figure 4.4 Chromatography of Wild-Type Tobacco Rubisco Reaction Products.

Wild-type tobacco Rubisco consumed [1-^{3}H]ribulose-P_2 under conditions that promoted carboxylase (*A*) or oxygenase (*B*) activity. The reaction products were chromatographed on an anion exchange column with a NaCl gradient (shown in Figure 4.3). The peak containing ribulose-P_2 and xylulose-P_2 under oxygenase conditions was collected and dephosphorylated before chromatography on a Bio-Rad HPX-87C column (*C*). The numbers in parentheses show the radioactivity recovered for each compound as a percentage of the total applied radioactivity.

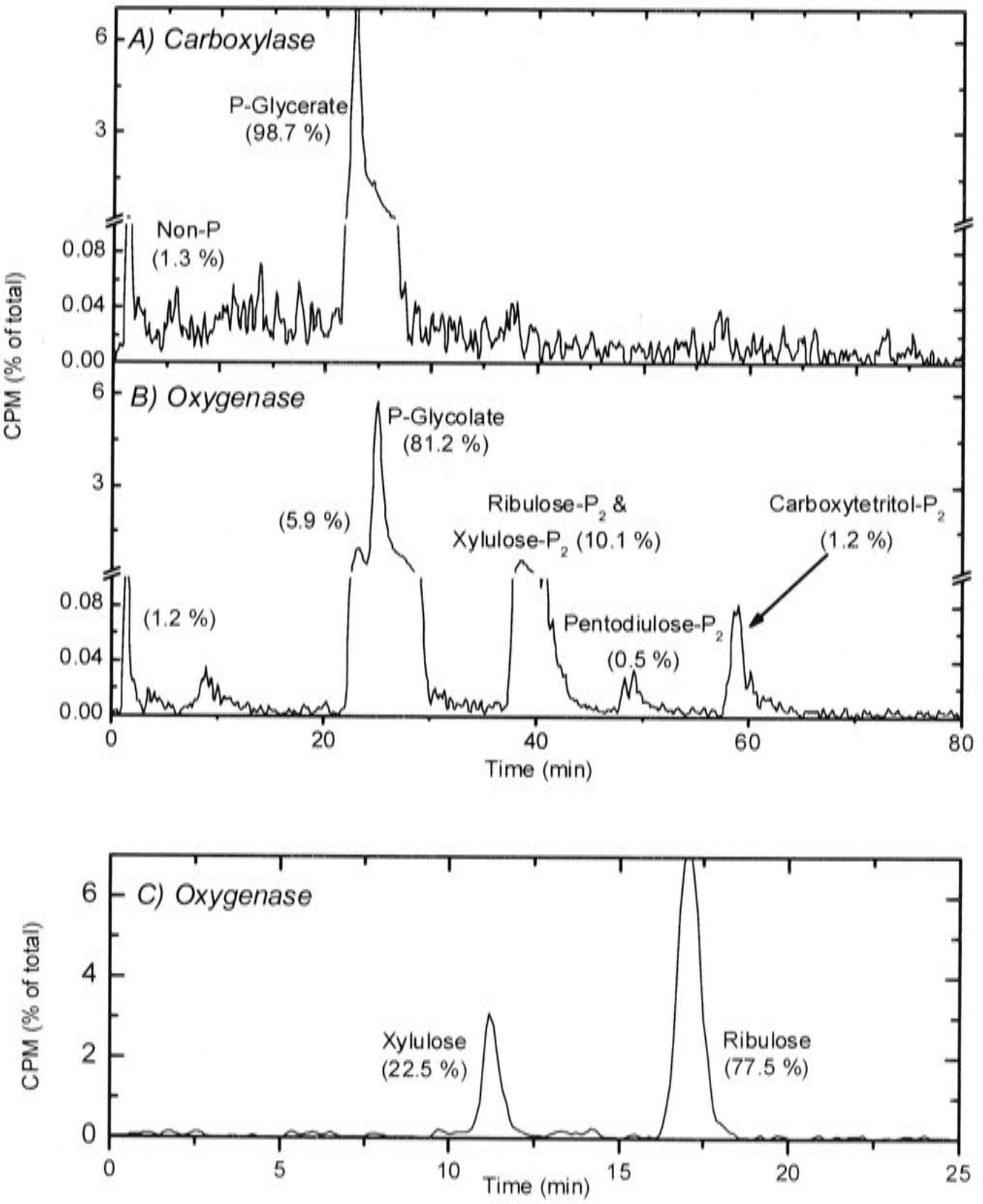

Figure 4.5 Chromatography of L335V Tobacco Rubisco Reaction Products.

L335V tobacco Rubisco consumed [1-^{3}H]ribulose-P_2 under conditions that promoted carboxylase (*A*) or oxygenase (*B*) activity. The reaction products were chromatographed on an anion exchange column with a NaCl gradient (shown in Figure 4.3). The peak containing ribulose-P_2 and xylulose-P_2 under oxygenase conditions was collected and dephosphorylated before chromatography on a Bio-Rad HPX-87C column (*C*). The numbers in parentheses show the radioactivity recovered for each compound as a percentage of the total applied radioactivity.

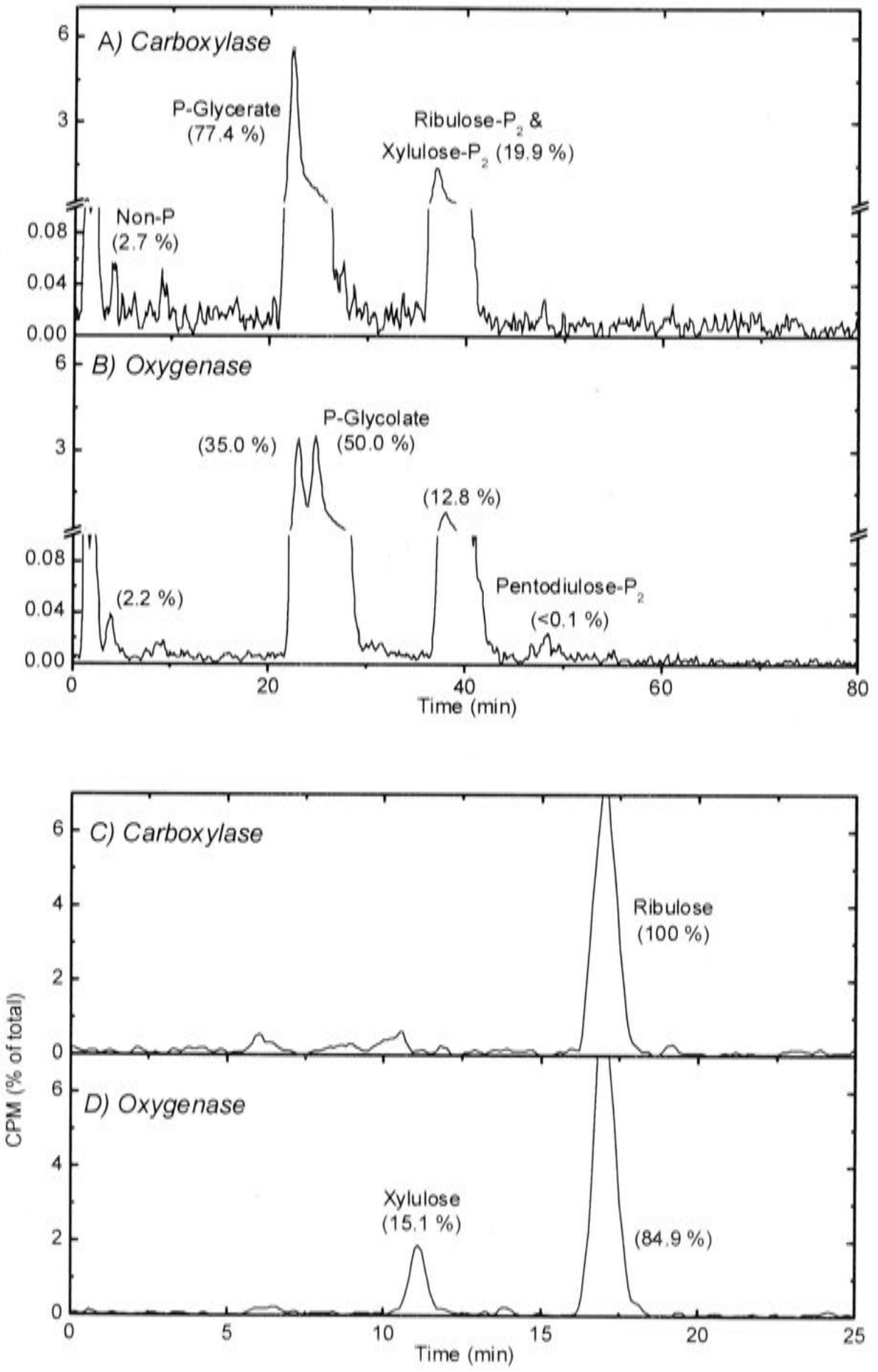

Figure 4.6 Chromatography of *G. sulphuraria* Rubisco Reaction Products.

G. sulphuraria Rubisco consumed [1-3H]ribulose-P_2 under conditions that promoted carboxylase (A) or oxygenase (B) activity. The reaction products were chromatographed on an anion exchange column with a NaCl gradient (shown in Figure 4.3). The peak containing ribulose-P_2 and xylulose-P_2 under oxygenase and carboxylase conditions were collected and dephosphorylated before chromatography on a Bio-Rad HPX-87C column (C, D). The numbers in parentheses show the radioactivity recovered for each compound as a percentage of the total applied radioactivity.

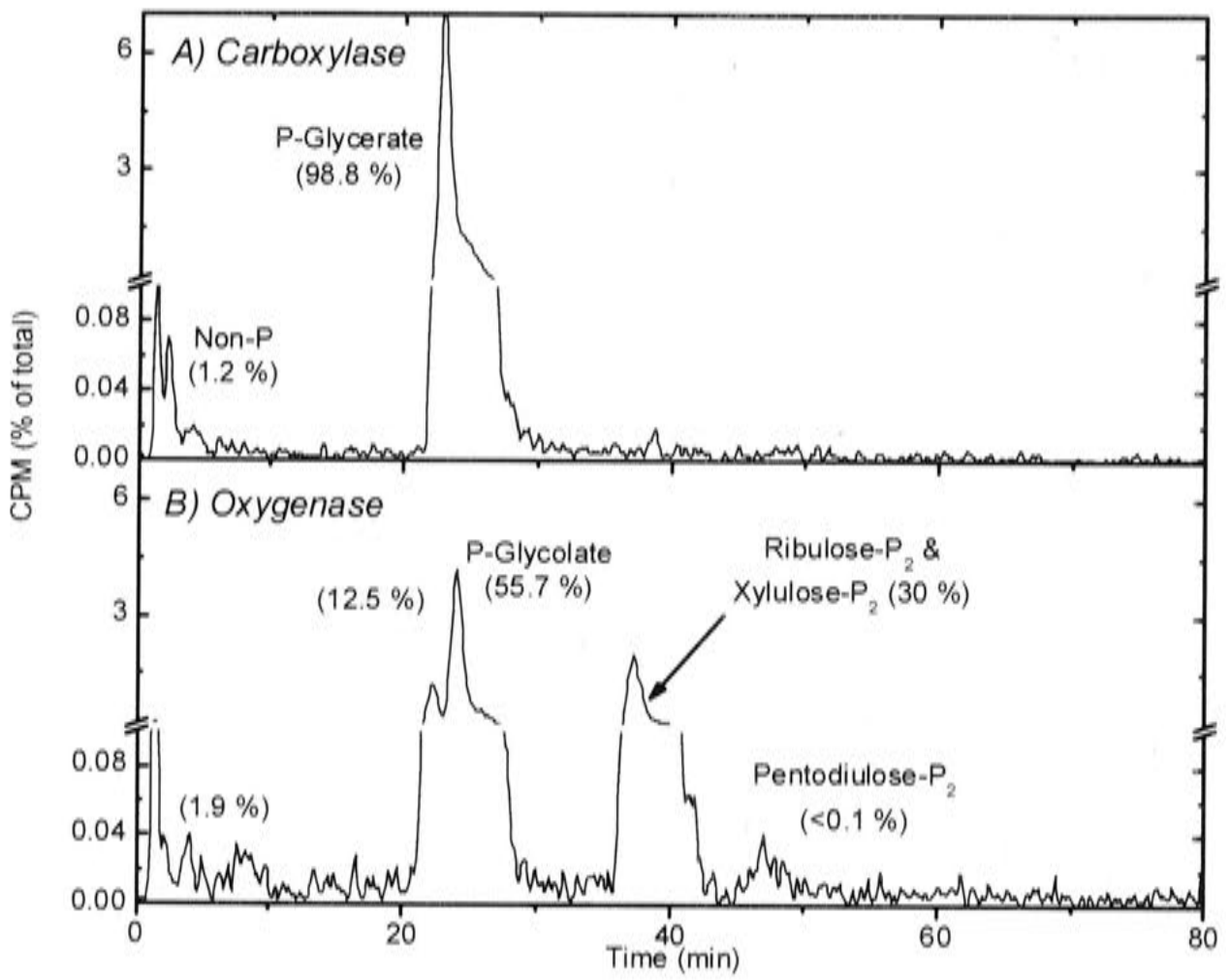

Figure 4.7 Chromatography of *Synechococcus* PCC6301 Reaction Products.

Synechococcus PCC6301Rubisco consumed [1-^{3}H]ribulose-P_2 under conditions that promoted carboxylase (*A*) or oxygenase (*B*) activity. The reaction products were chromatographed on an anion exchange column with a NaCl gradient (shown in Figure 4.3). The peak containing ribulose-P_2 and xylulose-P_2 under oxygenase conditions was collected and dephosphorylated before chromatography on a Bio-Rad HPX-87C column (*C*). The numbers in parentheses show the radioactivity recovered for each compound as a percentage of the total applied radioactivity.

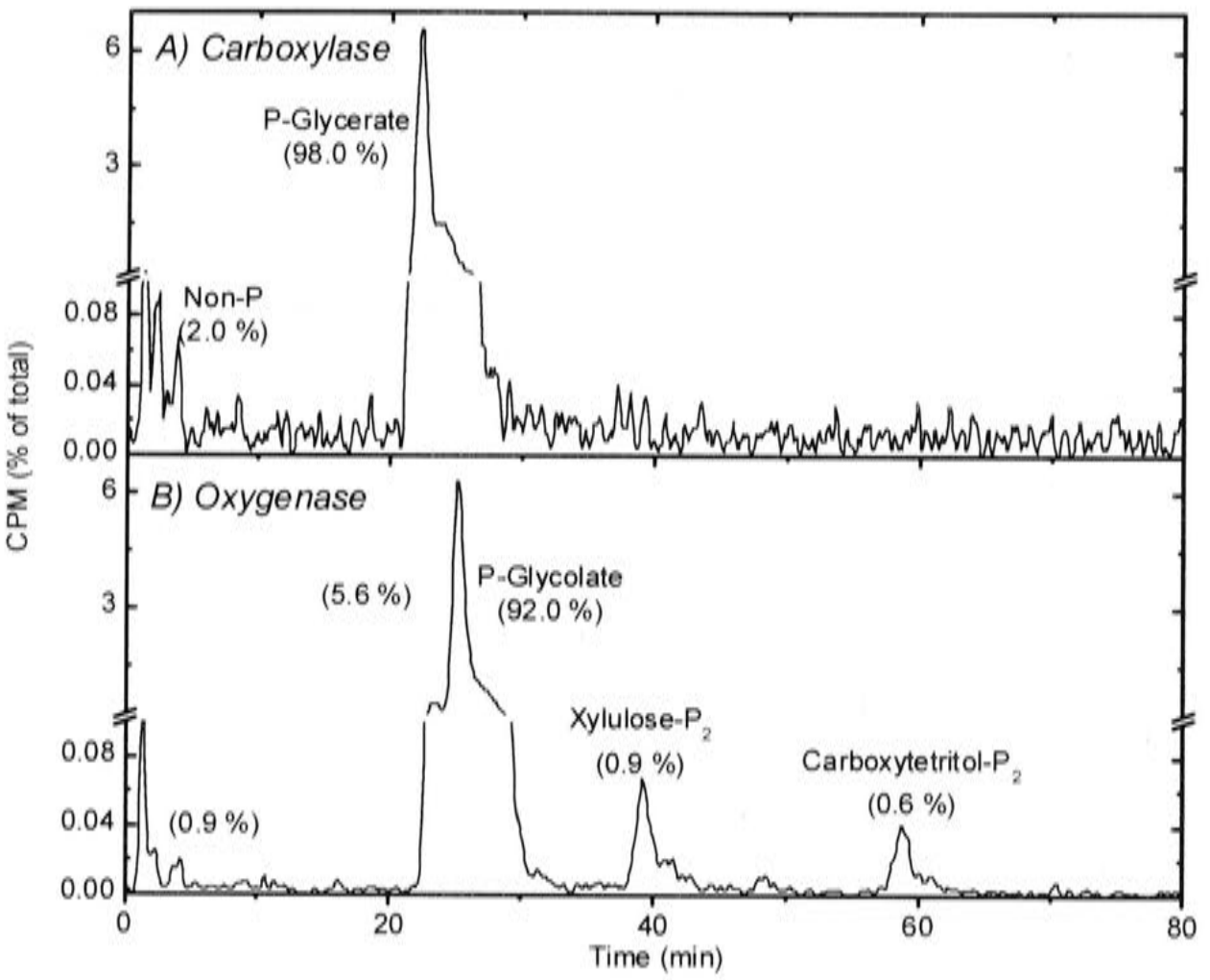

Figure 4.8 Chromatography of His-*Rubrum* Rubisco Reaction Products.

His-*Rubrum* Rubisco consumed [1-^{3}H]ribulose-P_2 under conditions that promoted carboxylase (*A, C*) or oxygenase (*B*) activity. The reaction products were chromatographed on an anion exchange column with a NaCl gradient (shown in Figure 4.3). The peak containing ribulose-P_2 and xylulose-P_2 under oxygenase conditions was collected and dephosphorylated before chromatography on a Bio-Rad HPX-87C column (*C*). The numbers in parentheses show the radioactivity recovered for each compound as a percentage of the total applied radioactivity.

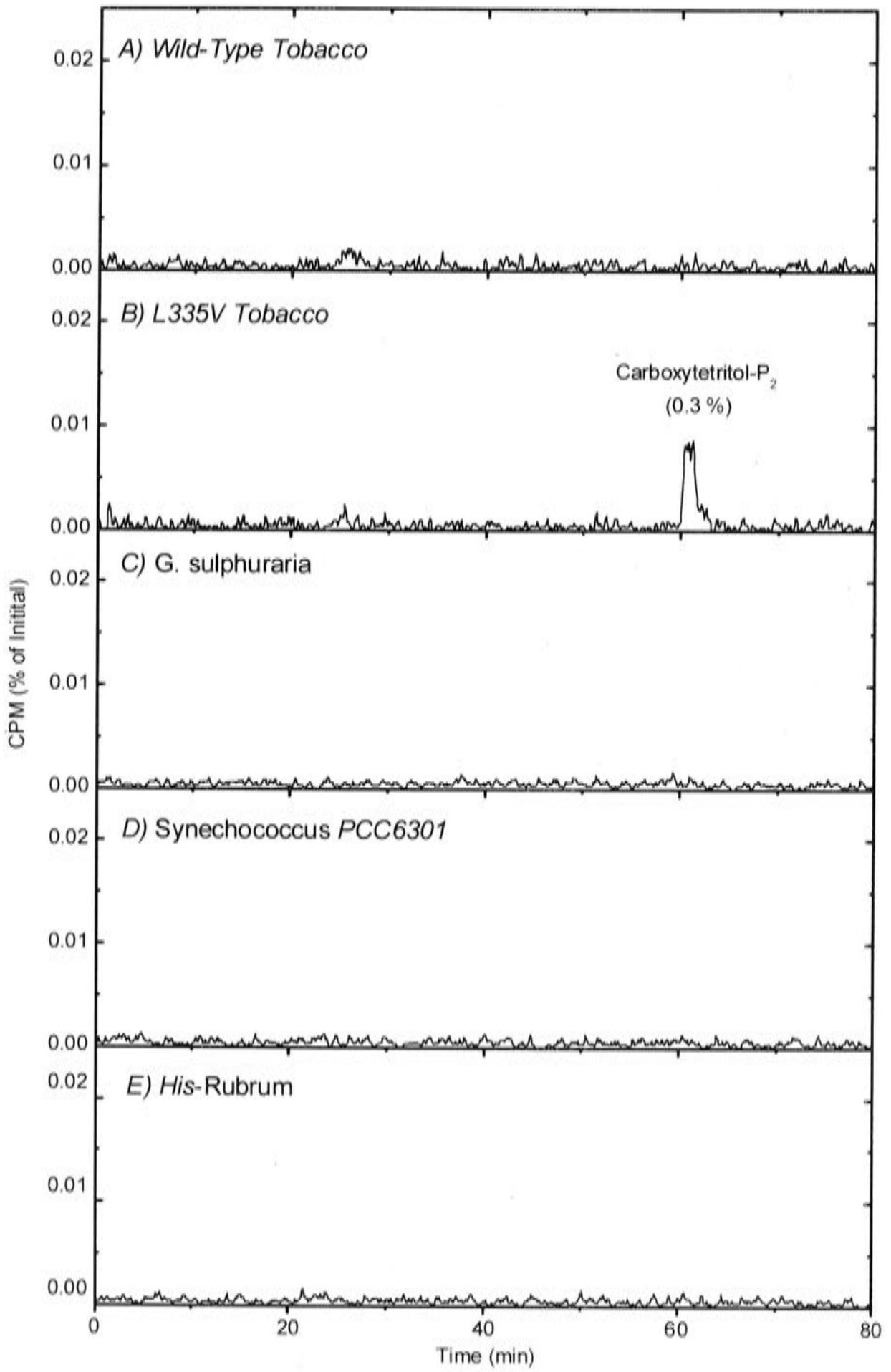

Figure 4.9 Chromatography of Reaction Products Produced Under Carboxylating Conditions That Remain Bound to Rubisco.

Wild-type Tobacco (*A*), L335V tobacco (*B*), *G. sulphuraria* (*C*), *Synechococcus* PCC6301 (*D*) and His-*Rubrum* (*E*) Rubisco consumed [1-^{3}H]ribulose-P_2 under conditions that promoted carboxylase activity. Unbound compounds were removed by ultrafiltration, and the reaction products remaining bound were released by treatment with SDS, then chromatographed on an anion exchange column with a NaCl gradient. The numbers in parentheses show the radioactivity recovered for each compound as a percentage of the total radioactivity.

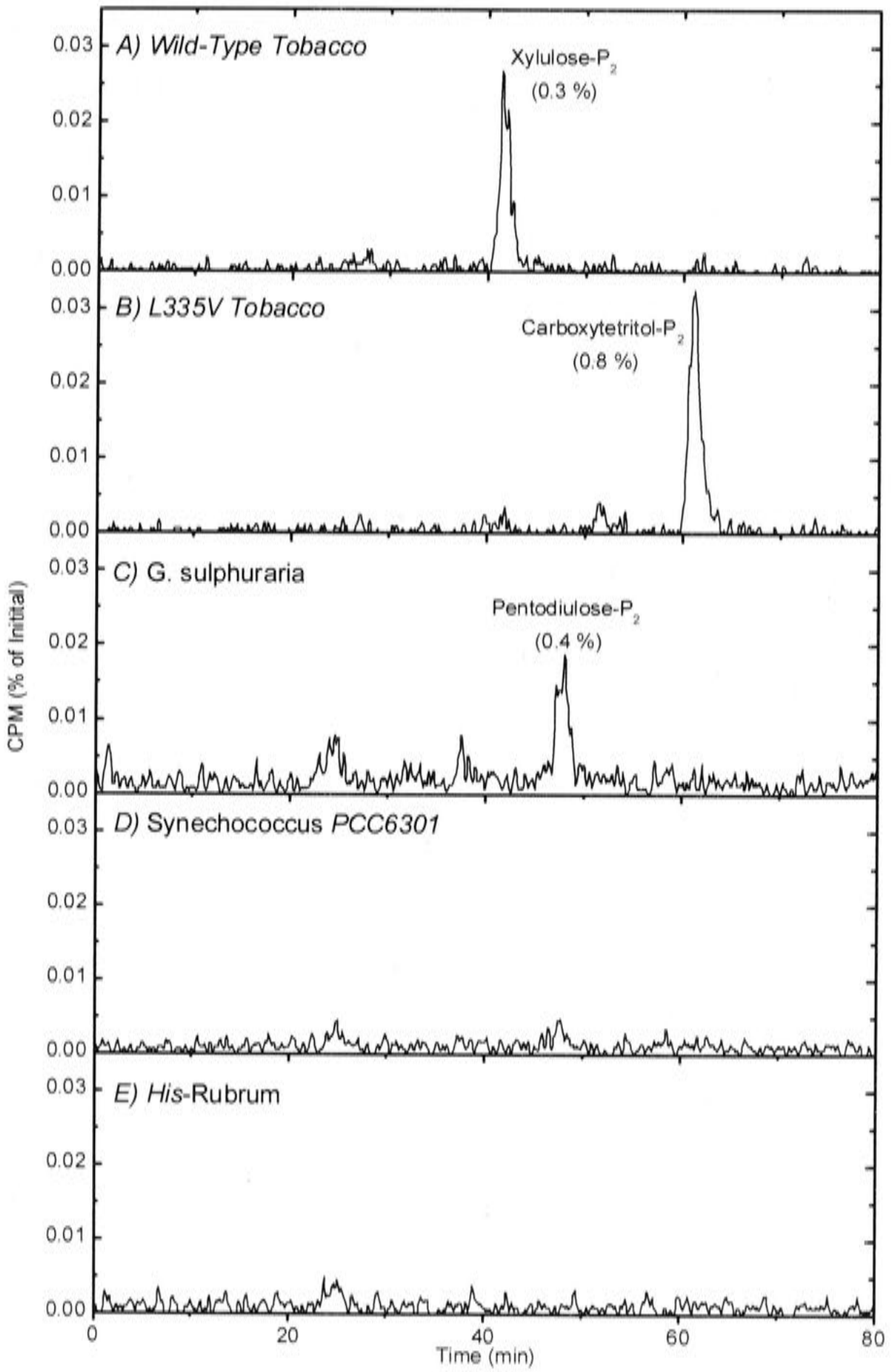

Figure 4.10 Chromatography of Reaction Products Produced Under Oxygenating Conditions That Remain Bound to Rubisco.

Wild-type Tobacco (*A*), L335V tobacco (*B*), *G. sulphuraria* (*C*), *Synechococcus* PCC6301 (*D*) and His-*Rubrum* (*E*) Rubisco consumed [1-^{3}H]ribulose-P_2 under conditions that promoted oxygenase activity. Unbound compounds were removed by ultrafiltration, and the reaction products remaining bound were released by treatment with SDS, then chromatographed on an anion exchange column with a NaCl gradient. The numbers in parentheses show the radioactivity recovered for each compound as a percentage of the total radioactivity.

4.3.5 Catalysis of Oxidised Ribulose-P_2

Exposure of ribulose-P_2 to Cu^{2+} ions results in the formation of several products, including pentodiulose-P_2 and carboxytetritol-P_2 (Kane et al. 1998). Chromatographic resolution of the oxidation products (Figure 4.11A) confirmed the presence of mostly ribulose-P_2 (~ 40 % of the initial ribulose-P_2 concentration) with some pentodiulose-P_2 (8.9 %) and carboxytetritol-P_2 (1.8 %), together with a variety of monophosphorylated and non-phosphorylated compounds arising from further degradation of the unstable pentodiulose-P_2 (Kane et al. 1998). The mixture of compounds was reacted with Rubisco to completion under carboxylase conditions, before unbound compounds were removed by gel filtration as quickly as possible to maximise the retention of bound pentodiulose-P_2.

Separation of the reaction products showed that wild-type tobacco, *G. sulphuraria*, and *Synechococcus* PCC6301 Rubisco converted the ribulose-P_2 into P-glycerate, but the proportions of pentodiulose-P_2 and carboxytetritol-P_2 were largely unchanged from the oxidised ribulose-P_2 mixture (Figure 4.11, Table 4.3). Most of the pentodiulose-P_2 and carboxytetritol-P_2 remained bound to the enzyme (Figure 4.12, Table 4.3).

L335V tobacco and His-*Rubrum* Rubisco also converted the ribulose-P_2 into P-glycerate, but had a higher proportion of carboxytetritol-P_2 to pentodiulose-P_2 (Figure 4.11). While both pentodiulose-P_2 and carboxytetritol-P_2 remained bound to L335V tobacco enzyme, there was negligible binding to His-*Rubrum* Rubisco (Figure 4.12).

4.3.6 The Effect of H_2O_2 on Reactions with Pentodiulose-P_2

In the presence of H_2O_2, pentodiulose-P_2 can be converted into P-glycolate and P-glycerate (Kane et al. 1998). Carboxytetritol-P_2 is formed by the benzylic acid-type rearrangement of pentodiulose-P_2, and to confirm the origin of carboxytetritol-P_2, H_2O_2 was included in some of the reaction assays. With both wild-type and L335V tobacco Rubisco, adding H_2O_2 simultaneously with the oxidized ribulose-P_2 preparation eliminated over 75 % of the bound radioactivity (Figure 4.13). When the H_2O_2 was added to the reaction mixture 5 min after the oxidized ribulose-P_2 preparation, when conversion to products had been completed, the result was similar with the wild-type Rubisco but different with the L335V mutant enzyme, which retained 80 % of the radioactivity bound in the absence of H_2O_2.

	Pentodiulose-P_2		Carboxytetritol-P_2	
	Total	Bound	Total	Bound
Wild-Type Tobacco	6.1 %	(4.2 %)	1.0 %	(0.6 %)
L335V Tobacco	1.1 %	(0.4 %)	4.8 %	(4.9 %)
G. sulphuraria	4.7 %	(5.2 %)	1.1 %	(1.2 %)
Synechococcus PCC6301	5.1 %	(3.8 %)	1.0 %	(1.3 %)
His-*Rubrum*	1.8 %	(< 0.1 %)	5.4 %	(1.0 %)

Table 4.3 Products of Catalysis Using Oxidised Ribulose-P_2.

Activated Rubisco was added to assays containing oxidised [1-^{3}H]ribulose-P_2 under CO_2 saturating conditions (as described in Section 4.2.5). Values shown are the amount of radiolabelled product as a percentage of total radioactivity. Number in parentheses show the percentage of initial radioactivity that remained bound to Rubisco after gel filtration

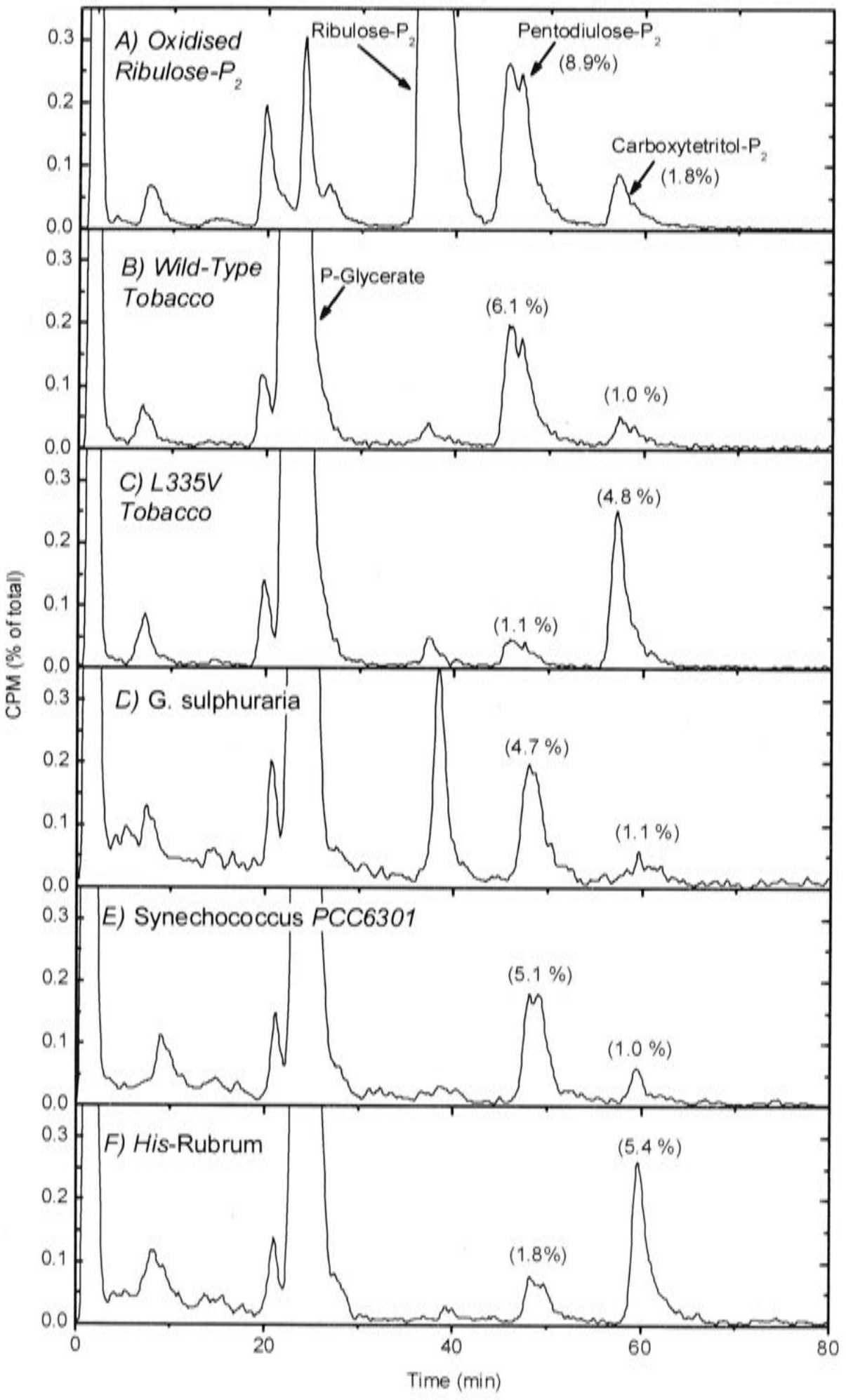

Figure 4.11 Chromatography of Total Reaction Products after Complete Consumption of Oxidised Ribulose-P_2.

[1-^{3}H]Ribulose-P_2 was oxidised with $CuSO_4$ (chromatogram of the oxidised products shown in *panel A*) and reacted to completion under carboxylating conditions with Wild-type tobacco (*B*), L335V tobacco (*C*), *G. sulphuraria* (*D*), *Synechococcus* PCC6301 (*E*) and His-*Rubrum* (*F*) Rubisco. Total reaction products were chromatographed on an anion exchange column with a NaCl gradient. The numbers in parentheses show the radioactivity for each compound as a percentage of the total radioactivity.

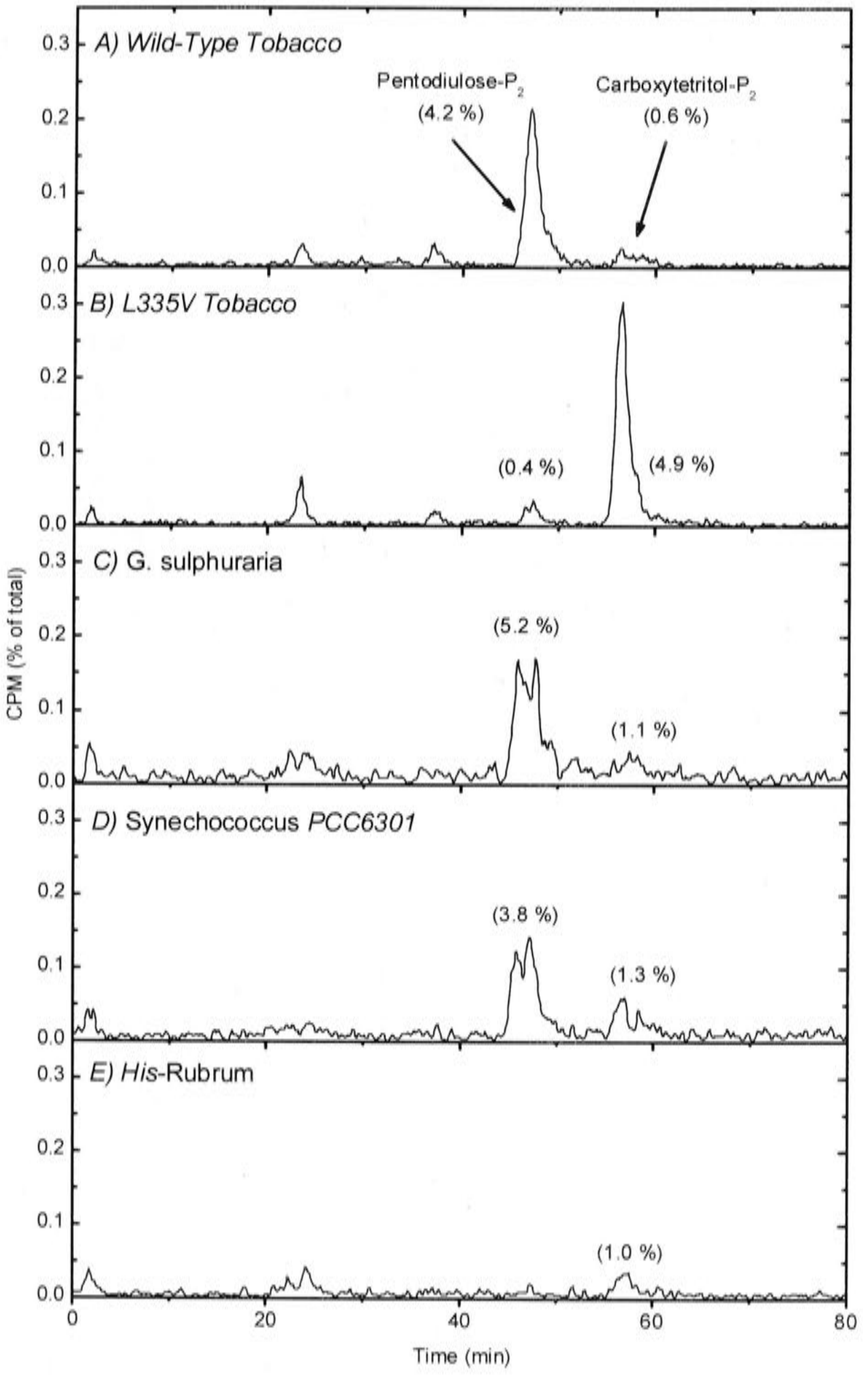

Figure 4.12 Chromatography of Enzyme-Bound Reaction Products after Complete Consumption of Oxidised Ribulose-P_2.

[1-^{3}H]Ribulose-P_2 was oxidised with $CuSO_4$ and reacted to completion under carboxylating conditions with Wild-type Tobacco (*A*), L335V tobacco (*B*), *G. sulphuraria* (*C*), *Synechococcus* PCC6301 (*D*) and His-*Rubrum* (*E*). Rubisco-bound compounds were isolated by gel filtration, released with SDS and chromatographed on an anion exchange column with a NaCl gradient. The numbers in parentheses show the radioactivity recovered for each compound as a percentage of the total initial radioactivity.

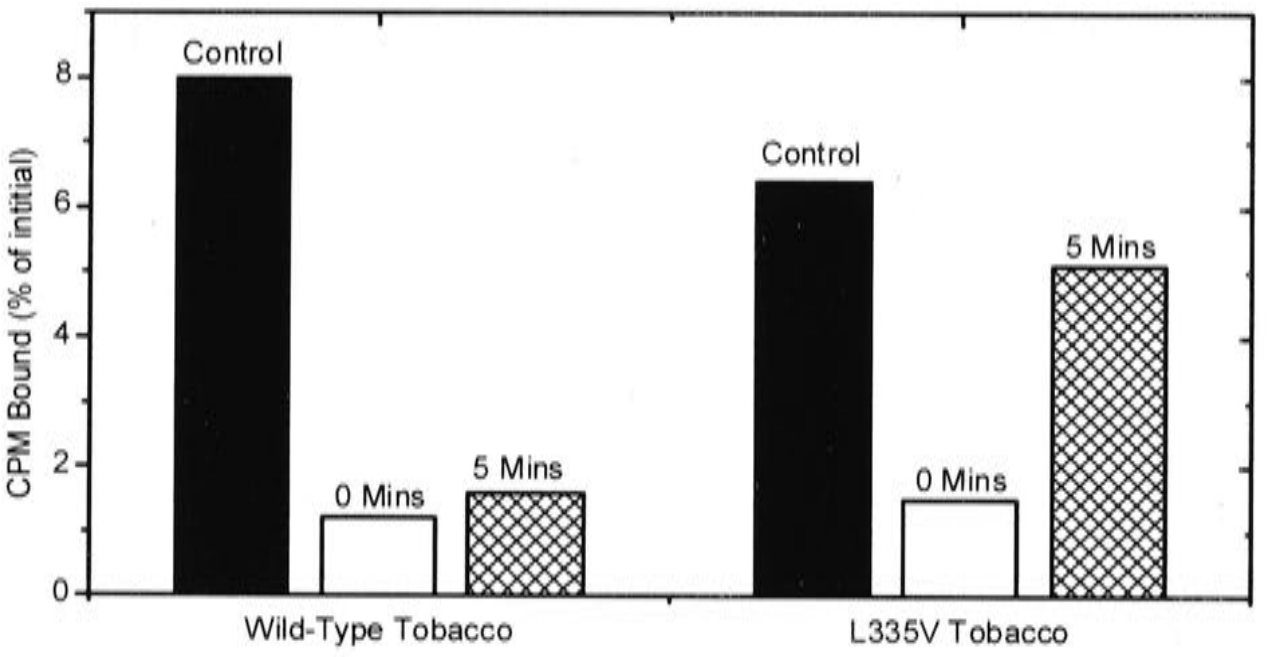

Figure 4.13 The Effect of H_2O_2 on the Binding of Ribulose-P_2 Oxidation Products to Rubisco.

[1-^{3}H]Ribulose-P_2 was oxidised with $CuSO_4$ and reacted to completion under carboxylating conditions with Wild-type tobacco, and L335V tobacco Rubisco. H_2O_2 was absent (black solid column) or added (5 mM final concentration) to Rubisco simultaneously with the oxidised ribulose-P_2 (0 min, white columns) or five min afterwards (5 min, hatched columns) when the reaction had proceeded to completion. Rubisco-bound compounds were isolated by gel filtration, and the radioactivity was determined using on-line scintillation counting.

4.4 Discussion

Self-inhibition of Rubisco is due to the formation of inhibitory compounds, including pentodiulose-P_2 and xylulose-P_2, which bind to the active site of the enzyme (Edmondson et al. 1990b). Initial studies suggested that keto-arabinitol-P_2 may have been present as an inhibitor (Zhu and Jensen 1991a), but this was later shown to have been due to the misidentification of reaction products, and was actually pentodiulose-P_2 (Chen and Hartman 1995). The formation of side-products can be seen by chromatographic analysis of the products formed after the complete conversion of labelled ribulose-P_2 into products. A NaCl gradient was optimised to separate bisphosphate and carboxylated-monophosphate products using anion-exchange chromatography.

4.4.1 More Compounds are Produced Under Predominantly Oxygenating Conditions

Assays that were performed over predominantly oxygenating conditions yielded the most side-products. Under low CO_2 concentrations, the fraction of active sites bound to the enediol intermediate is increased, and flux through the oxygenase pathway is promoted. Reducing the availability of gaseous substrates to react with the enediol bound to the active site increases the chance of side-reactions to form alternate products. Increasing the proportion of oxygenation compared to carboxylation also increased the chance of the peroxyketone intermediate undergoing alternate reactions. The possible consequences of this is discussed in Section 7.

Xylulose-P_2 was produced by all Rubisco enzymes to some extent under oxygenating conditions, but was not observed under carboxylating conditions (Table 4.2). As xylulose-P_2 is formed by the misprotonation of the enediol intermediate, there is a greater chance of formation under low CO_2 concentrations, when there is a high proportion of enediol bound to the active site because the reaction is limited by the availability of CO_2. When the CO_2 concentration is high, the proportion of active sites with enediol present is reduced due to a high availability of CO_2, and there is less opportunity for side reactions to occur.

Under predominantly oxygenating conditions, pentodiulose-P_2 was produced by both wild-type and L335V tobacco Rubisco, and traces were present for other Rubisco enzymes (Table 4.2). Pentodiulose-P_2 can be produced from the peroxyketone intermediate of the oxygenation pathway, or by the non-enzymatic oxidation of

ribulose-P_2 in solution, therefore it is not observed under anaerobic conditions when no O_2 is available for non-enzymatic oxidation or formation of the peroxyketone.

Under predominantly oxygenating conditions, the increased incubation times allow the opportunity for non-enzymatic oxidation of ribulose-P_2 to occur. An increased amount of pentodiulose-P_2 present for wild-type and L335V tobacco Rubisco compared to other Rubisco enzymes suggests that there was increased formation of pentodiulose-P_2 from the peroxyketone intermediate above the background levels of non-enzymatic oxidation. Tobacco Rubisco appears to be restricted in its ability to prevent peroxide elimination of the peroxyketone, when compared to the other enzymes studied. Despite a conservation of active site structure between different enzymes, there may be subtle differences in the active site due to differences remote to the active site that reduce the stability of the reaction intermediate.

A reduction in the level of pentodiulose-P_2 produced by other Rubisco enzymes could also be due to its consumption during the assay. In the presence of H_2O_2, Rubisco can catalyse the reverse reaction, and convert pentodiulose-P_2 into P-glycerate and P-glycolate (Kane et al. 1998). The reduced amounts of pentodiulose-P_2 during the assay may also be due to increased turnover by Rubisco in the presence of traces of H_2O_2 during the assay. While this turnover rate may be slow, the long incubation times inherent to the assay may be sufficient to allow nearly complete consumption.

However, when Rubisco is incubated with oxidised ribulose-P_2, which contains a mixture of compounds including pentodiulose-P_2, the concentration of pentodiulose-P_2 after the reaction is similar to the initial concentration. If the reduced level of pentodiulose-P_2 observed in the oxygenase product assays were due to increased turnover of the compound, it would be expected that the pentodiulose-P_2 in the oxidised ribulose-P_2 mixture would also be turned over. As this is not the case, the reduced level of pentodiulose-P_2 observed for *G. sulphuraria*, *Synechococcus* PCC6301 and His-*Rubrum* Rubisco must be due to a reduced rate of production, rather than an increased level of consumption.

4.4.2 L335V Tobacco and His-*Rubrum* Rubisco Rearrange Pentodiulose-P_2 into Carboxytetritol-P_2

Carboxytetritol-P_2 can be produced during catalysis by the benzylic acid-type rearrangement of pentodiulose-P_2 (Chen and Hartman 1995). This product was only formed by L335V tobacco and His-*Rubrum* Rubisco under oxygenating conditions,

which promoted the formation of pentodiulose-P_2 from the peroxyketone intermediate (Table 4.2).

To further investigate the processing of intermediate products, ribulose-P_2 can be incubated with Cu^{2+} ions to produce a mixture of compounds, including pentodiulose-P_2 and carboxytetritol-P_2 (Kane et al. 1998). Incubation of this mixture with Rubisco showed that only L335V tobacco and His-*Rubrum* Rubisco were able to carry out the rearrangement of pentodiulose-P_2 (Figure 4.11,Table 4.3). In other enzymes, the proportions of carboxytetritol-P_2 and pentodiulose-P_2 were similar to those found in the initial mixture. L335V tobacco and His-*Rubrum* Rubisco showed an increase in the proportion of carboxytetritol-P_2 and a corresponding decrease in the proportion of pentodiulose-P_2 due to the rearrangement of pentodiulose-P_2 into carboxytetritol-P_2.

The formation of carboxytetritol-P_2 from pentodiulose-P_2 was also demonstrated by adding H_2O_2 to the assay mixture, allowing the return of pentodiulose-P_2 to the catalytic pathway for oxygenation to produce P-glycerate and P-glycolate. Both pentodiulose-P_2 and carboxytetritol-P_2 bind tightly to wild-type and L335V Rubisco, thus the proportion of bound radioactivity reflects the total amount of carboxytetritol-P_2 and pentodiulose-P_2 present.

Addition of H_2O_2 to the assay altered the total amount of bound radioactivity, influencing the amount of carboxytetritol-P_2 and pentodiulose-P_2 that was bound to Rubisco (Figure 4.13). In the absence of H_2O_2, wild-type tobacco Rubisco bound only the initial concentrations of pentodiulose-P_2 and carboxytetritol-P_2. L335V tobacco Rubisco also bound the initial concentrations of carboxytetritol-P_2 and pentodiulose-P_2, and was able to rearrange pentodiulose-P_2 into carboxytetritol-P_2. When H_2O_2 was initially present in the assay, the pentodiulose-P_2 in the mixture could be converted back to the peroxyketone intermediate, and subsequently cleaved to produce P-glycolate and P-glycerate. These compounds do not bind tightly to the enzyme, leaving only the initial carboxytetritol-P_2 bound to the active site. When H_2O_2 was added to the assay after 5 min, L335V tobacco Rubisco was able to catalyse the rearrangement of pentodiulose-P_2 into carboxytetritol-P_2 before the peroxide was added. Even after the addition of H_2O_2 to the solution, the carboxytetritol-P_2 remained bound to the enzyme, while pentodiulose-P_2 was converted into P-glycolate and P-glycerate and released. The wild-type tobacco Rubisco enzyme could not catalyse this rearrangement into carboxytetritol-P_2, and the pentodiulose-P_2 was converted into P-glycolate and P-glycerate in the presence of H_2O_2, which were subsequently released. This experiment could not be

carried out using His-*Rubrum* Rubisco, due to the reduced binding of carboxytetritol-P_2 and pentodiulose-P_2.

Differences in the ability to rearrange pentodiulose-P_2 are most likely due to changes in the structure of the active site. The L335V tobacco enzyme has valine instead of leucine at position 335. Leu-335 is conserved in all Form I Rubisco enzymes, as is methionine in all Form II Rubisco enzymes, which includes the His-*Rubrum* enzyme. The presence of leucine in loop 6 apparently prevents the rearrangement of pentodiulose-P_2 into carboxytetritol-P_2. When the residue is not leucine, such as the alteration to valine in L335V tobacco Rubisco, or the naturally occurring methionine residue in His-*Rubrum* Rubisco, there is greater flexibility in the active site that allows the rearrangement of pentodiulose-P_2 into carboxytetritol-P_2 to occur.

4.4.3 Some Products Bind Tightly to Rubisco

Few side-products were produced under carboxylating conditions, and consequently, with the exception of some carboxytetritol-P_2 that was bound to L335V tobacco Rubisco, few compounds were isolated that were bound to Rubisco. The carboxytetritol-P_2 bound to L335V tobacco Rubisco had not been observed as a reaction product, but may have been present at low levels due to some of production of carboxytetritol-P_2 from traces of pentodiulose-P_2 that were formed non-enzymatically from ribulose-P_2 during the assay. In the chromatographic separations of the total reaction products there is a higher level of background radiation compared to the separation of bound products, and it is possible that carboxytetritol-P_2 and pentodiulose-P_2 were present at low concentrations.

More tightly bound compounds were isolated under oxygenating conditions, when more side-products were formed. Although xylulose-P_2 was produced by all Rubisco enzymes, it only bound tightly to wild-type tobacco Rubisco. Similarly, while pentodiulose-P_2 was present in the reaction product mixtures of all Rubisco enzymes, it only bound tightly to Rubisco enzymes from *G. sulphuraria*. Carboxytetritol-P_2 bound tightly to L335V tobacco Rubisco in larger amounts under oxygenating conditions than under carboxylating conditions, and no compounds were isolated that bound tightly to *Synechococcus* PCC6301 or His-*Rubrum* Rubisco.

Although little pentodiulose-P_2 and carboxytetritol-P_2 were produced under oxygenating or carboxylating conditions, the binding of these compounds to Rubisco could be demonstrated using a mixture of ribulose-P_2 oxidation and degradation products. Pentodiulose-P_2 and carboxytetritol-P_2 bound tightly to Rubisco enzymes

from wild-type tobacco, *G. sulphuraria* and *Synechococcus* PCC6301 in similar proportions to those in the initial ribulose-P_2 mixture and the total reaction products. This showed that there was negligible turnover of either compound, and that the rearrangement of pentodiulose-P_2 to carboxytetritol-P_2 was not catalysed by the enzymes. Carboxytetritol-P_2 and pentodiulose-P_2 also bound tightly to L335V tobacco Rubisco, but with an increased proportion of carboxytetritol-P_2 relative to pentodiulose-P_2. This altered ratio was due to the rearrangement of pentodiulose-P_2 into carboxytetritol-P_2 at the active site. Traces of carboxytetritol-P_2, but no pentodiulose-P_2 was observed to bind tightly to His-*Rubrum* Rubisco, despite a higher proportion of carboxytetritol-P_2 relative to pentodiulose-P_2 being present in the total reaction products, suggesting a reduced binding affinity of the enzyme for the inhibitors.

4.4.4 Implications for Self-Inhibition

Differences in the pattern of self-inhibition of Rubisco enzymes are due to variation in the formation and binding of inhibitory compounds. All Rubisco enzymes produce some side-products that may include xylulose-P_2, pentodiulose-P_2 and carboxytetritol-P_2. Formation of these compounds is increased when there is a low CO_2/O_2 ratio, due to greater proportion of enzyme bound to the enediol that may be misprotonated to form xylulose-P_2, and during oxygenation, when the peroxyketone intermediate can give rise to side-products. The same compound may bind tightly to some Rubisco enzymes, but not to others.

Wild-type tobacco Rubisco produces and tightly binds xylulose-P_2 and pentodiulose-P_2, while L335V tobacco Rubisco produces xylulose-P_2, pentodiulose-P_2 and carboxytetritol-P_2, but only accumulates carboxytetritol-P_2. This accounts for the decline in activity that was observed in the previous chapter, as xylulose-P_2 and pentodiulose-P_2 bind to the wild-type tobacco enzyme and carboxytetritol-P_2 binds to the L335V tobacco enzyme.

G. sulphuraria and *Synechococcus* PCC6301 Rubisco enzymes bind pentodiulose-P_2 and carboxytetritol-P_2 tightly, but do not produce either of them as side-products in significant amounts. The only compound that they do produce as a side-product, xylulose-P_2, does not bind tightly to the active site. Hence the lack of self-inhibition observed for these enzymes is due to a reduction in the formation of some pentodiulose-P_2 and carboxytetritol-P_2, in conjunction with prevention of the tight binding of xylulose-P_2, which is produced during catalysis.

His-*Rubrum* Rubisco produces xylulose-P_2, pentodiulose-P_2 and carboxytetritol-P_2, during catalysis, but none of them bind tightly to the active site. The lack of self-inhibition for this enzyme is due to a reduction in the tightness with which inhibitors bind to the enzyme.

4.4.5 Conclusions

During catalysis, Rubisco enzymes can produce a range of products that may bind tightly to the enzyme. While few side-products were present when conditions promoted carboxylating activity, more compounds were present under predominantly oxygenating conditions. Xylulose-P_2 and pentodiulose-P_2 were produced by several enzymes, confirming previous observations concerning their role in the inhibition of enzyme activity during *in vitro* assays. L335V tobacco and His-*Rubrum* Rubisco can convert pentodiulose-P_2 into carboxytetritol-P_2, which binds tightly to most Rubisco enzymes, but not to His-*Rubrum* Rubisco. Xylulose-P_2 only bound tightly to wild-type tobacco Rubisco, while pentodiulose-P_2 bound tightly to all Rubisco enzymes except that from His-*Rubrum*.

5 Continuous Measurement of Side- and Partial-Reactions

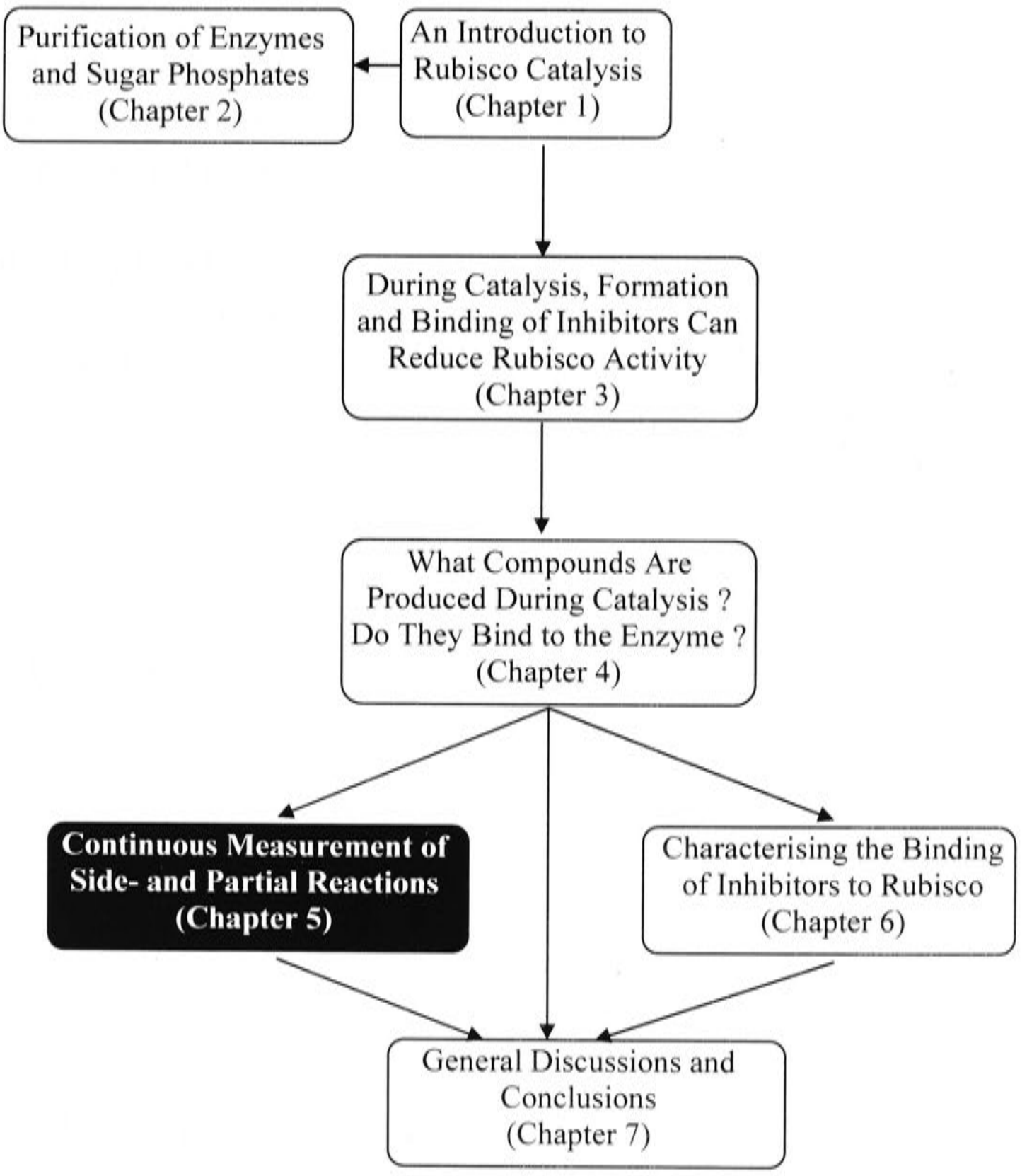

5.1 Introduction

As demonstrated in Chapter 4, Rubisco can catalyse a range of reactions other than the carboxylation and oxygenation of ribulose-P_2. While previous work has looked at the extent of production as a proportion of the initial ribulose-P_2 concentration, this chapter shows how the continuous rate of these side-reactions can be quantified, as can some of the partial-reactions. By observing the alternate partitioning of reaction intermediates, the relative tendencies of the enzyme to carry out side-reactions will be demonstrated., which will reflect the ability of the active site to stabilise intermediate compounds during catalysis.

5.1.1 Enolisation of Ribulose-P_2

In the initial step of catalysis, ribulose-P_2 is deprotonated at C-3 and O-3, and protonated at O-2 (as described in Section 1.4.3). The rate of enolisation can be measured by using ribulose-P_2 that has a labelled proton bound to the C-3 atom (Sue and Knowles 1982; Pierce and Reddy 1986). This proton is removed during enolisation, and is then replaced with a proton from solution if the enediol is reprotonated to form ribulose-P_2 (Figure 5.1).

5.1.2 Misprotonation of the Enediol

The enediol initially formed from ribulose-P_2 can be reprotonated at C-3 to form either ribulose-P_2 or xylulose-P_2. Re-protonation of the *Re* face yields xylulose-P_2, while reprotonation of the *Si* face produces ribulose-P_2 (shown in Figure 5.1).

Previous observations of xylulose-P_2 formation by Rubisco measured the proportion of initial ribulose-P_2 converted into xylulose-P_2, rather than by continuous measurement (Edmondson et al. 1990d). The rate of xylulose-P_2 production is affected by pH, with nearly eight times more being produced at pH 6.6 than at pH 8.0 (Zhu and Jensen 1991a).

...

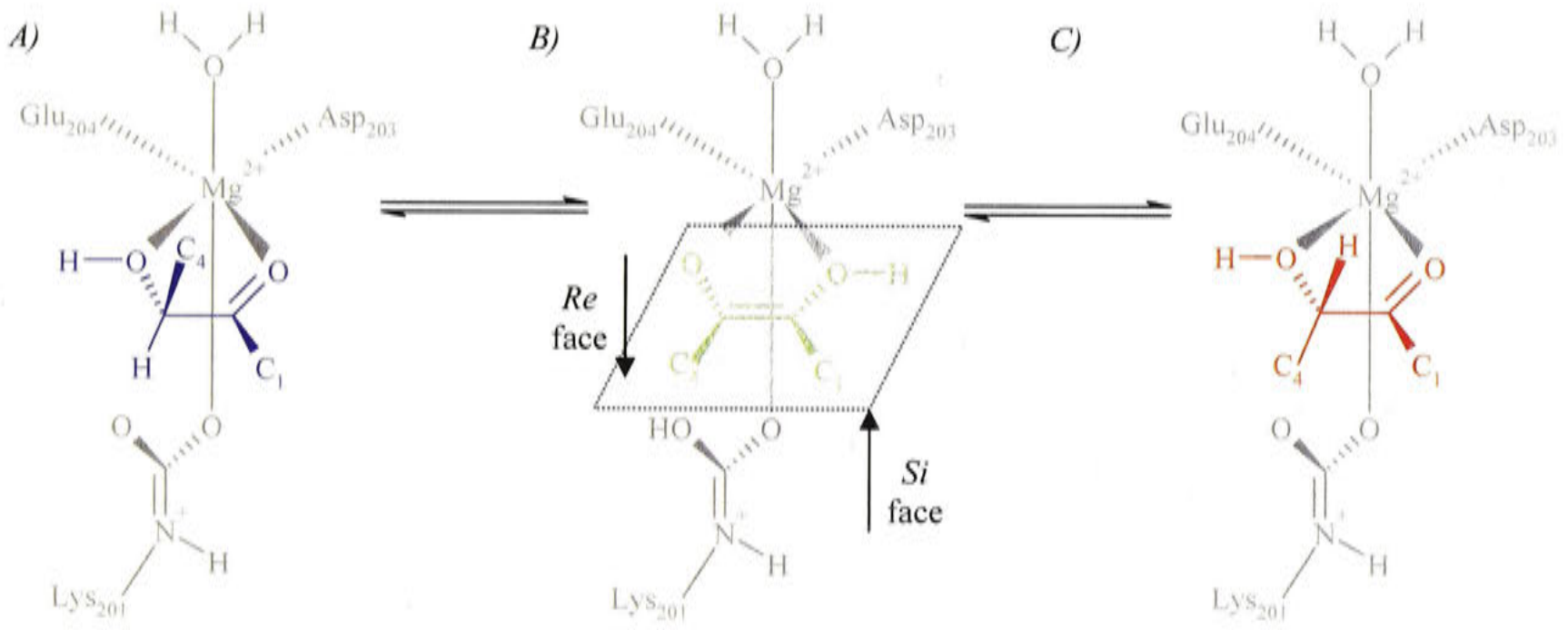

Figure 5.1 Reactions of the Enediol

Ribulose-P_2 (shown in blue) forms bonds with the metal ion to correctly orientate itself in the active site (*A*). Deprotonation of C-3 results in the formation of the enediol (shown in green), which adopts a similar orientation (*B*). Reprotonation of the enediol from the upper (*Re)* face results in the formation of xylulose-P_2 (*C*) (shown in red), while reprotonation from below (*Si*) forms ribulose-P_2. Enolisation of xylulose-P_2 is reduced because the carbamylated lysine residue is incorrectly positioned to deprotonate C-3.

Some mutations can increase the rate of production of xylulose-P_2. The E60Q (48) mutant of *R. rubrum*, which is restricted in its ability to form interactions in the active site, had a greatly reduced carboxylation rate and also showed self-inhibition characteristics (Lee et al. 1993). The self-inhibition was thought to be due to increased production of xylulose-P_2 and pentodiulose-P_2. The misprotonation rate was similar to the carboxylation rate, and initially high levels of xylulose-P_2 were observed in the reaction products. The xylulose-P_2 was eventually processed into P-glycerate and P-glycolate in the mutant enzyme, while no evidence of misprotonation by the wild-type *R. rubrum* enzyme was observed.

Mutations in the small subunit of *Synechococcus* PCC6301 also increased the misprotonation of the enediol to produce xylulose-P_2. While the wild-type enzyme converted 0.14 % of the initial ribulose-P_2 into xylulose-P_2, the Q99G and P108L SSU mutants produced 0.24 % and 0.40 % respectively and reduced the maximal rate of the enzyme (Flachmann et al. 1997). The decreased catalytic rate and increased misfire rate suggest a greater flexibility in the active site, probably due to weakened long range interactions between the small and large subunits. Increased xylulose-P_2 production may be due to the impaired ability of the mutant enzymes to stabilise the transition state forward reaction of enediol-ribulose-P_2 with CO_2.

5.1.3 β-Elimination of the Enediol

The enediol also has a tendency to undergo β-elimination reactions, resulting in a loss of phosphate to produce deoxy-pentodiulose-P (Paech et al. 1978; Morell et al. 1994). β-Elimination can be minimised if the bond between C-1 and the O atom of P-1 is in the same plane as the double bond between C-3 and C-2 (Rose 1981). The structure of spinach Rubisco activated with Ca^{2+} and bound to ribulose-P_2 showed that the bonds from C-2 to P-1 were indeed coplanar, as shown in Figure 5.2, and should minimize β-elimination (Taylor and Andersson 1997b). The P-1 phosphate is held in position by links to Gly-381, Gly-403 and Gly-404 residues in loops 7 and 8, and to Thr-65 from the adjoining large subunit (Cleland et al. 1998).

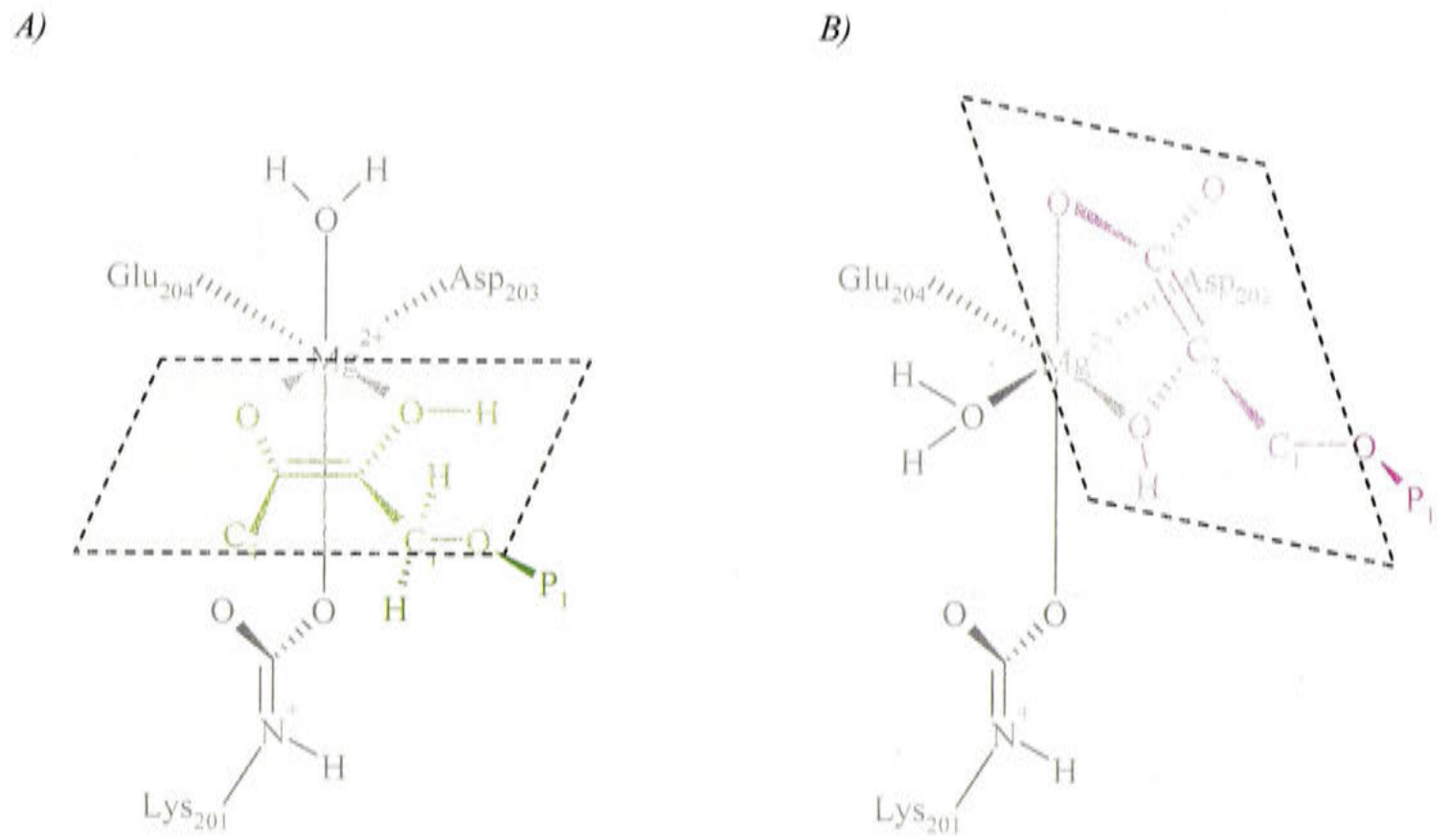

Figure 5.2 Planarity of the Enediol and *aci*-Acid

To reduce β-elimination of the enediol (A, shown in green) and *aci*-acid (B, shown in purple) intermediates, bonds must be kept planar. For the enediol, the C-1 to P-1 bond is kept in the same plane as the C-2 to C-3 double bond, and in the *aci*-acid, the C' to C-2 double bond is kept in the same plane as the C-1 to P-1 bond.

Some β-elimination can still be observed for spinach and *Synechococcus* PCC6301 Rubisco (Morell et al. 1997), with the T65V *Synechococcus* PCC6301 mutant converting 13 % of the initial ribulose-P_2 in the assay into deoxy-pentodiulose-P. The increased β-elimination in the mutant enzyme is due to an alteration of the P-1 binding site that reduces the ability of the intermediate compound to maintain bond planarity (Morell et al. 1994).

5.1.4 β-Elimination of the *aci*-Acid

The *aci*-acid that is produced after cleavage of the C-2 to C-3 bond of the carboxyketone intermediate is also prone to β-elimination. In this case, elimination of the phosphate group produces pyruvate. Like the enediol, β-elimination is minimised if the bond between C-1 and P-1 is kept in the same plane as the bond between the carboxyl-C and C-2, as shown in Figure 5.2. However this plane is perpendicular to the C-1 to P-1 plane of the enediol intermediate. The P-1 group is still held in position by hydrogen bonds, and coordinate covalent bonds also link O-2 to Mg^{2+} and the carboxylate to Mg^{2+}. As a result, C-1 and C-2 are able to move, maintaining a planar structure. This is supported by the observation of P-glycerate bound in this configuration in the structure of carbamylated enzyme with P-glycerate in the active site (Taylor and Andersson 1997a).

β-Elimination is not completely prevented during catalysis, and Rubisco normally produces pyruvate once every 150 turnovers, which is the equivalent of converting 0.7 % of the initial ribulose-P_2 concentration (Andrews and Kane 1991). Carrying out the reaction using ^2H_2O as a solvent increased the partitioning towards pyruvate to 2.2 %, due to the isotope effect, in which the deuteron is less likely to be donated than a proton, reducing the rate at which the *aci*-acid is protonated, and increasing the chance of β-elimination (Andrews and Kane 1991). Mutagenesis of the sites that position P-1 alter the binding orientation and can increase (Larimer et al. 1994), or decrease (Morell et al. 1994) the amount of pyruvate produced, by affecting the ability of the enzyme to maintain the planarity of the *aci*-acid molecule.

5.1.5 Carboxylation of Xylulose-P_2

Rubisco is able to carry out the enolisation of xylulose-P_2 by deprotonation of the C-3 atom, and protonation of the O-2 atom, in an analogous reaction to enolisation of ribulose-P_2 (Yokota 1991a). Enolisation is slower because the C-3 proton is not in a position where it can be removed by the carbamylated Lys-201 residue, as shown in

Figure 5.1. The resulting enediol can then undergo carboxylation or oxygenation in the same way as the enediol derived from ribulose-P_2.

Under saturating CO_2 concentrations, the rate of xylulose-P_2 carboxylation by *R. rubrum* Rubisco was 0.1–0.2 % of the rate of ribulose-P_2 carboxylation. The E60Q (48) mutant of *R. rubrum* Rubisco had a higher rate of xylulose-P_2 carboxylation, at 60 % of the ribulose-P_2 carboxylation rate (Lee et al. 1993). This mutant also had an increased rate of misprotonation to form xylulose-P_2, and a reduced carboxylation rate, due to altered interactions in the active site. Spinach Rubisco had a maximum xylulose-P_2 carboxylation rate that was 0.03 % of the rate of ribulose-P_2 carboxylation (Yokota 1991a), and *Synechococcus* PCC6301 had a slower xylulose-P_2 carboxylation rate, that was 0.005 % of ribulose-P_2 carboxylation (Newman and Gutteridge 1994).

5.1.6 Specific Aims and Objectives

While previous studies, and the experiments in Chapter 4, have looked at the products of catalysis, they have not directly looked at the absolute rate of formation. This chapter aims to measure the continuous rate of several side reactions, including β-elimination and misprotonation of the enediol intermediate and carboxylation of xylulose-P_2 for a range of different Rubisco enzymes. The continuous rate of [3-^{2}H]ribulose-P_2 enolisation is also measured, as is the β-elimination of the carbanion intermediate during catalysis.

Experiments used spectrophotometric and NMR assays to measure the rate of side- and partial-reactions carried out by Rubisco. Production of xylulose-P_2 and pyruvate were measured using coupled enzyme assays, while production of deoxy-pentodiulose-P was measured by the absorbance of a complex between the reaction product and o-phenylene-diamine. Enolisation of ribulose-P_2 was measured using NMR to observe the exchange of protons and deuterons.

5.2 Materials & Methods

5.2.1 Enolisation of Ribulose-P_2

The enolisation rate for wild-type and L335V tobacco Rubisco was measured by NMR spectrometry by observing the rate at which the deuteron of [3-^{2}H]ribulose-P_2 was exchanged with a proton from solution. Assays were carried out at 25 °C in buffer containing 50 mM Tris-HCl, pH 8.0, 10 mM $MgCl_2$, 1 mM EDTA, 10 % (v/v) ^2H_2O, and 2 mM [3-^{2}H] ribulose-P_2 that had been sparged with nitrogen. Reactions were initiated by the addition of Rubisco (to 3 μM sites) that had been activated as described in Section 2.2.2. The carry-over of $NaHCO_3$ was 100 μM. Spectra were collected at 2 minute intervals using a Varian INOVA 600 MHz NMR spectrometer. The water resonance was suppressed by the W5 WATERGATE pulse (Liu et al. 1998). The increasing intensity of the resonance at 4.37 ppm due to the 3-H proton with time was fitted to an exponential equation using non-linear regression software (OriginLab, Northampton, MA),

$$Area = A_f(1 - e^{-k_{obs}t}) \qquad \textbf{(Equation 5.1)}$$

where k_{obs} is the observed first-order rate constant and A_f is the final area. The rate of area.s^{-1} was calculated using the parameter estimates obtained and the differentiated form of Equation 5.1, in Equation 5.2.

$$Rate = A_f . k_{obs} . e^{-k_{obs}t} \qquad \textbf{(Equation 5.2)}$$

5.2.2 Carboxylation of [3-^{2}H]Ribulose-P_2

[3-^{2}H]Ribulose-P_2 carboxylase activity was measured using the same spectrophotometric assay as described in Section 2.2.2, but with 500 μM [3-^{2}H]ribulose-P_2 included in the assay instead of [3-^{1}H]ribulose-P_2. Data for product accumulation versus time were fitted to Equation 3.1 to estimate v_i, v_f and k_{obs}.

5.2.3 Misprotonation of the Enediol

Xylulose-P_2 formation was measured using a continuous spectrophotometric assay (Edmondson et al. 1990d). Assays were carried out in septum capped cuvettes that were flushed with N_2. Reaction mixtures (2 ml) contained 100 mM EPPS-NaOH, pH 8.0, 20 mM $MgCl_2$, 1 mM EDTA, 1 mg.ml^{-1} rabbit muscle aldolase, 0.16 mg.ml^{-1} rabbit muscle glycerol-P dehydrogenase, 10 mM NADH, 1 mM ribulose-P_2, and were sparged with

N_2. Reactions were initiated by the addition of Rubisco (final concentration 250 μg.ml^{-1}) that had been activated as in Section 3.2.1. Assays were carried out in duplicate on at least two separate runs, and the data pooled for the runs. Pooled data for product accumulation versus time were fitted to Equation 3.1. The reaction rate was calculated using a derivative of this equation, and the maximum rate (v_{max}) was estimated from this.

5.2.4 β-Elimination of the Enediol

Deoxy-pentodiulose-P formation was measured using a continuous spectrophotometric assay (Morell et al. 1997). Assays (2 ml) were carried out in buffer that had been sparged with N_2 containing 1 mM ribulose-P_2, 100 mM EPPS-NaOH, pH 8.0, 20 mM $MgCl_2$, 1 mM EDTA, 1 mg.ml^{-1} carbonic anhydrase and 20 mM *o*-phenylene-diamine in septum capped cuvettes that were flushed with N_2. Rubisco (final concentration in assay of 700 μg.ml^{-1}) was activated as described in Section 2.2.2, and approximately 180 μM $NaHCO_3$ was carried over to the final assay from the Rubisco activation process. Assays were carried out in duplicate on at least two separate runs, and the data pooled for the runs. Pooled data for product accumulation versus time were fitted to a fourth order polynomial equation. The reaction rate was calculated using a derivative of this equation, and the maximum rate (v_{max}) was estimated from this.

5.2.5 β-Elimination of the Carbanion

Pyruvate production during catalysis was measured using the method of (Andrews and Kane 1991), in which the pyruvate concentration was determined using a spectrophotometric assay. Rubisco (final concentration in assay of 50 μg.ml^{-1}) was activated as described in Section 2.2.2 and used to initiate assays (2 ml) in buffer containing 1 mM ribulose-P_2, 100 mM EPPS-NaOH, pH 8.0, 20 mM $MgCl_2$, 1 mM EDTA, 0.2 mM NADH, 0.1 mg.ml^{-1} carbonic anhydrase and 10 μg.ml^{-1} lactate dehydrogenase, which coupled the conversion of pyruvate into lactate with the consumption of NADH, which can be measured spectrophotometrically. After the ribulose-P_2 had been totally consumed, the amount of pyruvate produced was calculated by the total change in absorbance at 340 nm. Assays were carried out in duplicate on at least two separate runs, and the data pooled for the runs.

5.2.6 Carboxylation of Xylulose-P_2

Xylulose-P_2 carboxylase activity was measured using the same spectrophotometric assay as described in Section 2.2.2, but with 25–250 μM xylulose-P_2

included in the assay instead of ribulose-P_2, and using a final concentration of 30–130 $\mu g.ml^{-1}$ Rubisco. Assays were carried out in duplicate on at least two separate occasions, and the runs were pooled. The pooled data for product accumulation versus time were fitted to Equation 3.1 to estimate v_i, v_f and k_{obs}. Residual activity versus time was plotted using the parameter estimates obtained and Equation 3.2.

5.3 Results

5.3.1 Enolisation and Carboxylation of [3-^{2}H]Ribulose-P_2

Enolisation of ribulose-P_2 can be measured by monitoring the exchange of the C-3 proton of ribulose-P_2 with a proton from solution. This can be performed using [3-^{1}H]ribulose-P_2 in buffer containing ^2H_2O (Pierce et al. 1986b), or [3-^{3}H]ribulose-P_2 in buffer containing ^1H_2O (Sue and Knowles 1982).

In this experiment, the exchange of the deuteron of [3-^{2}H]ribulose-P_2 with an unlabelled proton from solution was measured by NMR. The level of [3-^{1}H]ribulose-P_2 (3.9 ppm) increased over time, as the deuteron was replaced with a proton from solution (Figure 5.3). This increase was fitted to Equation 5.1 to measure the rate of isotope exchange (Table 5.1). The level of [4-^{1}H]ribulose-P_2 (4.37 ppm) remained constant during the course of the assay, reflecting the restricted consumption of ribulose-P_2 under the anaerobic, CO_2 limited conditions of the assay. Some [3-^{1}H]P-glycolate (4.00 ppm) and [3-^{1}H]P-glycerate (4.10 ppm) were produced initially in the assay due to the 0.1 mM HCO_3^-/CO_2 carried over from the buffer in which Rubisco was activated, but this consumed only 5 % of the [3-^{2}H]ribulose-P_2 in the assay.

Carboxylation of [3-^{2}H]ribulose-P_2 was slower than [3-^{1}H]ribulose-P_2 carboxylation, but showed a similar decline in activity over time for wild-type and L335V tobacco Rubisco. The absolute enolisation rate was similar for wild-type and L335V tobacco Rubisco, but the rate relative to [3-^{2}H]ribulose-P_2 carboxylation was increased greatly in L335V tobacco Rubisco.

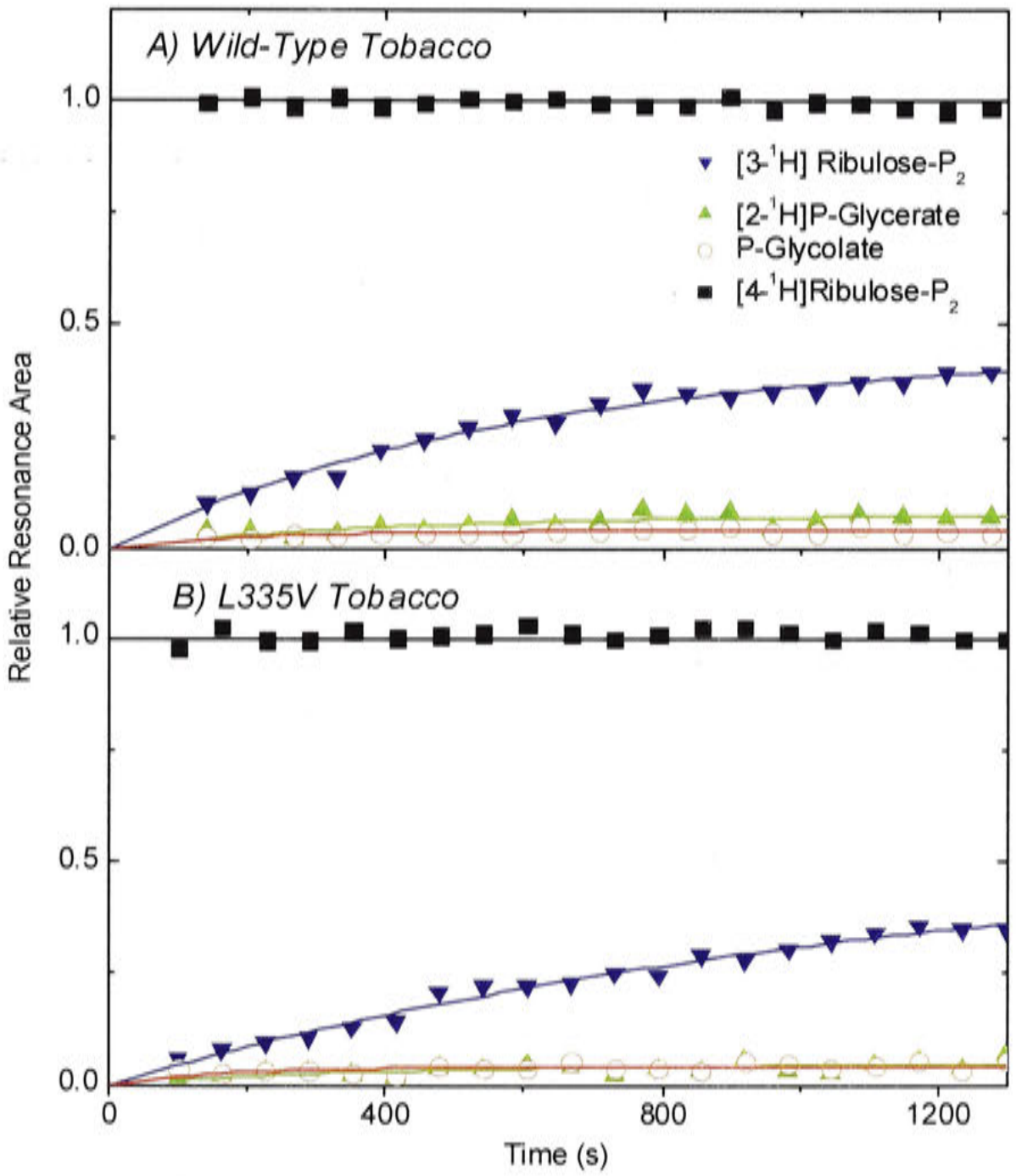

Figure 5.3 Enolisation of Ribulose-P_2 by Rubisco

Pre-activated wild-type (*A*) and L335V (*B*) tobacco Rubisco were used to initiate assays containing 2.9 mM [3-^{2}H]ribulose-P_2 and 10 % (v/v) ^2H_2O. Assays were carried out under anaerobic conditions designed to rapidly exhaust any remaining CO_2 carried over from the activation buffer. The rate at which the deuteron of [3-^{2}H]ribulose-P_2 was exchanged with a proton from solution was measured by NMR (as described in section 5.2.5). The increasing intensity of the resonance at 4.37 ppm ([3-^{1}H]ribulose-P_2) was fitted to Equation 5.1.

	[3-^{2}H]Ribulose-P_2 Enolisation Rate v_i (s^{-1})	[3-^{2}H]Ribulose-P_2 Carboxylation Rate v_i (s^{-1})	[3-^{1}H]Ribulose-P_2 Carboxylation Rate v_i (s^{-1})
Wild-Type Tobacco	0.92 ± 0.09	1.04 ± 0.01	2.82 ± 0.01
L335V Tobacco	0.61 ± 0.06	0.167 ± 0.002	0.477 ± 0.004

Table 5.1 The Rate of Enolisation and Carboxylation of [3-^{2}H]Ribulose-P_2 by Tobacco Rubisco.

Pre-activated Rubisco was incubated with [3-^{2}H]ribulose-P_2 in buffer containing 10 % (v/v) ^2H_2O. The rate at which the deuteron of [3-^{2}H]ribulose-P_2 was exchanged with a proton from solution was measured by NMR, and the initial enolisation rate calculated by fitting the data of Figure 5.3 to Equation 5.1. Activated Rubisco was also added to spectrophotometric assays containing 500 μM [3-^{2}H]ribulose-P_2 under CO_2 saturating conditions. Parameters (± S.E.) were calculated by fitting the data to Equation 3.1

5.3.2 Misprotonation of the Enediol

Reprotonation of the *Re* face of the enediol intermediate formed during catalysis results in the formation of xylulose-P_2. While this rate is slow compared with the rate of CO_2 addition to the enediol, it can be measured in the absence of CO_2 and O_2 where consumption of ribulose-P_2 by carboxylation and oxygenation is prevented and the fraction of enzyme with the enediol bound is maximised (Morell et al. 1997). Although CO_2 is required to activate Rubisco by carbamylation, this requirement can be met by activating the enzyme at high $NaHCO_3$ concentrations and adding a small volume of this to the assay mixture. Rubisco was pre-activated in 5 mM $NaHCO_3$ solution, and 20 µl of this was added to 2000 µl of the assay mixture, resulting in a carryover $NaHCO_3$ concentration of 50 µM. This is rapidly used up by carboxylation, which also uses only 50 µM of the 1000 µM ribulose-P_2 in solution. Decarbamylation of higher plant Rubisco in CO_2-free solutions occurs very slowly in the presence of ribulose-P_2 and was not considered to be a problem (Edmondson et al. 1990c).

Assuming that the xylulose-P_2 produced is released into solution, the rate of misprotonation can be measured using aldolase and glycerol-phosphate dehydrogenase. Controls that lacked Rubisco, ribulose-P_2, aldolase or glycerol-phosphate dehydrogenase showed negligible activity.

Assays showed an initial lag period, which is most likely due to delays while intermediates in the reaction reached steady-state concentration, and consumption of the last traces of CO_2/HCO_3^-, followed by a near linear rate. Increasing the concentration of the coupling enzymes did not reduce the lag period, demonstrating that the delay was not due to the coupling system. An exponential equation showed a good approximation to the data ($r^2 > 0.99$ for all fits, Figure 5.4 and Figure 5.5), and allowed calculation of xylulose-P_2.s^{-1}.active sites^{-1} (Table 5.2).

The absolute rate of xylulose-P_2 production was slowest for *Synechococcus* PCC6301 and L335V tobacco Rubisco. Wild-type tobacco and *G. sulphuraria* Rubisco had similar rates that were twice as fast, and His-*Rubrum* Rubisco had a rate that was ten times faster. When the rate of xylulose-P_2 production was compared to the ribulose-P_2 carboxylation rate, *Synechococcus* PCC6301 Rubisco produced the least xylulose-P_2, followed by wild-type tobacco, *G. sulphuraria*, L335V mutant tobacco and His-*Rubrum* Rubisco enzymes.

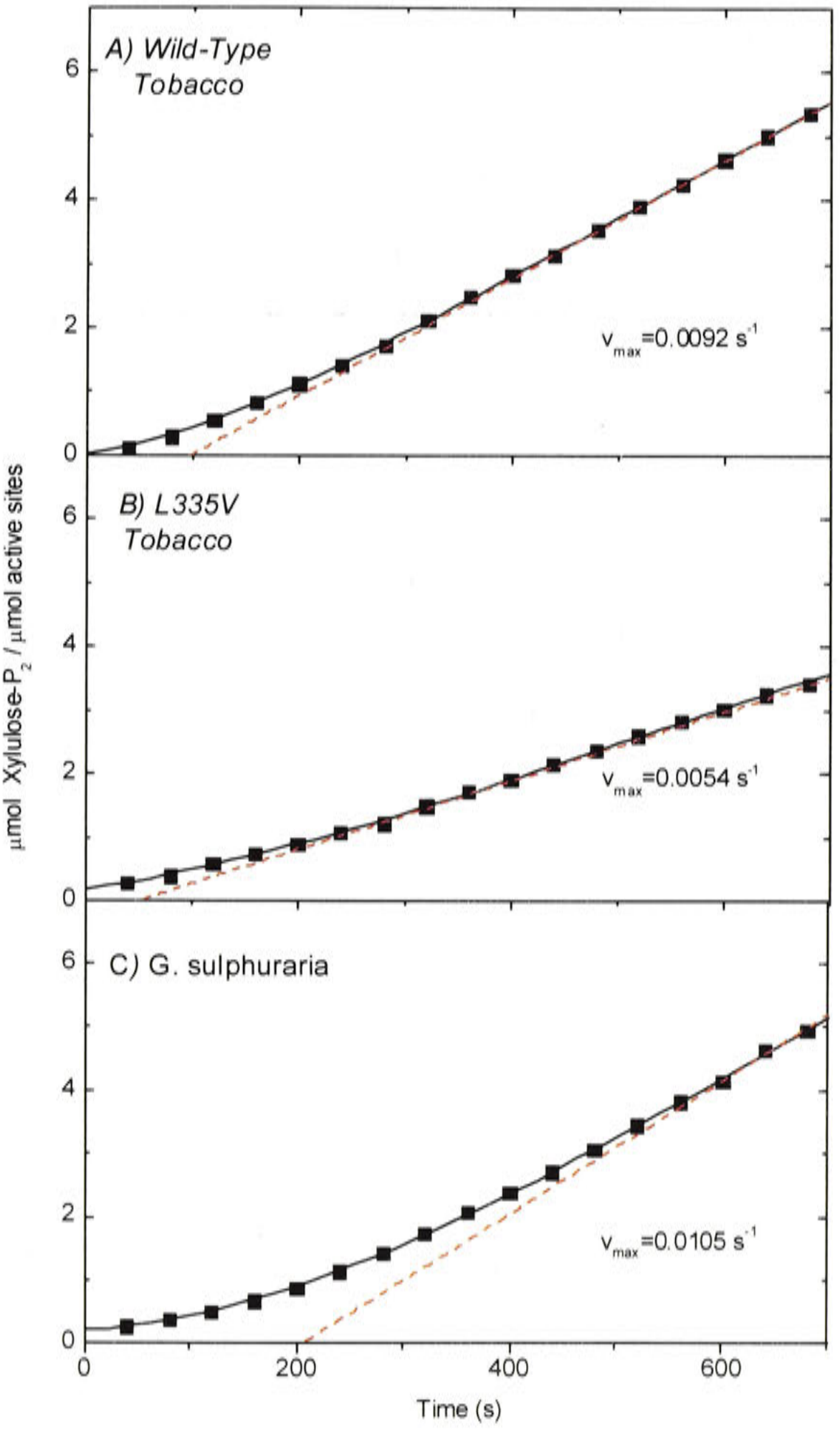

Figure 5.4 Xylulose-P_2 Production by Tobacco and *G. sulphuraria* Rubisco

Wild-type tobacco (*A*), L335V tobacco (*B*) and *G. sulphuraria* (*C*) Rubisco were activated as described (Section 3.2.3) before being added to the assay mixture to initiate the reaction. Assays were carried out under O_2 free conditions designed to rapidly exhaust any remaining CO_2 carried over from the activation buffer. Xylulose-P_2 production was measured spectrophotometrically, and the data for product accumulation (left ordinate, every eighth 5-s data point shown) versus time were fitted to an exponential equation, and the value for v_{max} was estimated (maximum rate shown as --) (Table 5.2).

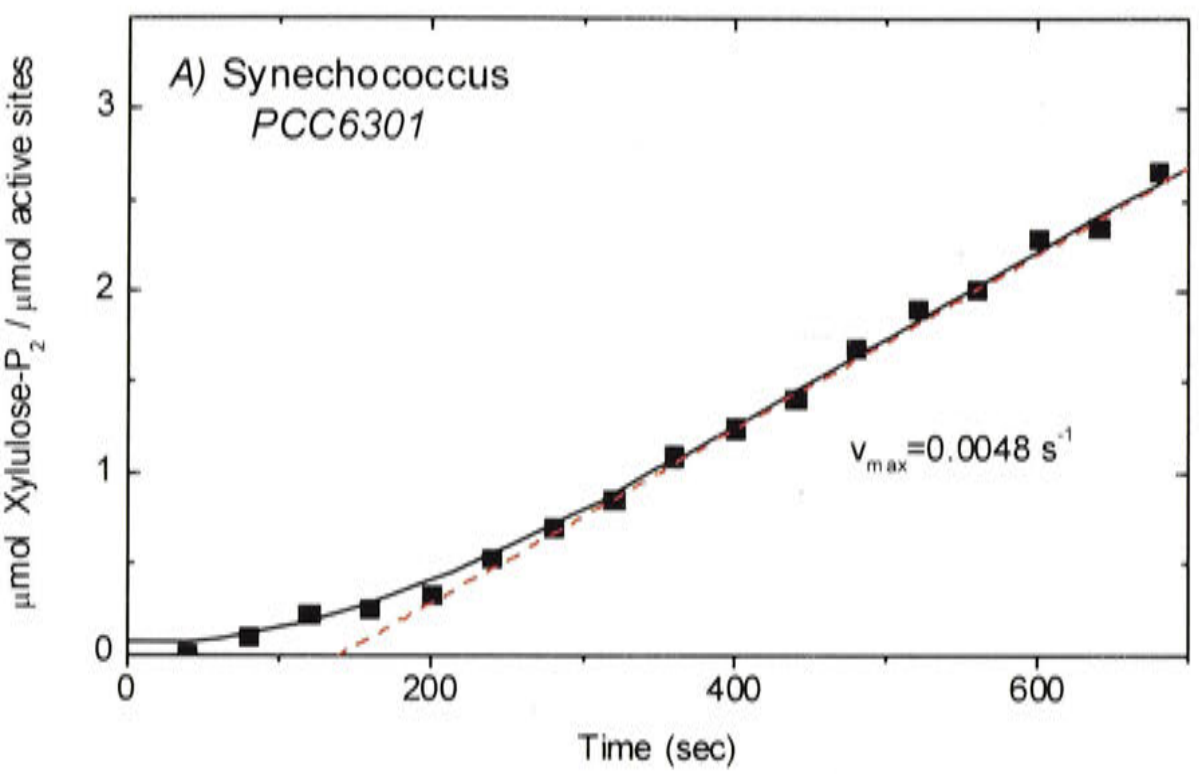

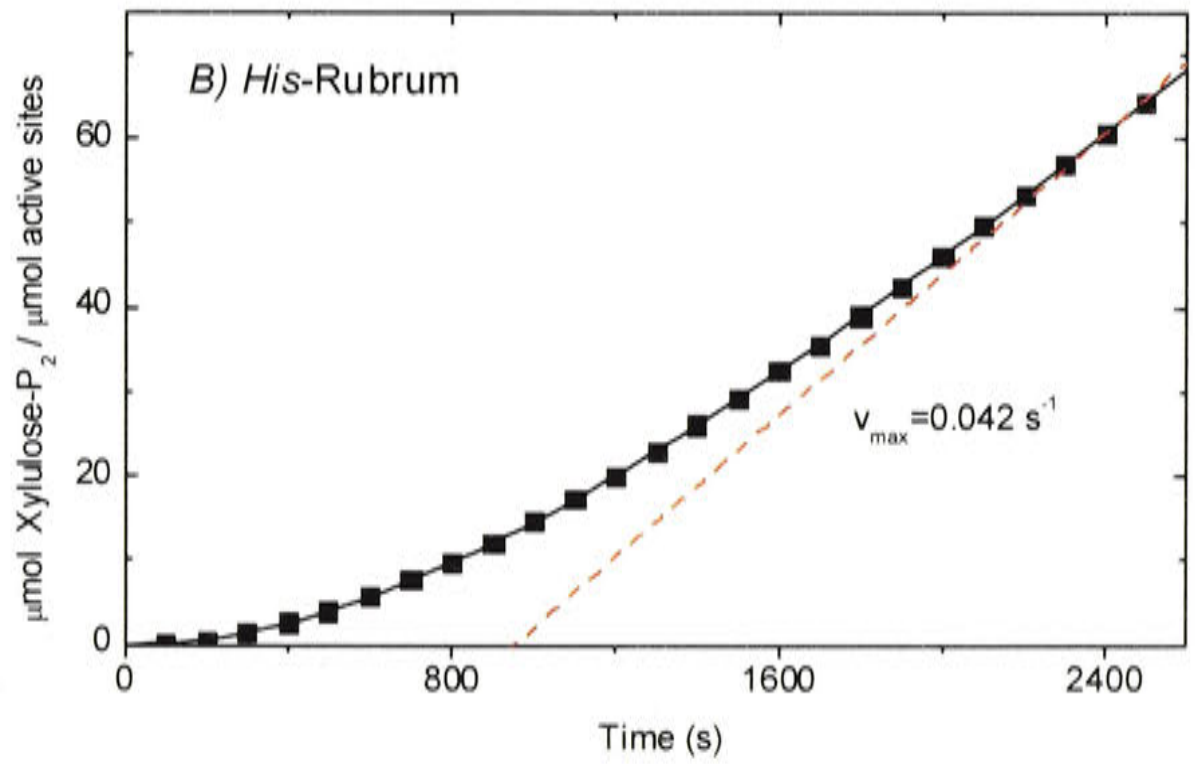

Figure 5.5 Xylulose-P_2 Production by *Synechococcus* PCC6301 and His-*Rubrum* Rubisco

Synechococcus PCC6301 (*A*) and His-*Rubrum* (*B*) Rubisco were activated as described (Section 2.2.2) before being added to the assay mixture to initiate the reaction. Assays were carried out under O_2 free conditions designed to rapidly exhaust any remaining CO_2 carried over from the activation buffer. Xylulose-P_2 production was measured spectrophotometrically, and the data for product accumulation (*Synechococcus* PCC6301 every eighth 5-s data point shown, His-*Rubrum* every twentieth 5-s data point shown) versus time were fitted to an exponential equation, and the value for v_{max} was estimated (maximum rate shown as --) (Table 5.2).

	Wild-Type Tobacco	L335V Tobacco	*G. sulphuraria*	*Synechococcus* PCC6301	His-*Rubrum*
Carboxylation k_{cat} (s^{-1})	2.9	0.45	1.2	11	6.6
Xylulose-P_2 production (s^{-1}) (*Figs 5.4,5.5*)	0.0092 (0.32 %)	0.0054 (1.20 %)	0.0105 (0.88 %)	0.0048 (0.044 %)	0.042 (1.4 %)
Deoxy-pentodiulose-P production (s^{-1}) (*Fig 5.6*)	0.0015 (0.05 %)	0.0023 (0.50 %)	ND[a]	ND	ND

[a], not determined

Table 5.2 Rates of Side-Reactions Arising From the Enediol Intermediate.

Rates of deoxy-pentodiulose-P and xylulose-P_2 production were measured spectrophotometrically in the absence of O_2, after exhaustion of CO_2, as described in Sections 5.2.1 and 5.2.2. These rates were compared to the carboxylation rate under CO_2 saturating conditions. Values in parentheses are the ratios of the rates of side reactions expressed as the percentage of the carboxylation k_{cat} at saturating ribulose-P_2 and CO_2 levels.

5.3.3 β-Elimination of the Enediol

The enediol intermediate is unstable, and has a tendency to undergo β-elimination reaction yielding deoxy-pentodiulose-P. Like the production of xylulose-P_2, this reaction is slow, but can be measured by maximising the fraction of enzyme with the enediol bound in the absence of CO_2 and O_2.

Deoxy-pentodiulose-P reacts with *o*-phenylene-diamine to form a quinoxaline adduct, the formation of which can be measured spectrophotometrically (Li and Kenyon 1995). The coloured quinoxaline adduct absorbs light at around 330 nm, allowing its formation to be monitored over time by the increase in absorption. Controls that lacked Rubisco showed some activity, due to the spontaneous formation of deoxy-pentodiulose-P or pentodiulose-P_2 from ribulose-P_2 in solution. Like deoxy-pentodiulose-P, pentodiulose-P_2 is a dicarbonyl compound that can also form the coloured quinoxaline adduct. This rate was subtracted from the assays that included Rubisco.

Like the previous assays that measured misprotonation of the enediol, there was an initial lag in activity due to the consumption of the last traces of CO_2/$NaHCO_3$. Deoxy-pentodiulose-P production peaked after 4 min and then decreased, possibly due to inhibition by side products or chemical modification of the enzyme by the *o*-phenylene-diamine. A fourth order polynomial showed a good fit to the data ($r^2 > 0.999$ for all fits, Figure 5.6), and allowed calculation of the deoxy-pentodiulose-P production rate (Table 5.2).

The absolute rate of deoxy-pentodiulose-P production was similar for both wild-type and L335V tobacco Rubisco, and consistent with previous observations for spinach Rubisco (Morell et al. 1997). However when compared to the rate of ribulose-P_2 carboxylation, L335V tobacco Rubisco had a much greater tendency, allowing β-elimination of the enediol. Parameters could not be estimated for other Rubisco enzymes, because of a low rate of β-elimination. Previous studies showed a low rate of β-elimination for *Synechococcus* PCC6301 Rubisco (Morell et al. 1997).

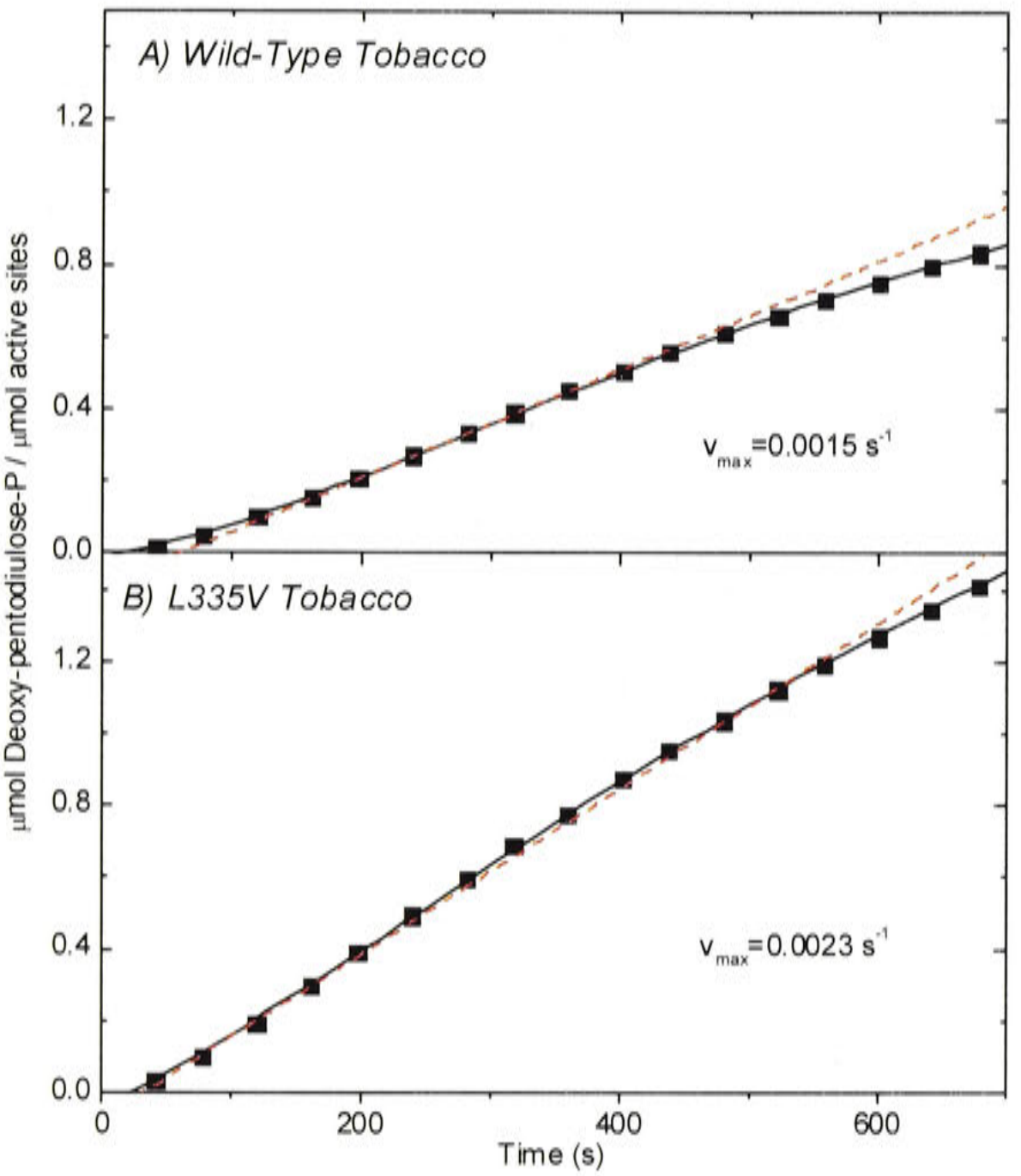

Figure 5.6 Deoxy-Pentodiulose-P Production by Tobacco Rubisco

Wild-type and L335V tobacco Rubisco were activated as described (Section 3.2,3) before being added to the assay mixture to initiate the reaction. Assays were carried out under O_2 free conditions designed to rapidly exhaust any remaining CO_2 carried over from the activation buffer. Deoxy-pentodiulose-P production was measured spectrophotometrically, and the data for product accumulation (every eighth 5-s data point shown) versus time were fitted to a 4th order polynomial equation to estimate the values for v_{max} (maximum rate shown as --) (Table 5.2).

5.3.4 β-Elimination of the Carbanion

Like the enediol formed early in catalysis, the *aci*-acid produced after C-C cleavage is also prone to β-elimination, yielding pyruvate. The level of pyruvate produced by Rubisco was measured by allowing complete consumption of 1000 μM ribulose-P_2 under conditions that promoted carboxylase activity. Any pyruvate produced was detected by using lactate dehydrogenase as a coupling enzyme. Controls lacking ribulose-P_2 or Rubisco showed negligible background activity.

The proportion of pyruvate produced by each enzyme is shown in Figure 5.7. Wild-type tobacco, *Synechococcus* PCC6301, and His-*Rubrum* Rubisco converted 0.7 % of ribulose-P_2 into pyruvate, which is consistent with previous observations (Andrews and Kane 1991). L335V tobacco Rubisco produced negligible pyruvate (< 0.1 %) and *G. sulphuraria* Rubisco converted 2 % of ribulose-P_2 into pyruvate.

5.3.5 Carboxylation of Xylulose-P_2

Xylulose-P_2 can also be used as a substrate by Rubisco, yielding P-glycerate and P-glycolate after carboxylation. Catalysis occurred at a very slow rate, consistent with previous observations (Yokota 1991a; Newman and Gutteridge 1994). For some enzymes, the activity showed an increase over time, while others showed a decrease in activity. Equation 3.1, which fits an exponential decline or increase in activity, showed a good approximation to the data ($r^2 > 0.998$ for all fits, Figure 5.8, Figure 5.9, Table 5.3). Controls lacking ribulose-P_2, Rubisco, or the coupling enzymes showed no activity. As expected, controls lacking triose-phosphate isomerase and glycerol-3-phosphate dehydrogenase reduced the rate of NADH oxidation to 2 NADH oxidised per CO_2 fixed.

Wild-type tobacco Rubisco showed a decline in activity that was similar to that observed during ribulose-P_2 carboxylation, while L335V tobacco, *G. sulphuraria*, *Synechococcus* PCC6301 and His-*Rubrum* Rubisco enzymes showed an increase in activity over time. This lag in activity may have been due to delays while intermediates in the reaction reached steady-state levels. Increasing the concentration of the coupling enzymes did not reduce the lag period, suggesting that the delay was not due to the coupling system. Wild-type tobacco had the slowest absolute rate after 10 minutes, followed by L335V tobacco, *G. sulphuraria*, *Synechococcus* PCC6301 and His-*Rubrum* Rubisco. When compared to the rate of ribulose-P_2 carboxylation, *G. sulphuraria* and L335V tobacco Rubisco had a rate that twice as fast as His-*Rubrum* and ten times faster than that of wild-type tobacco and *Synechococcus* PCC6301 Rubisco (Table 5.3).

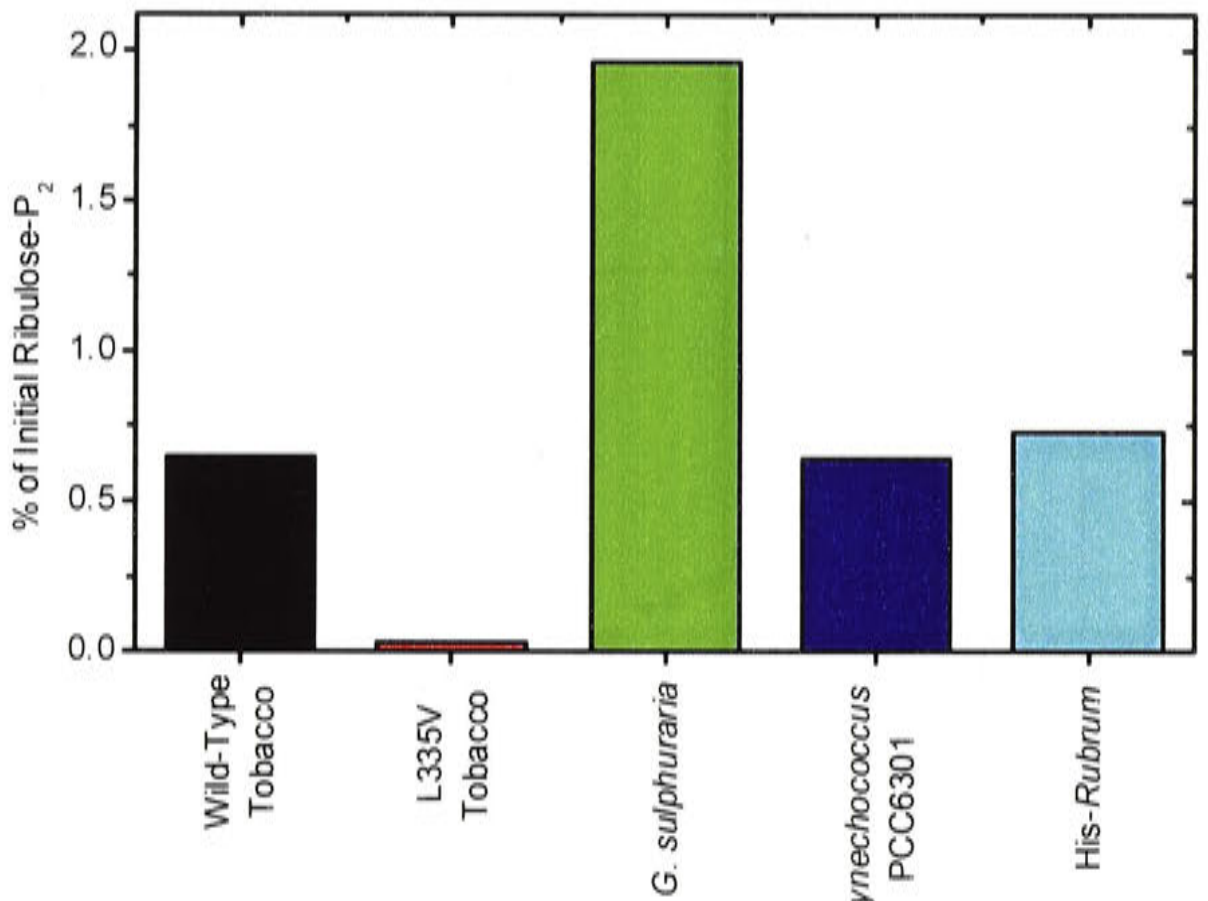

Figure 5.7 Pyruvate Production by Rubisco

Activated wild-type tobacco, L335V tobacco, *G. sulphuraria*, *Synechococcus* PCC6301 and His-*Rubrum* Rubisco were added to a complete assay mixture containing 1 mM ribulose-P_2 under CO_2-saturating conditions. Pyruvate production was measured spectrophotometrically to calculate the total amount of pyruvate produced.

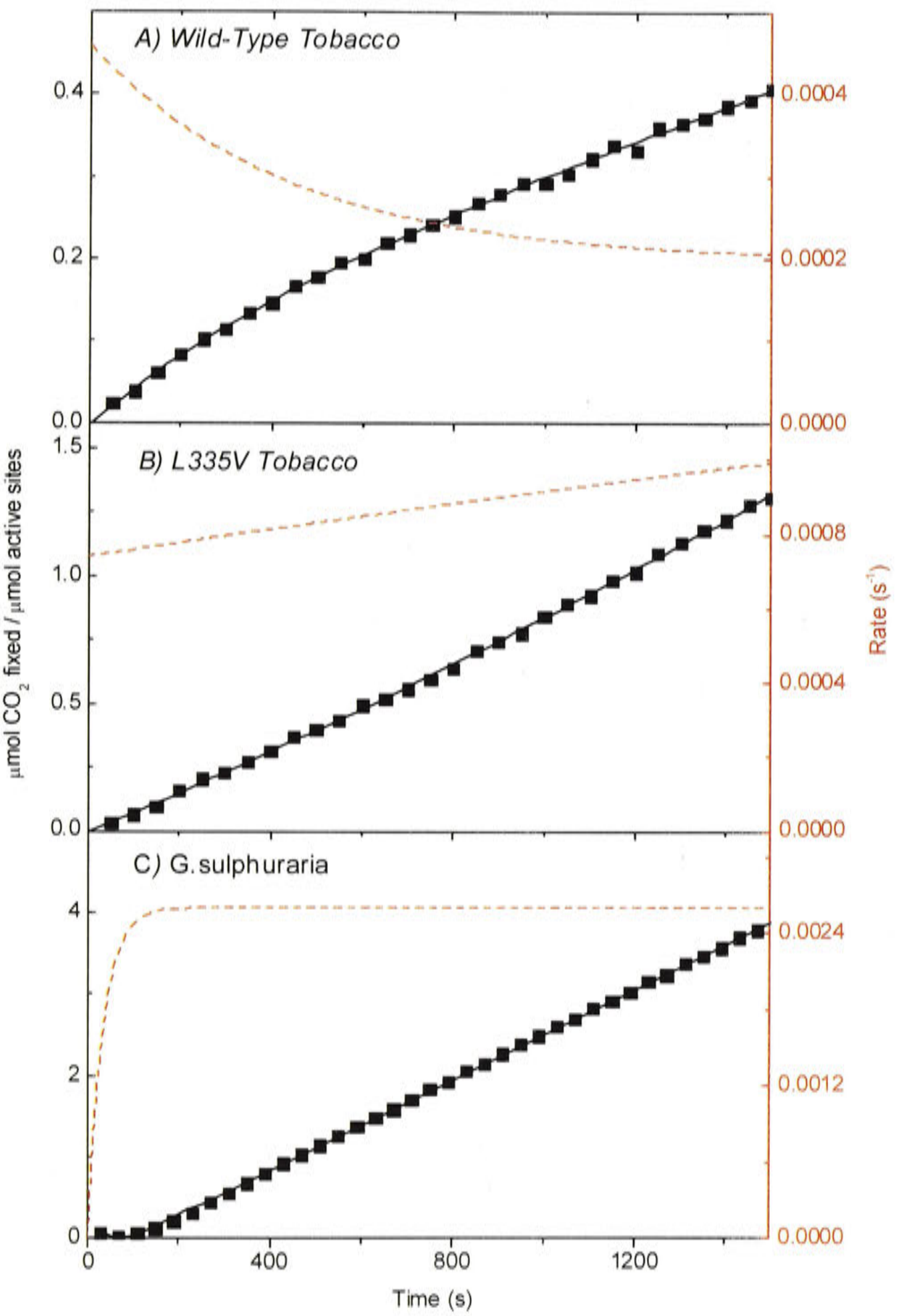

Figure 5.8 Xylulose-P_2 Carboxylation by Tobacco and *G. sulphuraria* Rubisco

Pre-activated wild-type tobacco (*A*), L335V (*B*) tobacco and *G. sulphuraria* (*C*) Rubisco (30–130 μg.ml^{-1}) was added to spectrophotometric assay mixture containing xylulose-P_2 (50 μM) to initiate the reaction. Xylulose-P_2 dependent carboxylase activity was measured spectrophotometrically at saturating CO_2 under aerobic conditions. The data for product accumulation (left ordinate, every tenth 5-s data point shown) versus time were fitted to Equation 3.1, and the values for v_i, v_f and k_{obs} were estimated (Table 5.3). Using these estimates, curves for the rate of catalysis (right ordinate, --) as a function of time were plotted using Equation 3.2.

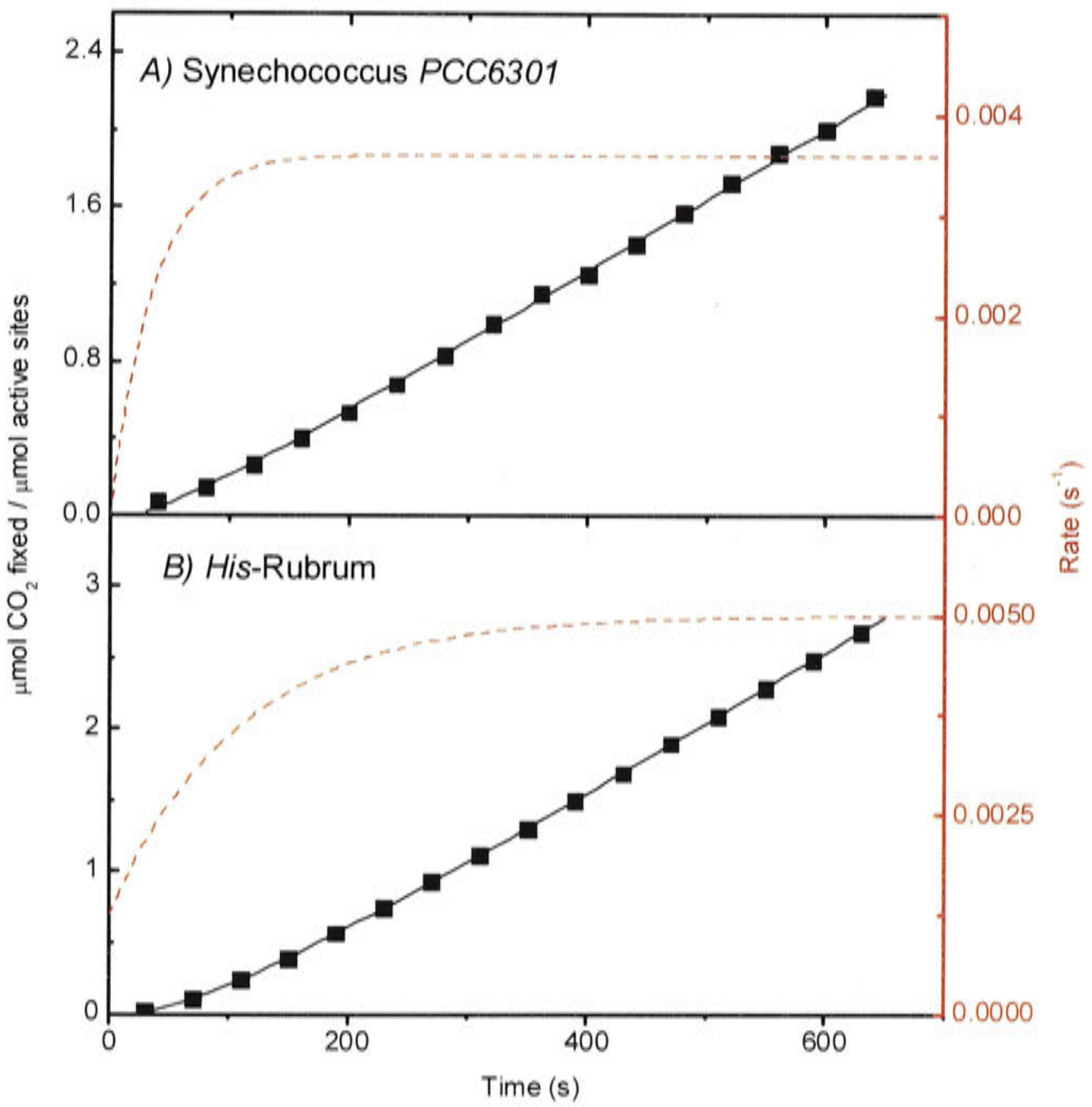

Figure 5.9 Xylulose-P_2 Carboxylation by *Synechococcus* PCC6301 and His-*Rubrum* Rubisco

Pre-activated *Synechococcus* PCC6301 (*A*) and His-*Rubrum* (*B*) Rubisco (30–130 $\mu g.ml^{-1}$) was added to spectrophotometric assay mixture containing xylulose-P_2 (50 µM) to initiate the reaction. Carboxylase activity was measured spectrophotometrically at saturating CO_2 under aerobic conditions. The data for product accumulation (left ordinate, every eighth 5-s data point shown) versus time were fitted to Equation 3.1, and the values for v_i, v_f and k_{obs} were estimated (Table 5.3). Using these estimates, curves for the rate of catalysis (right ordinate, - - -) as a function of time were plotted using Equation 3.2.

	v_i (s^{-1})	v_f (s^{-1})	k_{obs} (s^{-1})	r^2
Wild-Type Tobacco	$0.46 \pm 0.02 \times 10^{-3}$ (0.02 %)	$0.20 \pm 0.01 \times 10^{-3}$ (0.007 %)	$2.32 \pm 0.40 \times 10^{-3}$	0.9988
L335V Tobacco	$0.74 \pm 0.02 \times 10^{-3}$ (0.16 %)	$1.93 \pm 1.05 \times 10^{-3}$ (0.41 %)	$0.17 \pm 0.71 \times 10^{-3}$	0.9993
G. sulphuraria	0 -	$2.75 \pm 0.03 \times 10^{-3}$ (0.28 %)	$23.4 \pm 3.2 \times 10^{-3}$	0.9997
Synechococcus PCC6301	$1.20 \pm 1.58 \times 10^{-3}$ (0.01 %)	$3.66 \pm 0.03 \times 10^{-3}$ (0.03 %)	$15.9 \pm 6.8 \times 10^{-3}$	0.9989
His-*Rubrum*	$1.25 \pm 0.32 \times 10^{-3}$ (0.04 %)	$5.0 \pm 0.03 \times 10^{-3}$ (0.16 %)	$9.08 \pm 0.38 \times 10^{-3}$	0.9999

Table 5.3 Xylulose-P_2 Carboxylation by Rubisco.

Activated Rubisco was added to spectrophotometric assays containing 50 μM xylulose-P_2 under CO_2 saturating conditions. Parameters (± S.E.) were calculated by fitting the data of Figure 5.8 and Figure 5.9 to Equation 3.1. Values in parenthesis indicate the rate of xylulose-P_2 carboxylation as a percentage of the ribulose-P_2 carboxylation rate.

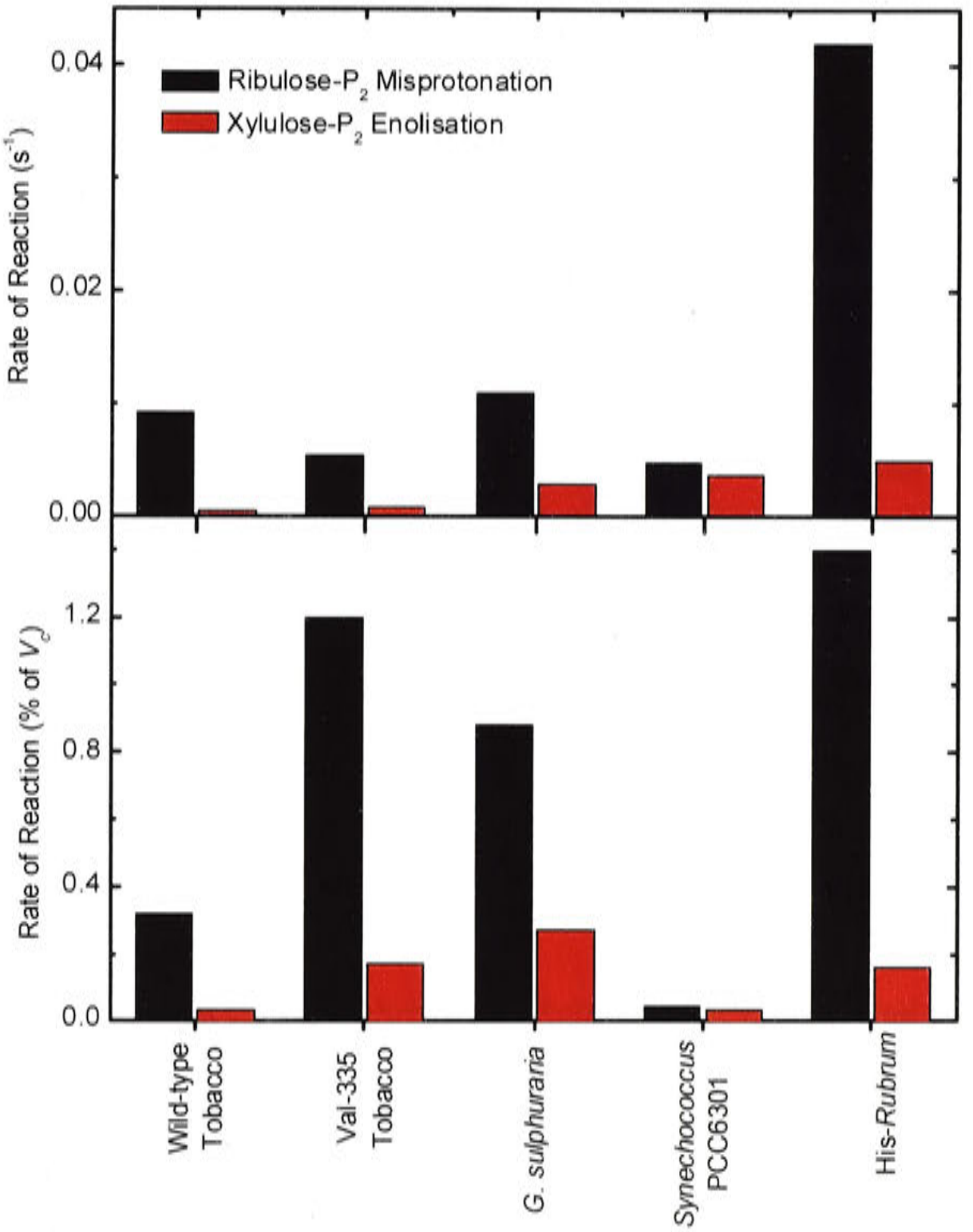

Figure 5.10 Comparison of Xylulose-P_2 Formation and Carboxylation Rates

The rate of ribulose-P_2 misprotonation and xylulose-P_2 enolisation was measured for wild-type tobacco, L335V tobacco, *G. sulphuraria*, *Synechococcus* PCC6301, and His-*Rubrum* Rubisco (Table 5.2 and Table 5.3).

5.4 Discussion

Despite having conserved active site geometry, there is significant variation in the rates of side- and partial-reactions carried out by the Rubisco enzyme. While previous studies and the experiments of Chapter 4 demonstrated the partitioning of reaction intermediates during catalysis, there has been little work to date aimed at measuring the continuous rates of reaction. The experiments described in this chapter are often carried out under substrate limiting conditions, which encourage the formation of side-products. By measuring the rate of these reactions a better understanding is obtained of how the rate of side- and partial-reactions can be different, despite the enzymes having a nearly identical active site. These variations in catalytic activity must be due to differences in the tertiary and quaternary structure that are remote from the active site.

5.4.1 Enolisation of Ribulose-P_2

The initial step of catalysis involves the abstraction of the ribulose-P_2 C-3 proton by the carbamylated Lys-201 residue (Cleland et al. 1998; Roy and Andrews 2000). The rate of this step was only slightly impaired by the substitution of Lys-335 with valine for tobacco Rubisco (Table 5.1), showing that while the mutation may affect carboxylation, oxygenation and some of the side- and partial-reactions, enolisation is not influenced to as great a degree.

Carboxylation of [3-^{2}H]ribulose-P_2 by Rubisco from wild-type tobacco was reduced three-fold due to isotope discrimination, which has been observed previously (Van Dyk and Schloss 1986). The larger deuteron atom is slower to be abstracted than the smaller proton, slowing the rate of enolisation. Fallover inhibition of the [3-^{2}H]ribulose-P_2 carboxylation rate was similar to that seen for unlabelled ribulose-P_2, because the [3-^{2}H] deuteron is abstracted to form the enediol and once removed, does not participate further in the reaction partitioning.

Surprisingly, the carboxylation of [3-^{2}H]ribulose-P_2 by L335V tobacco Rubisco was also reduced three-fold. The enolisation rate showed that the mutation did affect the enolisation rate to as great an extent as other parameters, and so the overall drop in catalysis is due to a limited ability to carry out the carboxylation or oxygenation of the enediol. However, there was an isotope effect on the [3-^{2}H]ribulose-P_2 carboxylation rate, despite previous suggestions that the [3-^{2}H] deuteron has no further role in catalysis after it has been abstracted. It is likely that the deuteron remains in the active

site, and has a limiting effect on the addition of CO_2 or O_2, as well as limiting the rate of enolisation.

5.4.2 The Enediol Intermediate is Not Well Stabilised

The enediol can be converted into several compounds, including carboxylation to form the carboxyketone, oxygenation to form the peroxyketone, misprotonation to form xylulose-P_2, β-elimination to form deoxy-pentodiulose-P, and correct reprotonation to form ribulose-P_2. All Rubisco enzymes studied showed an ability to catalyse the misprotonation and β-elimination of the enediol intermediate. The rate of misprotonation depends on the enzyme's ability to control access of protons to the *Re* face of the C-3 atom of the enediol, and suppression of the rate of β-elimination of the P-1 phosphate depends on the ability to maintain planarity of the O-1, C-1, C-2 and C-3 atoms. Closure of loop 6 over the active site during catalysis plays an important role in restricting the access of water molecules into the active site, which would increase the rate of misprotonation (Schreuder et al. 1993a). Increased misprotonation rates may be the consequence of some water molecules being able to penetrate the active site during catalysis.

Misprotonation of the enediol occurred at a similar rate for L335V tobacco and *Synechococcus* PCC6301 Rubisco, was faster in wild-type tobacco and *G. sulphuraria* Rubisco, and was faster again in His-*Rubrum* Rubisco (Table 5.2, Figure 5.4, Figure 5.5 and Figure 5.10). When compared to the carboxylation rate, L335V tobacco Rubisco showed the greatest tendency to carry out misprotonation, followed by *G. sulphuraria*, His-*Rubrum*, wild-type tobacco, and *Synechococcus* PCC6301 Rubisco, which had the lowest tendency. The rate of misprotonation gives an indication of how well the enzyme is able to restrict the access of protons to the enediol. The high rate of misprotonation in L335V tobacco and *G. sulphuraria* Rubisco suggests that protons have greater access to the *Re* face of the enediol in these enzymes than in *Synechococcus* PCC6301 and wild-type tobacco Rubisco.

The enediol must be kept in a planar configuration to avoid β-elimination, producing deoxy-pentodiulose-P. L335V and wild-type tobacco Rubisco showed similar absolute rates of β-elimination, but when compared to the carboxylation rate, L335V tobacco Rubisco showed a greater tendency to partition the enediol to deoxy-pentodiulose-P (Table 5.2 and Figure 5.6). This suggests that the substitution has caused a loosening of the active site, and the L335V mutant Rubisco is less able to stabilise the enediol in a planar configuration.

5.4.3 Pyruvate Production Varies Between Rubisco Enzymes

Like the enediol intermediate, the *aci*-acid produced after C-C cleavage is also prone to β-elimination. This is minimised if the C-1 to P-1 bond is in the same plane as the carboxyl C to C-2 bond, which requires movement of the C-1 atom. Consistent with previous observations, wild-type tobacco, *Synechococcus* PCC6301 and His-*Rubrum* Rubisco partitioned some of ribulose-P_2 into pyruvate (Andrews and Kane 1991). This partitioning was increased for *G. sulphuraria* Rubisco and decreased for L335V tobacco Rubisco. Apparently loosening the active site, as predicted for the L335V mutant tobacco Rubisco, can sometimes aid the stereospecific protonation that completes the carboxylation sequence. A decrease in pyruvate partitioning was also seen in a previous site-directed mutant of *Synechococcus* PCC6301 Rubisco (Morell et al. 1994). The increased partitioning by *G. sulphuraria* is one of the highest observed, and may represent a less flexible active site that restricts the movement, mostly of the C-1 atom, away from being planar with C-2 and C-3 in the enediol towards being planar with C-2 and the carbonyl C atom..

5.4.4 Xylulose-P_2 as a Substrate for Rubisco

Carboxylation of xylulose-P_2 by Rubisco requires abstraction of the C-3 proton, which would normally be carried out on ribulose-P_2 by the carbamylated Lys-201 residue (Cleland et al. 1998; Roy and Andrews 2000). However, if xylulose-P_2 binds to Rubisco in a similar fashion to the binding of ribulose-P_2, the residue would not be positioned appropriately. Thus the rate of xylulose-P_2 enolisation gives an indication of the flexibility of the active site.

Wild-type tobacco Rubisco had the slowest rate of xylulose-P_2 carboxylation after 10 minutes, followed by L335V tobacco, *G. sulphuraria*, *Synechococcus* PCC6301, and His-*Rubrum* Rubisco (Table 5.3 and Figure 5.10). The increased rate of the L335V tobacco mutant Rubisco suggests that there is increased flexibility in the active site that allows proton abstraction to occur, which is in agreement with the increased rate of misprotonation and β-elimination of the enediol. Similarly, the higher rate of xylulose-P_2 carboxylation by His-*Rubrum* Rubisco is likely to reflect greater flexibility of the active site, substantiating the other results. When compared to the rate of ribulose-P_2 carboxylation, *G. sulphuraria* Rubisco had the highest rate of xylulose-P_2 carboxylation out of all the enzymes studied, suggesting that there may be another base positioned above the plane that can act to deprotonate the C-3 atom of xylulose-P_2.

The fallover-like drop in activity shown by wild-type tobacco Rubisco is similar to the time-course of xylulose-P_2 inhibition of Rubisco due to the progressive decarbamylation of the active site that is induced by xylulose-P_2 (Yokota 1991a; Zhu and Jensen 1991b). The decrease in xylulose-P_2 carboxylation activity was only apparent for wild-type tobacco Rubisco, with other Rubisco enzymes exhibiting an increase in xylulose-P_2 carboxylation over time. An increase in activity may be due to a limited rate of 3-epimerisation of xylulose-P_2, to form ribulose-P_2, even at saturating CO_2 concentrations. The traces of ribulose-P_2 produced would initially be overwhelmed by the high xylulose-P_2 concentration, but as the concentration slowly increased over time there would be an increased rate of turnover until eventually a steady state was reached where carboxylation of xylulose-P_2 by the normal pathway matched the rate of production by epimerization.

The delay in establishing a steady state of activity may provide an insight into the catalytic reaction mechanism. It would be expected that the enediol formed by the deprotonation of xylulose-P_2 would undergo carboxylation at the saturating levels of CO_2 in the assay. The potential formation of ribulose-P_2 suggests that there may be several different tautomeric forms of the enediol. Deprotonation of xylulose-P_2 generates one form of the enediol, which must undergo tautomerisation to another form of the enediol before the addition of CO_2. If this tautomerisation step is slow, there would be an increased chance of reprotonation of the initial enediol to form ribulose-P_2.

5.4.5 Loosening the Active Site Promotes Side-Reactions

Intermediates formed during catalysis need to be stabilised to prevent side-reactions from occurring. The L335V mutant of tobacco Rubisco has a substitution located in loop 6, which closes over the active site during catalysis. The rate of enolisation is not affected to a large degree, but the rate of ribulose-P_2 carboxylation is reduced 6-fold, suggesting that the enzyme is less proficient in promoting carboxylation. The reduction in specificity that is exhibited by this enzyme shows a reduced ability to discriminate between CO_2 and O_2 as substrates (Whitney et al. 1999). The rate of xylulose-P_2 carboxylation and misprotonation of the enediol intermediate is increased, reflecting an increased ability for abstraction of the C-3 proton from xylulose-P_2, and greater opportunity for access of protons to the enediol intermediate. A decrease in pyruvate production showed that the C-1 to P-1 bond of the carbanion intermediate was maintained in a linear state, and was significantly less prone to β-elimination.

Rubisco from *G. sulphuraria* has a high specificity, reflecting good discrimination between CO_2 and O_2 as substrates. An increased partitioning of pyruvate is a result of a rigid active site, which does not allow for maintaining the C-1 to P-1 bind in a linear state. However, the ability of the enzyme to carry out the enolisation of xylulose-P_2 at a relatively high level suggests that there is some flexibility in the active site, or another basic group that allows for the abstraction of a proton from the *Si* face of xylulose-P_2.

Misprotonation of the enediol and enolisation of xylulose-P_2 are slow in *Synechococcus* PCC6301 Rubisco, despite the reduced specificity suggesting that the active site may be looser than that of tobacco or *G. sulphuraria* Rubisco. It is possible that *Synechococcus* PCC6301 Rubisco has a similar active site to that of higher plants, considering that they are both 'green-like' types of Form I Rubisco.

His-*Rubrum* Rubisco had consistently higher rates of xylulose-P_2 carboxylation and enediol misprotonation compared to other Rubisco enzymes. Coupled with a low ability to discriminate between CO_2 and O_2 as substrates, it is also likely that this active site has greater flexibility, and is less able to stabilise reaction intermediates.

The different rates of side-reactions reflect the flexibility of the active site. The formation of xylulose-P_2 was consistent with that observed in Chapter 4, although misprotonation is faster under CO_2 and O_2 free conditions than when the assay favours carboxylation or oxygenation of ribulose-P_2. While there are differences in the rates of side reactions between the different enzymes, the variation does not appear to be sufficient to solely explain the differences in patterns of self-inhibition observed for Rubisco enzymes. These disparities may be due to altered interactions with inhibitors, the possibility of which is investigated in Chapter 6.

5.4.6 Conclusions

The rates of Rubisco partial- and side-reactions can be directly measured, providing an insight into the catalytic chemistry occurring in the active site. Xylulose-P_2 was produced by most Rubisco enzymes at a similar rate, but at a faster rate in His-*Rubrum* Rubisco, suggesting differences in the stability of the enediol intermediate that allows for misprotonation from the *Re* face. β-Elimination of the enediol was similar for wild-type and L335V tobacco Rubisco, while pyruvate production by β-elimination of the *aci*-carbanion was decreased in L335V tobacco Rubisco and increased in *G. sulphuraria* Rubisco, implying differences in the ability to accommodation movement of the C-1 atom during catalysis. All Rubisco enzymes could carry out enolisation of xylulose-P_2, but the rate was faster in Rubisco from L335V tobacco, His-*Rubrum* and

G. sulphuraria, possibly due to an increased ability of the active site to abstract a proton from the C-3 atom. The rate of ribulose-P_2 enolisation was similar for wild-type and L335V tobacco Rubisco, demonstrating that the mutation had only a small effect on the enolisation of ribulose-P_2.

6 Interaction of Rubisco with Ligands

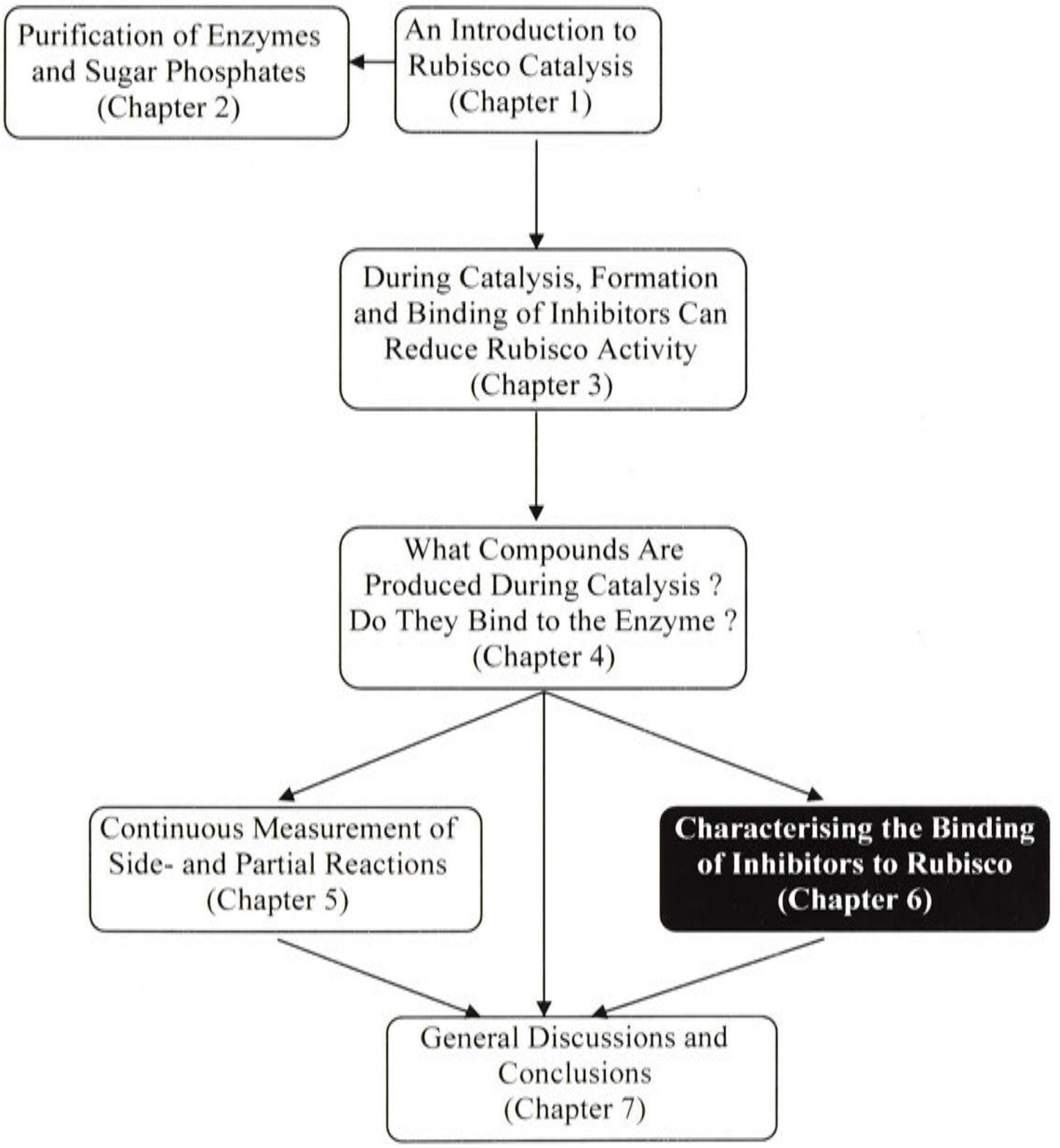

6.1 Introduction

In addition to controlling the reactions of Rubisco, the structure of the enzyme also influences the interaction of the active site with regulatory ligands. Regulation of Rubisco activity by inhibitors controls the flux thought the CBB cycle, and maintains the concentration of metabolites at a constant level. These inhibitory ligands are often analogues of intermediate compounds formed during catalysis or analogues of the substrate. The substrate, ribulose-P_2, can also bind to uncarbamylated Rubisco and act as an inhibitor, because the enzyme cannot carry out the initial enolisation reaction without the carbamylated residue and coordinated Mg^{2+} ion. Xylulose-P_2, an isomer of ribulose-P_2, is derived from misprotonation of the enediol by Rubisco itself. Carboxyarabinitol-1-P, which is produced by other pathways in some higher plants, has a similar structure to the carboxyketone intermediate compound. Carboxyarabinitol-P_2, which does do not occur naturally in nature, also mimics the carboxyketone intermediate compound.

Intermediate compounds have a very slow release rate from the active site, to prevent them from being released into solution and degraded. It therefore follows that inhibitors that mimic intermediate compounds also have a very slow release rate (Schloss 1988a). The reduced rate of release was often accompanied by a slow rate of binding, and a delay in inhibition after exposure to the inhibitor (Morrison 1982).

Slow, tight-binding inhibition involves two distinct steps. The initial step is similar to competitive inhibition, and involves a rapid equilibrium step to form EI, in which the inhibitor is loosely associated with the enzyme, and is easily released. The second step is a slow conformational change to form EI*, the tightly bound enzyme-inhibitor complex. Release of inhibitor from this compound is a slow process, and may be irreversible. For Rubisco, the slow conformation change is likely to involve the closure of loop 6 over the active site (Duff et al. 2000).

6.1.1 Ribulose-P_2

Rubisco requires activation by the co-ordination of a Mg^{2+} ion and carbamylation of Lys-201 in order to carry out catalysis, as described in Section 1.4.2. If the active site lacks the metal ion and carbamylated residue, ribulose-P_2 can bind to form the E:ribulose-P_2 complex, but catalysis cannot take place.

It was initially observed that ribulose-P_2 could bind to the uncarbamylated form, as well as the carbamylated form (Laing and Christeller 1976). Uncarbamylated

Rubisco, that showed negligible activity, was assayed with varying concentrations of ribulose-P_2. Over the course of the assay, Rubisco showed an increase in activity over time that was inversely related to the ribulose-P_2 concentration. At low concentrations of ribulose-P_2, the activity was restored faster than at high concentrations. The rate of activation reflects the speed at which ribulose-P_2 is released from the EI* complex, which varies widely between different Rubisco enzymes.

Release of ribulose-P_2 from the uncarbamylated form of spinach Rubisco was very slow, taking over an hour for full activation (Jordan and Chollet 1983). The activation of the E:ribulose-P_2 complex from spinach Rubisco was much faster in the absence of ribulose-P_2 than in its presence (Edmondson et al. 1990c). Activation of the Form II *R. rubrum* Rubisco enzyme was relatively rapid, with most activation occurring within a few min (Jordan and Chollet 1983).

Activation has been described for a number of species. *Thiobacillus denitrificans* is an autotrophic bacterium with genes encoding a Form II and 'green-type' Form I Rubisco. The Form II enzyme showed rapid E:ribulose-P_2 activation, while the Form I enzyme had a slower rate of activation (Hernandez et al. 1996).

Rhodobactor capsulatus (a non-sulphur purple bacterium) has the 'green-type' Form I Rubisco and a slow E:ribulose-P_2 activation rate (Horken and Tabita 1999a). *Rhodobactor sphaeroides* has a Form I 'red-type' Rubisco that formed a tight E:ribulose-P_2 complex that had a slow release rate, and a Form II Rubisco that showed rapid activation (Gibson and Tabita 1979). *Anabaena* is a cyanobacterium with a 'green-type' Form I Rubisco that shows rapid release of ribulose-P_2 from the E:ribulose-P_2 complex. Nearly half of the activity of the inhibited enzyme was recovered within a minute (Li and Tabita 1997).

6.1.2 Xylulose-P_2

Xylulose-P_2 is an isomer of ribulose-P_2 that can be formed by misprotonation of the enediol intermediate compound (Edmondson et al. 1990d). Incubation of spinach Rubisco with xylulose-P_2 resulted in a reduction of activity (McCurry and Tolbert 1977). The drop in activity was biphasic, with initial slow binding of inhibitors at low concentrations of xylulose-P_2, and then faster rates of binding at higher concentrations. When ribulose-P_2 and xylulose-P_2 were added simultaneously to the assay, it was found that the inhibition was competitive with respect to ribulose-P_2 (McCurry and Tolbert 1977), which both ligands competing for the same active site.

The binding of xylulose-P_2 to spinach Rubisco was a slow process, with maximum inhibition reached after 20-30 min incubation (Zhu and Jensen 1991b). The binding of xylulose-P_2 to the enzyme induced the loss of the activating CO_2 group, even in the presence of saturating levels of CO_2 and Mg^{2+}. Apparently xylulose-P_2 bound more tightly to inactive, decarbamylated sites than to carbamylated sites (Zhu and Jensen 1991b). The binding and release of xylulose-P_2 to spinach Rubisco was affected by pH, with tighter binding and a slower rate of release at lower pH (Zhu and Jensen 1991a).

Mutation of the small subunits has been observed to alter the inhibitory effects of xylulose-P_2. *Synechococcus* PCC6301 Rubisco enzymes that had substitutions in the small subunits (Q99G and P108L) had a reduced binding affinity for xylulose-P_2 (Flachmann et al. 1997), which was accompanied by an increase in the rate of xylulose-P_2 production.

6.1.3 Carboxyarabinitol-P_2

Early studies showed that carboxypentitol-P_2 was a competitive inhibitor of Rubisco with respect to ribulose-P_2 (Siegel and Lane 1972), and that Mg^{2+} was required for maximal inhibition. Carboxypentitol-P_2 contains a mixture of carboxyarabinitol-P_2 and carboxyribinitol-P_2, which are analogues of the carboxyketone intermediate that is produced during catalysis. Both were found to be competitive inhibitors, with carboxyarabinitol-P_2 exhibiting slow, tight binding to the carbamylated enzyme (Pierce et al. 1980).

Studies of the binding of carboxyarabinitol-P_2 to Rubisco suggested that carboxyarabinitol-P_2 bound quickly to half of the sites, and slowly to the other half of sites, which is consistent with the idea of negative cooperativity (Johal et al. 1985; Zhu and Jensen 1990). With fully activated Rubisco the rate of tight binding was rapid, with most binding occurring within a matter of seconds for higher plant Rubisco (Pierce et al. 1980).

6.1.4 Carboxyarabinitol-1-P

Some higher plants produce the inhibitory compound carboxyarabinitol-1-P to regulate Rubisco activity at night (Gutteridge et al. 1986; Berry et al. 1987). Carboxyarabinitol-1-P mimics the structure of the carboxyketone intermediate compound formed during carboxylation of ribulose-P_2, and binds tightly to carbamylated active sites (Seemann et al. 1985).

Binding of carboxyarabinitol-1-P to French bean Rubisco was slow and tight, with an apparent first order-binding constant of 0.03 s^{-1}. The rate of release when the inactive ECM:carboxyarabinitol-1-P complex was incubated with alkaline phosphatase, which degrades the released inhibitor, was 0.001 s^{-1}, (Seemann et al. 1985). Recovery of the inhibited enzyme is faster in the presence of ribulose-P_2, and is also increased by the presence of the Rubisco activase enzyme (Robinson and Portis 1988).

6.1.5 Specific Aims and Objectives

While many studies have focussed on the binding of ribulose-P_2 to the Rubisco active site, and the use of radiolabelled carboxyarabinitol-P_2 to measure the level of carbamylated actives has become routine, there has been relatively little research carried out on the binding of inhibitory compounds to Rubisco. This chapter aims to quantify the interaction of the Rubisco enzyme with inhibitory compounds that have been observed in Chapter 4 and other studies. Previous studies have shown that ribulose-P_2 and xylulose-P_2 bind to the active site of the decarbamylated enzyme, while carboxyarabinitol-1-P and carboxyarabinitol-P_2 bind to the carbamylated form of the enzyme.

The interaction of Rubisco with ligands was measured by incubating different Rubisco enzymes with a range of inhibitors under different conditions. The rate of binding and release was measured by monitoring either the enzyme activity or the exchange of radiolabelled ligands. Kinetic parameters for rapid equilibrium and slow, tight binding were calculated using models for the interaction of enzyme with ligands.

6.2 Materials & Methods

6.2.1 Activation of the E:Ribulose-P_2 Complex

6.2.1.1 Decarbamylation of Rubisco

Tobacco, *Synechococcus* PCC6301 and His-*Rubrum* Rubisco were decarbamylated by incubating at 25 °C for 5 min in buffer containing 100 mM EPPS-NaOH, pH 8.0, 1 mM EDTA.

G. sulphuraria Rubisco was decarbamylated by dialysing overnight at 4°C against buffer containing 100 mM EPPS-NaOH, pH 8.0, 1 mM EDTA that was continually sparged with N_2.

6.2.1.2 Measurement by Spectrophotometric Assay

Rubisco (2–7 μM) was decarbamylated (as described in Section 6.2.1.1) and incubated at 25°C in 100 mM EPPS-NaOH, pH 8.1, 1 mM EDTA with 2 mM ribulose-P_2. To initiate activation, these solutions were added to complete assay mixtures containing 20 mM $MgCl_2$, 1–50 mM $NaHCO_3$ and 0.5 mM ribulose-P_2 as described in Section 2.2.2 (final Rubisco concentration of 150 nM sites). Assays were carried out in duplicate on at least two separate occasions, and the runs were pooled. The pooled data for product accumulation versus time were fitted to Equation 3.1, which describes an exponential change in activity over time, to estimate values for v_i, v_f and k_{obs}. Residual activity versus time was plotted using the parameter estimates obtained with Equation 3.2, which is the derived function of Equation 3.1.

6.2.1.3 Measurement by Gel Filtration

Rubisco (3 μM) was decarbamylated (as described in Section 6.2.1.1) and incubated with [1-^{3}H]ribulose-P_2 (6 μM) in a buffer containing 50 mM EPPS-NaOH, pH 8.0, 1 mM EDTA, for 10 min prior to separation of Rubisco-bound radioactivity from unbound by gel filtration using Sephadex G-50 fine (10 mm x 200 mm) resin equilibrated with the reaction buffer. The protein peak was collected and unlabelled ribulose-P_2 (400 μM) added. At intervals thereafter, samples were taken and reapplied to the gel filtration column. The Rubisco-bound and unbound radioactivity was measured by online scintillation counting (Ultima-Flo, Packard). Assays were carried out on two separate occasions and the runs were pooled.

Data for the release of labelled inhibitor versus time were fitted to the following exponential equation,

$$\frac{I^*}{I_t} = 1 - e^{-k_{obs}t} \qquad \textbf{(Equation 6.1)}$$

where I^* is the amount of labelled inhibitor that has been released from the enzyme, I_t is the total amount of labelled inhibitor, and k_{obs} is the observed first-order rate constant.

6.2.2 Activation of the E:Xylulose-P_2 Complex

Rubisco (2-7 μM) was decarbamylated (as described in Section 6.2.1.1) and incubated at 25°C in 100 mM EPPS-NaOH, pH 8.0, 1 mM EDTA with 80 μM xylulose-P_2. To initiate activation, these solutions were added to complete assay mixtures containing 20 mM $MgCl_2$, 1 – 50 mM $NaHCO_3$ and 0.5 mM ribulose-P_2 as described in Section 2.2.2 (final Rubisco concentration of 150 nM sites). Assays were carried out in duplicate on at least two separate occasions, and the runs were pooled. To estimate values for v_i, v_f and k_{obs}, data for product accumulation versus time were fitted to Equation 3.1, which describes an exponential change in activity over time. Residual activity versus time was plotted using the parameter estimates obtained and Equation 3.2, which is the derived function of Equation 3.1.

6.2.2.1 Activation of the G. sulphuraria *E:Xylulose-P_2 Complex*

Rubisco (3 μM) was decarbamylated (as described in Section 6.2.1.1) and incubated with xylulose-P_2 (200 μM) in a buffer containing 100 mM EPPS-NaOH, pH 8.0, 1 mM EDTA, for 10 min prior to separation of Rubisco-bound compounds from unbound by gel filtration on a 10 x 200 mm column of Sephadex G-50 fine (Pharmacia) equilibrated with the reaction buffer. The protein peak was collected and added to a spectrophotometric assay mixture lacking ribulose-P_2 as described in Section 2.2.2. At intervals thereafter samples were taken and ribulose-P_2 (0.5 mM) was added to initiate the reaction. Assays were carried out on two separate occasions and the runs were pooled. To estimate values for v_f and k_{obs}, the pooled data for rate versus time was fitted to Equation 3.2, which describes an exponential change in activity over time.

6.2.3 Binding of Xylulose-P_2 to Rubisco

Rubisco was activated as described in Section 2.2.2 (0.05 μM sites) and incubated with xylulose-P_2 (0.1–50 μM) at 25 °C for 60 min. 200 μl was then used to initiate a 2

ml spectrophotometric assay containing 0.5 mM ribulose-P_2 as described in Section 2.2.2. Assays were carried out in duplicate on two separate occasions and the runs were pooled.

The initial rate was calculated by fitting Equation 3.1, which describes an exponential change in activity over time, to the pooled data and compared to Rubisco activity in the absence of xylulose-P_2. The data were then fitted to equations describing the slow, tight, reversible binding of ligands to the active site, as described in Section 6.2.8.

6.2.4 Competitive inhibition by Xylulose-P_2

Rapid-equilibrium, competitive inhibition of activated Rubisco by xylulose-P_2 was measured as described (McCurry and Tolbert 1977) by adding pre-activated enzyme (final concentration of 12 nM sites) to initiate spectrophotometric assays (as described in Section 2.2.2) containing mixtures of ribulose-P_2 (2.5–320 μM) and xylulose-P_2 (0–40 μM). Assays were carried out in duplicate on at least two separate occasions, and the runs were pooled. Initial activities for each inhibitor concentrations were measured by fitting Equation 3.1 to the pooled data, and for each inhibitor concentration the data were fitted to the following hyperbolic equation,

$$v = \frac{k_{cat}[S]}{[S] + K_{app}} \qquad \textbf{(Equation 6.2)}$$

where v is the Rubisco activity at substrate concentration $[S]$, k_{cat} is the maximum Rubisco activity, and K_{app} is the observed Michaelis constant for the given inhibitor concentration $[I]$. The data for K_{app} versus $[I]$ was then fitted to a linear equation,

$$K_{app} = K_m + \frac{K_m[I]}{K_i} \qquad \textbf{(Equation 6.3)}$$

to calculate the Michaelis constant (K_m) for ribulose-P_2 and the inhibition constant (K_i) for xylulose-P_2. These equations are derived from the Michaelis equation for competitive inhibition,

$$v = \frac{k_{cat}[S]}{[S] + K_m(1 + {}^{[I]}\!/\!_{K_i})} \qquad \textbf{(Equation 6.4)}$$

6.2.5 Release of Inhibitor from the ECM:Carboxyarabinitol-P_2 complex

Rubisco (1.5 μM) was activated as described in Section 2.2.2, and incubated with ^{14}C-carboxypentitol-P_2 (18 μM) in a buffer containing 50 mM EPPS-NaOH, pH 8.0, 10 mM $MgCl_2$, 1 mM EDTA, 10 mM $NaHCO_3$ for 10 min prior to separation of Rubisco-bound radioactivity from unbound by gel filtration using Sephadex G-50 fine resin (10 mm x 200 mm) equilibrated with the reaction buffer. The protein peak was collected and unlabelled carboxypetitiol-P_2 was added to a final concentration of 200 μM. At intervals thereafter, samples were taken and reapplied to the gel filtration column, and the Rubisco-bound and unbound radioactivity were measured by online scintillation counting (Ultima-Flo, Packard). Assays were carried out on two separate occasions and the runs were pooled.

To estimate the value for k_{obs}, data for the release of labelled inhibitor versus time was fitted to Equation 6.1, which described the exchange of labelled inhibitors.

6.2.6 Binding of Carboxyarabinitol-P_2 to Rubisco

Rubisco (final concentration in assay of 5–30 nM) was activated and added to 2 ml spectrophotometric assays as described in Section 2.2.2. Carboxyarabinitol-P_2 was added to the assay (final concentration of 0.1–2.0 μM) and the mixture was incubated at 25°C for 0–240 s, before ribulose-P_2 (final concentration of 0.5 mM) was added to initiate the reaction.

Alternatively, Rubisco was activated as described in Section 2.2.2 and incubated with carboxyarabinitol-P_2 (5 – 600 μM) at 25°C. At intervals thereafter, 20 μl was then used to initiate a 2 ml assay containing 0.5 mM ribulose-P_2 (final concentration in assay of 5–30 nM).

Assays were carried out in duplicate on at least two separate occasions, and the runs were pooled. Initial activities for each time and inhibitor concentration were measured by fitting Equation 3.1 to the pooled data, and the data was analysed and parameters for slow tight binding were estimated as described in Section 6.2.8.

6.2.7 Release of Inhibitor from the ECM:Carboxyarabinitol-1-P Complex

Rubisco was activated as described in Section 2.2.2, and incubated with 20 μM carboxyarabinitol-1-P, in a buffer containing 100 mM EPPS-NaOH, pH 8.0, 1 mM EDTA, 20 mM $MgCl_2$ and 5–50 mM $NaHCO_3$ for 60 min to form the

ECM:carboxyarabinitol-1-P complex..A 10 µl aliquot of the ECM:carboxyarabinitol-1-P complex (final concentration in assay of 5–30 nM) was then used to initiate a 2000 µl spectrophotometric assay containing 0.5 mM ribulose-P_2, as described in Section 2.2.2. Assays were carried out on at least two separate occasions and the runs were pooled. To estimate values for v_i, v_f and k_{obs}, the pooled data for product accumulation versus time were fitted to Equation 3.1, which describes an exponential change in activity over time. Residual activity versus time was plotted using the parameter estimates obtained and Equation 3.2, which is the derived function of Equation 3.1.

6.2.8 Binding of Carboxyarabinitol-1-P to Rubisco

Rubisco was activated as described in Section 2.2.2, and incubated with 0.5–15 µM carboxyarabinitol-1-P, in a buffer containing 100 mM EPPS-NaOH, pH 8.0, 1 mM EDTA, 20 mM $MgCl_2$ and 5–50 mM $NaHCO_3$ for 60 min to form the ECM:carboxyarabinitol-1-P complex. A 20 µl aliquot of the ECM:carboxyarabinitol-1-P complex was then used to initiate a 2000 µl spectrophotometric assay containing 0.5 mM ribulose-P_2, as described in Section 2.2.2. Assays were carried out on at least two separate occasions and the runs were pooled. Equation 3.1 was fitted to the pooled data to estimate the initial rate of the enzyme. To estimate values for k_3 and K_i, the data were simultaneously fitted to Equations 6.7 and 6.8, assuming that the value for k_4 was equal to the estimate of k_{obs} calculated in Section 6.2.7.

6.2.9 Analysis of Slow Binding Inhibition

Slow binding inhibition of Rubisco has previously been modelled as a two-step process (Pierce et al. 1980). Initially there is a rapid equilibrium where the inhibitor competes with the substrate for the active site. This is followed by a slow isomerisation of the complex to form a much tighter complex that is likely to be associated with closure of flexible loops of the protein over the ligand in the active site (Duff et al. 2000). This is indicated by the following scheme:

$$E + I \underset{k_2}{\overset{k_1}{\rightleftharpoons}} EI \underset{k_4}{\overset{k_3}{\rightleftharpoons}} EI^* \qquad \textbf{(Equation 6.5)}$$

where E represents enzyme, I, the inhibitor, EI the complex in rapid equilibrium with E and I, EI^*, the slowly exchanging complex, and k_1 to k_4 are the rate constants of the individual forward and reverse reactions.

Assuming that k_3 and k_4 are much smaller than k_1 and k_2 and that $[I] >> [E]$, the rate equation for this process is,

$$\frac{v}{v_i} = \frac{E_a}{E_t} = \left(1 - \frac{k_4}{k_{obs}}\right) e^{-k_{obs} \cdot t} + \frac{k_4}{k_{obs}} \qquad \textbf{(Equation 6.6)}$$

where

$$k_{obs} = \frac{k_3 I}{K_i + I} + k_4 \qquad \textbf{(Equation 6.7)}$$

v is the Rubisco activity at time t, v_i is the Rubisco activity at time zero, E_a (= $[E]$ + $[EI]$) and E_t are the concentrations of non-tightly-complexed and total Rubisco active sites respectively, I is the inhibitor concentration, and $K_i = k_2/k_1$. This is also demonstrated in Figure 6.1.

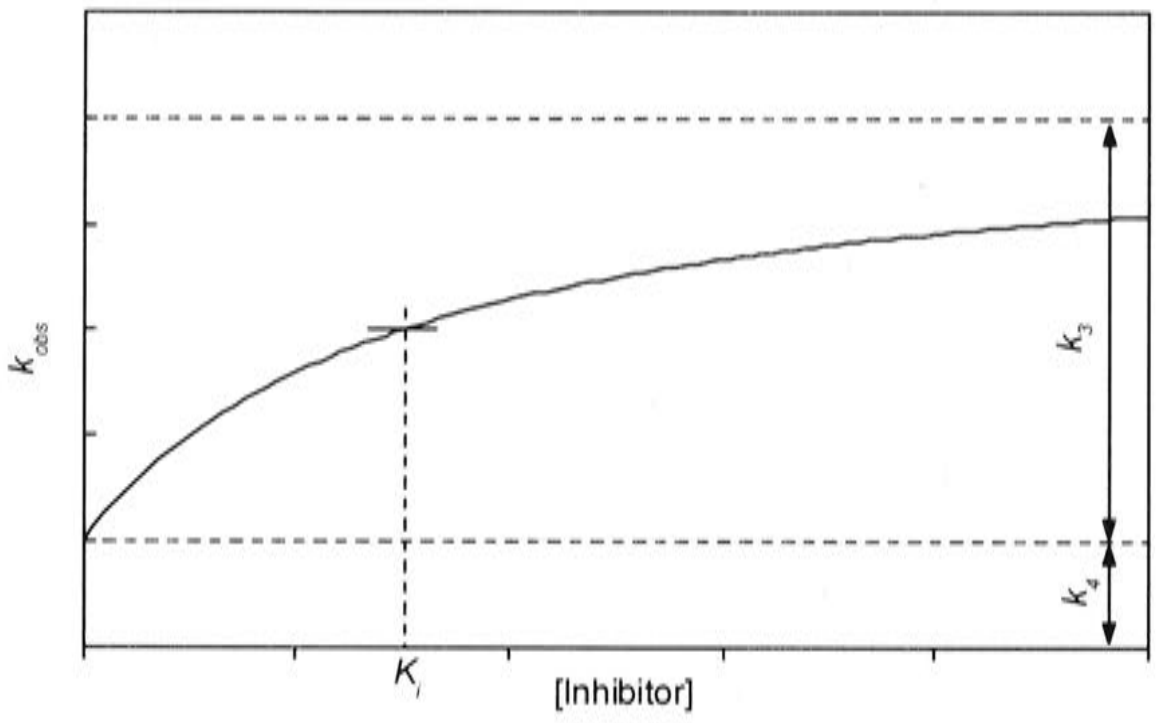

Figure 6.1 The Kinetics of Slow, Tight-Binding Inhibition

When an inhibitor is incubated with an enzyme, the rate at which the final equilibrium is reached (k_{obs}) is made up of two components, k_3 and k_4. The rate of inhibitor release (k_4) is constant and independent of inhibitor concentration. The rate of inhibitor binding increases with increasing inhibitor concentration before reaching an upper limit (k_3).

When $k_4 = 0$ (i.e. the tight complex is non-exchangeable and inhibition proceeds to completion, as it does with carboxyarabinitol-P_2), these relationships simplify to those used previously (Pierce et al. 1986a). However, if k_4 is finite, inhibition proceeds until equilibrium is reached at which a portion of the enzyme remains unsequestered in the tight complex and active. This active fraction is given by

$$\frac{v_f}{v_i} = \frac{E_a}{E_t} = \frac{k_4}{k_{obs}} \qquad \textbf{(Equation 6.8)}$$

where v_f is the final steady state activity. Because of the saturation of the inhibitor binding rate that is inherent in the model (Equation 6.7), a residual active fraction persists even at saturating concentrations of the slow-binding inhibitor. This fraction is given by $k_4/(k_3+k_4)$. Substituting Equation 6.8 into Equation 6.6 leads to Equation 3.2 and, by integration, to Equation 3.1. These relationships are analogous to those derived by Morrison (1982) for slow-isomerization binding.

Release of inhibitor from non-carbamylated, metal free Rubisco was modelled by using Equation 3.1. Under these conditions, where $[I] << K_i$ but still much greater than the enzyme concentration, Equation 6.7 simplifies so that k_{obs} approximates k_4.

To model the binding of xylulose-P_2 to Rubisco, the enzyme was incubated over a range of periods with various concentrations of inhibitor and its activity was measured immediately after mixing with ribulose-P_2 as described in Section 6.3.6. To estimate K_i, k_3, and k_4, these data were fitted simultaneously to Equations 6.5 and 6.6, using multiple curve-fitting software (OriginLab, Northampton, MA).

6.3 Results

6.3.1 Decarbamylation of Rubisco

Tobacco, *Synechococcus* PCC6301, and His-*Rubrum* Rubisco showed a decrease in activity following a 30 minute incubation with EPPS/EDTA buffer, sufficient to decarbamylate the enzyme with EDTA chelation of the Mg^{2+} ion. When this treatment was used for *G. sulphuraria* Rubisco, there was negligible apparent reduction in activity, suggesting that decarbamylation was slow, or that carbamylation could be maintained in the absence of the divalent metal by the low levels of CO_2 present in the solution. Effective decarbamylation of *G. sulphuraria* required dialysis overnight against buffer that was sparged with N_2 to remove all traces of CO_2. Even after this treatment, some activity remained, indicating that some sites were still carbamylated.

6.3.2 Activation of the Decarbamylated Enzyme

When decarbamylated Rubisco is added to an assay mixture containing saturating concentrations of CO_2, Mg^{2+}, and ribulose-P_2, the activity increases as the essential Mg^{2+}-stabilized carbamate (ECM) is formed in the active site. Although the rate of ECM formation is slowed by the presence of ribulose-P_2, which binds tightly to E (Jordan and Chollet 1983), the activity increases from an initial low rate to a final steady state which matches that seen in controls where full Mg^{2+}/CO_2 activation occurred prior to ribulose-P_2 addition.

Results for activity versus time were fitted to Equation 3.2, which showed a good approximation to the data ($r^2 > 0.999$ for all fits) and provided an estimation of the k_{obs}, the observed rate constant value. Equation 6.7 shows the relationship between k_{obs}, and k_4, the rate constant for inhibitor release. In this assay, the ribulose-P_2 concentration is high, thus k_{obs} gives a higher value than the actual value of k_4.

After showing no initial activity, wild-type and L335V tobacco Rubisco showed similar rates of ribulose-P_2 release, with a half-time of around four min (Figure 6.2, Figure 6.6, Table 6.1). His-*Rubrum* and *Synechococcus* PCC6301 Rubisco showed rapid activation, reaching full activity within two min after showing no initial activity (Figure 6.3, Figure 6.5, Table 6.1). *G. sulphuraria* Rubisco had an initial activity that was 5–10 % of the control activity, but had negligible detectable increase over 20 min, suggesting a very slow activation rate in the presence of saturating concentrations of ribulose-P_2 (Figure 6.4).

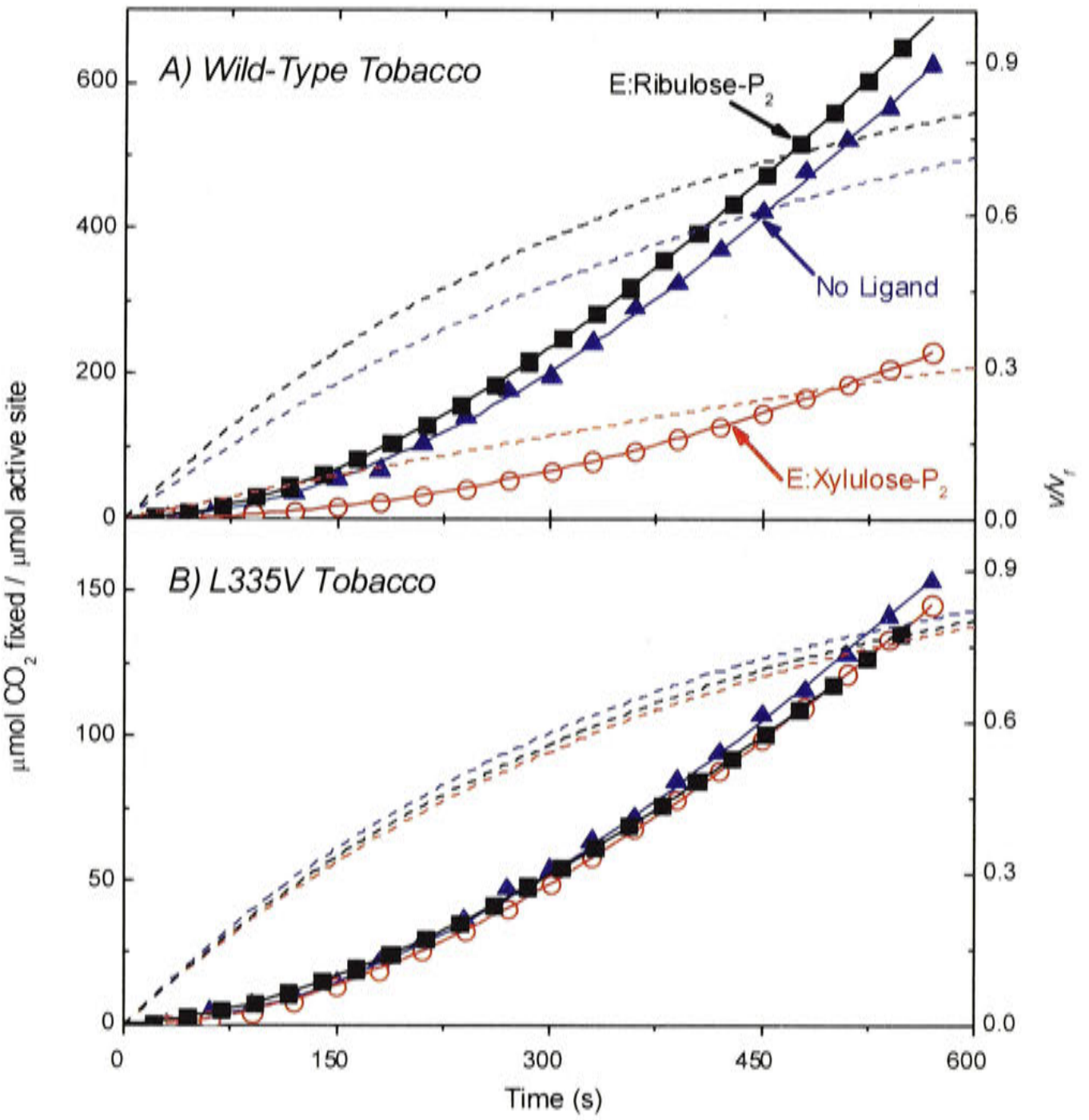

Figure 6.2 Activation of Uncarbamylated, Metal-free Tobacco Rubisco

Uncarbamylated metal-free complexes of wild-type (*A*) and L335V (*B*) tobacco Rubisco were incubated with no ligand (▲, blue lines), ribulose-P_2 (■, black lines) or xylulose-P_2 (○, red lines). These complexes were added at zero time to spectrophotometric assay mixtures containing saturating Mg^{2+}, ribulose-P_2 and CO_2 concentrations (as described in Sections 6.2.1 & 6.2.2). The data for product accumulation (left ordinate, ▲, ■ & ○) versus time was fitted to Equation 3.1 (solid lines) and the values for v_f and k_{obs} were estimated (Table 6.1). Using these estimates, curves for the rate as a proportion of the final activity (right ordinate) as a function of time were plotted using Equation 3.2 (dashed lines).

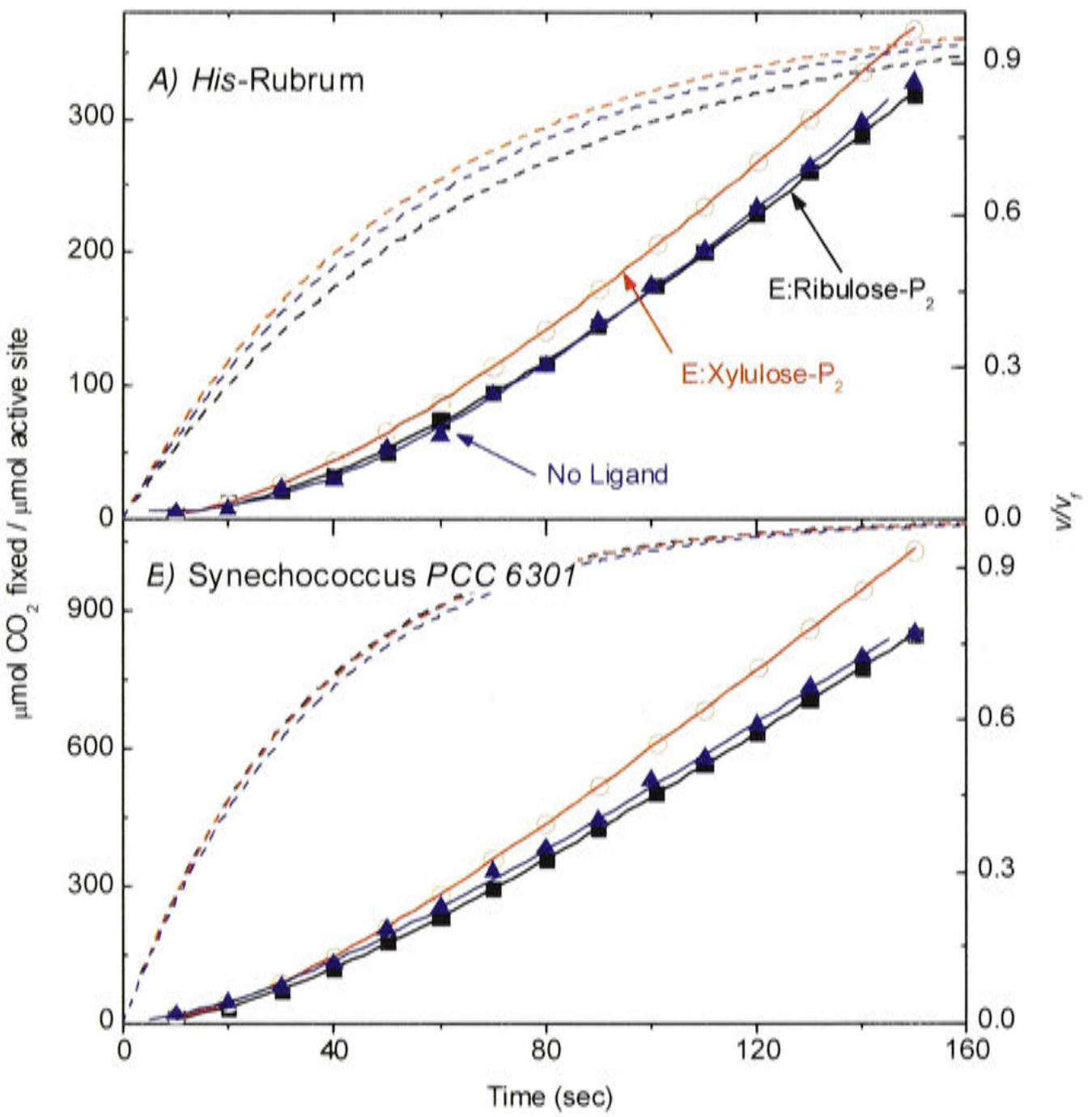

Figure 6.3 Activation of Uncarbamylated, Metal-free His-*Rubrum* and *Synechococcus* PCC6301 Rubisco

Uncarbamylated metal-free complexes of His-*Rubrum* (*A*) and *Synechococcus* PCC6301 (*B*) Rubisco were incubated with no ligand (▲, blue lines), ribulose-P_2 (■, black lines) or xylulose-P_2 (○, red lines). These complexes were added at zero time to spectrophotometric assay mixtures containing saturating Mg^{2+}, ribulose-P_2 and CO_2 concentrations (as described in Sections 6.2.1 & 6.2.2). The data for product accumulation (left ordinate, ▲, ■ & ○) versus time was fitted to Equation 3.1 (solid lines) and the values for v_f and k_{obs} were estimated (Table 6.1). Using these estimates, curves for rate as a proportion of the final activity (right ordinate) as a function of time were plotted using Equation 3.2 (dashed lines).

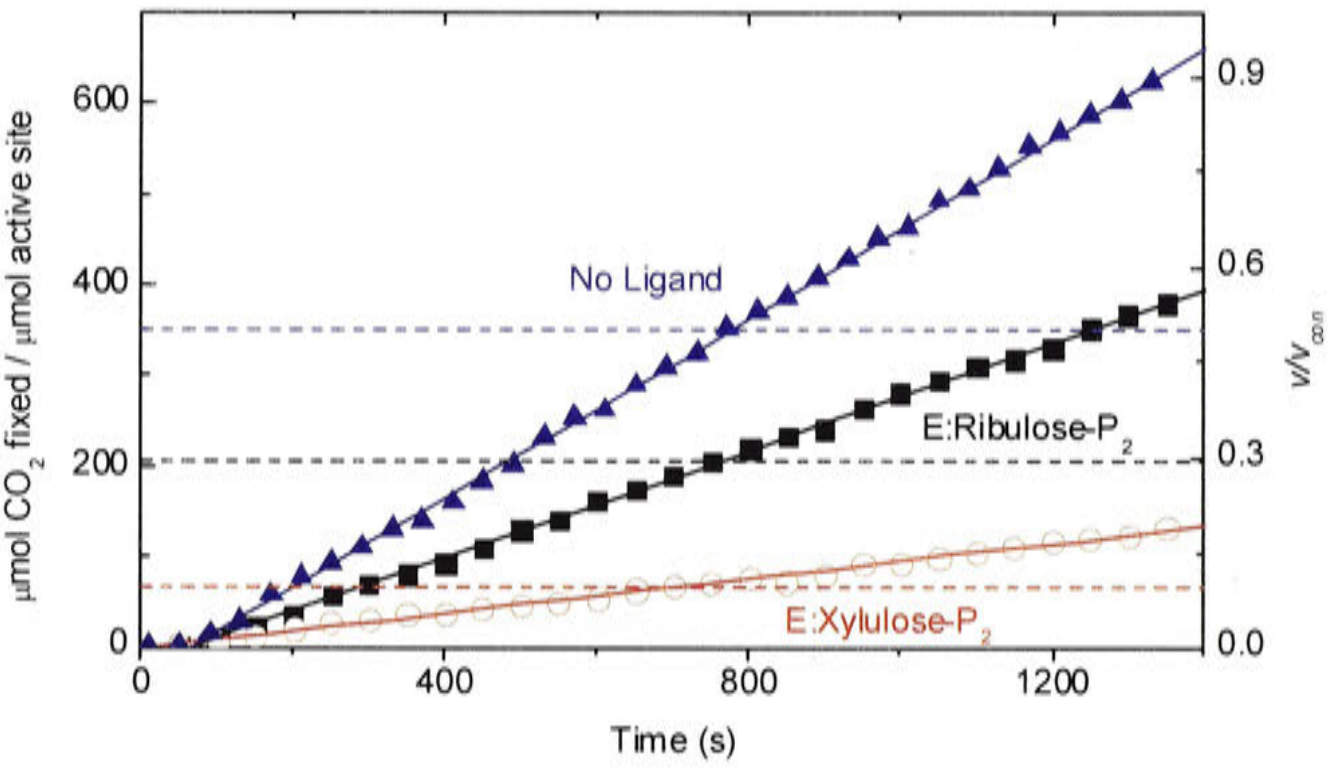

Figure 6.4 Activation of Uncarbamylated, Metal-free *G. sulphuraria* Rubisco

Uncarbamylated metal-free complexes of *G. sulphuraria* Rubisco were incubated with no ligand (▲, blue lines), ribulose-P_2 (■, black lines) or xylulose-P_2 (○, red lines). These complexes were added at zero time to spectrophotometric assay mixtures containing saturating Mg^{2+}, ribulose-P_2 and CO_2 concentrations (as described in Sections 6.2.1 & 6.2.2). The data for product accumulation (left ordinate, ▲, ■ & ○) versus time was fitted to a linear equation. Using this estimate, curves for the rate as a proportion of the fully activated activity (right ordinate) as a function of time were plotted (dashed lines).

6.3.3 Activation of the E:Ribulose-P_2 Complex

The decarbamylated Rubisco enzyme can form a complex with the substrate, ribulose-P_2, which slowly dissociates over time. The rates of ribulose-P_2 release from the E:ribulose-P_2 complex were analogous to the activation rate of adding decarbamylated enzyme to the assay without preincubation with ribulose-P_2. Activation rates seen in these experiments were faster than some previous observations for spinach and *R. rubrum* Rubisco enzymes (Jordan and Chollet 1983). However the previous work had been carried out at 2°C, and it would be expected that the rate of inhibitor binding and release would be slower at lower temperatures.

To detect the release of ribulose-P_2 from the E:ribulose-P_2 complex of *G. sulphuraria* Rubisco, the exchange of labelled inhibitors was measured because the increase in activity during spectrophotometric assays was too slow. Uncarbamylated Rubisco was incubated with [1-^{3}H]ribulose-P_2 to form the E:ribulose-P_2 complex, and unbound inhibitors were removed by gel filtration. An excess of unlabelled ribulose-P_2 was added, so that when a labelled ribulose-P_2 molecule was released from the active site, an unlabelled ribulose-P_2 molecule would replace it. The exchange of bound [1-^{3}H]ribulose-P_2 with [1-^{1}H]ribulose-P_2 was measured by gel filtration (Figure 6.5, Table 6.1), allowing k_{obs} to be calculated using Equation 6.1 ($r^2 > 0.99$). Release of ribulose-P_2 was much slower than other enzymes, with a half-time of 74 min (Figure 6.5).

In this experiment, k_{obs} should give a good approximation to k_4, because the concentration of labelled inhibitor is much lower than that of unlabelled inhibitor, which effectively reduces Equation 6.7 to $k_{obs} = k_4$. When this method was used for His-*Rubrum*, *Synechococcus* PCC6301, or tobacco Rubisco, the [1-^{3}H]ribulose-P_2, was released during the initial gel filtration step.

6.3.4 Competitive Inhibition by Xylulose-P_2

Xylulose-P_2 can act as a competitive inhibitor of Rubisco by binding loosely to the carbamylated active site. The action of xylulose-P_2 as a competitive inhibitor with respect to ribulose-P_2 was determined by measuring the initial activity of the Rubisco at different ribulose-P_2 and xylulose-P_2 concentrations. Estimates of the inhibition parameters were obtained by calculating the K_{app} value for each xylulose-P_2 concentration using Equation 6.2, and then calculating K_i using Equation 6.3 ($r^2 > 0.96$ for all fits). These values are shown in Table 6.2 as 'rapid equilibrium data'.

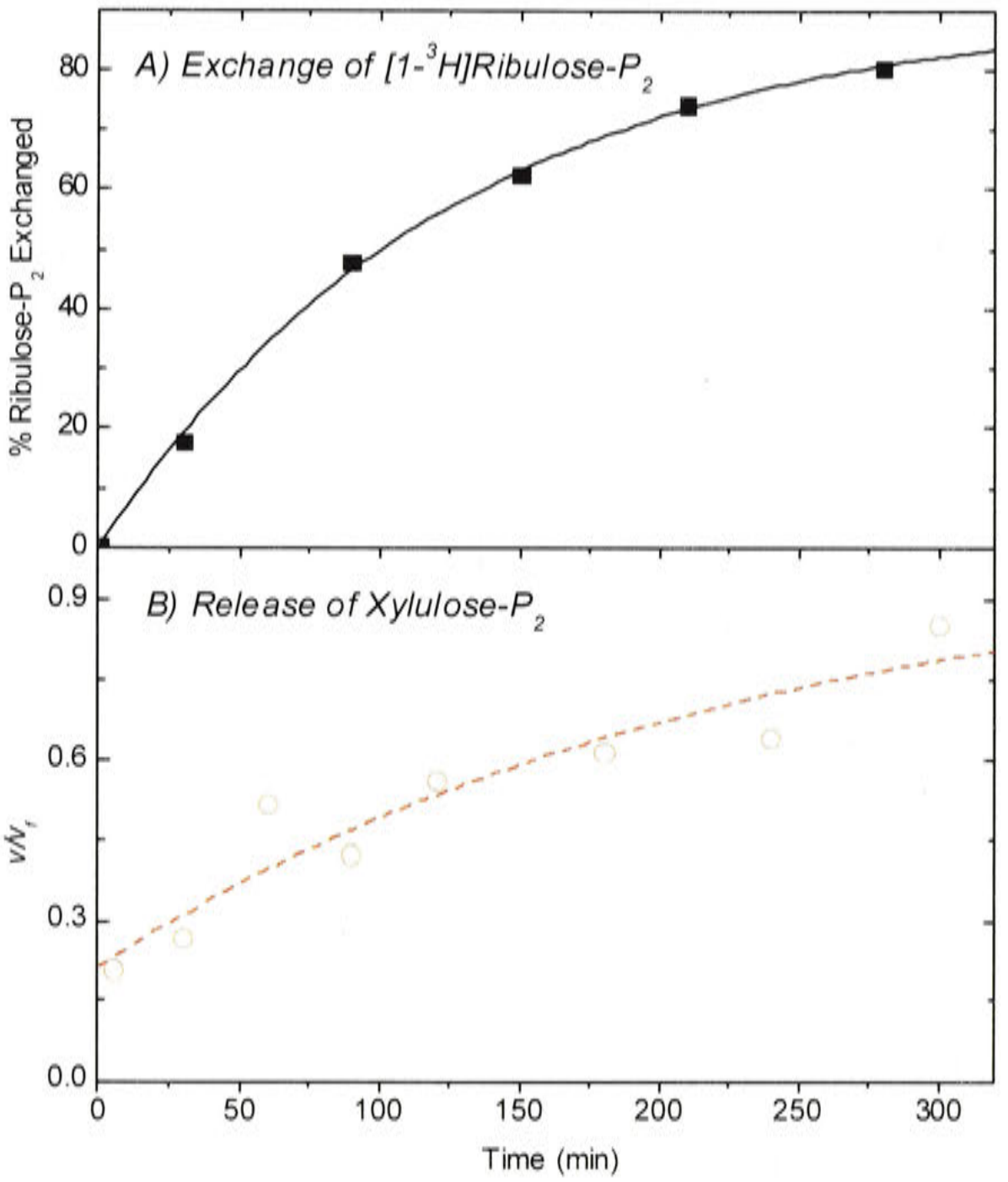

Figure 6.5 Release of Ribulose-P_2 and Xylulose-P_2 by Uncarbamylated, Metal-free *G. sulphuraria* Rubisco

Uncarbamylated metal-free complexes of *G. sulphuraria* Rubisco were incubated with [1-^{3}H]ribulose-P_2 (*A*) or xylulose-P_2 (*B*). Unbound [1-^{3}H]ribulose-P_2 was removed by gel filtration, and an excess of unlabelled ribulose-P_2 was added. At time intervals thereafter, samples were taken and the amount of Rubisco-bound radioactivity measured by gel filtration (as described in Section 6.2.1). Data was fitted to Equation 6.1 to calculate k_{obs} (Table 6.1). Unbound xylulose-P_2 was removed by gel filtration, and the Rubisco was added to assay buffer lacking ribulose-P_2. At time intervals thereafter, samples were taken and ribulose-P_2 added to initiate the reaction, allowing the rate to be measured (as described in Section 6.2.2). Data were fitted to Equation 6.6 to calculate k_{obs} (Table 6.1).

	Ribulose-P_2 k_{obs} (s^{-1})	Xylulose-P_2 k_{obs} (s^{-1})	No ligand k_{obs} (s^{-1})
Wild-Type Tobacco	$2.74 \pm 0.01 \times 10^{-3}$	$0.60 \pm 0.01 \times 10^{-3}$	$2.09 \pm 0.01 \times 10^{-3}$
L335V Tobacco	$2.83 \pm 0.02 \times 10^{-3}$	$2.87 \pm 0.02 \times 10^{-3}$	$2.60 \pm 0.01 \times 10^{-3}$
G. sulphuraria	$0.13 \pm 0.01 \times 10^{-3}$	$0.07 \pm 0.03 \times 10^{-3}$	
Synechococcus PCC6301	$28.9 \pm 0.5 \times 10^{-3}$	$29.8 \pm 0.5 \times 10^{-3}$	$34.4 \pm 9.0 \times 10^{-3}$
His-*Rubrum*	$20.0 \pm 0.5 \times 10^{-3}$	$19.5 \pm 0.5 \times 10^{-3}$	$18.3 \pm 0.3 \times 10^{-3}$

Table 6.1 Kinetic Parameters (± S.E.) for the Activation of Uncarbamylated, Metal-free Rubisco
Uncarbamylated wild-type tobacco, L335V tobacco, *G. sulphuraria*, *Synechococcus* PCC6301 and His-*Rubrum* Rubisco were incubated with ribulose-P_2 or xylulose-P_2 (as described in Sections 6.2.1 & 6.2.2). For wild-type tobacco, L335V tobacco, *Synechococcus* PCC6301 and His-*Rubrum* Rubisco Equation 3.1 was fitted to the activity versus time data (Figure 6.2 and Figure 6.3)to estimate k_{obs}. For *G. sulphuraria* Rubisco, Equation 6.1 was fitted to the data in Figure 6.5 to estimate k_{obs}.

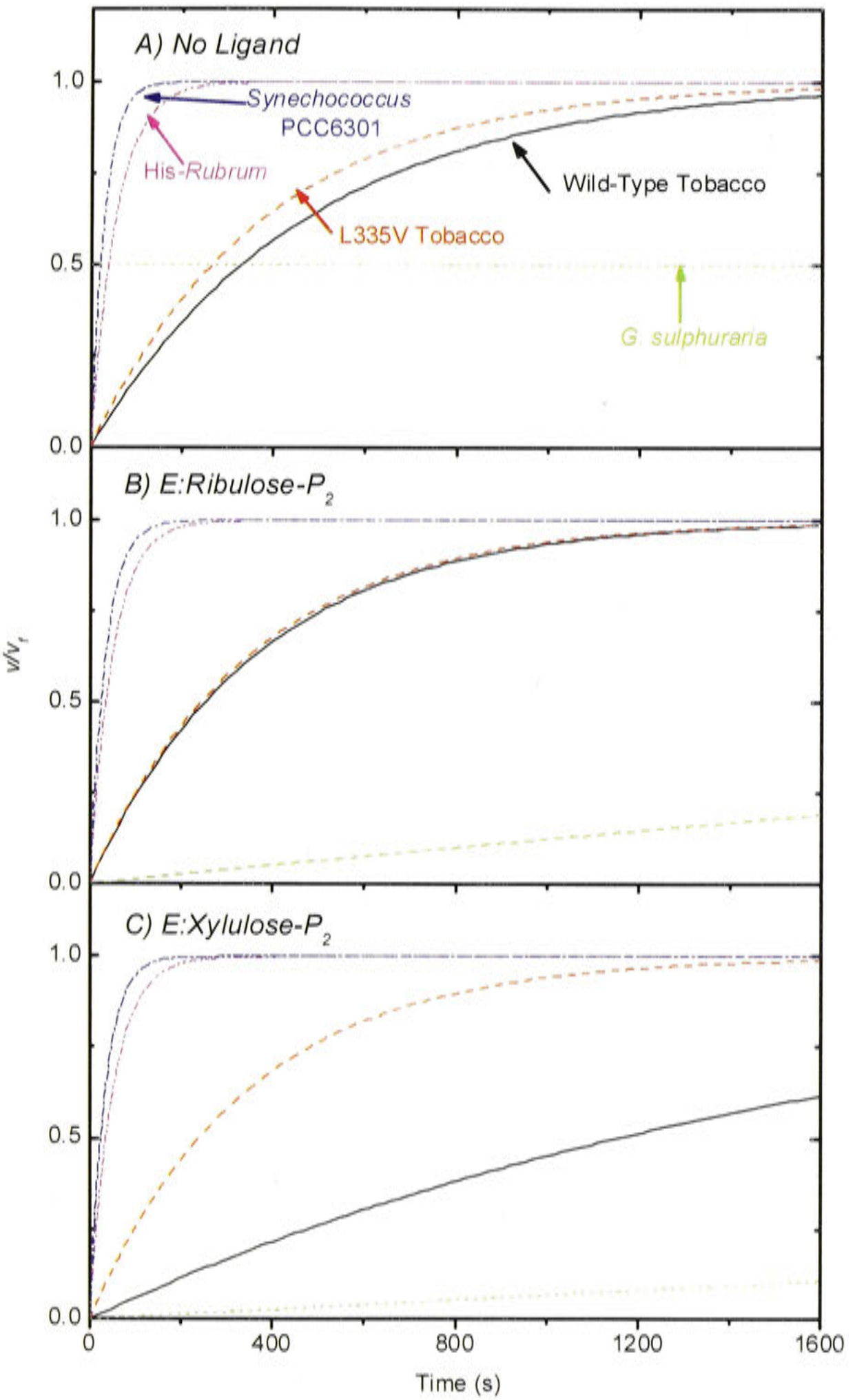

Figure 6.6 Activation of Uncarbamylated, Metal-free Rubisco

Uncarbamylated metal-free complexes of wild-type tobacco, L335V tobacco, His-*Rubrum*, *Synechococcus* PCC6301 and *G. sulphuraria* Rubisco were incubated with no inhibitor (A), ribulose-P_2 (B) or xylulose-P_2 (C). These complexes were added at zero time to spectrophotometric assay mixtures containing saturating Mg^{2+}, ribulose-P_2 and CO_2 concentrations (as described in 6.2.1 & 6.2.2). Using the estimates of v_f, v_i and k_{obs}, (Table 6.1) curves for the percentage of the final activity as a function of time were plotted using Equation 3.2.

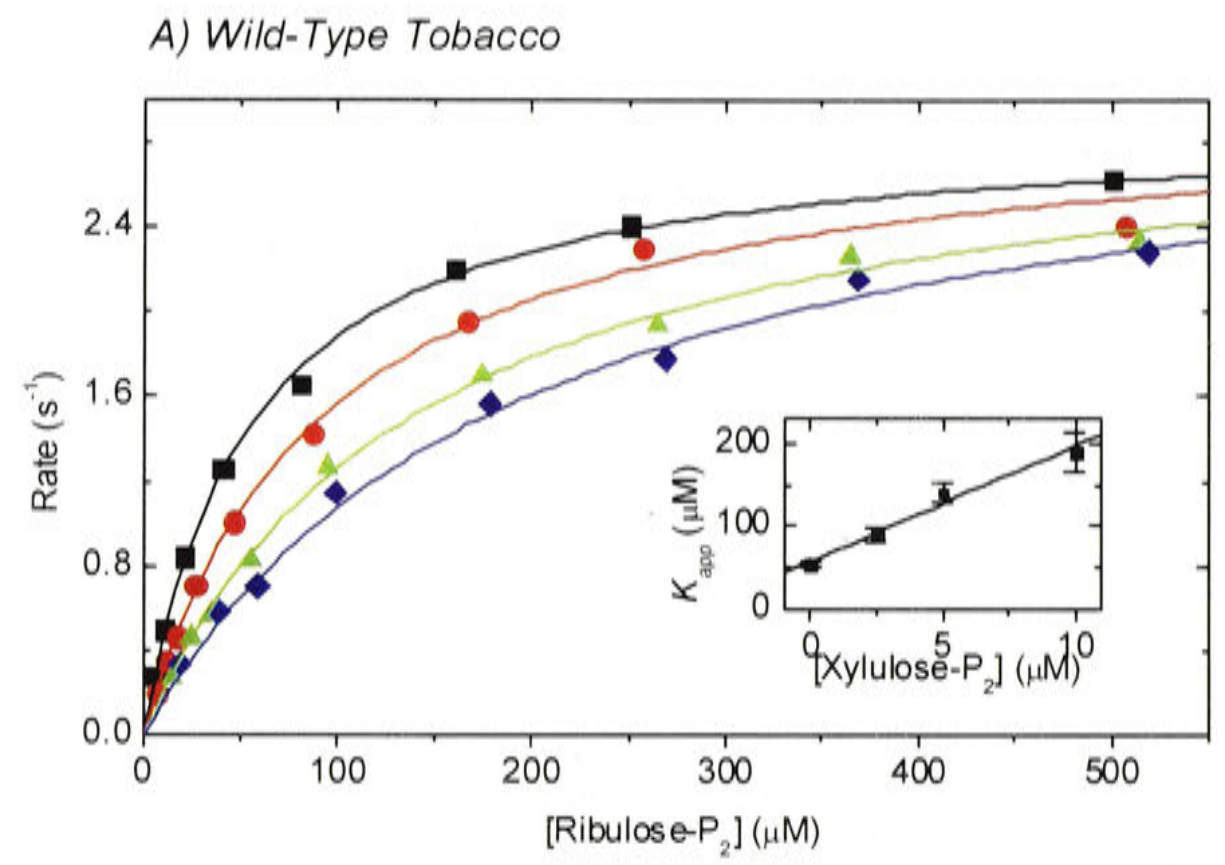

Figure 6.7 Competitive Inhibition of Wild-Type and L335V Tobacco Rubisco by Xylulose-P_2

Spectrophotometric assays were carried out in buffers containing a range of ribulose-P_2 concentrations and xylulose-P_2 concentrations for wild-type (■ 0 μM xylulose-P_2; ● 2.5 μM; ▲ 5.0 μM; ◆ 10 μM) and L335V (■ 0 μM xylulose-P_2; ● 10 μM; ▲ 20 μM; ◆ 40 μM) tobacco Rubisco. K_{app} was calculated by fitting the data to Equation 6.2. This was plotted versus [xylulose-P_2] (inset) and fitted to Equation 6.3, allowing K_i and K_m to be calculated (Table 6.2).

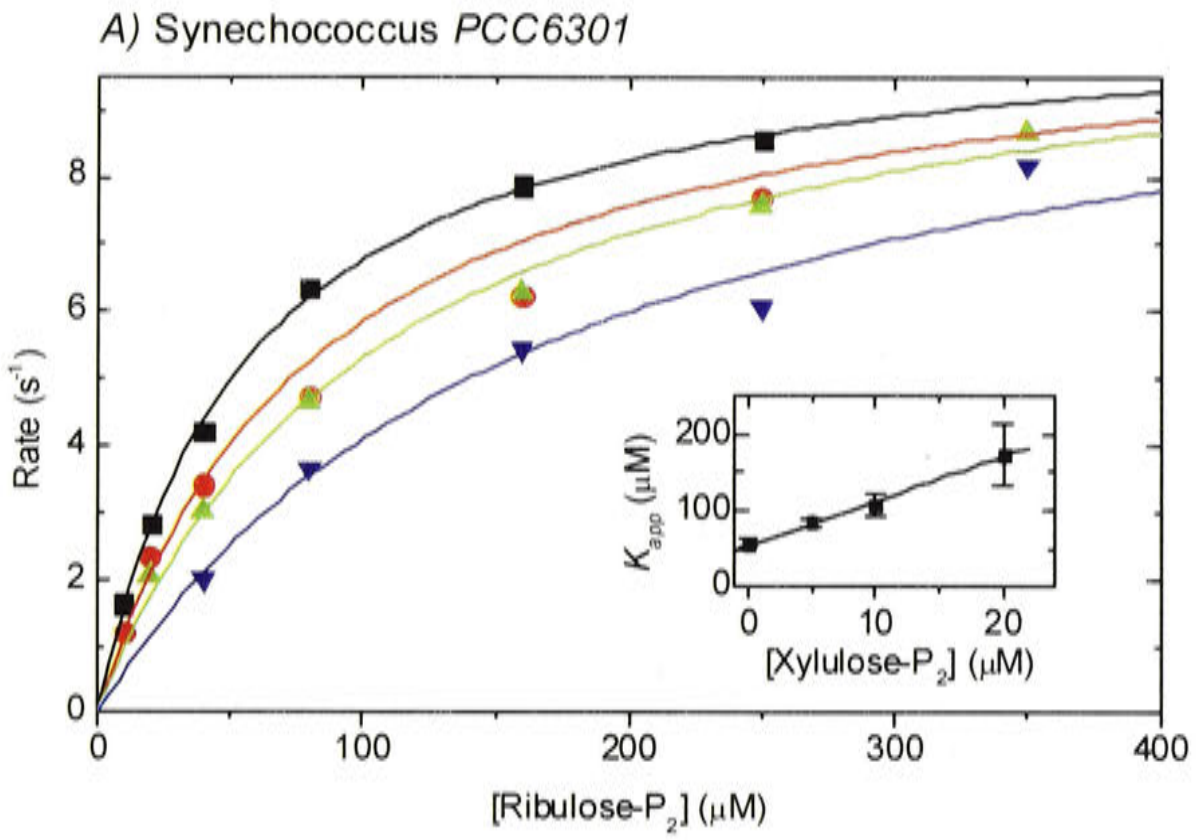

Figure 6.8 Competitive Inhibition of *Synechococcus* PCC6301 and His-*Rubrum* Rubisco by Xylulose-P_2

Spectrophotometric assays were carried out in buffers containing a range of ribulose-P_2 concentrations and xylulose-P_2 concentrations for *Synechococcus* PCC6301 (■ 0 μM xylulose-P_2; ● 5.0 μM; ▲ 10 μM; ◆ 20 μM) and His-*Rubrum* (■ 0 μM xylulose-P_2; ● 2.5 μM; ▲ 5.0 μM; ◆ 10 μM) Rubisco. K_{app} was calculated by fitting the data to Equation 6.2. This was plotted versus [xylulose-P_2] (inset) and fitted to Equation 6.3, allowing K_i and K_m to be calculated (Table 6.2).

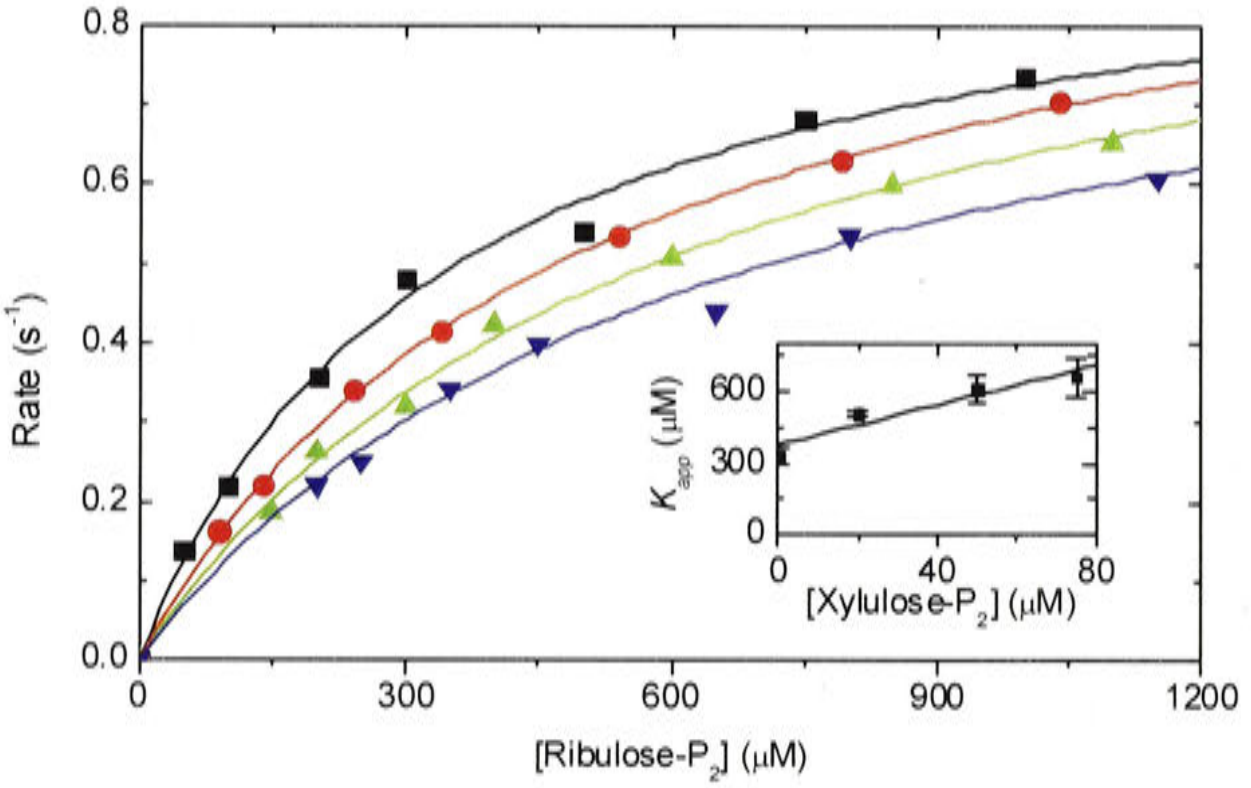

Figure 6.9 Competitive Inhibition of *G. sulphuraria* Rubisco by Xylulose-P_2

Spectrophotometric assays were carried out in buffers containing a range of ribulose-P_2 concentrations and xylulose-P_2 concentrations for *G. sulphuraria* (■ 0 μM xylulose-P_2; ● 20 μM; ▲ 50 μM; ◆ 75 μM) Rubisco. K_{app} was calculated by fitting the data to Equation 6.2. This was plotted versus [xylulose-P_2] (inset) and fitted to Equation 6.3, allowing K_i and K_m to be calculated (Table 6.2).

	Rapid Equilibrium Inhibition		Slow Binding Inhibition		
	K_i(xylulose-P_2) (μM)	K_m(ribulose-P_2) (μM)	K_i (μM)	k_3 (s^{-1})	k_4 (s^{-1})
Wild-Type Tobacco	4.8 ± 0.4	58 ± 9	1.9 ± 0.5	15 ± 2 x 10^{-4}	5 ± 1 x 10^{-4}
L335V Tobacco	20.7 ± 4.6	17 ± 3	NA[a]	NA	NA
G. sulphuraria	89 ± 29	376 ± 42	89[b]	1.2 ± 0.1 x 10^{-4}	0.7 x 10^{-4} [c]
Synechococcus PCC6301	12.2 ± 1.0	54 ± 3	NA	NA	NA
His-*Rubrum*	3.1 ± 0.7	3.9 ± 1	NA	NA	NA

[a] Not applicable (no slow inhibition detected)
[b] Assumed to be equal to the value for rapid binding equilibrium
[c] Assumed to be equal to k_{obs} for E:xylulose-P_2 activation (from Table 6.1)

Table 6.2 Kinetic Parameters (± S.E.) for the Inhibition of Rubisco by Xylulose-P_2.

Parameters for slow binding inhibition were calculated for wild-type tobacco by fitting Equations 6.6 and 6.7 to the data in Figure 6.12, and for *G. sulphuraria* by fitting Equations 6.7 and 6.8 to the data in Figure 6.10. Rapid equilibrium inhibition parameters were calculated by fitting Equations 6.2 and 6.4 to the data in Figure 6.7, Figure 6.8 and Figure 6.9.

Wild-type tobacco, *Synechococcus* PCC6301 and *G. sulphuraria* Rubisco had a K_i for xylulose-P_2 that was 3–10 times less than the K_m for ribulose-P_2 (Table 6.2). For L335V tobacco and His-*Rubrum* Rubisco, the K_i for xylulose-P_2 was similar to the K_m for ribulose-P_2. The value for wild-type tobacco Rubisco was consistent with previous observation for spinach Rubisco (McCurry and Tolbert 1977). The estimates of K_m for ribulose-P_2 were slightly higher than previously observed, which may be due to the presence of amines. A Schiff's base can form between primary amines and aldehydes and ketones, such as ribulose-P_2. The EPPS buffer used in the assay solutions, while of the highest commercially available purity, nevertheless may have contained low levels of contaminating aromatic compounds that could bind to ribulose-P_2 and lower the effective concentration.

6.3.5 Activation of the E:Xylulose-P_2 Complex

Like ribulose-P_2, xylulose-P_2 can also bind to uncarbamylated Rubisco to form an inactive complex that can undergo further conformational change to form a tightly bound complex, referred to as E:xylulose-P_2. The rate constant for release of xylulose-P_2 from the E:xylulose-P_2 complex could be measured in a similar way to that for the release of ribulose-P_2 from the E:ribulose-P_2 complex, by adding E:xylulose-P_2 to an assay containing saturating Mg^{2+}, CO_2 and ribulose-P_2 concentrations (Figure 6.2, Figure 6.3, Figure 6.4). When these assays were carried out using L335V tobacco, *Synechococcus* PCC6301 or His-*Rubrum* Rubisco that had been incubated with xylulose-P_2, the rate of activation was similar to the rate observed for activation of E:ribulose-P_2 in the presence of ribulose-P_2 (Table 6.1,Figure 6.6). Wild-type tobacco Rubisco had a slower rate of inhibitor release from the E:xylulose-P_2 complex than from the E:ribulose-P_2 complex, with a half-time of 20 min. This is similar to the previous observation of a half-time of 16 min for spinach Rubisco (Zhu and Jensen 1991b). *G. sulphuraria* Rubisco showed negligible activation during the spectrophotometric assay, but had an initial rate that was 30 % of the fully activated rate.

To measure the release of xylulose-P_2 from the *G. sulphuraria* E:xylulose-P_2 complex, gel filtration was used to remove all traces of unbound xylulose-P_2 from the enzyme, reducing the possibly that the released inhibitor would bind to the enzyme again. The Rubisco was then added to an assay mixture that lacked ribulose-P_2, but contained high levels of Mg^{2+} and $NaHCO_3$, allowing activation of the active sites once the xylulose-P_2 was released. Samples were taken over time and ribulose-P_2 was added to initiate the reaction allowing calculation of the reaction rate. The activity increased

over time (Figure 6.5), reflecting the release of xylulose-P_2, and was fitted to Equation 6.6 to calculate k_{obs}, the first order rate constant ($r^2 > 0.98$). In this assay, [*I*] is low due to the gel filtration step, thus Equation 6.7 simplifies to $k_{obs}=k_4$. The initial activity was 20 % of the fully activated rate, and increased with a half-time of nearly three min, much slower than that of other Rubisco enzymes.

6.3.6 Binding of Xylulose-P_2 to Rubisco

In addition to the release of xylulose-P_2 from the E:xylulose-P_2 complex, parameters for the formation of the E:xylulose-P_2 complex can also be measured. Fully carbamylated Rubisco enzymes were incubated with varying xylulose-P_2 concentrations for 60 min to allow the formation of the E:xylulose-P_2 complex. Samples were then used to initiate a spectrophotometric assay to determine the Rubisco activity. As well as the tight binding of xylulose-P_2 to Rubisco, competitive inhibition of Rubisco can also occur from xylulose-P_2 carried over from the inhibition incubation step, resulting in a lower reaction rate. This competitive inhibition of carbamylated Rubisco is minimised by the 10-fold dilution of Rubisco and xylulose-P_2 that occurs when the sample is added to the spectrophotometric assay. The high ribulose-P_2 concentration in the solution also reduces the level of competitive inhibition. Despite these factors, at high xylulose-P_2 concentrations the effect of competitive inhibition is increased, particularly for *G. sulphuraria* Rubisco, which has a high K_m for ribulose-P_2. For L335V tobacco, *Synechococcus* PCC6301 and His-*Rubrum* Rubisco, the decline in activity was consistent with the K_i for competitive inhibition calculated in Section 6.3.4 (Figure 6.10Figure 6.11).

Wild-type tobacco and *G. sulphuraria* Rubisco exhibited a decline in activity that exceeded the drop expected for competitive inhibition (Figure 6.10). As predicted for slow isomerisation binding (Equation 6.8), where release from the tight complex occurs at an appreciable rate relative to isomerisation, this inhibition was less than complete, with some activity (25 % of initial) remaining, even after prolonged exposure to saturating xylulose-P_2 concentrations. Maximum inhibition of wild-type tobacco Rubisco occurred in the presence of more than 2 μM xylulose-P_2, which is similar to that previously observed for spinach Rubisco, and was attributed to the formation of a decarbamylated enzyme-xylulose-P_2 complex (Zhu and Jensen 1991b). Maximum inhibition of *G. sulphuraria* Rubisco occurred in the presence of more than 200 μM xylulose-P_2, which suggests a lower binding affinity than the wild-type tobacco enzyme.

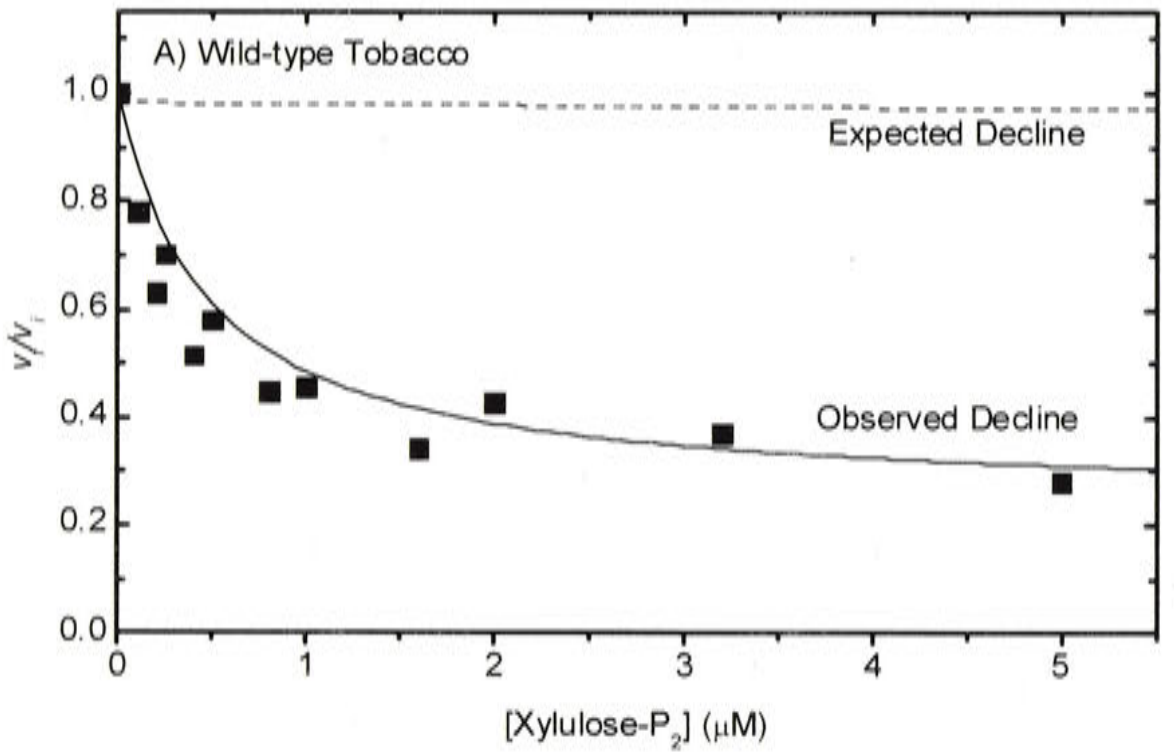

Figure 6.10 Inhibition of Carbamylated Rubisco Following Exposure to Xylulose-P_2

Pre-activated wild-type tobacco (panel A, ■), and *G. sulphuraria* (panel A, ▲), Rubisco were exposed to xylulose-P_2 for 60 min before assay. The residual activity (v_f) is plotted as a proportion of the activity seen in controls lacking xylulose-P_2 (v_i). The solid line is drawn according to Equations 6.6 and 6.7 using the parameter estimates in Table 6.2 for wild-type tobacco and *G. sulphuraria* Rubisco. The dashed lines show the expected decease in activity due to competitive inhibition using parameters from Table 6.2 and Equation 6.4.

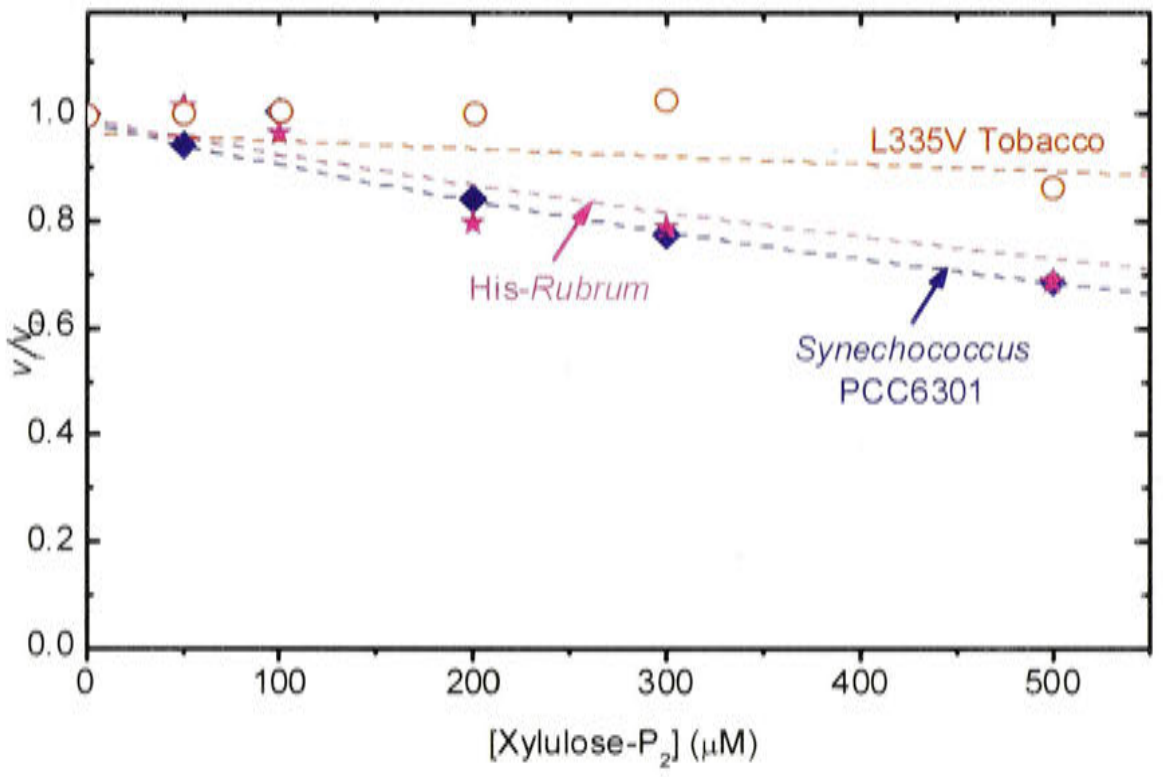

Figure 6.11 Inhibition of Carbamylated Rubisco Following Exposure to Xylulose-P_2

Pre-activated L335V tobacco (○), *Synechococcus* PCC6301 (◆), and His-*Rubrum* (★) Rubisco were exposed to xylulose-P_2 for 60 min before assay. The residual activity (v_f) is plotted as a proportion of the activity seen in controls lacking xylulose-P_2 (v_i). The dashed lines show the expected decease in activity due to competitive inhibition using parameters from Table 6.2 and Equation 6.4.

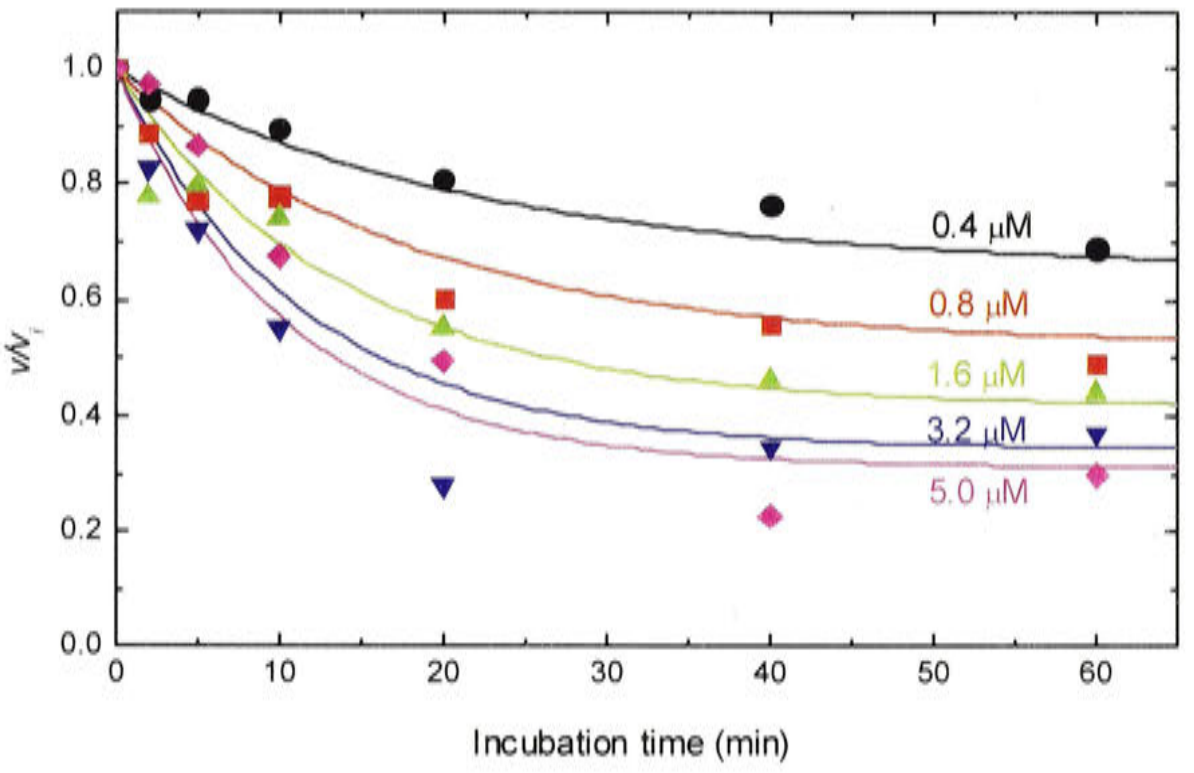

Figure 6.12 Inhibition of Carbamylated Wild-Type Tobacco Rubisco Following Exposure to Xylulose-P_2

Pre-activated wild-type tobacco Rubisco was exposed to the indicated concentrations of xylulose-P_2 at zero time, and assayed at intervals thereafter (as described in 6.2.3). The data for all five time courses were fitted simultaneously to Equations 6.6 and 6.7 to estimate K_i, k_3 and k_4 (Table 6.2). The solid fitted lines were plotted using these estimates.

For wild-type Rubisco, the rate constants for slow binding and release of xylulose-P_2, k_3 and k_4, were obtained by incubating the enzyme with varying xylulose-P_2 concentrations for up to 60 min, and assuming that the carboxylation rate gave an accurate indication of the level of inhibition. The initial carboxylation rate was measured, because the dilution of xylulose-P_2 inherent to the assay procedure allowed the release of xylulose-P_2 from the active sites, resulting in an increase in activity over time. The dilution of xylulose-P_2 and the high concentration of ribulose-P_2 also eliminated any rapid-equilibrium inhibition by xylulose-P_2 during the assay. Data for the rate of inhibition versus time (Figure 6.12) were simultaneously fitted to Equations 6.5 and 6.6 (Table 6.2), which showed that the rate of binding and extent of inhibition was greater at higher xylulose-P_2 concentrations.

Although the data for v_f/v_i versus [xylulose-P_2] (Figure 6.10) can be fitted simultaneously to Equations 6.6 and 6.7 to calculate K_i, k_3 and k_4, the values of the parameter estimates are limited by the strong interdependency between k_3 and k_4. The curve drawn for wild-type tobacco Rubisco using the estimates of these values from Table 6.2 approximately fit these data. For *G. sulphuraria* Rubisco, the curve was drawn under the assumptions that the value of xylulose-P_2 binding to the uncarbamylated form (K_i, Figure 6.9, Table 6.2) was the same as binding to the carbamylated form, and that the rate of release is the same as the constant for activation of the E:xylulose-P_2 complex (k_{obs}, Figure 6.5B, Table 6.1). This gave a good approximation to the data and suggested that the binding of xylulose-P_2 to *G. sulphuraria* Rubisco was 10-fold slower than binding to wild-type tobacco Rubisco.

The results for inhibition of wild-type tobacco Rubisco are similar to the results observed for inhibition of spinach Rubisco with 5 μM xylulose-P_2 (Zhu and Jensen 1991b). However, they did not use the same models for the binding of ligands, and their value is likely to indicate k_{obs}, rather than k_3.

6.3.7 Release of Carboxyarabinitol-P_2 from the ECM:Carboxyarabinitol-P_2 Complex

Carbamylated Rubisco can form a tight complex with carboxyarabinitol-P_2, termed ECM:carboxyarabinitol-P_2. Wild-type tobacco, Val-353 tobacco, *G. sulphuraria* and *Synechococcus* PCC6301 Rubisco enzymes showed negligible exchange of bound ^{14}C-carboxyarabinitol-P_2 for unbound, unlabelled carboxyarabinitol-P_2 over several days (Figure 6.13). This is consistent with an exchange rate for higher plants of around 1×10^{-8} s^{-1}, which would take over two years for half of the inhibitor to be exchanged

(Schloss 1988a). His-*Rubrum* Rubisco showed slow release of bound inhibitor, with half of the inhibitor being exchanged after two days (Figure 6.13). This data could be fitted to Equation 6.1 and used to calculate the values of k_{obs}. Due to the low concentration of free inhibitor in the assay, Equation 6.7 simplifies to $k_{obs} = k_4$ (Table 6.3). The increased rate of release by His-*Rubrum* is also consistent with the previously observed rates for *R. rubrum* (Harpel et al. 1991; Harpel et al. 1998).

6.3.8 Binding of Carboxyarabinitol-P_2 to Rubisco

Carboxyarabinitol-P_2 binds tightly to carbamylated Rubisco to form the ECM:carboxyarabinitol-P_2 complex, with a resulting drop in activity (Pierce et al. 1980). By incubating Rubisco with carboxyarabinitol-P_2 and observing the decrease in activity over time, the rate of binding, k_3, can be measured. Like other inhibitors, carboxyarabinitol-P_2 binds in a two-step process, involving an initial rapid equilibrium phase followed by slow isomerisation to form the non-exchangeable complex (Pierce et al. 1980). Data for Rubisco inhibition (v/v_f) versus time (Figure 6.14, Figure 6.15, Figure 6.16, Figure 6.17, Figure 6.18) were fitted to Equation 6.6 to calculate the binding constant (k_{obs}) for each carboxyarabinitol-P_2 concentration. This was then plotted against the carboxyarabinitol-P_2 concentration and fitted to Equation 6.7 to calculate the binding rate (k_3) and inhibition constant (K_i) ($r^2 > 0.905$ for all fits, Table 6.3). It was assumed that $k_4 = 0$, i.e. that binding was irreversible and the rate of inhibitor release was effectively zero. This is supported by the observation that there was a complete abolition of activity after long incubation periods, which has also been observed in other experiments (Pierce et al. 1980). Attempts to fit the data using a non-zero value of k_4 resulted in large error values.

Wild-type and L335V tobacco Rubisco had similar binding rates and inhibition constants, while *Synechococcus* PCC6301 Rubisco had a slightly faster binding rate and slightly higher inhibition constant (Figure 6.19). *G. sulphuraria* Rubisco had a similar binding rate to that of tobacco Rubisco, but the binding constant was nearly 400 times greater (Figure 6.19). His-*Rubrum* Rubisco had a very fast binding rate, with half of the sites occupied after 1 s at a concentration of 1.6 μM carboxyarabinitol-P_2. As a result, it was not possible to measure the binding rate at higher carboxyarabinitol-P_2 concentrations. These results are consistent with the previous observation for the binding of carboxyarabinitol-P_2 to spinach Rubisco (Pierce et al. 1980).

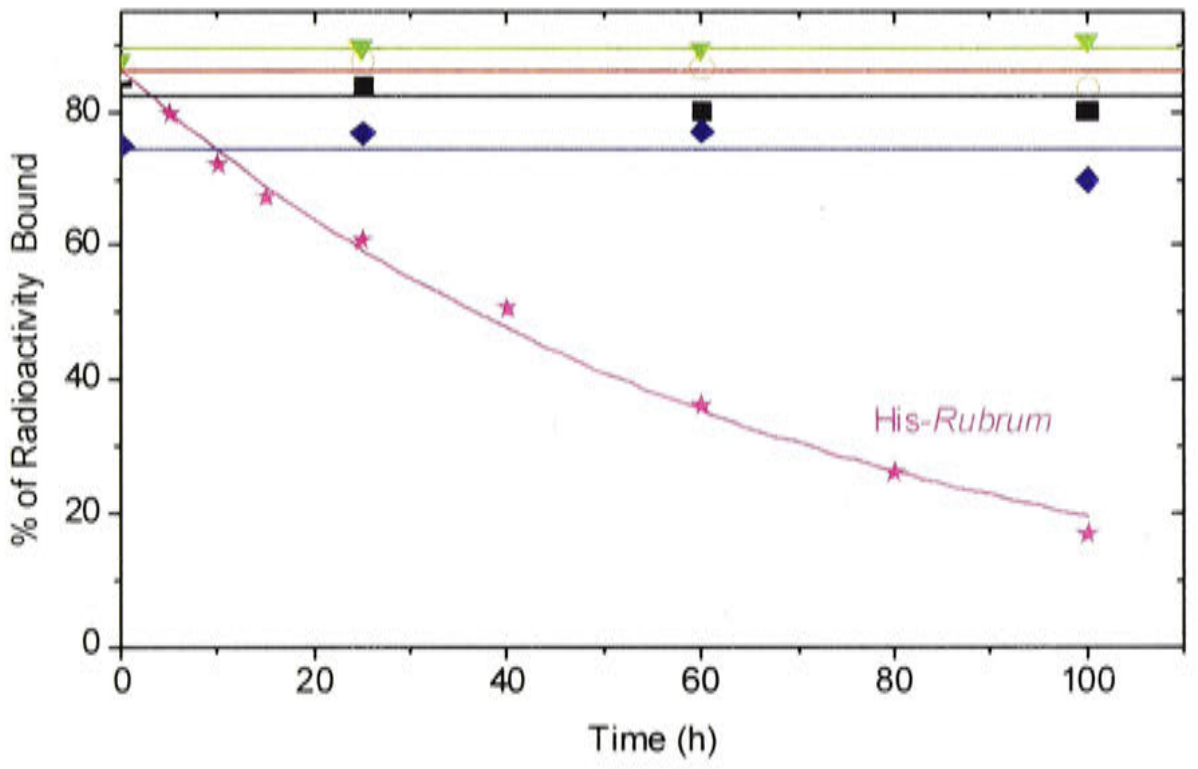

Figure 6.13 Release of Carboxyarabinitol-P_2 from Rubisco

Pre-activated wild-type tobacco (■), L335V tobacco (○), *G. sulphuraria* (▼), *Synechococcus* PCC6301 (◆), and His-*Rubrum* (★) Rubisco incubated with [^{14}C]carboxyarabinitol-P_2. Enzyme-bound radioactivity was separated from unbound radioactivity by gel filtration, and an excess of unlabelled carboxyarabinitol-P_2 was added. At intervals thereafter, samples were taken and the proportion of radioactivity bound to Rubisco was determined by gel filtration. This was fitted to Equation 6.1 to calculate k_{obs}.

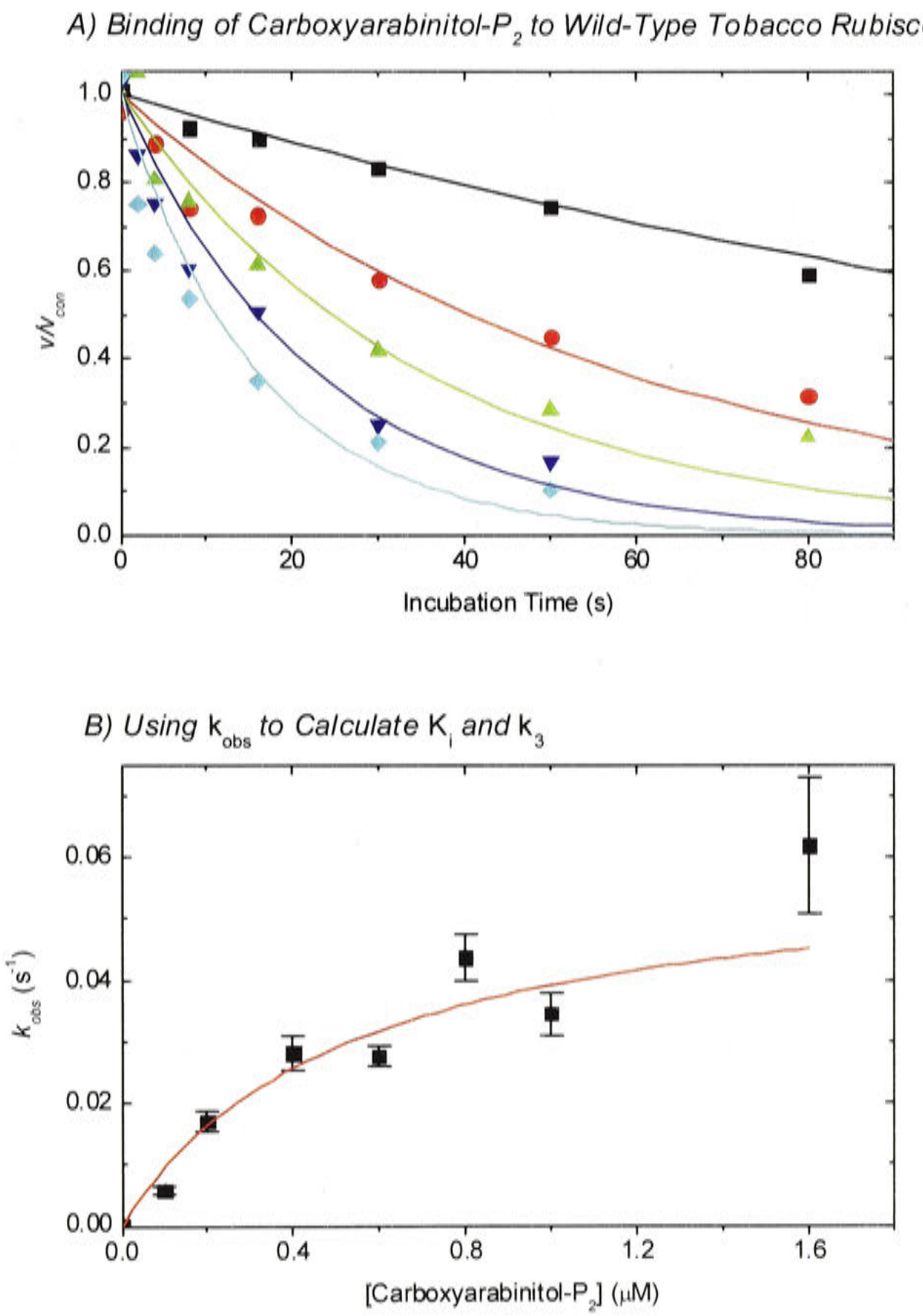

Figure 6.14 Binding of Carboxyarabinitol-P_2 to Wild-Type Tobacco Rubisco

Pre-activated Rubisco was exposed to the indicated concentrations of carboxyarabinitiol-P_2 at zero time (■ 0.1 μM; ● 0.2 μM; ▲ 0.4 μM; ▼ 0.8 μM; ◆ 1.6 μM), and assayed at intervals thereafter (as described in 6.2.6). Equation 6.6 was fitted to the data for each concentration to estimate k_{obs}. These values were plotted against the carboxyarabinitol-P_2 concentration, and Equation 6.7 used to estimate K_i and k_3 (*B*) (Table 6.3).

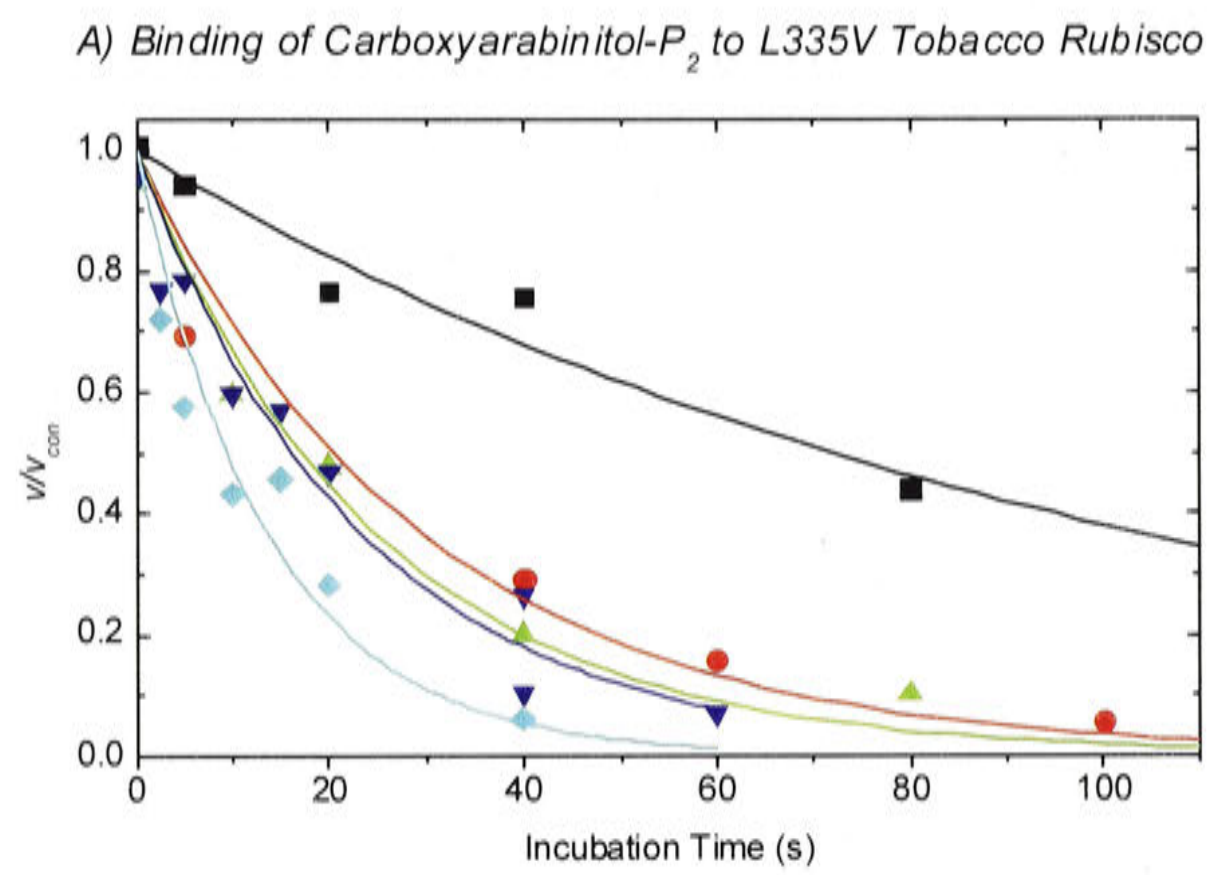

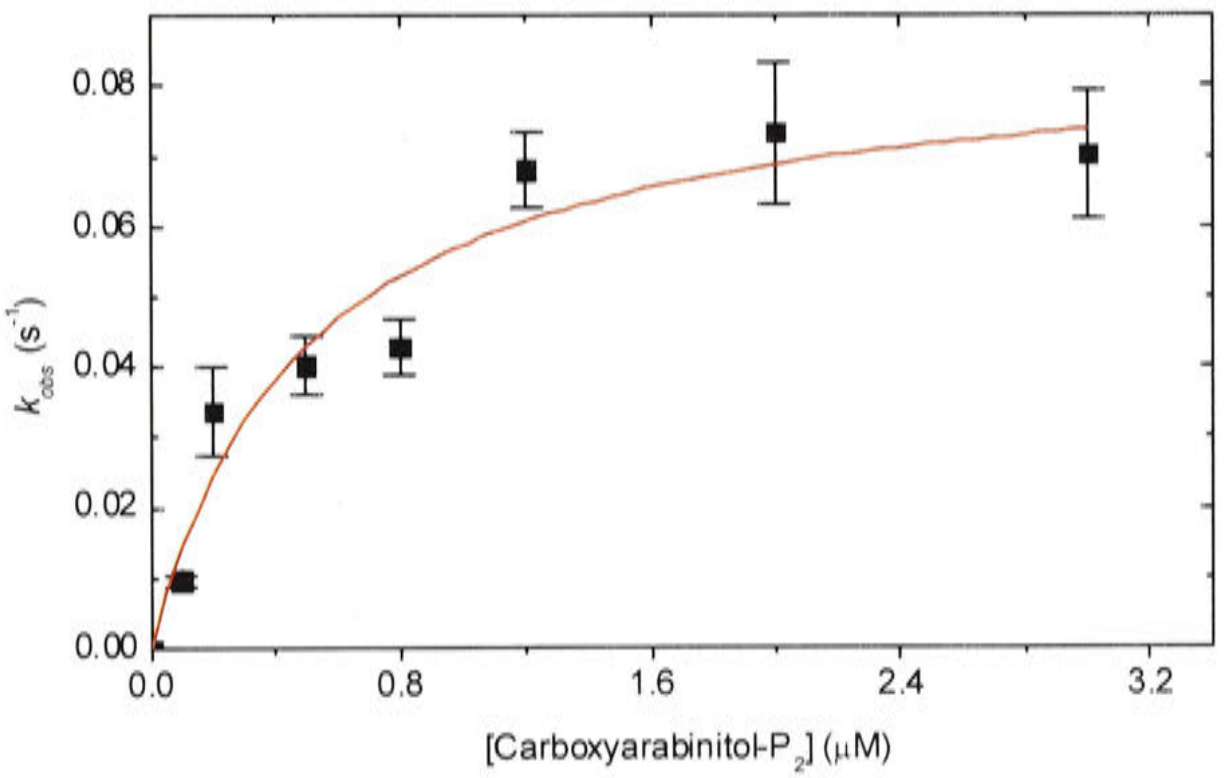

Figure 6.15 Binding of Carboxyarabinitol-P_2 to L335V Tobacco Rubisco

Pre-activated Rubisco was exposed to the indicated concentrations of carboxyarabinitiol-P_2 (■ 0.1 μM; ● 0.2 μM; ▲ 0.5 μM; ▼ 0.8 μM; ◆ 2.0 μM) at zero time, and assayed at intervals thereafter (as described in 6.2.6). Equation 6.6 was fitted to the data for each concentration to estimate k_{obs}. These values were plotted against the carboxyarabinitol-P_2 concentration, and Equation 6.7 used to estimate K_i and k_3 (*B*) (Table 6.3).

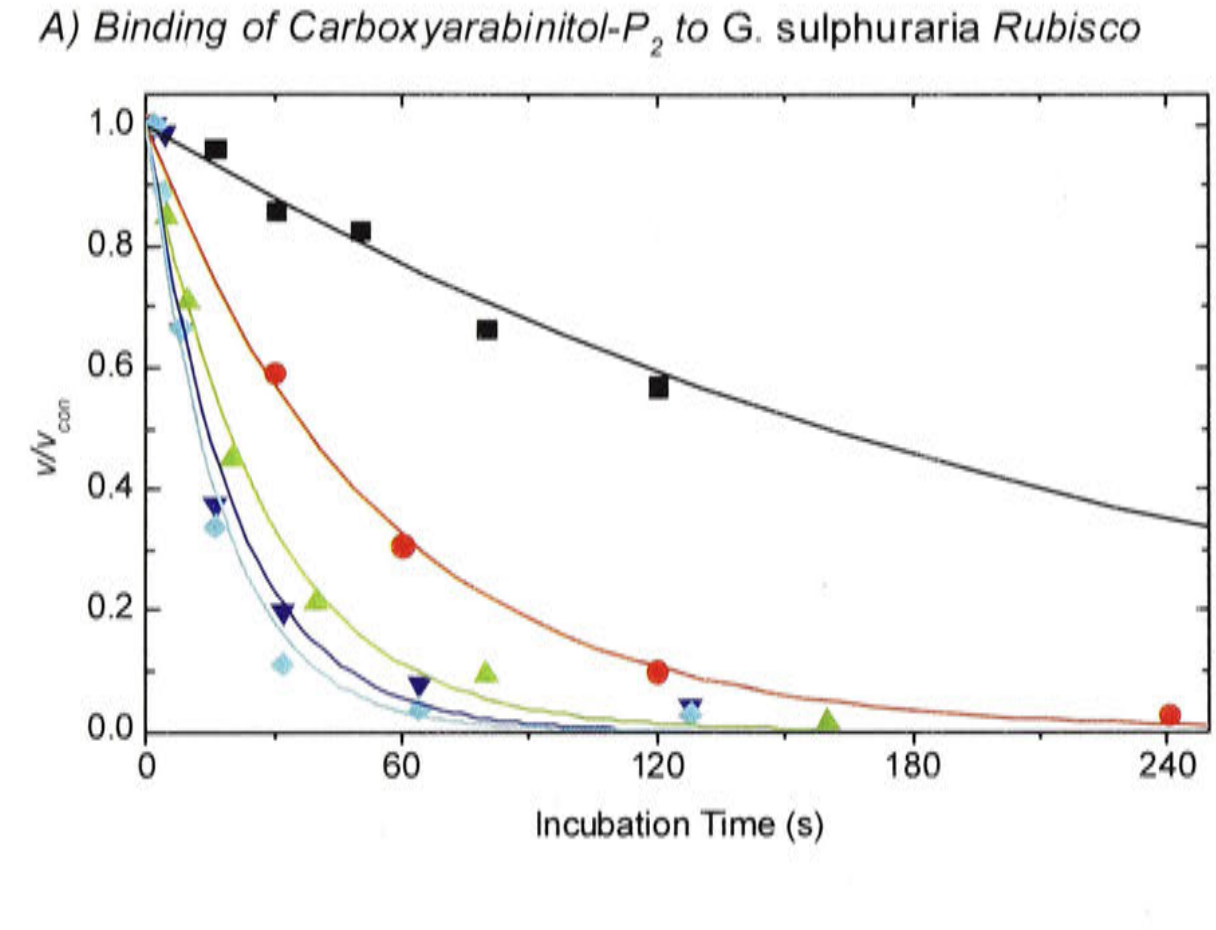

Figure 6.16 Binding of Carboxyarabinitol-P_2 to *G. sulphuraria* Rubisco

Pre-activated Rubisco was exposed to the indicated concentrations of carboxyarabinitiol-P_2 (■ 30 μM; ● 60 μM; ▲ 200 μM; ▼ 300 μM; ◆ 500 μM) at zero time, and assayed at intervals thereafter (as described in 6.2.6). Equation 6.6 was fitted to the data for each concentration to estimate k_{obs}. These values were plotted against the carboxyarabinitol-P_2 concentration, and Equation 6.7 used to estimate K_i and k_3 (*B*) (Table 6.3).

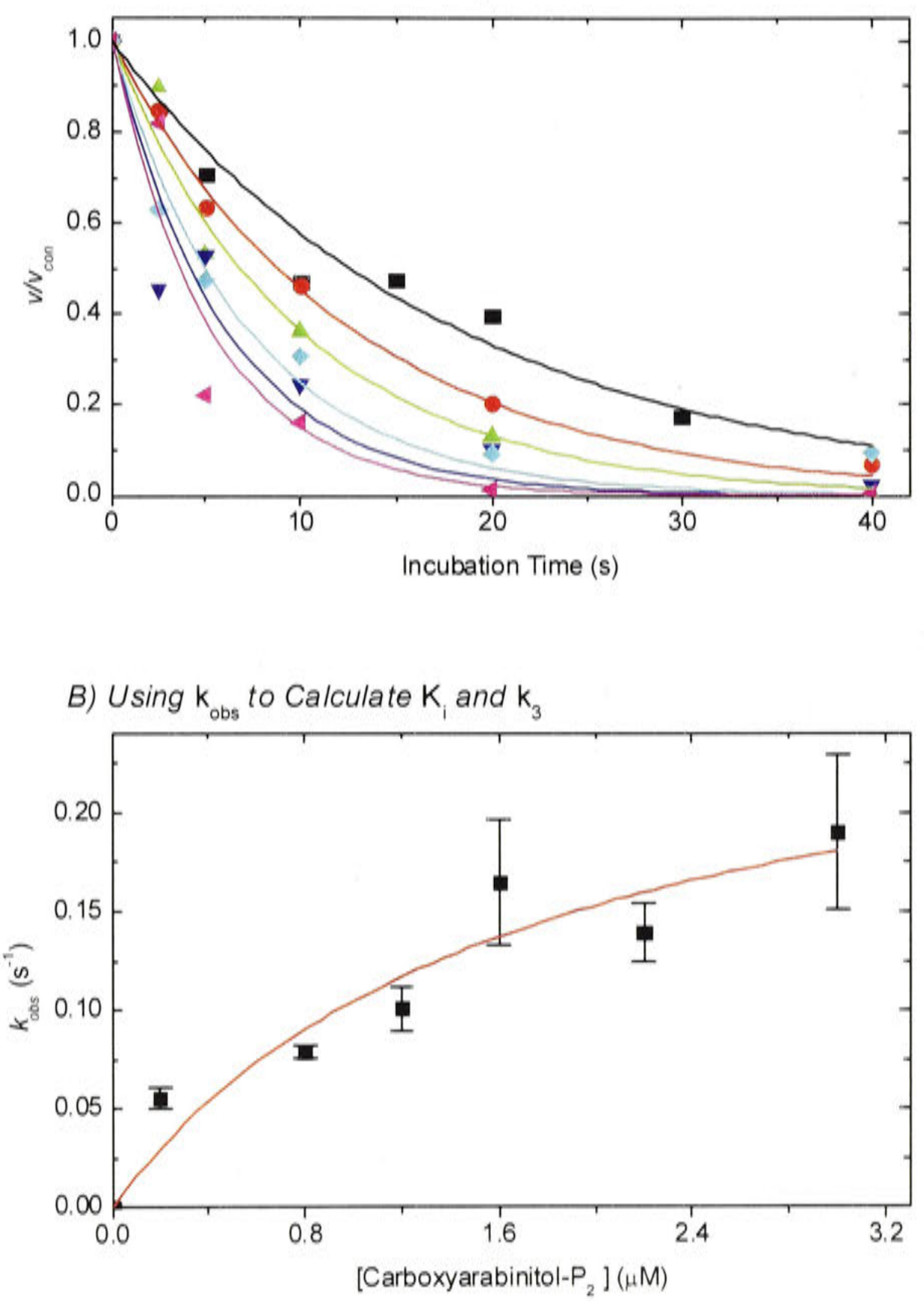

Figure 6.17 Binding of Carboxyarabinitol-P_2 to *Synechococcus* PCC6301 Rubisco

Pre-activated Rubisco was exposed to the indicated concentrations of carboxyarabinitiol-P_2 at zero time (■ 0.2 μM; ● 0.8 μM; ▲ 1.2 μM; ▼ 1.6 μM; ◆ 2.2 μM; ◀ 3.0 μM), and assayed at intervals thereafter (as described in 6.2.6). Equation 6.6 was fitted to the data for each concentration to estimate k_{obs}. These values were plotted against the carboxyarabinitol-P_2 concentration, and Equation 6.7 used to estimate K_i and k_3 (*B*) (Table 6.3).

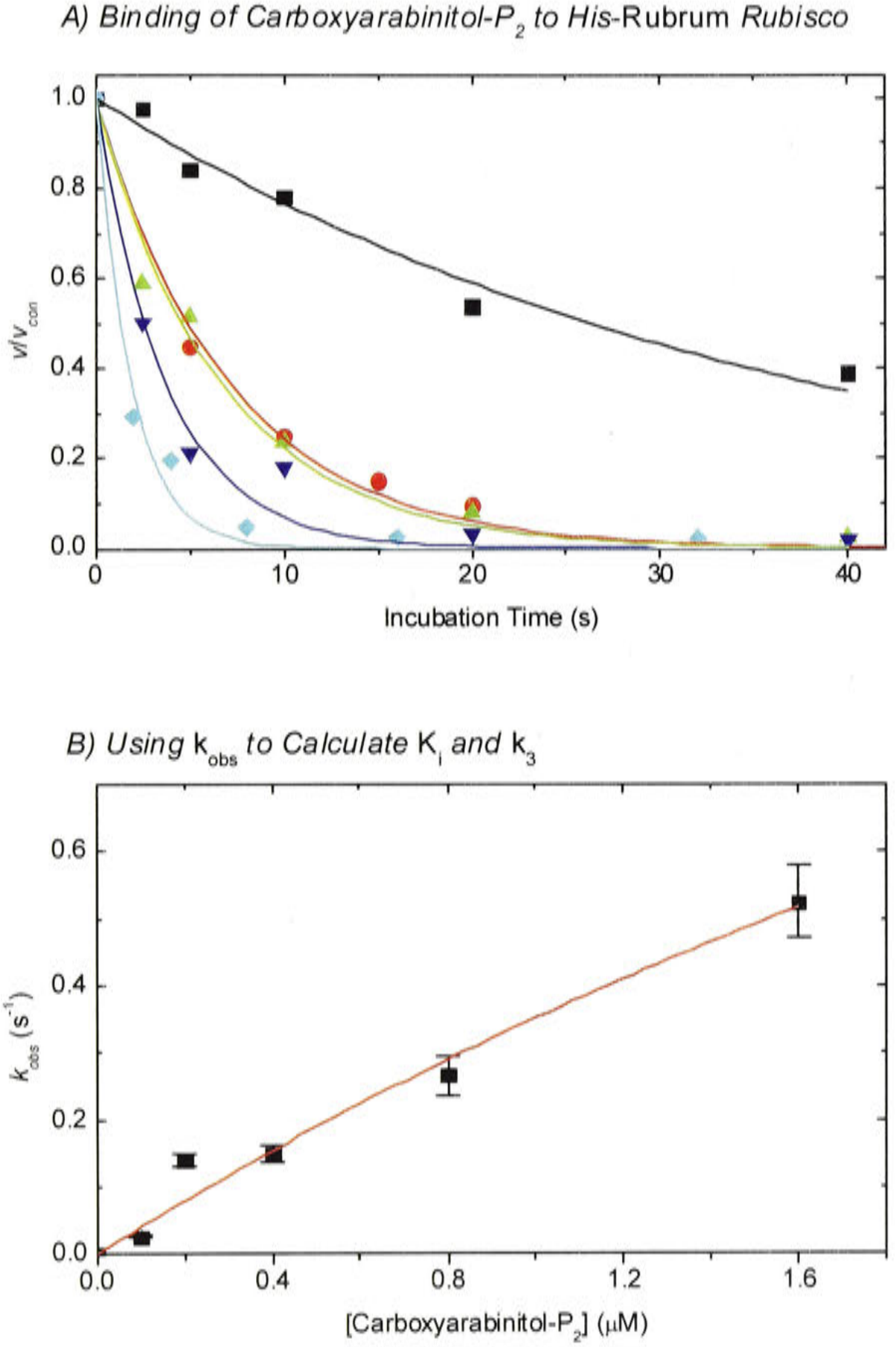

Figure 6.18 Binding of Carboxyarabinitol-P_2 to His-*Rubrum* Rubisco

Pre-activated Rubisco was exposed to the indicated concentrations of carboxyarabinitiol-P_2 at zero time (■ 0.1 μM; ● 0.2 μM; ▲ 0.4 μM; ▼ 0.8 μM; ◆ 1.6 μM), and assayed at intervals thereafter (as described in 6.2.6). Equation 6.6 was fitted to the data for each concentration to estimate k_{obs}. These values were plotted against the carboxyarabinitol-P_2 concentration, and Equation 6.7 used to estimate K_i and k_3 (*B*) (Table 6.3).

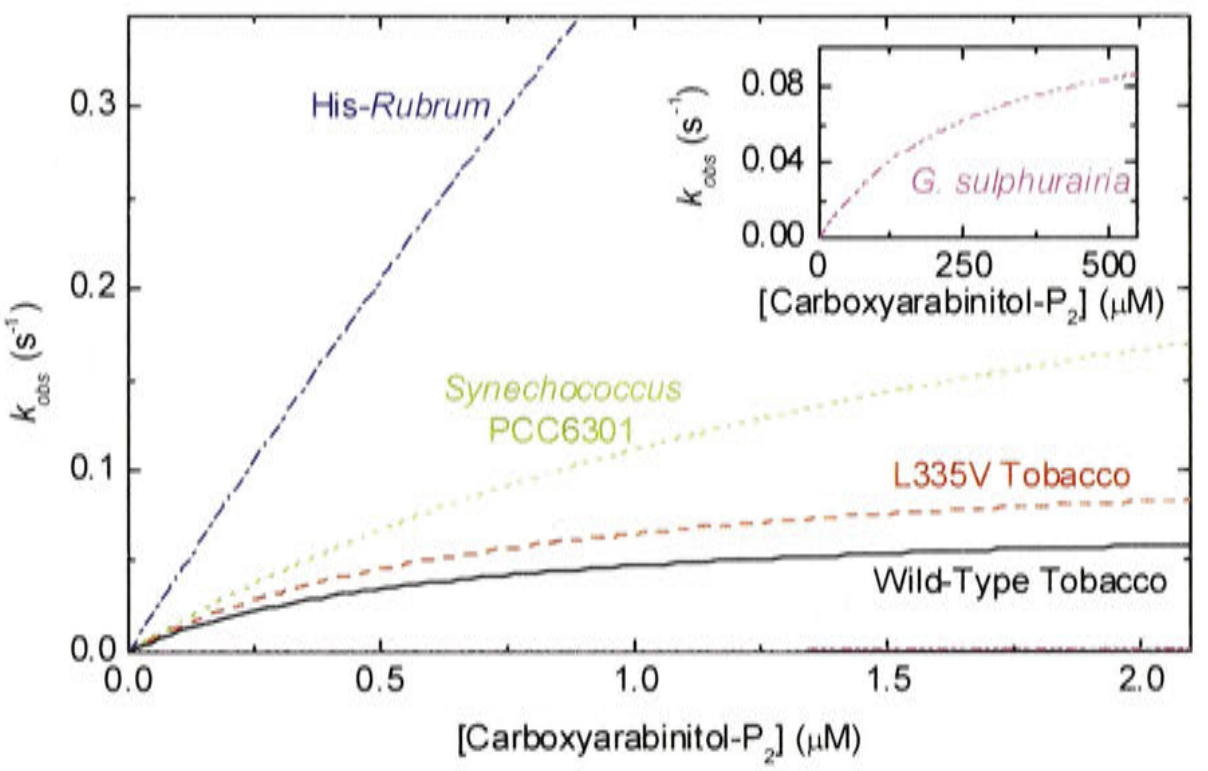

Figure 6.19 Binding of Carboxyarabinitol-P_2 to Rubisco

Pre-activated wild-type tobacco, L335V tobacco, *G. sulphuraria*, *Synechococcus* PCC6301 and His-*Rubrum* Rubisco was exposed to different carboxyarabinitiol-P_2 concentrations and assayed at intervals thereafter (as described in 6.2.6) to estimate k_{obs}. Equation 6.7 was used to estimate K_i and k_4 (Table 6.3).

	K_i (μM)	k_3 (s^{-1})	r^2	k_4 (s^{-1})
Wild-Type Tobacco	0.54 ± 0.33	0.060 ± 0.017	0.9196	$< 10^{-7}$ [b]
L335V Tobacco	0.50 ± 0.17	0.087 ± 0.009	0.9435	$< 10^{-7}$ [b]
G. sulphuraria	220 ± 101	0.086 ± 0.016	0.9050	$< 10^{-7}$ [b]
Synechococcus PCC6301	1.72 ± 1.10	0.28 ± 0.09	0.9093	$< 10^{-7}$ [b]
His-*Rubrum*	> 2[c]	> 1[c]		$4.1 \pm 0.2 \times 10^{-6}$

[a] Goodness of fit value shown for calculating K_i and k_3
[b] No detectable exchange of labelled carboxypentitol-P_2 after 9 days
[c] Rate too fast to measure above 1.6 μM carboxyarabinitol-P_2

Table 6.3 Kinetic Parameters (± S.E.) for the Slow Binding Inhibition of Rubisco by Carboxyarabinitol-P_2.

K_i and k_3 were calculated by fitting Equations 3.2 and 6.7 to the data in Figure 6.14, Figure 6.15, Figure 6.16, Figure 6.17, and Figure 6.18. k_4 was calculated by fitting Equation 6.1 to the data in Figure 6.13.

6.3.9 Release of Carboxyarabinitol-1-P from the ECM:Carboxyarabinitol-1-P Complex

Carboxyarabinitol-1-P can bind to the carbamylated form of Rubisco to form the ECM:carboxyarabinitol-1-P complex. The dissociation of carboxyarabinitol-1-P from this complex was measured by adding a small aliquot of the ECM:carboxyarabinitol-1-P complex to a spectrophotometric assay and monitoring the increase in activity. Adding a small aliquot reduces the concentration of carboxyarabinitol-1-P around the enzyme, and the high ribulose-P_2 concentration in the assay reduces the rate of inhibitor binding. The data was fitted to Equation 6.7, which showed a good approximation to the data (r^2 > 0.999 for all fits).

During the assay, the activity increased over time, after initially showing negligible activity (Figure 6.20, Figure 6.21). The release of carboxyarabinitol-1-P was faster for His-*Rubrum* Rubisco, followed by *Synechococcus* PCC6301, wild-type and tobacco Rubisco, which had similar rates, and *G. sulphuraria* Rubisco, which had the slowest activation rate (Table 6.4). Activation was less than complete, with *G. sulphuraria* Rubisco regaining only 20 % of the control activity (in the absence of carboxyarabinitol-1-P), and other Rubisco enzymes regaining 80 % of the control activity. Lack of full activation may be due to inhibition by the low levels of carboxyarabinitol-1-P (0.1 μM) that are carried over into the spectrophotometric assay with the enzyme to initiate the assay, as previous experiments have shown a K_i of 0.8 μM for the competitive inhibition of *Phaseolus vulgaris* Rubisco by carboxyarabinitol-1-P (Seemann et al. 1985). These experiments also showed that the inhibitor binds to the carbamylated form of the enzyme (Seemann et al. 1985), suggesting that residual inhibition was not due to the formation of an E:carboxyarabinitol-1-P complex.

Carboxyarabinitol-1-P appeared to be released from the carbamylated wild-type and L335V tobacco and His-*Rubrum* Rubisco enzymes at a similar rate to the release of ribulose-P_2 from the decarbamylated forms of the enzyme (Table 6.1 and Table 6.4). *Synechococcus* PCC6301 Rubisco released carboxyarabinitol-1-P slower than it released ribulose-P_2, while *G. sulphuraria* had a faster rate of release of carboxyarabinitol-1-P than for xylulose-P_2 or ribulose-P_2.

6.3.10 Binding of Carboxyarabinitol-1-P to Rubisco

Preliminary work was also carried out that investigated the binding of carboxyarabinitol-1-P to the carbamylated form of Rubisco. Incubation of the enzyme

with carboxyarabinitol-1-P resulted in the formation of the ECM:carboxyarabinitol-1-P complex, and the extent of inhibition increased as the inhibitor concentration was increased (Figure 6.22), due to a higher proportion of the enzyme being present as the ECM:carboxyarabinitol-1-P complex.

The degree of inhibition could be used to estimate the parameters for the rate of binding (k_3) and inhibition constant (K_i) using Equations 6.7 and 6.8, which describe slow, tight binding, and assuming that the value for activation of the ECM:carboxyarabinitol-1-P complex (k_{obs}) calculated in Section 6.3.9 was equal to the value for inhibitor release (k_4) and that the rate of uninhibited enzyme (v_{con}) was equivalent to the initial enzyme activity (v_i). There was a high degree of error in the parameter estimates (Table 6.4), due to the interdependency of the k_3 and k_4 values in the model, and a large amount of variation in the data.

Nevertheless, there are general trends apparent in the data. Wild-type and L335V tobacco Rubisco showed similar degrees of inhibition by carboxyarabinitol-1-P, while His-*Rubrum* Rubisco showed negligible inhibition. Rubisco from *G. sulphuraria* exhibited some inhibition, but the extent was limited by having a higher value for K_i, which is consistent with the higher K_i values for carboxyarabinitol-P_2 and xylulose-P_2. *Synechococcus* PCC6301 Rubisco also showed some inhibition, but the extent may be limited by the higher rate of release, relative to the rate of inhibitor binding.

	K_i (μM)[a]	k_3 (s^{-1}) [a]	r^2 [b]	k_4 (s^{-1}) [c]
Wild-Type Tobacco	1.3 ± 1.0	19.5 ± 8.8 x 10^{-3}	0.924	2.8 ± 0.1 x 10^{-3}
L335V Tobacco	3.4 ± 2.3	28.5 ± 10.1 x 10^{-3}	0.973	2.3 ± 0.1 x 10^{-3}
G. sulphuraria	250 ± 200	200 ± 200 x 10^{-3}	0.756	0.8 ± 0.1 x 10^{-3}
Synechococcus PCC6301	8.8 ± 8.0	4.2 ± 4.1 x 10^{-3}	0.879	8.3 ± 0.1 x 10^{-3}
His-*Rubrum*	ND [d]	ND		19.4 ± 0.2 x 10^{-3}

[a] Calculated by fitting Equations 6.7 and 6.8 to the data in Figure 6.22, and estimates for k_4
[b] Goodness of fit value shown for calculating K_i and k_3
[c] Assumes that k_4 is equal to the observed k_{obs} for ECM:carboxyarabinitol-1-P activation
[d] Could not be measured from data

Table 6.4 Kinetic Parameters (± S.E.) for the Slow Binding Inhibition of Rubisco by Carboxyarabinitol-1-P (Preliminary Results).

Values for k_4 were calculated from the data in Figure 6.20 and Figure 6.21 using Equation 6.6 and assuming that k_4 is equal to the observed k_{obs} value. Parameters for K_i and k_3 were calculated by fitting Equations 6.7 and 6.8 to the data in Figure 6.22.

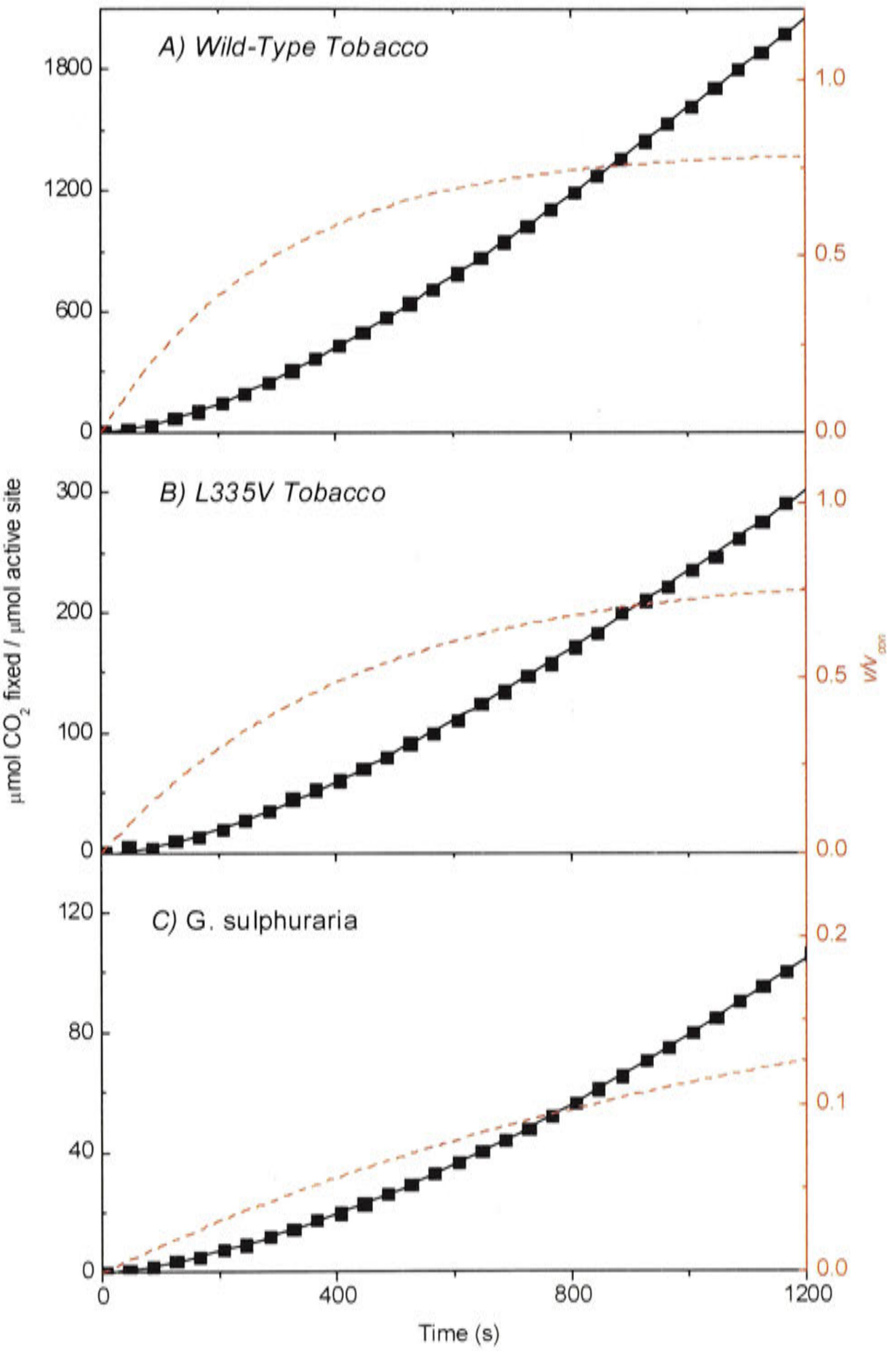

Figure 6.20 Activation of the Tobacco and *G. sulphuraria* ECM:Carboxyarabinitol-1-P Complex

Carbamylated wild-type tobacco (*A*), L335V tobacco (*B*) and *G. sulphuraria* (*C*) Rubisco enzymes were incubated with carboxyarabinitol-1-P to form the ECM:carboxyarabinitol-1-P complex, which was used to initiate spectrophotometric assays, as described in Section 6.2.7. The data for product accumulation (left ordinate, every eighth 5-s data point shown) were fitted to Equation 3.1 (solid lines) and the values for v_f and k_{obs} were estimated (Table 6.4). Using these estimates, curves for the proportion of the non-inhibited activity (right ordinate, - -) as a function of time were plotted using Equation 6.6.

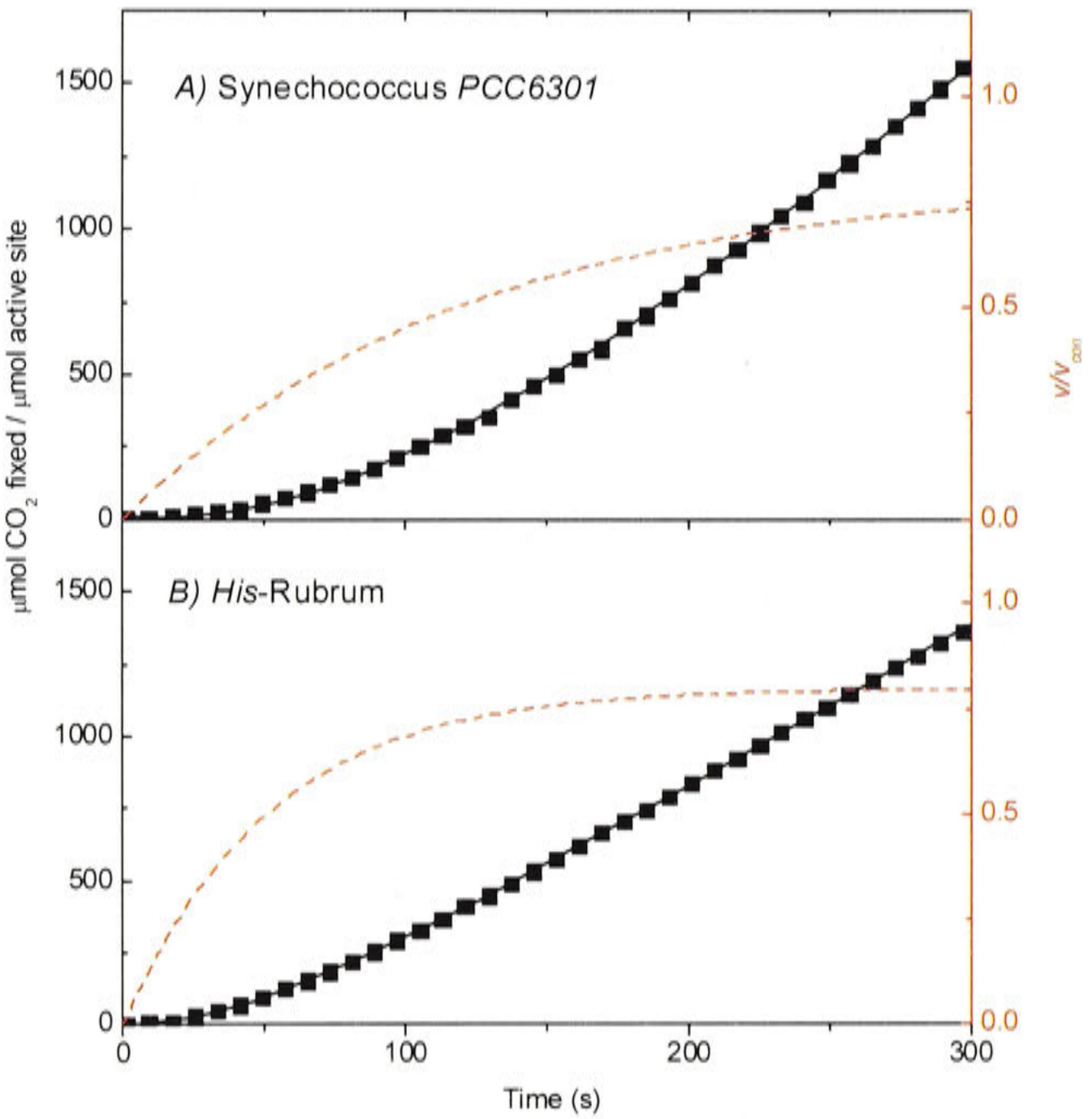

Figure 6.21 Activation of the *Synechococcus* PCC6301 and His-*Rubrum* ECM:Carboxyarabinitol-1-P Complex

Carbamylated *Synechococcus* PCC6301 (*A*) His-*Rubrum* (*B*) Rubisco enzymes were incubated with carboxyarabinitol-1-P to form the ECM:carboxyarabinitol-1-P complex, which was used to initiate spectrophotometric assays, as described in Section 6.2.7. The data for product accumulation (left ordinate, every eighth 1-s data point shown) were fitted to Equation 3.1 (solid lines) and the values for v_f and k_{obs} were estimated (Table 6.4). Using these estimates, curves for the proportion of the non-inhibited activity (right ordinate, - -) as a function of time were plotted using Equation 6.6.

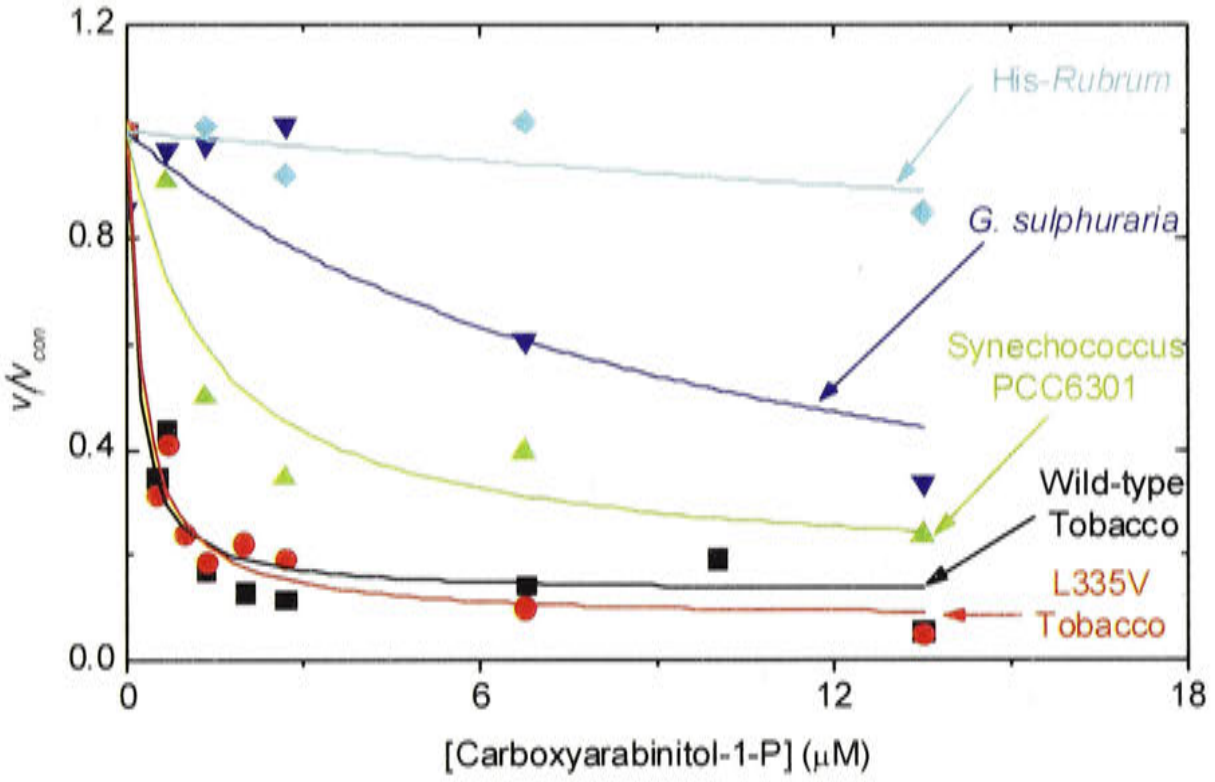

Figure 6.22 Binding of Carboxyarabinitol-1-P to Carbamylated Rubisco

Pre-activated wild-type tobacco (■), L335V tobacco (●), *G. sulphuraria* (▼), *Synechococcus* PCC6301 (▲), and His-*Rubrum* (◆) Rubisco were exposed to carboxyarabinitol-1-P for 60 min before assaying activity. The residual activity (v_f) is plotted as a proportion of the activity seen in controls lacking carboxyarabinitol-1-P (v_{con}). The solid lines are drawn according to Equations 6.7 and 6.8 using the parameter estimates in Table 6.4, with the assumption that $v_{con} = v_i$.

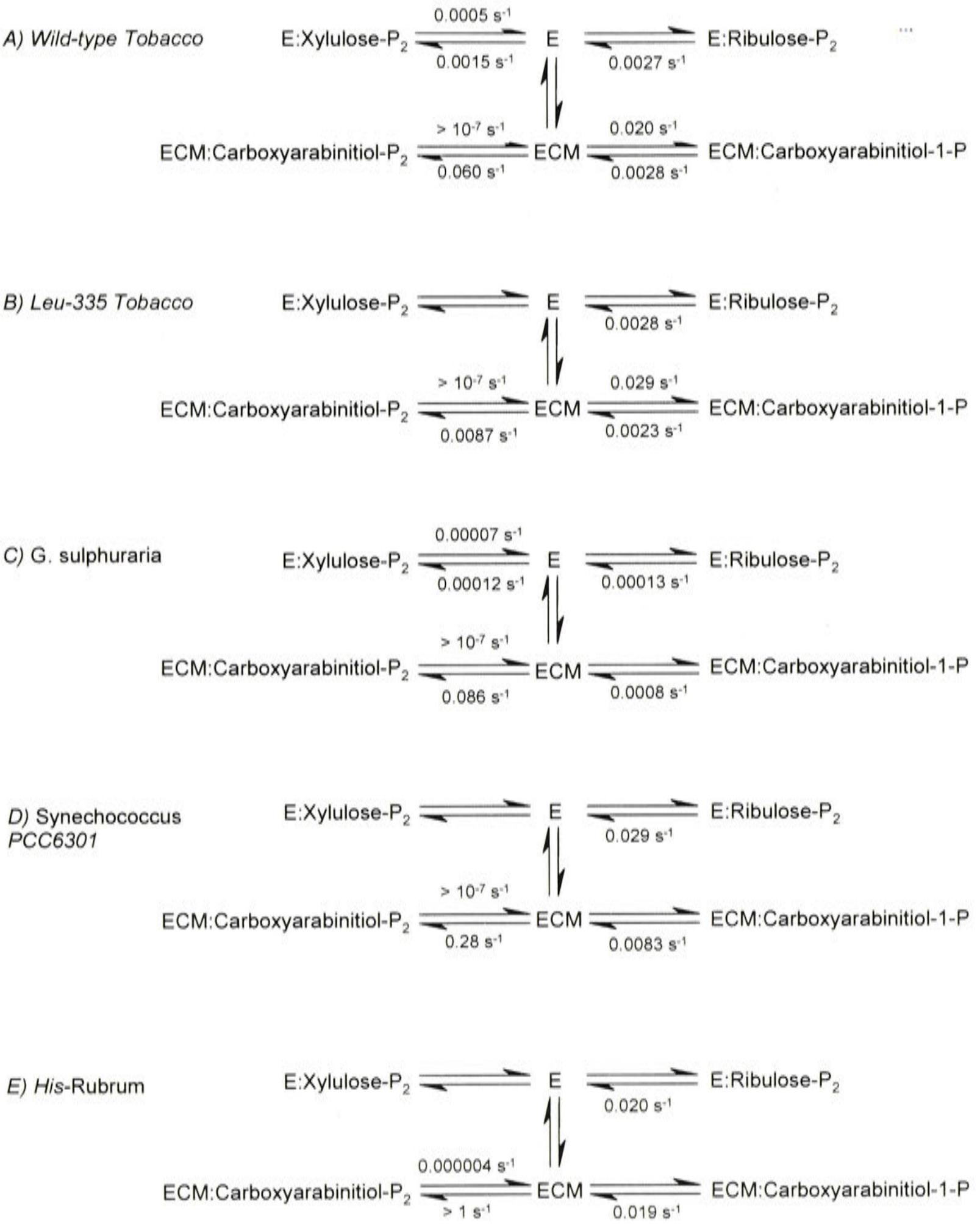

Figure 6.23 Summary of Ligand Binding and Release Rates

The kinetic parameters for the binding and release of ligands (where known) is indicated, with data from Table 6.1, Table 6.2, Table 6.3 and Table 6.4.

6.4 Discussion

Like the variations observed in catalytic parameters for Rubisco enzymes from different groups, there is extensive variation in the binding and release of inhibitors for different Rubisco enzymes, as shown in Figure 6.23. Inhibitors can bind tightly to some forms of the enzyme, but not to others, and the strength of these interactions is likely to be determined by how closely the inhibitors resemble intermediates of catalysis. The exact trigger for closure of the loop 6 region over the active site is not known, but it is thought to involve the distance between the terminal phosphate groups of the ligand (Duff et al. 2000). When a ligand binds to the active site, the inter-phosphate distance is shortened by the curved conformation of the ligand around the metal ion or charged groups in the metal binding site if the ion is absent. This shortening of the inter-phosphate distance triggers loop closure, and loop opening is normally triggered by the cleavage of the ribulose-P_2, which increases the inter-phosphate distance. Closure of loop 6 over the active site is important in excluding solvent from the active site, and is accompanied by an ordering of the C-terminal and N-terminal regions (Schreuder et al. 1993a). A tight binding inhibitor is more likely to trigger the closure of loop 6 over the active site, and so the tightness of binding provides an insight into how well the loop 6 region is maintained in an ordered state rather than a disordered, open state.

6.4.1 Xylulose-P_2 Competitively Inhibits Carbamylated Rubisco

Xylulose-P_2 has a similar structure to that of ribulose-P_2, and can act as a rapid equilibrium inhibitor that competes with ribulose-P_2 for the active site. The inhibitor binds loosely to the active site of carbamylated Rubisco, and does not involve the slow conformational change of the enzyme that occurs during slow, tight binding. While L335V tobacco and His-*Rubrum* Rubisco had a K_i value that was similar to the K_m for ribulose-P_2, wild-type tobacco, *Synechococcus* PCC6301 and *G. sulphuraria* Rubisco had a K_i that was less than the K_m. These results suggest that the affinity of the active site is similar for the two isomers, but Rubisco enzymes from wild-type tobacco, *Synechococcus* PCC6301 and *G. sulphuraria* have a higher affinity for xylulose-P_2 than for ribulose-P_2.

6.4.2 Release of Inhibitors from Uncarbamylated Rubisco

Ribulose-P_2 and xylulose-P_2 can act as slow, tight-binding inhibitors of uncarbamylated Rubisco. When decarbamylated Rubisco was added to assay conditions containing saturating levels of Mg^{2+}, CO_2 and ribulose-P_2, there was initially little

activity, but the activity increased over time. This was due to a faster binding of ribulose-P_2 to the decarbamylated active site than the rate of CO_2 and Mg^{2+} activation. As ribulose-P_2 was released from the active site, CO_2 and Mg^{2+} were able to access the active site and activate the enzyme, resulting in an increase in activity. There was negligible difference of preincubation of the decarbamylated enzyme with ribulose-P_2 prior to the assay, suggesting the there is a rapid binding of ribulose-P_2 as soon as the enzyme was exposed to the saturating ribulose-P_2 concentrations in the assay.

Rubisco from *Synechococcus* PCC6301 and His-*Rubrum* showed fast activation of the E:ribulose-P_2 complex, with full activity restored within minutes due to the rapid release of ribulose-P_2 from the E:ribulose-P_2 complex. Activation of the E:xylulose-P_2 complex followed a similar pattern, suggesting that xylulose-P_2 or ribulose-P_2 may bind to the active site with a similar affinity. Since structural studies have shown that loop 6 can close over the *Synechococcus* PCC6301 active site bound to xylulose-P_2 (Newman and Gutteridge 1993), it is likely that the enzyme can undergo a conformational change, however closure of loop 6 over the active site does not appear to be strongly maintained in an ordered state, and can be rapidly disordered to release the ligand. The activation observed is due to the release of xylulose-P_2 or ribulose-P_2 from the active site, followed by competition between binding of ribulose-P_2 to the uncarbamylated active site and the activation of the active site by CO_2 and Mg^{2+}.

Wild-type and L335V tobacco Rubisco exhibited a similar rate of activation, which was slower than *Synechococcus* PCC6301 and His-*Rubrum* Rubisco. For wild-type tobacco Rubisco, the rate of xylulose-P_2 release was slower than the release of ribulose-P_2 (Figure 6.2A), whereas L335V tobacco Rubisco did not show additional inhibition by xylulose-P_2 (Figure 6.2B). The mutation of residue 335 from leucine to valine in tobacco Rubisco appears to have prevented the tight binding of xylulose-P_2 to the active site, and the observed inhibition is due to the rapid release of xylulose-P_2 from the active site followed by competition between binding of ribulose-P_2 to the uncarbamylated active site and the activation of the active site by CO_2 and Mg^{2+}.

Release of ribulose-P_2 and xylulose-P_2 from *G. sulphuraria* Rubisco was much slower than for tobacco Rubisco, taking several hours for full activation to occur. This required gel filtration to remove all unbound inhibitors before activation would occur. Ribulose-P_2 was released faster than xylulose-P_2, showing that xylulose-P_2 binds more tightly to the decarbamylated enzyme than ribulose-P_2 does.

The tighter binding of ligands to *G. sulphuraria* Rubisco is likely to be the result of greater stabilisation of the loop 6 region. Structural studies have shown that the closure of loop 6 in *G. partita* is accompanied by a unique hydrogen-bond between loop 6 and the large subunit (Okano et al. 2002). This hydrogen bond would be expected to stabilise the closure of loop 6, and assist in maintaining loop 6 and the C-terminus and N-terminus in an ordered state, preventing the release of the inhibitor.

6.4.3 Slow, Tight Binding of Xylulose-P_2 to Rubisco

The observation that xylulose-P_2 bound tightly to uncarbamylated wild-type tobacco and *G. sulphuraria* Rubisco suggested that slow, tight binding of xylulose-P_2 to Rubisco was taking place to a greater extent than for the binding of ribulose-P_2. This was confirmed by incubating activated Rubisco with increasing concentrations of xylulose-P_2. While L335V Tobacco, *Synechococcus* PCC6301 and *His-Rubrum* Rubisco showed only competitive, rapid equilibrium, inhibition by xylulose-P_2, wild-type tobacco and *G. sulphuraria* Rubisco showed a greater decrease in activity than that expected for purely competitive inhibition, due to a second, slow isomerisation state that further inhibits the enzyme.

Slow binding of xylulose-P_2 to Rubisco involves an isomerisation step as loop 6 becomes ordered over the active site. The rate of binding was measured by incubating wild-type Rubisco with xylulose-P_2 and monitoring the drop in activity over time; the data could be modelled using equations describing classic two-step, slow isomerisation inhibition (Morrison 1982).

Saturation of the xylulose-P_2 binding rate for wild-type tobacco Rubisco is consistent with the models for slow, tight binding, in which the rate of binding reaches an upper limit (Figure 6.1). This occurs when inhibitor binding is limited by the rate of conformational change, rather than the inhibitor concentration. For rapid equilibrium inhibition, the rate of binding is directly proportional to the inhibitor concentration, and will effectively increase in a linear manner.

It is not known if the slow rate of xylulose-P_2 binding is due to the tighter binding of xylulose-P_2 to uncarbamylated sites than to activated sites. The observed binding rate assumes that there is a spontaneous release of Mg^{2+} and the carbamate by Rubisco, and that xylulose-P_2 then preferentially binds to the uncarbamylated sites. The reduced binding of xylulose-P_2 to *G. sulphuraria* Rubisco may be due to the low $K_c.K_{Mg}$ exhibited by the enzyme (Saska 2001), which reduces the amount of decarbamylated Rubisco that is available to bind to xylulose-P_2.

Structural studies show that xylulose-P_2 binds as a C-2 diol to the uncarbamylated form of *Synechococcus* PCC6301 and spinach Rubisco, and that inhibitor binding is accompanied by the closure of loop 6 over the active site (Newman and Gutteridge 1994; Taylor et al. 1996). Xylulose-P_2 is a C-3 epimer of ribulose-P_2, and binds with the C-3 hydroxyl in a similar position to that of the C-3 hydroxyl of carboxyarabinitol-P_2 or ribulose-P_2. As there is different stereochemistry with xylulose-P_2 compared with ribulose-P_2, this configuration can only be achieved with a considerable distortion of the metal binding site. O-3 and one of the C-2 diol oxygen molecules form interactions with Glu-204 and Asp-203, which would not be possible in the presence of Mg^{2+}, and would not allow closure of loop 6 (Taylor et al. 1996). Hence while xylulose-P_2 is a rapid equilibrium binding inhibitor of both carbamylated and uncarbamylated forms of the enzyme, the second step of slow, tight binding inhibition, which involves a conformational change, only occurs with the decarbamylated form of the enzyme. It also appears that xylulose-P_2 is much more adept than ribulose-P_2 at maintaining loop 6 in an ordered state for Rubisco from wild-type tobacco and *G. sulphuraria*. The mutation of Leu-335 of tobacco Rubisco alters the interactions of loop 6 with xylulose-P_2 bound to the uncarbamylated enzyme, and prevents the conformational change associated with slow, tight binding inhibition.

6.4.4 Carboxyarabinitol-P_2 Binds Very Tightly to Rubisco

Carboxyarabinitol-P_2 binds to the activated form of Rubisco, inducing the closure of loop 6 over the active site (Lundqvist and Schneider 1989b; Newman and Gutteridge 1993; Schreuder et al. 1993a; Andersson 1996). Binding occurs with O-2 and O-3 in the *cis* conformation, with carboxyarabinitol-P_2 providing three ligands to the Mg^{2+} ion. This structure is analogous to the 6-carbon intermediate, 3-keto-2-carboxyarabinitol-P_2, but has a hydroxyl group at C-3.

While carboxyarabinitol-P_2 does not occur naturally *in vivo*, it has a similar structure to that of carboxytetritol-P_2, which has been observed to be produced by some mutant enzymes, and by His-*Rubrum* Rubisco. Unfortunately there are currently no protocols available for the synthesis of carboxytetritol-P_2, however inferences may be made between the binding of carboxytetritol-P_2 and the binding of carboxyarabinitol-P_2 to different Rubisco enzymes.

Binding of carboxyarabinitol-P_2 to wild-type and L335V tobacco, *G. sulphuraria* and *Synechococcus* PCC6301 Rubisco was virtually irreversible, with no exchange observed after a week. His-*Rubrum* Rubisco had a detectable release of

carboxyarabinitol-P_2, with a half-time of 2 days, which was still several orders of magnitude slower than the release of ribulose-P_2.

The binding of carboxyarabinitol-P_2 to Rubisco fitted slow binding models well, giving an indication of the binding rate and binding affinity for each enzyme. Tobacco, *G. sulphuraria* and *Synechococcus* PCC6301 Rubisco had similar rates of binding, although *G. sulphuraria* Rubisco had a binding constant that was higher than for other Rubisco enzymes. His-*Rubrum* Rubisco had a rapid binding rate that was too fast to be measured, but was at least ten-fold faster than other Rubisco enzymes. Unlike the inhibition by xylulose-P_2 and ribulose-P_2, in which some activity remained at saturating inhibitor concentrations, inhibition of Rubisco by carboxyarabinitol-P_2 was effectively complete at high inhibitor concentrations. This is due to the rate of carboxyarabinitol-P_2 binding being several orders of magnitude higher than the rate of release, which effectively reduces Equations 6.7 and 6.8 to $v_f/v_i=0$.

6.4.5 Carboxyarabinitol-1-P Inhibits Rubisco

Like carboxyarabinitol-P_2, carboxyarabinitol-1-P inhibits Rubisco by binding to the carbamylated form of the enzyme. Preliminary experiments showed that carboxyarabinitol-1-P could bind tightly to Rubisco from wild-type and L335V tobacco, *G. sulphuraria*, and *Synechococcus* PCC6301. Release of the inhibitor from the enzyme occurred at a similar rate for wild-type and L335V tobacco Rubisco, showing that the mutation did not affect the binding of carboxyarabinitol-1-P to the active site. Activation of the ECM:carboxyarabinitol-1-P complex also occurred at a similar rate to the activation of E:ribulose-P_2 complex, suggesting that the inhibitors have a similar affinity for the active site. Carboxyarabinitol-1-P was released from the ECM:carboxyarabinitol-1-P complex of *Synechococcus* PCC6301 Rubisco slower than ribulose-P_2 was released from the E:ribulose-P_2 complex, showing that *Synechococcus* PCC6301 Rubisco is able to bind carboxyarabinitol-1-P more tightly than ribulose-P_2. For *G. sulphuraria* Rubisco, dissociation of the ECM:carboxyarabinitol-1-P complex was faster than the dissociation of the E:ribulose-P_2 complex, because the carboxyarabinitol-1-P binds to the active site less tightly than ribulose-P_2.

Carboxyarabinitol-1-P acts as an inhibitor by mimicking the carboxyketone intermediate compound that is formed during catalysis. The main differences between the inhibitor and the intermediate structure are the lack of the P-5 phosphate group, and presence of a hydroxyl group at C-3 instead of a ketone. Sufficient homology exists between the two structures to trigger closure of loop 6 over the inhibitor for most

Rubisco enzymes, although maintaining the loop in a closed state occurs at different levels for the different Rubisco enzymes, depending on the stability of the ECM:carboxyarabinitol-1-P complex.

6.4.6 Slow Binding Inhibition of Rubisco

As noted previously, most inhibitors of Rubisco are structurally similar to the substrate or to intermediates of catalysis. Many molecules that mimic reaction intermediates are slow, tight binding inhibitors, in which the rapid equilibrium binding is followed by a slow step that involves a conformational change (Schloss 1988b). In Rubisco, this conformational change is accompanied by the closure of loop 6 over the active site that is triggered by a shortening of the inter-phosphate distance as the ligand binds to the active site (Duff et al. 2000).

Ribulose-P_2, the substrate for Rubisco, may act as a slow, tight binding inhibitor of the uncarbamylated enzyme, which is slowly released over time. A prolonged time taken for the recovery of activity for the inhibited enzyme would suggest a degree of slow, tight binding inhibition. This is evident in the long activation time of *G. sulphuraria* Rubisco (half-activation time of 90 min), and also in the activation time of wild-type and Leu-335 tobacco Rubisco (half-activation time of 5 min). Slow, tight binding inhibition of *Synechococcus* PCC6301 and His-*Rubrum* Rubisco is less apparent, and it is possible that the delay is due to inhibition that does not involve a conformational change in the enzyme. While the structure of uncarbamylated spinach Rubisco coordinated with ribulose-P_2 shows a closed loop (Taylor and Andersson 1997b), showing that a conformational change can occur, there is currently little structural data available for other enzymes.

Xylulose-P_2 is a competitive inhibitor of activated Rubisco and is a slow binding inhibitor of uncarbamylated wild-type tobacco and *G. sulphuraria* Rubisco. The stereochemistry of the active site prevents the loop closing over xylulose-P_2 in the active site of activated enzyme. While structural studies have shown that the loop can close over xylulose-P_2 bound to uncarbamylated *Synechococcus* PCC6301 enzyme (Newman and Gutteridge 1994), this does not appear to be sufficient to cause sustained tight binding, as negligible inhibition was observed for the enzyme. The substitution of Leu-335 for valine in tobacco Rubisco was sufficient to prevent xylulose-P_2 acting as a tight binding inhibitor, most likely due to the altered interactions of loop 6 with the ligand.

Inhibition by xylulose-P_2 and carboxyarabinitol-1-P was not complete, with some activity remaining at saturating concentrations. This subsaturating level of inhibition has also been observed for mixtures of fallover inhibitors, and pentodiulose-P_2. This has previously been attributed to anti-cooperativity effects, in which binding of the ligand to one or more active sites on the Rubisco octomer reduces the affinity of binding to the remaining sites. However it is more economically explained as simply being the expected consequence of the model embodied in Scheme 6.1, where a rate of inhibition that becomes saturated at high concentrations of inhibitor is coupled with an appreciable rate of release.

The carbamylated form of Rubisco is tightly inhibited by carboxyarabinitol-1-P and carboxyarabinitol-P_2. The degree of inhibition demonstrates the extent to which the inhibitors mimic the carboxyketone intermediate compound. Carboxyarabinitol-1-P has only one phosphate group, and does not bind as tightly as carboxyarabinitol-P_2, which has two phosphate groups. The release of carboxyarabinitol-P_2 by His-*Rubrum* is four orders of magnitude slower than the release of ribulose-P_2, and the rate of binding by wild-type tobacco Rubisco is two orders of magnitude faster than the binding of xylulose-P_2. It appears that carboxyarabinitol-P_2 is more effective than xylulose-P_2 or carboxyarabinitol-1-P at triggering and maintaining closure of loop 6, possibly because of the extent to which it mimics the inter-phosphate distance of the carboxyketone intermediate compound. As carboxyarabinitol-P_2 and carboxytetritol-P_2 have similar structures, it may be inferred that carboxytetritol-P_2, which has two phosphate groups, will bind tightly to most Rubisco enzymes.

6.4.7 Negative Cooperativity in Binding

Previous studies have also observed the saturation of inhibition by xylulose-P_2 at less than complete inhibition (McCurry and Tolbert 1977; Zhu and Jensen 1991b), as well as for one or more of the inhibitors remaining after complete consumption of ribulose-P_2 (Edmondson et al. 1990c), carboxyarabinitol-1-P (Gutteridge et al. 1986; Berry et al. 1987) and pentodiulose-P_2 (Kane et al. 1998). This has previously been attributed to negative cooperativity (Edmondson et al. 1990c), in which binding of a ligand to one or more sites on the Rubisco octomer reduces the affinity of binding to the remaining sites. While no direct evidence has been found for the existence or lack of negative cooperativity, the less than complete inhibition can be accounted for as being simply the expected consequence of the model for slow inhibition (Equation 6.8), where

a rate of inhibition that becomes saturated at high inhibitor concentrations is coupled with an appreciable rate of ligand release.

6.4.8 Conclusions

The differences in ligand binding and release between Rubisco enzymes may account for the observed differences in self-inhibition that were observed in Chapter 4. While there have been few previous studies on the binding of inhibitory compounds to Rubisco, the results obtained here provide a complete comparison for a range of inhibitory ligand and different Rubisco enzymes.

Inhibition of Rubisco occurs as a two step process, with initial rapid equilibrium inhibition followed by a second, slow tight binding step. Ribulose-P_2 binds quickly, but not very tightly to the decarbamylated form of Rubisco from His-*Rubrum* and *Synechococcus* PCC6301, moderately tightly to tobacco Rubisco, and very tightly to Rubisco from *G. sulphuraria*. While xylulose-P_2 is a rapid equilibrium competitive inhibitor of all Rubisco enzymes, the second tight binding step does not appear to occur in some enzymes. Although xylulose-P_2 binds tightly to Rubisco from wild-type tobacco and very tightly to Rubisco from *G. sulphuraria*, Rubisco enzymes from His-*Rubrum*, *Synechococcus* PCC6301, and L335V tobacco did not show tight binding inhibition by xylulose-P_2.

Unlike xylulose-P_2 and ribulose-P_2, the inhibitors carboxyarabinitol-1-P and carboxyarabinitol-P_2 bind to the carbamylated form of the enzyme. The binding of carboxyarabinitol-P_2 is very tight, with negligible release from most Rubisco enzymes, and the rate of binding is also several orders of magnitude faster than the binding of xylulose-P_2.

7 General Discussion and Conclusions

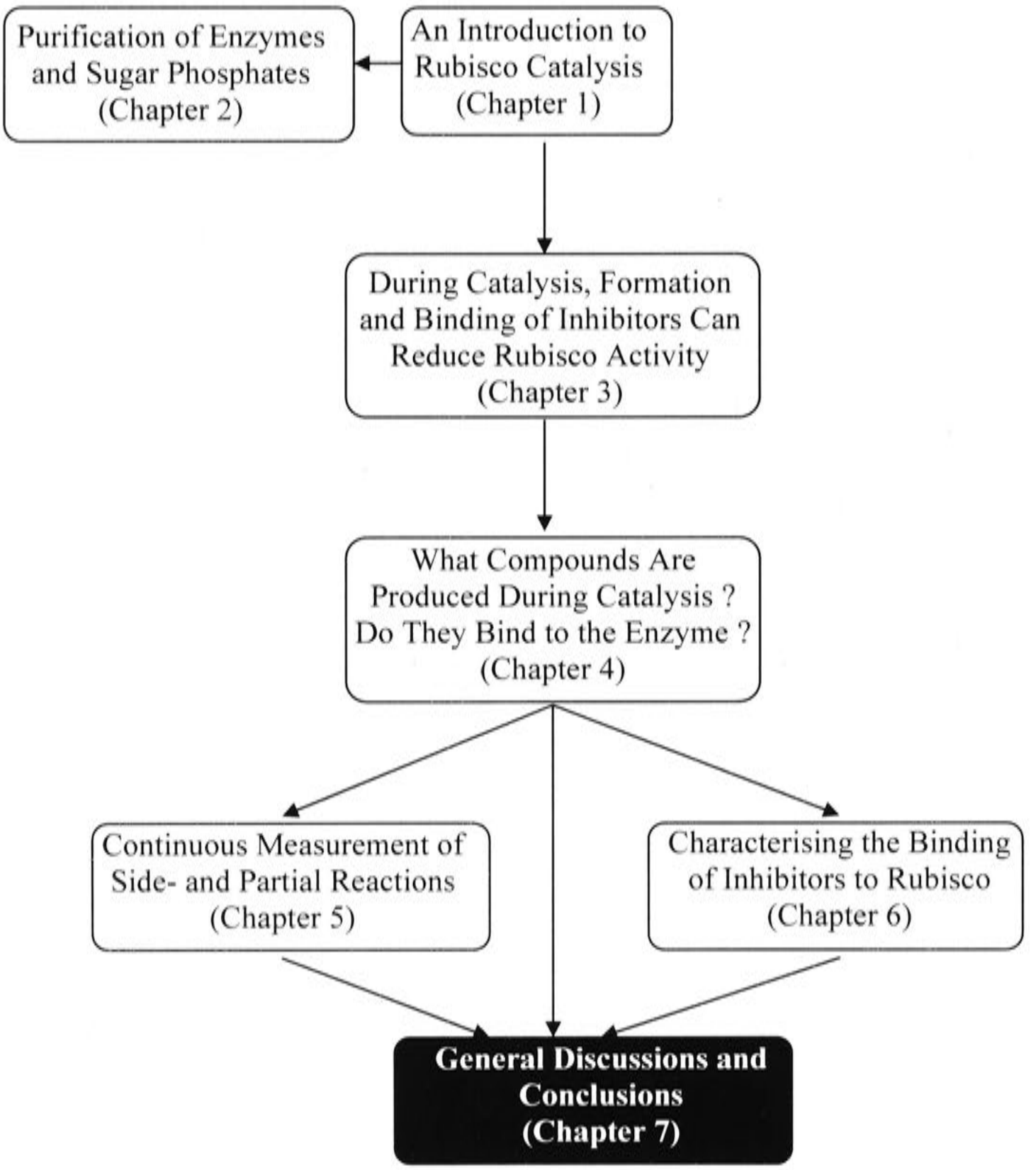

7.1 Introduction

Photosynthesis is often limited by both the ability of Rubisco to differentiate between CO_2 and O_2 as a substrate and the slow catalytic rate of the enzyme, and a long-term goal of Rubisco research is to improve photosynthesis in crop plants by the replacement or modification of the endogenous enzyme. Reduced substrate specificity increases the photorespiratory rate, with a subsequent loss of energy and reducing power, and also causes a decrease in the water use efficiency of higher plants. The low catalytic rate of the enzyme means that the organism needs to invest large amounts of protein in order to maintain viable rates of growth.

Natural variations have been observed in the kinetic parameters of Rubisco enzymes from different groups, however structural comparisons have shown that there is little difference in the structure of the active site. The difference in catalytic chemistry must be due to the variation in tertiary and quaternary enzyme structure, which is remote from the active site. These long-distance interactions are complex, and it is often difficult to establish how these large differences in tertiary and quaternary structure are translated into subtle differences in the active site structure. An increased knowledge of these interactions is required before rational design of Rubisco enzymes is possible.

Computational studies have progressed over recent years, allowing sophisticated modelling of the reaction mechanism, and predicting the relative importance of different residues and the possible consequences of mutational changes. However, these predications do not always correlate with the observed results, and a concerted effort is required, in which the computational predictions are compared with the actual result, to improve the models that are used. Biorational design of the Rubisco enzyme is progressing, but the models are not yet sufficiently accurate to allow reliable mutational studies and predictions.

Significant research is also currently going on in the development of high-throughput screening for 'improved' Rubisco enzymes, which allows many different random combinations of mutations to be analysed (Spreitzer and Salvucci 2002; Emlyn-Jones et al. 2003). These enzymes are usually only screened for faster catalytic rates or for a lower rate of oxygenase activity relative to the carboxylase activity. While this strategy may identify improvements in some kinetic parameters, it is important to undertake a full biochemical characterisation of the different enzymes, including

measuring the formation of catalytic by-products and interactions of the enzyme with regulatory ligands.

To improve the knowledge of how subtle changes in the geometry of the active site may affect the catalytic chemistry and binding of ligands, this thesis has carried out a comprehensive study of the kinetic parameters for a range of naturally occurring classes of Rubisco and a site directed mutant from higher plants. This study has been based on elucidating the differences that have previously been observed in the pattern of self-inhibition between different forms of Rubisco enzymes.

7.2 Self-Inhibition of Rubisco

During *in vitro* assays, higher plant Rubisco shows a decline in activity that has been termed 'fallover' and involves the formation of inhibitory complexes that bind tightly to the enzyme, but can be released or converted into products that can be released. This decline has not been observed for Form II, cyanobacterial, or 'Red-type' Form I Rubisco, and the kinetics of the decline are similar to that of slow, tight binding inhibition, with a final rate that is not completely inhibited.

The results of this thesis supported the earlier identification of inhibitors as xylulose-P_2 and pentodiulose-P_2, formed by misprotonation of the enediol intermediate and from the peroxyketone intermediate respectively (Edmondson et al. 1990d; Kane et al. 1998). Previous studies of the self-inhibition of Rubisco have often been limited by the purity of the ribulose-P_2 preparations, as care needs to be taken to avoid the introduction of additional inhibitors with the ribulose-P_2 substrate (Paech et al. 1978; Kane et al. 1998).

7.2.1 Self-Inhibition of Higher Plant Rubisco

When higher plant Rubisco was assayed, a greater degree of inhibition was observed under aerobic conditions than under anaerobic conditions. When oxygen was present, pentodiulose-P_2 could be formed from the peroxyketone intermediate in the oxygenation pathway, and acted in conjunction with xylulose-P_2 to inhibit the enzyme to a high degree. Under anaerobic conditions, pentodiulose-P_2 was not formed, and inhibition was solely by xylulose-P_2.

7.2.2 Consequences of Self-Inhibition

The extent of self-inhibition depended on the levels of CO_2 and O_2. When assay conditions promoted oxygenase activity over carboxylation, there was an increase in the

production of pentodiulose-P_2 due to the possibility of side-reactions arising from the enediol intermediate. If the level of CO_2 and O_2 were low, the addition of gaseous substrates to the enediol intermediate will be slow, and there is an increased chance of misprotonation to form xylulose-P_2.

In vivo, self-inhibition may be a way for Rubisco to regulate its own activity during catalysis. If the conditions are unfavourable, due to low levels of CO_2, and the proportion of oxygenation to carboxylation is high, pentodiulose-P_2 may be produced to down-regulate the enzyme and avoid photorespiration. The low levels of carboxylation will also increase the chance of misprotonation of the enediol to form xylulose-P_2. It has also been suggested that the extent of self-inhibition in maize is increased at higher temperatures (Crafts-Brandner and Salvucci 2002), which may be a mechanism to maintain the active sites in a carbamylated state.

It has been argued that the oxygenation activity of Rubisco has an important role in maintaining turnover of photosynthesis under low CO_2 conditions, which minimises photoinhibition. This would ensure that the components of the light reactions are not damaged by a build-up of high levels of ATP and reducing energy during high-light conditions and low CO_2 levels. This would be important as a rapid response to the adverse environmental effects, however if the oxygenase activity occurred over a prolonged period of time, self-regulation would allow for the down-regulation of Rubisco activity, which would correspond with a down-regulation of the light reactions.

This regulation of activity also involves the regulatory protein Rubisco activase, which has a role in removing inhibitors from the Rubisco active site. Any down-regulation of Rubisco activity by the binding of inhibitors requires a corresponding down-regulation of Rubisco activase activity. As Rubisco activase is regulated by the level of ATP, this coordinated approach couples the inhibition of Rubisco with the amount of chemical energy available.

7.2.3 Mutations can Change Patterns of Self-Inhibition

Mutation of Leu-335 to valine in the tobacco enzyme changes the pattern of inhibition during *in vitro* assay. Under anaerobic conditions, when inhibition is solely due to xylulose-P_2, no decline is observed because the mutation prevents the slow, tight binding of xylulose-P_2 to the active site. When the presence of O_2 allows the formation of pentodiulose-P_2, inhibition is slower, but proceeds to completion. Unlike the wild-type enzyme, the mutant tobacco Rubisco is able to rearrange pentodiulose-P_2 to

form carboxytetritol-P_2, which is a much tighter binding inhibitor, and is not released or catalysed by the enzyme, as shown in Figure 7.1.

7.2.4 Other Rubisco Enzymes Lack Self-Inhibition

Self-inhibition is due to the slow, tight binding of inhibitors to the enzyme, therefore a lack of self-inhibition reflects the reduced formation of inhibitors by the enzyme, or a lack of slow tight binding. Analysis of reaction products and rates of side reactions of non-higher plant Rubisco enzymes showed that inhibitors were being formed during catalysis. For cyanobacterial and Form II Rubisco, inhibitors did not bind tightly to the enzyme, as shown in Figure 7.1. Like the L335V tobacco mutant Rubisco, His-*Rubrum* Rubisco could rearrange pentodiulose-P_2 into carboxytetritol-P_2, but unlike the mutant tobacco enzyme, His-*Rubrum* Rubisco rapidly released carboxytetritol-P_2 and was not inhibited.

'Red-type' Form I Rubisco could be tightly inhibited by pentodiulose-P_2 and xylulose-P_2, and produced both of these, but did not show the expected self-inhibition. This is partly due to a low $K_C.K_{Mg}$ that results in a high proportion of enzyme remaining carbamylated, even after exhaustive lengths are taken to remove extraneous CO_2 (Saska 2001). Xylulose-P_2 binds to the decarbamylated form of Rubisco, thus it might be suggested that the 'red-type' Rubisco avoids inhibition by maintaining the Rubisco in a carbamylated state, as shown in Figure 7.1. Inhibition by pentodiulose-P_2 is compensated for by the high specificity for CO_2 over O_2, reducing the partitioning down the oxygenation pathway. The tendency to convert the peroxyketone intermediate into pentodiulose-P_2 is also negligible.

7.3 Correlation between Structure and Function

A long-term goal of Rubisco research is the replacement of the native higher plant Rubisco with one that has an improved specificity and catalytic rate, which could improve the water and nitrogen efficiency of crop plants. The improved Rubisco may be one that is naturally occurring in another organism, or an altered version of the native enzyme. Few mutagenic studies have been able to improve the kinetic characteristics of Rubisco, therefore it is more likely that a naturally occurring enzyme will be used, providing the chaperone compatibility problems can be solved.

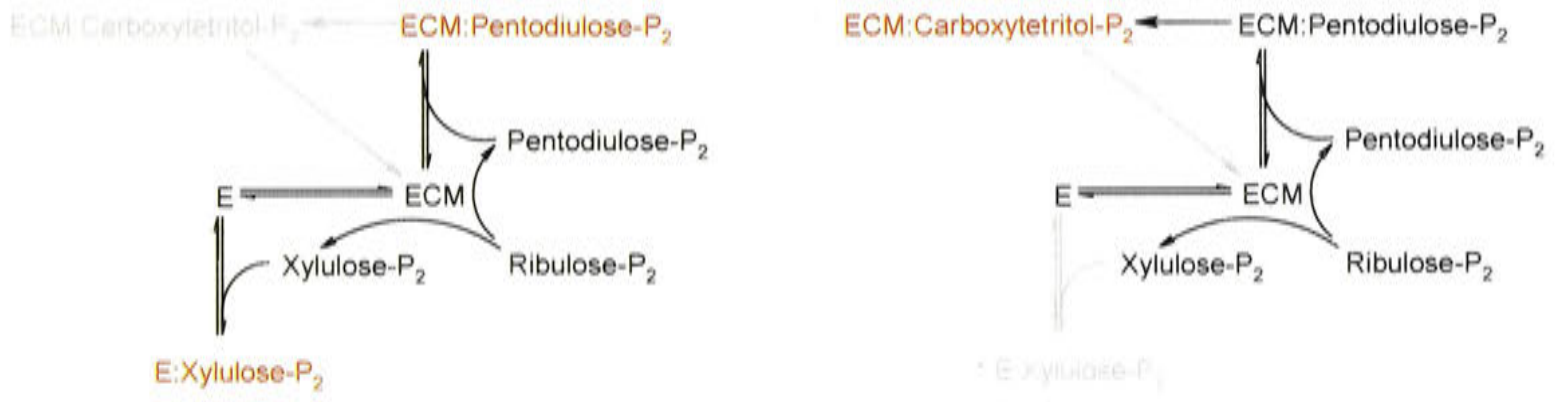

Figure 7.1 Self-Regulation of Different Rubisco Enzymes

Rubisco can produce pentodiulose-P_2 after oxygenation or xylulose-P_2 as side-products during catalysis. These inhibitors can then bind to the carbamylated (ECM) or decarbamylated form (E). In some enzymes, complexes are produced in which the inhibitors are slowly released (shown in red), while other enzymes avoid inhibition by reducing inhibitor formation or binding (shown in grey).

While most of the previous studies have focussed only on the specificity and catalytic rate, the work in this thesis has looked at a wider range of kinetic parameters, and how they relate to each other, allowing some elucidation of how the active site can be structured to carry out different reactions (Table 7.1).

7.3.1 Flexible Active Sites are Prone to Side Reactions

Side-products other than P-glycerate and P-glycolate may be formed during catalysis. Reprotonation of the *Re* face of the enediol intermediate results in the formation of xylulose-P_2, while β-elimination of the enediol P-1 phosphate group produces deoxy-pentodiulose-P. The *aci*-acid intermediate of carboxylation is also prone to β-elimination, forming pyruvate, and the peroxyketone intermediate of oxygenation may eliminate H_2O_2 to produce pentodiulose-P_2, which can be rearranged to form carboxytetritol-P_2. Like ribulose-P_2, xylulose-P_2 can be enolised by the abstraction of the C-3 proton.

In order to prevent side reactions, the reaction intermediates must be stabilised in the active site. β-Elimination is reduced by maintaining the C-1 to P-1 bond in the same plane as the C-2 to C-3 bond. Xylulose-P_2 formation gives an indication of the ability of the active site to protect the enediol from attack by protons, while enolisation of xylulose-P_2 reflects the ability of the active site to abstract a proton from the *Re* face. The peroxyketone must be stabilised to avoid H_2O_2 elimination, forming pentodiulose-P_2, and the active site may allow rearrangement of this into carboxytetritol-P_2.

		Higher Plants	L335V Tobacco	'Red-type' Form I	Cyanobacterial Form I	Form II
	Specificity for CO_2 (τ)	80	20	180	43	10
	Carboxylation of Ribulose-P_2 (s^{-1})	2.9	0.45	1	11	7
Chapter 4	Formation of Pentodiulose-P_2	+++	++	+	+	+
	Rearrangement of Pentodiulose-P_2 into Carboxytetritol-P_2	-	+++	-	-	+++
Chapter 5	Misprotonation of the Enediol (s^{-1})	0.0092 (0.32 %)	0.0054 (1.20 %)	0.011 (0.88 %)	0.0048 (0.04%)	0.042 (1.44 %)
	β-Elimination of Enediol (s^{-1})	0.0015 (0.05 %)	0.0023 (0.50 %)			
	β-Elimination of Carbanion	0.68 %	0.13 %	1.96 %	0.73 %	0.68 %
	Enolisation of Xylulose-P_2 (s^{-1})	0.00046 (0.03 %)	0.00074 (0.17 %)	0.0028 (0.27 %)	0.0036 (0.03 %)	0.0050 (0.16 %)
Chapter 6	Affinity for ribulose-P_2 (K_m, μM)	60	17	300	59	4.3
	Half-Activation of E:Ribulose-P_2 (s)	330	265	5300	24	35
	Affinity for Xylulose-P_2 (Competitive) (K_i, μM)	4.8	20.7	89	12.2	3.1
	Binding of Xylulose-P_2 (k_3, s^{-1})	0.0015	-	0.00012	-	-
	Half-Activation of E:Xylulose-P_2 (s)	1200	-	9900	-	-
	Affinity for Carboxyarabinitol-P_2 (K_i, μM)	0.54	0.50	220	1.72	> 2
	Binding of Carboxyarabinitol-P_2 (k_3, s^{-1})	0.060	0.087	0.086	0.28	> 1
	Half-Activation of ECM:Carboxyarabinitol-P_2 (days)	> 100	> 100	> 100	> 100	2
	Half-Activation of ECM:Carboxyarabinitol-1-P (s)	250	300	865	85	36

Table 7.1 Summary of Kinetic Parameters

Where the exact values are not known, the relative rate for each enzymes is indicated by symbols, with '+' showing least activity, and '+++' showing the highest activity.

7.3.2 Increased Flexibility Reduces the Tightness of Binding

Slow tight binding occurs when an inhibitor is an analogue of a reaction intermediate or substrate. The inhibition is accompanied by a conformational change in the enzyme, which, in Rubisco, is the closure of loop 6 over the active site. Loop 6 closure is thought to be triggered by a reduction in the inter-phosphate distance of the ligand, which is reduced when the ligand is coordinated in the active site (Duff et al. 2000). This closure is associated with the ordering of the C-terminal and N-terminal residues, which hold loop 6 in a closed position, and is important in excluding the solvent from the active site and positioning Lys-334 in the active site (Schreuder et al. 1993a). Thus the degree to which an inhibitor binds to the enzyme reflects how tightly the intermediate would normally bind, and how securely loop 6 is maintained in an ordered state over the active site.

7.3.3 Higher Plants Have a Tight Active Site

Rubisco from higher plants has a relatively high specificity for CO_2 over O_2. This improved ability to differentiate between substrates suggests that the active site is able to control catalysis by differentially stabilising the transition states. Formation of side products is moderate compared to other enzymes, with negligible misprotonation or β-elimination of the enediol. Some pentodiulose-P_2 is formed during catalysis, suggesting reduced stability of the peroxyketone intermediate.

A consequence of the stability of intermediate compounds is that inhibitors can bind tightly to the active site, and are released very slowly. Xylulose-P_2 and ribulose-P_2 bind tightly to the decarbamylated form, and carboxyarabinitol-P_2 binds extremely tightly to the carbamylated form.

7.3.4 Mutations Can Loosen the Active Site

In tobacco Rubisco, Leu-335 is located adjacent to the catalytically important Lys-334 residue, which is involved in the addition of CO_2 to the enediol. Mutation of this residue to valine reduced the ability of the active site to stabilise the reaction intermediates, presumably due to the reduced interaction between Lys-334 and the reaction intermediates. This was apparent by the reduced catalytic rate and specificity for CO_2 over O_2, and was accompanied by an increase in the rate of misprotonation or β-elimination of the enediol.

Interestingly, the mutation nearly abolished the β-elimination of the carbanion during carboxylation. Loosening the active site configuration may improve its ability to switch quickly between the different conformations required to stabilise the enediol and the *aci*-carbanion intermediates.

The mutation prevented the slow, tight binding of xylulose-P_2 to the decarbamylated active site, but did not significantly alter the binding of other inhibitors. Changing the composition of loop 6 must either prevent xylulose-P_2 from coordinating to the active site and triggering loop closure, or reduce the ability of the enzyme to maintain loop 6 in an ordered state while xylulose-P_2 is coordinated in the active site.

7.3.5 'Red-Type' Rubisco Has a Rigid Active Site

The specificity of 'red-type' Form I Rubisco is the highest observed yet, suggesting that the active site is very effective in differentially stabilising the carboxylation and oxygenation transition states. Despite this, the rate of enediol misprotonation is still high compared to other enzymes. Configuring the active site to favour carboxylation over oxygenation has reduced the ability to maintain the planarity of the carbanion bonds, resulting in increased pyruvate production. The active site must also have an increased ability to abstract protons from the *Re* face of xylulose-P_2, as the xylulose-P_2 enolisation rate is high compared to other enzymes.

The biggest consequence of the rigid active site is to increase the tightness with which inhibitors bind to the enzyme. Ribulose-P_2 and xylulose-P_2 were released from the decarbamylated enzyme at least an order of magnitude slower than other Rubisco enzymes. Tightness of binding may be due to a unique hydrogen bond between loop 6 and the large subunit, which is lacking in other Rubisco enzymes and assists in maintaining loop 6 in an ordered state (Okano et al. 2002). To make up for this potentially debilitating inhibition, the 'red-type' Form I Rubisco has a reduced $K_C.K_{Mg}$ value, which effectively prevents decarbamylation of the active site. These enzymes also have a reduced binding affinity for most ligands, including the substrate, ribulose-P_2, which may be a consequence of the rigid active site.

7.3.6 Cyanobacterial Rubisco Releases Inhibitors

Cyanobacterial 'green-type' Rubisco is similar to the higher plant 'green-type' enzyme, both in terms of the formation of side-products and the other kinetic constants. The major difference between the enzymes is in the release of inhibitors. Ribulose-P_2 is released from the decarbamylated active site nearly ten times faster than the higher plant

enzyme, and xylulose-P_2 does not bind tightly to the cyanobacterial enzyme. The binding and release of carboxyarabinitol-P_2 to the active site has similar parameters for both enzymes, suggesting that the active site has a similar configuration to higher plants. However inhibitors do not bind tightly to the decarbamylated enzyme, suggesting that either coordination of inhibitors in the absence of a metal ion does not trigger closure of loop 6, or that loop 6 is not as stable in the ordered state, allowing the subsequent disordering and ligand release.

7.3.7 Form II Rubisco Active Sites Are Very Loose

While enzymes with high specificities seem to have a rigid active site, enzymes with low specificities, such as Form II Rubisco, appear to have a loose active site. Misprotonation of the enediol is high, and the active site allows the rearrangement of pentodiulose-P_2 into carboxytetritol-P_2. Increased flexibility of the active site is also apparent in the reduced binding of inhibitors to the enzyme due to either restrictions in the coordinated ligand triggering closure of loop 6, or that like cyanobacterial Rubisco loop 6 is not as stable in the ordered state as in higher plant or red algal Rubisco. Ribulose-P_2 is released quickly from the active site of decarbamylated enzyme, and xylulose-P_2 does not bind. Carboxyarabinitol-P_2 binds more quickly to Form II Rubisco than to other enzymes, but is also released at a detectable, albeit slow rate.

7.4 Conclusions

Rubisco is limited by its ability to catalyse reactions other than the carboxylation of ribulose-P_2. The predominant competing reaction is the oxygenation of ribulose-P_2, but other reactions can also take place, mainly involving the intermediates of catalysis. Products of these reactions can act as inhibitors of Rubisco, and may be a mechanism by which the enzyme regulates its own activity.

Comparing a range of phylogenetic representatives of Rubisco enzymes demonstrates how the nature of the active site can influence the kinetic parameters. The degree to which the enzyme controls side-reactions is correlated to the binding of inhibitors to the active site, thus enzymes that are able to reduce the level of side reactions are often limited by the tight binding of inhibitors. Similarly, enzymes that do not bind inhibitors tightly are less able to control the partitioning of side reactions.

These results have implications for future work on the replacement of Rubisco in crop plants with a more efficient form. Along with the specificity and catalytic rate, consideration must also be given to production of side-products, and the interaction of

these with the enzyme. An enzyme with high specificity and catalytic rate may be less effective if it is strongly inhibited by ligands. This work also demonstrates that while there are some general correlations between different kinetic parameters, it is difficult to make direct inferences as to how the active site structure influences the enzyme function. These relationships can only be determined by observing the changes caused by mutating specific residues.

Future Rubisco research is almost certainly going to unearth many Rubisco mutants that have an increased specificity, and/or catalytic rate through rapid screening techniques (Spreitzer and Salvucci 2002). However, a full characterisation of the mutants will have to be carried out to ensure that these mutants are not impaired by the formation or binding of side-products, which could have implications for their *in vivo* properties. Improvement of photosynthesis in crop plants will most likely involve the identification of a naturally occurring more efficient Rubisco, which will be strongly supported by the current research aimed at the expression and assembly of Rubisco in a foreign host (Andrews and Whitney 2003).

8 Literature Cited

Allen, M. B. (1959). "Studies with Cyanidium caldarium, an anomalously pigmented chlorophyte." Archives of Microbiology **32**: 270-277.

Andersson, I. (1996). "Large structures at high resolution: The 1.6Å crystal structure of spinach ribulose-1,5-bisphosphate carboxylase/oxygenase complexed with 2-carboxyarabinitol bisphosphate." Journal of Molecular Biology **259**(1): 160-174.

Andersson, I., S. Knight, G. Schneider, Y. Lindqvist, T. Lundqvist, *et al.* (1989). "Crystal structure of the active site of ribulose-bisphosphate carboxylase." Nature **337**: 229-234.

Andersson, I. and T. C. Taylor (2003). "Structural framework for catalysis and regulation in ribulose-1,5-bisphosphate carboxylase/oxygenase." Archives of Biochemistry and Biophysics **414**(2): 130-140.

Andrés, J., V. S. Safont, J. Queralt and O. Tapia (1993). "A theoretical study of the singlet-triplet energy gap dependence upon rotation and pyramidalization for 1,2-dihydroxyethylene. A simple model to study the enediol moiety in Rubisco's substrate." Journal of Physical Chemistry **97**: 7888-7893.

Andrews, T. J. (1988). "Catalysis by cyanobacterial ribulosebisphosphate carboxylase large subunits in the complete absence of small subunits." Journal of Biological Chemistry **263**: 12213-12220.

Andrews, T. J. and K. M. Abel (1981). "Kinetics and subunit interactions of ribulose bisphosphate carboxylase-oxygenase from the cyanobacterium, *Synechococcus* sp." Journal of Biological Chemistry **256**: 8445-8451.

Andrews, T. J., M. R. Badger and G. H. Lorimer (1975). "Factors affecting interconversion between kinetic forms of ribulose diphosphate carboxylase-oxygenase from spinach." Archives of Biochemistry and Biophysics **171**: 93-103.

Andrews, T. J. and M. D. Hatch (1971). "Activity and properties of ribulosediphosphate carboxylase from plants with the C_4-dicarboxylic pathway of photosynthesis." Phytochemistry **10**: 9-15.

Andrews, T. J. and H. J. Kane (1991). "Pyruvate is a by-product of catalysis by ribulosebisphosphate carboxylase/oxygenase." Journal of Biological Chemistry **266**: 9447-9452.

Andrews, T. J. and G. H. Lorimer (1987). Rubisco: Structure, mechanisms, and prospects for improvement. The Biochemistry of Plants: A Comprehensive Treatise, Vol. 10, Photosynthesis. N. K. Boardman. New York, Academic Press: 131-218.

Andrews, T. J., S. von Caemmerer, C. J. Mate, G. S. Hudson and J. R. Evans (1995). The regulation of Rubisco catalysis by Rubisco activase. Photosynthesis: from Light to Biosphere. P. Mathis. Dordrecht, Kluwer Academic Publishers: 17-22.

Andrews, T. J. and S. M. Whitney (2003). "Manipulating ribulose bisphosphate carboxylase/oxygenase in the chloroplasts of higher plants." Archives of Biochemistry and Biophysics **414**(2): 159-169.

Ashida, H., Y. Saito, C. Kojima, K. Kobayashi, N. Ogasawara, *et al.* (2003). "A functional link between RuBisCO-like protein of Bacillus and photosynthetic RuBisCO." Science **302**(5643): 286-290.

Badger, M. R. and T. J. Andrews (1974). "Effects of CO_2, O_2 and temperature on a high-affinity form of ribulose diphosphate carboxylase-oxygenase from spinach." Biochemical and Biophysical Research Communications **60**: 204-210.

Barcena, J. A. (1983). "Differential effect of CA-2+ and MN-2+ on activation and catalyasis of spinach ribulose-1,5-bisphosphate carboxylase oxygenase." Biochemistry International **7**: 755-760.

Barraclough, R. and R. J. Ellis (1980). "Protein-synthesis in chloroplasts .9. assembly of newly-synthesized large subunits into ribulose bisphosphate carboxylase in isolated intact pea-chloroplasts." Biochimica et Biophysica Acta **608**: 19-31.

Bateman, J. M. and S. Purton (2000). "Tools for chloroplast transformation in Chlamydomonas: expression vectors and a new dominant selectable marker." Molecular and General Genetics **263**: 404-410.

Berry, J. A., G. H. Lorimer, J. Pierce, J. R. Seemann, J. Meek, *et al.* (1987). "Isolation, identification, and synthesis of 2-carboxyarabinitol 1-phosphate, a diurnal regulator of ribulose-bisphosphate carboxylase activity." Proceedings of the National Academy of Sciences of the United States of America **84**: 734-738.

Berrylow, S. L., T. D. McKnight, D. M. Shah and R. B. Meagher (1982). "The nucleotide sequence, expression, and evolution of one member of a multigene family encoding the small subunit of ribulose-1,5-bisphosphate carboxylase in soybean." Journal of Molecular and Applied Genetics **1**: 483-498.

Byrne, W. L. and H. A. Lardy (1954). "Pentose Phosphates Formed by Muscle Aldolase." Biochimica et Biophysica Acta **14**: 495-501.

Calvin, M. and A. A. Benson (1948). "The Path of Carbon in Photosynthesis." Science **107**: 476-480.

Carrer, H., T. N. Hockenberry, Z. Svab and P. Maliga (1993). "Kanamycin resistance as a selection marker for plastid transformation in tobacco." Molecular and General Genetics **241**(241): 49-56.

Chen, Y.-R. and F. C. Hartman (1995). "A signature of the oxygenase intermediate in catalysis by ribulose-bisphosphate carboxylase/oxygenase as provided by a site-directed mutant." Journal of Biological Chemistry **270**: 11741-11744.

Chifflet, S., A. Torriglia, R. Chiesa and S. Tolosa (1988). "A method for the determination of inorganic phosphate in the presence of labile organic phosphate and high concentrations of protein: application to lens ATPases." Analytical Biochemistry **168**: 1-4.

Chu, D. K. and J. A. Bassham (1975). "Regulation of RuDP carboxylase by substrates and other metabolites. Further evidence for several types of binding sites." Plant Physiology **55**: 720-726.

Cleland, W. W., T. J. Andrews, S. Gutteridge, F. C. Hartman and G. H. Lorimer (1998). "Mechanism of Rubisco - the carbamate as general base [review]." Chemical Reviews **98**(2): 549-561.

Crafts-Brandner, S. J. and M. E. Salvucci (2002). "Sensitivity of photosynthesis in a C4 plant, maize, to heat stress." Plant Physiology **129**(4): 1773-1780.

Curmi, P. M. G., D. Cascio, R. M. Sweet, D. Eisenberg and H. Schreuder (1992). "Crystal structure of the unactivated form of ribulose-1, 5-bisphosphate carboxylase/oxygenase from tobacco refined at 2.0-Å resolution." Journal of Biological Chemistry **267**: 16980-16989.

Daniell, H., B. Muthukumar and S. B. Lee (2001). "Marker tree transgenic plants: engineering the chloroplast genome without the use of antibiotic selection." Current Genetics **39**(2): 109-116.

Dean, C., P. Vandenel., S. Tamaki, P. Dunsmuir and J. Bedbrook (1985). "Linkage and homology analysis divides the 8 genes for the small subunit of petunia ribulose 1,5-bisphosphate carboxylase into 3 gene families." Proceedings of the National Academy of Sciences of the United States of America **82**: 4964-4968.

Delwiche, C. F. and J. D. Palmer (1996). "Rampant horizontal transfer and duplication of rubisco genes in eubacteria and plastids." Molecular Biology & Evolution **13**(6): 873-882.

Dorner, R. W., A. Kahn and S. G. Wildman (1957). "The Proteins of Green leaves. VII. Synthesis and decay of the cytoplasmic proteins during the life of a tobacco leaf." Journal of Biochemistry **229**: 945-952.

Duff, A., T. J. Andrews and P. M. G. Curmi (2000). "The Transition between the Open and Closed States of Rubisco is Triggered by the Inter-Phosphate Distance of the Bound Bisphosphate." Journal of Biological Chemistry **298**: 903-916.

Edmondson, D. L., M. R. Badger and T. J. Andrews (1990a). "A kinetic characterization of slow inactivation of ribulosebisphosphate carboxylase during catalysis." Plant Physiology **93**: 1376-1382.

Edmondson, D. L., M. R. Badger and T. J. Andrews (1990b). "Slow inactivation of ribulosebisphosphate carboxylase during catalysis is caused by accumulation of a slow, tight-binding inhibitor at the catalytic site." Plant Physiology **93**: 1390-1397.

Edmondson, D. L., M. R. Badger and T. J. Andrews (1990c). "Slow inactivation of ribulosebisphosphate carboxylase during catalysis is not due to decarbamylation of the catalytic site." Plant Physiology **93**: 1383-1389.

Edmondson, D. L., H. J. Kane and T. J. Andrews (1990d). "Substrate isomerization inhibits ribulosebisphosphate carboxylase- oxygenase during catalysis." FEBS Lett **260**: 62-66.

Ellis, R. J. (1979). "The most abundant protein in the world." Trends in Biochemical Sciences **4**: 241-244.

Emlyn-Jones, D., G. D. Price and T. J. Andrews (2003). "Nitrogen-regulated hypermutator strain of Synechococcus sp for use in in vivo artificial evolution." Applied and Environmental Microbiology **69**(11): 6427-6433.

Esquivel, M. G., M. Anwaruzzaman and R. J. Spreitzer (2002). "Deletion of nine carboxy-terminal residues of the Rubisco small subunit decreases thermal stability but does not eliminate function." FEBS Lett **520**(1-3): 73-76.

Ezaki, S., N. Maeda, T. Kishimoto, H. Atomi and T. Imanaka (1999). "Presence of a structurally novel type ribulose-bisphosphate carboxylase/oxygenase in the hyperthermophilic archaeon, *Pyrococcus kodakaraensis* KOD1." Journal of Biological Chemistry **274**(8): 5078-5082.

Flachmann, R., G. H. Zhu, R. G. Jensen and H. J. Bohnert (1997). "Mutations in the small subunit of ribulose-1,5-bisphosphate carboxylase/oxygenase increase the formation of the misfire product xylulose-1,5-bisphosphate." Plant Physiology **114**(1): 131-136.

Gatenby, A. A. and J. A. Castleto (1982). "Amplification of maize ribulose bisphosphate carboxylase large subunit synthesis in *Escherichia coli* by transcriptional fusion with the lambda-N operon." Molecular and General Genetics **185**: 424-429.

Gatenby, A. A., S. M. Van der vies and D. Bradley (1985). "Assembly in E. coli of a functional multi-subunit ribulose bisphosphate carboxylase from a blue-green alga." Nature **314**: 617-620.

Gibson, J. L. and F. R. Tabita (1979). "Activation of ribulose 1,5-bisphosphate carboxylase from *Rhodopseudomonas sphaeroides*: Probable role of the small subunit." Journal of Bacteriology **140**: 1023-1027.

Gibson, J. L. and F. R. Tabita (1986). "Isolation of the *Rhodopseudomonas sphaeroides* form 1 ribulose 1,5-biphosphate carboxylase oxygenase large and small subunit genes and expression of the active hexadecameric enzyme in escherichia-coli." GENE **44**: 271-278.

Gibson, J. L. and F. R. Tabita (1997). "Analysis of the *cbbXYZ* operon in *Rhodobacter sphaeroides*." Journal of Bacteriology **179**(3): 663-669.

Grimm, R., M. Grimm, C. Eckerskorn, K. Pohlmeyer, T. Röhl, *et al.* (1997). "Postimport methylation of the small subunit of ribulose-1,5- bisphosphate carboxylase in chloroplasts." FEBS Lett. **408**(3): 350-354.

Gutteridge, S. and A. A. Gatenby (1995). "Rubisco synthesis, assembly, mechanism, and regulation." Plant Cell **7**: 809-819.

Gutteridge, S., G. H. Lorimer and J. Pierce (1988). "Details of the reactions catalysed by mutant forms of rubisco." Plant Physiology & Biochemistry **26**: 675-682.

Gutteridge, S., M. A. J. Parry, S. Burton, A. J. Keys, A. Mudd, *et al.* (1986). "A nocturnal inhibitor of carboxylation in leaves." Nature **324**: 274-276.

Hall, N. P., J. Pierce and N. E. Tolbert (1981). "Formation of a carboxyarabinitol bisphosphate complex with ribulose bisphosphate carboxylase-oxygenase and theoretical specific activity of the enzyme." Archives of Biochemistry and Biophysics **212**: 115-119.

Hanson, T. E. and F. R. Tabita (2001). "A ribulose-1,5-bisphosphate carboxylase/oxygenase (RubisCO)-like protein from *Chlorobium tepidum* that is involved with sulfur metabolism and the response to oxidative stress." Proceedings of the National Academy of Sciences of the United States of America **98**(8): 4397-4402.

Harpel, M. R. and F. C. Hartman (1994). "Chemical rescue by exogenous amines of a site-directed mutant of ribulose 1,5-bisphosphate carboxylase/oxygenase that lacks a key lysyl residue." Biochemistry **33**: 5553-5561.

Harpel, M. R. and F. C. Hartman (1996). "Facilitation of the terminal proton transfer reaction of ribulose 1,5-bisphosphate carboxylase oxygenase by active-site Lys166." Biochemistry **35**(44): 13865-13870.

Harpel, M. R., F. W. Larimer and F. C. Hartman (1991). "Functional analysis of the putative catalytic bases His- 321 and Ser-368 of *Rhodospirillum rubrum* ribulose bisphosphate carboxylase/oxygenase by site-directed mutagenesis." Journal of Biological Chemistry **266**: 24734-24740.

Harpel, M. R., F. W. Larimer and F. C. Hartman (1998). "Multiple catalytic roles of His 287 of *Rhodospirillum rubrum* ribulose 1,5-bisphosphate carboxylase/oxygenase." Protein Science **7**(3): 730-738.

Harpel, M. R., F. W. Larimer and F. C. Hartman (2002). "Multifaceted roles of Lys166 of ribulose-bisphosphate carboxylase/oxygenase as discerned by product analysis and chemical rescue of site-directed mutants." Biochemistry **41**(4): 1390-1397.

Harpel, M. R., E. H. Serpersu, J. A. Lamerdin, Z. H. Huang, D. A. Gage, *et al.* (1995). "Oxygenation mechanism of ribulose-bisphosphate carboxylase/oxygenase. Structure and origin of 2-carboxytetritol 1,4-bisphosphate, a novel O_2-dependent side product generated by a site- directed mutant." Biochemistry **34**: 11296-11306.

Hartman, F. C. and E. H. Lee (1989). "Examination of the function of active site lysine 329 of ribulose-bisphosphate carboxylase/oxygenase as revealed by the proton exchange reaction." Journal of Biological Chemistry **264**: 11784-11789.

Hartman, F. C., T. S. Soper, S. K. Niyogi, R. J. Mural, R. S. Foote, *et al.* (1987). "Function of Lys-166 of *Rhodospirillum rubrum* ribulosebisphosphate carboxylase oxygenase as examined by site-directed mutagenesis." Journal of Biological Chemistry **262**: 3496-3501.

Hernandez, J. M., S. H. Baker, S. C. Lorbach, J. M. Shively and F. R. Tabita (1996). "Deduced amino acid sequence, functional expression, and unique enzymatic properties of the form I and form II ribulose bisphosphate carboxylase oxygenase from the chemoautotrophic bacterium *Thiobacillus denitrificans*." Journal of Bacteriology **178**(2): 347-356.

Holbrook, G. P., G. Bowes and M. E. Salvucci (1989). "Degradation of 2-carboxyarabinitol 1-phosphate by a specific chloroplast phosphatase." Plant Physiology **90**: 673-678.

Horken, K. M. and F. R. Tabita (1999a). "Closely related form I ribulose bisphosphate carboxylase/oxygenase molecules that possess different CO_2/O_2 substrate specificities." Archives of Biochemistry and Biophysics **361**(2): 183-194.

Horken, K. M. and F. R. Tabita (1999b). "The "green" form I ribulose 1,5-bisphosphate carboxylase oxygenase from the nonsulfur purple bacterium *Rhodobacter capsulatus*." Journal of Bacteriology **181**(13): 3935-3941.

Houtz, R. L., L. Poneleit, S. B. Jones, M. Royer and J. T. Stults (1992). "Posttranslational modifications in the amino-terminal region of the large

subunit of ribulose-1,5-bisphosphate carboxylase/oxygenase from several plant species." Plant Physiology **98**: 1170-1174.

Houtz, R. L. and J. Portis, Archie R. (2003). "The life of ribulose 1,5-bisphosphate carboxylase/oxygenase--posttranslational facts and mysteries." Archives of Biochemistry and Biophysics **414**(2): 150-158.

Houtz, R. L., J. T. Stults, R. M. Mulligan and N. E. Tolbert (1989). "Post-translational modifications in the large subunit of ribulose bisphosphate carboxylase/oxygenase." Proceedings of the National Academy of Sciences of the United States of America **86**: 1855-1859.

Hudson, G. S., J. R. Evans, S. von Caemmerer, Y. B. C. Arvidsson and T. J. Andrews (1992). "Reduction of ribulose-1,5-bisphosphate carboxylase/oxygenase content by antisense RNA reduces photosynthesis in transgenic tobacco plants." Plant Physiol. **98**: 294-302.

Hudson, G. S., J. D. Mahon, P. A. Anderson, M. J. Gibbs, M. R. Badger, *et al.* (1990). "Comparisons of *rbc*L genes for the large subunit of ribulose- bisphosphate carboxylase from closely related C_3 and C_4 plant species." Journal of Biological Chemistry **265**: 808-814.

Iamtham, S. and A. Day (2000). "Removal of antibiotic resistance genes from transgenic tobacco plants." Nature Biotechnology **18**: 1172-1176.

Johal, S., B. E. Partridge and R. Chollet (1985). "Structural characterization and the determination of negative cooperativity in the tight-binding of 2-carboxyarabinitol bisphosphate to higher-plant ribulose bisphosphate carboxylase." Journal of Biological Chemistry **260**: 9894-9904.

Jordan, D. B. and R. Chollet (1983). "Inhibition of ribulose bisphosphate carboxylase by substrate ribulose 1,5-bisphosphate." Journal of Biological Chemistry **258**: 13752-13758.

Kane, H. J., J. Viil, B. Entsch, K. Paul, M. K. Morell, *et al.* (1994). "An improved method for measuring the CO_2/O_2 specificity of ribulosebisphosphate carboxylase-oxygenase." Australian Journal of Plant Physiology **21**: 449-461.

Kane, H. J., J. M. Wilkin, A. R. Portis and T. J. Andrews (1998). "Potent inhibition of ribulose-bisphosphate carboxylase by an oxidized impurity in ribulose-1,5-bisphosphate." Plant Physiology **117**(3): 1059-1069.

Kanevski, I. and P. Maliga (1994). "Relocation of the plastid *rbcL* gene to the nucleus yields functional ribulose-1,5-bisphosphate carboxylase in tobacco chloroplasts." Proceedings of the National Academy of Sciences of the United States of America **91**: 1969-1973.

Kanevski, I., P. Maliga, D. F. Rhoades and S. Gutteridge (1999). "Plastome engineering of ribulose-1,5-bisphosphate carboxylase/oxygenase in tobacco to form a sunflower large subunit and tobacco small subunit hybrid." Plant Physiology **119**(1): 133-141.

Kawashima, N., S. Singh and S. G. Wildman (1971). "Reversible cold inactivation and heat reactivation of RuDP carboxylase activity of crystallised tobacco fraction 1 protein." Biochemical & Biophysical Research Communications **42**(4): 664-668.

Keys, A. J., I. Major and M. A. J. Parry (1995). "Is there another player in the game of Rubisco regulation?" Journal of Experimental Botany **46**(290): 1245-1251.

King, W. A., J. E. Gready and T. J. Andrews (1998). "Quantum chemical analysis of the enolization of ribulose bisphosphate - the first hurdle in the fixation of CO_2 by Rubisco." Biochemistry **37**(44): 15414-15422.

Kitano, K., N. Maeda, T. Fukui, H. Atomi, T. Imanaka, *et al.* (2001). "Crystal structure of a novel-type archaeal rubisco with pentagonal symmetry." Structure (Camb) **9**(6): 473-81.

Klenk, H. P., R. A. Clayton, J. F. Tomb, O. White, K. E. Nelson, *et al.* (1997). "The complete genome sequence of the hyperthermophilic, sulphate-reducing archaeon *Archaeoglobus fulgidus*." Nature **390**(6658): 364-&.

Knight, S., I. Andersson and C.-I. Brändén (1989). "Reexamination of the three-dimensional structure of the small subunit of RuBisCo from higher plants." Science **244**: 702-705.

Knight, S., I. Andersson and C.-I. Brändén (1990). "Crystallographic analysis of ribulose 1,5-bisphosphate carboxylase from spinach at 2.4 Å resolution. Subunit interactions and active site." Journal of Molecular Biology **215**: 113-160.

Kung, S. D., R. Chollet and T. V. Marsho (1980). "Crystallization and Assay Procedures of Tobacco Ribulose-1,5-bisphosphate Carboxylase-Oxygenase." Methods in Enzymology **69**: 326-336.

Kunst, F., N. Ogasawara, I. Moszer, A. M. Albertini, G. Alloni, *et al.* (1997). "The complete genome sequence of the Gram-positive bacterium *Bacillus subtilis*." Nature **390**(6657): 249-256.

Laing, W. A. and J. T. Christeller (1976). "A model for the kinetics of activation and catalysis of ribulose 1,5-bisphosphate carboxylase." Biochemical Journal **159**: 563-570.

Laing, W. A., W. L. Ogren and R. H. Hageman (1974). "Regulation of soybean net photosynthetic CO_2 fixation by the interaction of CO_2, O_2, and ribulose 1,5-bisphosphate carboxylase." Plant Physiol. **54**: 678-685.

Lan, Y. and K. A. Mott (1991). "Determination of apparent K_m values for ribulose 1,5-bisphosphate carboxylase/oxygenase (Rubisco) activase using the spectrophotometric assay of Rubisco activity." Plant Physiology **95**: 604-609.

Larimer, F. W., M. R. Harpel and F. C. Hartman (1994). "Beta-Elimination of Phosphate from Reaction Intermediates by Site-Directed Mutants of Ribulose-Bisphosphate Carboxylase Oxygenase." Journal of Biological Chemistry **269**(15): 11114-11120.

Larson, E. M., C. M. O'Brien, G. H. Zhu, R. J. Spreitzer and A. R. Portis, Jr. (1997). "Specificity for activase is changed by a Pro-89 to Arg substitution in the large subunit of ribulose-1,5-bisphosphate carboxylase/oxygenase." Journal of Biological Chemistry **272**(27): 17033-17037.

Lee, B., B. A. Read and F. R. Tabita (1991). "Catalytic properties of recombinant octameric, hexadecameric, and heterologous cyanobacterial/bacterial ribulose-1,5- bisphosphate carboxylase/oxygenase." Archives of Biochemistry and Biophysics **291**: 263-269.

Lee, E. H., M. R. Harpel, Y.-R. Chen and F. C. Hartman (1993). "Perturbation of reaction-intermediate partitioning by a site-directed mutant of ribulose-bisphosphate carboxylase/oxygenase." Journal of Biological Chemistry **268**: 26583-26591.

Li, L.-A., J. L. Gibson and F. R. Tabita (1993). "The Rubisco activase (*rca*) gene is located downstream from *rbcS* in *Anabaena* sp. strain CA and is detected in other *Anabaena/Nostoc* strains." Plant Molecular Biology **21**: 753-764.

Li, L. A. and F. R. Tabita (1997). "Maximum activity of recombinant ribulose 1,5-bisphosphate carboxylase/oxygenase of *Anabaena* sp. strain CA requires the product of the *rbcX* gene." Journal of Bacteriology **179**(11): 3793-3796.

Li, L. A., M. R. Zianni and F. R. Tabita (1999). "Inactivation of the monocistronic rca gene in *Anabaena variabilis* suggests a physiological ribulose bisphosphate carboxylase oxygenase activase-like function in heterocystous cyanobacteria." Plant Molecular Biology **40**(3): 467-478.

Li, R. S. and G. L. Kenyon (1995). "A spectrophotometric determination of α-dicarbonyl compounds and its application to the enzymatic formation of α-ketobutyrate." Analytical Biochemistry **230**: 37-40.

Lilley, R. M. and D. A. Walker (1974). "An improved spectrophotometric assay for ribulosebisphosphate carboxylase." Biochimica et Biophysica Acta **358**: 226-229.

Liu, M. L., X. A. Mao, C. H. Ye, H. Huang, J. K. Nicholson, *et al.* (1998). "Improved WATERGATE pulse sequences for solvent suppression in NMR spectroscopy." Journal of Magnetic Resonance **132**(1): 125-129.

Lorimer, G. and F. C. Hartman (1988). "Evidence supporting lysine-166 of Rhodospirillum rubrum ribulosebisphosphate carboxylase as the essential base which initiates catalysis." Journal of Biological Chemistry **263**: 6468-6471.

Lorimer, G. H. (1979). "Evidence for the existence of discrete activator and substrate sites for CO_2 on ribulose-1,5-bisphosphate carboxylase." Journal of Biological Chemistry **254**: 5599-5601.

Lorimer, G. H. (1981). "Ribulosebisphosphate carboxylase - amino-acid sequence of a peptide bearing the activator carbon-dioxide." Biochemistry **20**: 1236-1240.

Lorimer, G. H., M. R. Badger and T. J. Andrews (1976). "The activation of ribulose-1,5-bisphosphate carboxylase by carbon dioxide and magnesium ions. Equilibria, kinetics, a suggested mechanism and physiological implications." Biochemistry **15**: 529-536.

Lorimer, G. H., Y.-R. Chen and F. C. Hartman (1993). "A role for the ε-amino group of lysine-334 of ribulose-1, 5-bisphosphate carboxylase in the addition of carbon dioxide to the 2,3-enediol(ate) of ribulose 1,5-bisphosphate." Biochemistry **32**: 9018-9024.

Lorimer, G. H. and H. M. Miziorko (1980). "Carbamate formation on the epsilon-amino group of lysyl residue as the basis for the activation of ribulosbisphosphate carboxylase by CO2 and MG2+." Biochemistry **19**: 5321-5328.

Loring, H. S., L. W. Levy, L. K. Moss and J. M. Ploeser (1956). "Periodate Oxidation of Sugar Phosphates in Neutral Solution. I. D-Ribose 5-Phosphate." Journal of the American Chemical Society **78**: 3724-3727.

Lundqvist, T. and G. Schneider (1989a). "Crystal structure of the binary complex of ribulose-1,5- bisphosphate carboxylase and its product, 3-phospho-D-glycerate." Journal of Biological Chemistry **264**: 3643-3646.

Lundqvist, T. and G. Schneider (1989b). "Crystal structure of the complex of ribulose-1,5-bisphosphate carboxylase and a transition state analogue, 2-carboxy-D-arabinitol 1,5-bisphosphate." Journal of Biological Chemistry **264**: 7078-7083.

Lundqvist, T. and G. Schneider (1991). "Crystal structure of activated ribulose-1,5-bisphosphate carboxylase complexed with its substrate, ribulose-1,5-bisphosphate." Journal of Biological Chemistry **266**: 12604-12611.

Maeda, N., T. Kanai, H. Atomi and T. Imanaka (2002). "The unique pentagonal structure of an archaeal Rubisco is essential for its high thermostability." Journal of Biological Chemistry **277**(35): 31656-62.

Maliga, P. (1993). "Towards plastid transformation in flowering plants." Trends in Biotechnology **11**: 101-107.

Mauser, H., W. A. King, J. E. Gready and T. J. Andrews (2001). "CO2 fixation by Rubisco: Computational dissection of the key steps of carboxylation, hydration, and C-C bond cleavage " Journal of the American Chemical Society **123**(44): 10821-10829.

McCurry, S. D. and N. E. Tolbert (1977). "Inhibition of ribulose-1,5-bisphosphate carboxylase/oxygenase by xylulose 1,5-bisphosphate." Journal of Biological Chemistry **252**: 8344-8346.

Mizohata, E., M. Anwaruzzaman, H. Okuno, K. I. Tomizawa, S. Shigeoka, *et al.* (2003). "Chemical modification of arginine alleviates the decline in activity during catalysis of spinach Rubisco." Biochemical and Biophysical Research Communications **301**(2): 591-597.

Moore, B. D., J. Kobza and J. R. Seemann (1991). "Measurement of 2-carboxyarabinitol 1-phosphate in plant leaves by isotope dilution." Plant Physiology **96**: 208-213.

Morell, M. K., H. J. Kane, G. S. Hudson and T. J. Andrews (1992). "Effects of mutations at residue 309 of the large subunit of ribulosebisphosphate carboxylase from *Synechococcus* PCC 6301." Archives of Biochemistry & Biophysics **299**: 295-301.

Morell, M. K., K. Paul, N. J. O'Shea, H. J. Kane and T. J. Andrews (1994). "Mutations of an active site threonyl residue promote β elimination and other side reactions of the enediol intermediate of the ribulosebisphosphate carboxylase reaction." Journal of Biological Chemistry **269**: 8091-8098.

Morell, M. K., J.-M. Wilkin, H. J. Kane and T. J. Andrews (1997). "Side reactions catalyzed by ribulose-bisphosphate carboxylase in the presence and absence of small subunits." Journal of Biological Chemistry **272**(9): 5445-5451.

Morrison, J. F. (1982). "The slow-binding and slow, tight-binding inhibition of enzyme-catalysed reactions." Trends in Biochemical Sciences **7**: 102-105.

Newman, J. and S. Gutteridge (1993). "The X-ray structure of *Synechococcus* ribulose-bisphosphate carboxylase/oxygenase-activated quaternary complex at 2.2- Å resolution." Journal of Biological Chemistry **268**: 25876-25886.

Newman, J. and S. Gutteridge (1994). "Structure of an effector-induced inactivated state of ribulose 1,5-bisphosphate carboxylase/oxygenase: the binary complex between enzyme and xylulose 1,5-bisphosphate." Structure **2**: 495-502.

Newman, S. M., J. Derocher and R. A. Cattolico (1989). "Analysis of chromophytic and rhodophytic ribulose-1,5-bisphosphate carboxylase indicates extensive structural and functional similarities among evolutionarily diverse algae." Plant Physiology **91**: 939-946.

Nierzwicki-Bauer, S. A., S. E. Curtis and R. Haselkorn (1984). "Cotranscription of genes encoding the small and large subunits of ribulose-1,5-bisphosphate carboxylase in the cyanobacterium *Anabaena*-7120." Proceedings of the National Academy of Sciences of the United States of America **81**: 5961-5965.

Ogren, W. L. and G. Bowes (1971). "RuDP carboxylase regulates soybean photorespiration." Nature **230**: 159-160.

Okano, Y., E. Mizohata, Y. Xie, H. Matsumura, H. Sugawara, *et al.* (2002). "X-ray structure of *Galdieria* Rubisco complexed with one sulfate ion per active site." FEBS Lett **527**(1-3): 33.

Ott, C. M., B. D. Smith, A. R. Portis and R. J. Spreitzer (2000). "Activase region on chloroplast ribulose-1,5-bisphosphate carboxylase/oxygenase - Nonconservative substitution in the large subunit alters species specificity of protein interaction." Journal of Biological Chemistry **275**(34): 26241-26244.

Paech, C., J. Pierce, S. D. McCurry and N. E. Tolbert (1978). "Inhibition of ribulose-1,5-bisphosphate carboxylase/oxygenase by ribulose-1,5-bisphosphate epimerization and degradation products." Biochemical and Biophysical Research Communications **83**: 1084-1092.

Paech, C., F. J. Ryan and N. E. Tolbert (1977). "Essential primary amino groups of ribulose bisphosphate carboxylase/oxygenase indicated by reaction with pyridoxal 5'-phosphate." Archives of Biochemistry & Biophysics **179**: 279-288.

Parry, M. A. J., P. J. Andralojc, R. A. C. Mitchell, P. J. Madgwick and A. J. Keys (2003). "Manipulation of Rubisco: the amount, activity, function and regulation." Journal of Experimental Botany **54**(386): 1321-1333.

Paul, M. J., P. J. Andralojc, F. M. Banks, M. A. J. Parry, J. S. Knight, *et al.* (1996). "Altered Rubisco activity and amounts of a daytime tight-binding inhibitor in transgenic tobacco expressing limiting amounts of phosphoribulokinase." Journal of Experimental Botany **47**(305): 1963-1966.

Paulsen, J. M. and M. D. Lane (1966). "Spinach ribulose diphosphate carboxylase. I. Purification and properties of the enzyme." Biochemistry **5**: 2350-2357.

Pierce, J., T. J. Andrews and G. H. Lorimer (1986a). "Reaction intermediate partitioning by ribulose-bisphosphate carboxylases with differing substrate specificities." Journal of Biological Chemistry **261**: 10248-10256.

Pierce, J., G. H. Lorimer and G. S. Reddy (1986b). "Kinetic mechanism of ribulosebisphosphate carboxylase: Evidence for an ordered, sequential reaction." Biochemistry **25**: 1636-1644.

Pierce, J. and G. S. Reddy (1986). "The sites for catalysis and activation of ribulosebisphosphate carboxylase share a common domain." Archives of Biochemistry & Biophysics **245**: 483-493.

Pierce, J., N. E. Tolbert and R. Barker (1980). "Interaction of ribulosebisphosphate carboxylase/oxygenase with transition-state analogues." Biochemistry **19**: 934-942.

Pon, N. G., B. R. Rabin and M. Calvin (1963). "Mechanism of the carboxydismutase reaction. I. The effect of preliminary incubation of substrates, metal ion and enzyme on activity." Biochemische Zeitschrift **338**: 7-19.

Portis, A. R. (2003). "Rubisco activase - Rubisco's catalytic chaperone [Review]." Photosynthesis Research **75**(1): 11-27.

Portis, A. R., Jr. (1995). "The regulation of Rubisco by Rubisco activase." Journal of Experimental Botany **46**(290): 1285-1291.

Portis, A. R., Jr., R. M. Lilley and T. J. Andrews (1995). "Subsaturating ribulose-1,5-bisphosphate concentration promotes inactivation of ribulose-1,5-bisphosphate carboxylase/oxygenase (Rubisco) - Studies using continuous substrate addition in the presence and absence of Rubisco activase." Plant Physiology **109**(4): 1441-1451.

Portis, A. R., Jr., M. E. Salvucci and W. L. Ogren (1986). "Activation of ribulose bisphosphate carboxylase/oxygenase at physiological CO2 and ribulosebisphosphate concentrations by rubisco activase." Plant Physiology **82**: 967-971.

Robinson, S. P. and A. R. Portis, Jr. (1988). "Release of the nocturnal inhibitor, carboxyarabinitol-1-phosphate, from ribulose bisphosphate carboxylase/oxygenase by rubisco activase." FEBS Lett. **233**: 413-416.

Robinson, S. P. and A. R. Portis, Jr. (1989a). "Adenosine triphosphate hydrolysis by purified rubisco activase." Archives of Biochemistry & Biophysics **268**: 93-99.

Robinson, S. P. and A. R. Portis, Jr. (1989b). "Ribulose-1,5-bisphosphate carboxylase/oxygenase activase protein prevents the *in vitro* decline in activity of ribulose-1,5-bisphosphate carboxylase/oxygenase." Plant Physiology **90**: 968-971.

Rose, I. A. (1981). "Chemistry of proton abstraction by glycolytic enzymes (aldolase, isomerases and pyruvate kinase)." Philosphical Transactions of the Royal Society of London,Series B **293**: 131-143.

Roy, H. and T. J. Andrews (2000). Rubisco: Assembly and Mechanism. Photosynthesis: Physiology and Metabolism. S. von Caemmerer. Dordrecht, Kluwer Academic Publishers: 53-83.

Salvucci, M. E. (1992). "Subunit interactions of Rubisco activase: Polyethylene glycol promotes self-association, stimulates ATPase and activation activities, and enhances interactions with Rubisco." Archives of Biochemistry & Biophysics **298**: 688-696.

Salvucci, M. E., G. P. Holbrook, J. C. Anderson and G. Bowes (1988). "Nadph-dependent metabolism of the ribulose bisphosphate carboxylase oxygenase inhibitor 2-carboxyarabinitol 1-phosphate by a chloroplast protein." FEBS Lett. **231**: 197-201.

Salvucci, M. E. and W. L. Ogren (1996). "The mechanism of Rubisco activase: Insights from studies of the properties and structure of the enzyme." Photosynthesis Research **47**(1): 1-11.

Salvucci, M. E., A. R. Portis, Jr. and W. L. Ogren (1985). "A soluble chloroplast protein catalyzes ribulosebisphosphate carboxylase oxygenase activation invivo (technical note)." Photosynthesis Research **7**: 193-201.

Saska, I. (2001). "Activation Properties of Rubisco from Red Algae." The Australian National University.

Schloss, J. V. (1988a). "Comparative affinities of the epimeric reaction-intermediate analogs 2-carboxy-D-arabinitol and 4-carboxy-D-arabinitol 1,5-bisphosphate for spinach ribulose 1,5-bisphosphate carboxylase." Journal of Biological Chemistry **263**: 4145-4150.

Schloss, J. V. (1988b). "Significance of slow-binding enzyme inhibition and its relationship to reaction-intermediate analogues." Accounts of Chemical Research **21**: 348-353.

Schneider, G., C.-I. Brändén and G. Lorimer (1986a). "New crystal forms of ribulose-1,5-bisphosphate carboxylase/oxygenase from *Rhodospirillum rubrum*." Journal of Molecular Biology **187**: 141-143.

Schneider, G., Y. Lindqvist, C.-I. Brändén and G. Lorimer (1986b). "3-dimensional structure of ribulose-1,5-bisphosphate carboxylase-oxygenase from *Rhodospirillum rubrum* at 2.9 a resolution." EMBO Journal **5**: 3409-3415.

Schneider, S. U., M. B. Leible and X.-P. Yang (1989). "Strong homology between the small subunit of ribulose-1, 5-bisphosphate carboxylase/oxygenase of two species of *Acetabularia* and the occurrence of unusual codon usage." Molecular and General Genetics **218**: 445-452.

Schreuder, H. A., S. Knight, P. M. G. Curmi, I. Andersson, D. Cascio, *et al.* (1993a). "Formation of the active site of ribulose-1,5-bisphosphate carboxylase/oxygenase by a disorder-order transition from the unactivated to the activated form." Proceedings of the National Academy of Sciences of the United States of America **90**: 9968-9972.

Schreuder, H. A., S. Knight, P. M. G. Curmi, I. Andersson, D. Cascio, *et al.* (1993b). "Crystal structure of activated tobacco rubisco complexed with the reaction-intermediate analogue 2-carboxy-arabinitol 1,5-bisphosphate." Protein Science **2**: 1136-1146.

Seemann, J. R., J. A. Berry, S. Freas and M. A. Krump (1985). "Regulation of ribulose bisphosphate carboxylase activity *in vivo* by a light-modulated inhibitor of catalysis." Proceedings of the National Academy of Sciences of the United States of America **82**: 8024-8028.

Seemann, J. R., J. Kobza and B. D. Moore (1990). "Metabolism of 2-carboxyarabinitol 1-phosphate and regulation of ribulose-1,5-bisphosphate carboxylase activity." Photosynthesis Research **23**: 119-130.

Servaites, J. C. (1985a). "Binding of a phosphorylated inhibitor to ribulose bisphosphate carboxylase/oxygenase during the night." Plant Physiology **78**: 839-843.

Servaites, J. C. (1985b). "Crystalline ribulose bisphosphate carboxylase/oxygenase of high integrity and catalytic activity from *Nicotiana tabacum*." Archives of Biochemistry & Biophysics **238**: 154-160.

Shibata, N., H. Yamamoto, T. Inoue, K. Uemura, A. Yokota, *et al.* (1996). "Crystallization and preliminary crystallographic studies of ribulose 1,5-bisphosphate carboxylase/oxygenase from a red alga, *Galdieria partita*, with a high specificity factor." Journal of Biochemistry **120**(6): 1064-1066.

Shinozaki, K. and M. Sugiura (1983). "The gene for the small subunit of ribulose-1,5-bisphosphate carboxylase oxygenase is located close to the gene for the large subunit in the cyanobacterium *Anacystis nidulans* 6301." Nucleic Acids Research **11**: 6957-6964.

Siegel, M. I. and M. D. Lane (1972). "Interaction of ribulose diphosphate carboxylase with 2-carboxy-ribitol diphosphate, an analogue of the proposed carboxylated intermediate in the CO2 fixation reaction." Biochemical and Biophysical Research Communications **48**: 508-516.

Somerville, C. R., A. R. Portis, Jr. and W. L. Ogren (1982). "A mutant of *Arabidopsis thaliana* which lacks activation of RUBP carboxylase invivo." Plant Physiology **70**: 381-387.

Somerville, C. R. and S. C. Somerville (1984). "Cloning and expression of the *Rhodospirillum rubrum* ribulosebisphosphate carboxylase gene in *Escherichia coli*." Molecular and General Genetics **193**: 214-219.

Spreitzer, R. J. and M. E. Salvucci (2002). "Rubisco: Structure, Regulatory Interactions, and Possibilities for a Better Enzyme." Annual Review of Plant Biology **53**: 449-75.

Sue, J. M. and J. R. Knowles (1982). "Ribulose-1,5-bisphosphate carboxylase - fate of the tritium label in ^{3}H-3-labeled ribulose 1,5-bisphosphate during the enzyme-catalyzed reaction." Biochemistry **21**: 5404-5410.

Sugawara, H., H. Yamamoto, N. Shihata, T. Inoue, S. Okada, *et al.* (1999). "Crystal structure of carboxylase reaction-oriented ribulose 1,5-bisphosphate carboxylase oxygenase from a thermophilic red alga, *Galdieria partita*." Journal of Biological Chemistry **274**(22): 15655-15661.

Svab, Z. and P. Maliga (1993). "High-frequency plastid transformation in tobacco by selection for a chimeric *aadA* gene." Proceedings of the National Academy of Sciences of the United States of America **90**: 913-917.

Tabita, F. R. (1995). The biochemistry and metabolic regulation of carbon metabolism and CO2 fixation in purple bacteria. Anoxygenic Photosynthetic Bacteria. C. E. Bauer. Dordrecht, Kluwer Academic Publishers: 885-914.

Tabita, F. R. (1999). "Microbial ribulose 1,5-bisphosphate carboxylase/oxygenase: A different perspective [Review]." Photosynthesis Research **60**(1): 1-28.

Tapia, O. and J. Andrés (1992). "Towards and explanation of the carboxylation/oxygenation bifunctionality in Rubisco. Transition structure for the carboxylation reaction of 2,3,4-pentanetriol." Molecular Engineering **2**: 37-41.

Taylor, T. C. and I. Andersson (1996). "Structural transitions during activation and ligand binding in hexadecameric Rubisco inferred from the crystal structure of the activated unliganded spinach enzyme." Nature Structural Biology **3**(1): 95-101.

Taylor, T. C. and I. Andersson (1997a). "Structure of a product complex of spinach ribulose-1,5- bisphosphate carboxylase/oxygenase." Biochemistry **36**(13): 4041-4046.

Taylor, T. C. and I. Andersson (1997b). "The structure of the complex between rubisco and its natural substrate ribulose 1,5-bisphosphate." Journal of Molecular Biology **265**(4): 432-444.

Taylor, T. C., A. Backlund, K. Bjorhall, R. J. Spreitzer and I. Andersson (2001). "First crystal structure of rubisco from a green alga, *Chlamydomonas reinhardtii*." Journal of Biological Chemistry **276**(51): 48159-48164.

Taylor, T. C., M. D. Fothergill and I. Andersson (1996). "A common structural basis for the inhibition of ribulose 1,5- bisphosphate carboxylase by 4-carboxyarabinitol 1,5-bisphosphate and xylulose 1,5-bisphosphate." Journal of Biological Chemistry **271**(51): 32894-32899.

Terzaghi, B. E., W. A. Laing, J. T. Christeller, G. B. Petersen and D. F. Hill (1986). "Ribulose 1,5-bisphosphate carboxylase - effect on the catalytic properties of changing methionine-330 to leucine in the rhodospirillum-rubrum enzyme." Biochemical Journal **235**: 839-846.

Uemura, K., Anwaruzzaman, S. Miyachi and A. Yokota (1997). "Ribulose-1,5-bisphosphate carboxylase/oxygenase from thermophilic red algae with a strong specificity for CO_2 fixation." Biochemical and Biophysical Research Communications **233**(2): 568-571.

Uemura, K., H. Tokai, T. Higuchi, H. Murayama, H. Yamamoto, *et al.* (1998). "Distribution of fallover in the carboxylase reaction and fallover-inducible sites among ribulose 1,5-bisphosphate carboxylase/oxygenases of photosynthetic organisms." Plant & Cell Physiology **39**(2): 212-219.

Van Dyk, D. E. and J. V. Schloss (1986). "Deuterium isotope effects in the carboxylase reaction of ribulose-1,5-bisphosphate carboxylase/oxygenase." Biochemistry **25**: 5145-5156.

von Caemmerer, S., A. Millgate, G. D. Farquhar and R. T. Furbank (1997). "Reduction of ribulose-1,5-bisphosphate carboxylase/oxygenase by antisense RNA in the C_4 plant *Flaveria bidentis* leads to reduced assimilation rates and increased carbon isotope discrimination." Plant Physiol. **113**(2): 469-477.

Vu, J. C. V., L. H. Allen and G. Bowes (1984). "Dark/light modulation of ribulose biosphosphate carboxylase activity in plants from different photosynthetic categories." Plant Physiology **76**: 843-845.

Wang, Z.-Y., G. W. Snyder, B. D. Esau, A. R. Portis, Jr. and W. L. Ogren (1992). "Species-dependent variation in the interaction of substrate- bound ribulose-1,5-bisphosphate carboxylase/oxygenase (Rubisco) and Rubisco activase." Plant Physiology **100**: 1858-1862.

Watson, G. M. F. and F. R. Tabita (1997). "Microbial ribulose 1,5-bisphosphate carboxylase/oxygenase: A molecule for phylogenetic and enzymological investigation." Fems Microbiology Letters **146**(1): 13-22.

Weissbach, A., B. L. Horecker and J. Hurwitz (1956). "The Enzymatic Formation of Phosphoglyceric Acid From Ribulose Diphosphate and Carbon Dioxide." Journal of Biological Chemistry **218**: 795-810.

Weissbach, A., P. Z. Smyrniotis and B. L. Horecker (1954). "Pentose phosphate and CO2 fixation with spinach extracts." Journal of the American Chemical Society **76**: 3611-3612.

Whitney, S. M. and T. J. Andrews (2001a). "The gene for the ribulose-1,5-bisphosphate carboxylase/oxygenase (Rubisco) small subunit relocated to the plastid genome of tobacco directs the synthesis of small subunits that assemble into Rubisco." Plant Cell **13**(1): 193-205.

Whitney, S. M. and T. J. Andrews (2001b). "Plastome-encoded bacterial ribulose-1,5-bisphosphate carboxylase/oxygenase (RubisCO) supports photosynthesis and growth in tobacco." Proceedings of the National Academy of Sciences of the United States of America **98**(25): 14738-43.

Whitney, S. M., P. Baldett, G. S. Hudson and T. J. Andrews (2001). "Form I Rubiscos from non-green algae are expressed abundantly but not assembled in tobacco chloroplasts." Plant Journal **26**(5): 535-547.

Whitney, S. M., D. C. Shaw and D. Yellowlees (1995). "Evidence that some dinoflagellates contain a ribulose-1, 5-bisphosphate carboxylase/oxygenase related to that of the α-proteobacteria." Proceedings of the Royal Society of London.B:Biological Sciences **259**: 271-275.

Whitney, S. M., S. von Caemmerer, G. S. Hudson and T. J. Andrews (1999). "Directed mutation of the Rubisco large subunit of tobacco influences photorespiration and growth." Plant Physiology **121**(2): 579-588.

Woodrow, I. E. and J. A. Berry (1988). "Enzymatic regulation of photosynthetic CO_2 fixation in C_3 plants." Annual Review of Plant Physiology & Plant Molecular Biology **39**: 533-594.

Yokota, A. (1991a). "Carboxylation and Detoxification of Xylulose Bisphosphate by Spinach Ribulose Bisphosphate Carboxylase Oxygenase." Plant and Cell Physiology **32**(6): 755-762.

Yokota, A. (1991b). "Ribulose bisphosphate-induced, slow conformational changes of spinach ribulose bisphosphate carboxylase cause the two types of inflections in the course of its carboxylase reaction." Journal of Biochemistry (Tokyo) **110**: 246-252.

Yokota, A. and S. Kitaoka (1989). "Linearity and functioning forms in the carboxylase reaction of spinach ribulose 1,5-bisphosphate carboxylase/oxygenase." Plant and Cell Physiology **30**: 183-191.

Zhang, K. Y. J., D. Cascio and D. Eisenberg (1994). "Crystal structure of the unactivated ribulose 1,5-bisphosphate carboxylase/oxygenase complexed with a transition state analog, 2-carboxy-D-arabinitol 1,5-bisphosphate." Protein Science **3**: 64-69.

Zhu, G. and R. G. Jensen (1990). "Status of the substrate binding sites of ribulose bisphosphate carboxylase as determined with 2-C-carboxyarabinitol 1,5-bisphosphate." Plant Physiology **93**: 244-249.

Zhu, G. and R. G. Jensen (1991a). "Fallover of ribulose 1,5-bisphosphate carboxylase/oxygenase activity. Decarbamylation of catalytic sites depends on pH." Plant Physiology **97**: 1354-1358.

Zhu, G. and R. G. Jensen (1991b). "Xylulose 1,5-bisphosphate synthesized by ribulose 1,5-bisphosphate carboxylase/oxygenase during catalysis binds to decarbamylated enzyme." Plant Physiology **97**: 1348-1353.

Zhu, G. H., H. J. Bohnert, R. G. Jensen and G. F. Wildner (1998). "Formation of the tight-binding inhibitor, 3-ketoarabinitol-1,5-bisphosphate by ribulose-1,5-bisphosphate carboxylase/oxygenase is O_2-dependent." Photosynthesis Research **55**(1): 67-74.